Biologically produced sulfur particles and polysulfide ions

Effects on a biotechnological process for the removal of hydrogen sulfide from gas streams

Promotoren: Prof. dr. ir. A.J.H. Janssen
hoogleraar biologische gas- en waterreiniging
Wageningen Universiteit

Prof. dr. M.A. Cohen Stuart
hoogleraar fysische chemie, met bijzondere aandacht voor de kolloïdchemie
Wageningen Universiteit

Co-promotor: Dr. A. de Keizer
universitair docent bij de leerstoelgroep fysische chemie en kolloïdkunde
Wageningen Universiteit

Samenstelling promotiecommissie:

Prof. dr. R. Steudel, Technische Universität Berlin
Prof. dr. ir. G.F. Versteeg, Universiteit Twente
Prof. dr. ir. A.J.M. Stams, Wageningen Universiteit
Prof. dr. ir. C.J.N. Buisman, Wageningen Universiteit

Biologically produced sulfur particles and polysulfide ions

Effects on a biotechnological process for the removal of hydrogen sulfide from gas streams

Wilfred Kleinjan

Proefschrift
ter verkrijging van de graad van doctor
op gezag van de rector magnificus
van Wageningen Universiteit,
prof. dr. ir. L. Speelman,
in het openbaar te verdedigen
op donderdag 23 juni 2005
des namiddags te vier uur in de Aula.

ISBN: 90-8504-232-1

Contents

Chapter 1

Introduction

1.1. Sulfur compounds in the environment

Sulfur compounds are abundant throughout the world and, as a matter of fact, also outside this world. Our soils contain sulfur compounds in large quantities in, for instance, sulfide minerals (pyrite, FeS_2) or sulfate minerals (gypsum, $CaSO_4 \cdot 2H_2O$). Our atmosphere contains gases like sulfur dioxide (SO_2) and hydrogen sulfide (H_2S), emitted by volcanic activities, evaporation from oceans, or fossil fuel combustion, and the oceans are full of sulfate (about 28 mM, the second most abundant anion after chloride) [1]. The element sulfur is an essential component in all living organisms, as it is needed in several amino acids. Furthermore, sulfur compounds have been found in meteorites and, for instance, on Jupiter's volcanic moon Io.

On earth, sulfur components are cycled between soil, oceans, atmosphere, and living matter in the so-called geochemical and biological sulfur cycles. The geochemical sulfur cycle involves processes such as evaporation from surface waters, sedimentation, and rain [1]. The biological sulfur cycle, which is described in more detail in section 2.1 of this thesis, involves the continuous oxidation and reduction of sulfur compounds by microorganisms, plants, and animals [2].

A substantial part of today's environmental problems, such as 'acid rain' and acidified lakes, are related to sulfur compounds and disturbances of the sulfur cycles. Acidification of lakes can result from acid mine drainage. Many metals, such as copper, lead, zinc, and iron (pyrite) are present in ores as sulfide minerals. In these ores, sulfide minerals are stable at conditions without oxygen and water. Upon extraction of the metal by mining, however, the conditions change to moist and aerobic, and sulfide can be oxidized to sulfate (sulfuric acid). Wastewaters discharged from mining sites (acid mine drainage) are therefore often rich in toxic metals and have a low pH [3].

Acid rain is mainly related to the emission of SO_2, which can be oxidized in the atmosphere to sulfuric acid. Growing industrialization in North America and Europe resulted in a fast increase of SO_2 emission after the Second World War, mainly because of combustion of fossil fuels containing H_2S or organic S-compounds. Since the 1970s a number of emission control strategies were introduced to prevent SO_2 emission, such as coal desulfurization, waste gas treatment, and selection of fossil fuels with lower sulfur content. Fortunately, the introduction of emission controls has resulted in a considerable decrease of SO_2 emissions since the 1970s. Over the period 1990-1998, SO_2 emissions decreased by 52% in the EU and by 17% in the United States and Canada. In Asia, however, an overall increase of 16% of SO_2 emissions occurred in this period [4].

1.2. Removal of hydrogen sulfide from gas streams

An important aspect of emission control is the treatment of gas streams. When H_2S is combusted, SO_2 is formed, and therefore H_2S has to be removed from gas streams prior to combustion. Apart from environmental concerns, H_2S has to be removed from gas streams as it is a malodorous ('rotten eggs'), toxic, and corrosive gas. Gas streams that can contain H_2S are, e.g., natural gas, synthesis gas, refinery gases, LPG, and biogas. For the removal of H_2S from these gases a number of physicochemical processes are available, such as the Sulfinol, Claus, or Stretford process. Some of the processes only remove the H_2S from a gas stream (e.g., the Sulfinol process), whereas others remove the H_2S and subsequently convert H_2S to the less harmful elemental sulfur (e.g., the Claus process in combination with amine treating and the Stretford process). In physicochemical H_2S removal processes where H_2S is oxidized to elemental sulfur, this oxidation is catalyzed by metals, such as vanadium in the Stretford process, or by high pressure and temperature and a catalyst (Claus process). Generally, the process conditions and the need for special chemicals are drawbacks of these processes, which can be overcome by the use of biotechnological processes, where bacteria act as 'biocatalyst' at ambient conditions. A number of good reviews on physicochemical and biotechnological H_2S removal processes are available [5-7]. In general, physicochemical processes, such as the Claus process, are considered most economical for relatively large quantities of sulfur (> 50 ton /day). In smaller natural gas fields with a relatively high H_2S concentration, biotechnological processes can be considered most economical, depending on local conditions [8]. As with a continuing search for gas fields, more smaller natural gas fields with a relatively high H_2S concentration are expected to be explored in the near future, the interest in biotechnological H_2S removal processes increases.

In the 1980s and 1990s, the basic concepts of a biotechnological H_2S removal process were developed at the department of Environmental Technology of Wageningen University [9, 10]. This process was further developed by Paques B.V. and was applied for the treatment of biogas, a mixture of methane (CH_4), carbon dioxide (CO_2), and H_2S at atmospheric pressure, which is a product from anaerobic wastewater treatment plants. In 1993, the first unit for biogas desulfurization was started up and in 2000 16 units treating biogas were in operation [11, 12]. Currently, the process is also used for the treatment of high-pressure natural gas (as the *Shell-Paques* process, a cooperation between Paques B.V. and Shell Global Solutions International B.V.), and the treatment of refinery gas (*Thiopaq*™ process, a cooperation of Paques B.V., Shell Global Solutions International B.V., and U.O.P.).

The basic concepts of this process are illustrated in Figure 1.1. The process consists of a gas absorber (G) where H_2S is washed from a gas stream (Eqs. 1.1 and 1.2), and a bioreactor (B) where dissolved sulfide (HS^-) is oxidized to elemental sulfur (Eq. 1.3). Part of the formed solid elemental sulfur is separated from the liquid by sedimentation

in a settler (S), whereas another part is led back to the gas absorber with a liquid recycle. To prevent oxidation of sulfide to sulfate (Eq. 1.4), which would yield more energy for the bacteria than formation of sulfur [13], oxygen-limiting conditions are applied in the bioreactor. Production of elemental sulfur is preferred over the production of sulfate as elemental sulfur is less harmful than sulfate. Furthermore, hydroxyl ions, consumed in the absorption of H_2S in the alkaline liquid, are regenerated upon oxidation of sulfide to elemental sulfur. This saves costs of dosing NaOH to the process. Solid elemental sulfur is also easily separated from the solution by sedimentation and the resulting sulfur product can be reused. The dominant organism in the mixed culture in the biotechnological H_2S removal process (*Shell-Paques* or *Thiopaq*™ process) was found to be the organism *Thiobacillus* sp. W5 [14]. In this thesis, the terms 'biologically produced sulfur' or 'biosulfur' are generally used to refer to sulfur produced in such a process. The process is generally operated around pH 8.

$$H_2S(g) \rightarrow H_2S(aq) \qquad (1.1)$$

$$H_2S(aq) + OH^- \rightarrow HS^- + H_2O \qquad (1.2)$$

$$HS^- + \tfrac{1}{2}O_2 \rightarrow S^0 + OH^- \qquad (1.3)$$

$$HS^- + 2\,O_2 \rightarrow SO_4^{2-} + H^+ \qquad (1.4)$$

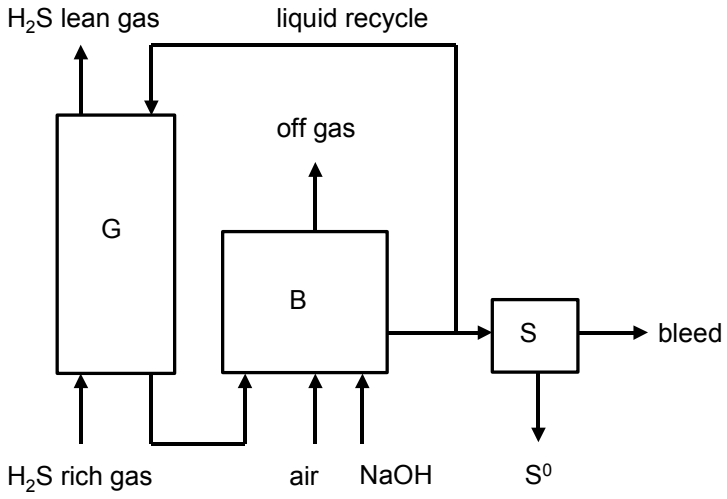

Figure 1.1. Scheme of the process for the biotechnological removal of H_2S from gas streams. G = Gas absorber, B = Bioreactor, S = Settler.

1.3. Sulfur and polysulfide chemistry in a biotechnological H_2S removal process

The sulfur formed in the process described above is of oxidation state zero (S^0) and is often called biologically produced sulfur, or biosulfur. This is a form of sulfur that is formed through oxidation of sulfide by sulfide-oxidizing bacteria. Biologically produced sulfur can occur in different modifications for different sulfide-oxidizing bacteria. In general, the biologically produced sulfur has some distinctly different properties as compared to "normal" inorganic sulfur. First, biologically produced sulfur particles are hydrophilic and can be dispersed in water, whereas inorganic sulfur is hydrophobic and poorly soluble in water (5 μg L^{-1}). Next, the density of biosulfur (1.3 g cm^{-3} for sulfur globules produced by *Allochromatium vinosum* [15]) has been reported to be lower than the density of crystalline forms of sulfur (1.95–2.26 g cm^{-3}) [16]. Furthermore, the nature of the sulfur structure can differ from the crystalline structures of inorganic sulfur. In **chapter 2** of this thesis an overview is given of the properties of biologically produced sulfur produced by bacteria in biotechnological H_2S removal systems and by other sulfide-oxidizing bacteria.

The chemistry of sulfur compounds is highly complex. Sulfur atoms are known to occur in nine different oxidation states (see Table 1.1), of which the oxidation states –2, 0, +4, and +6 are most common. Furthermore, sulfur of oxidation state zero tends to form long chains or rings of various sizes. Therefore, there are numerous forms of elemental sulfur allotropes [16]. The most common form of elemental sulfur is the cyclo S_8 molecule, which crystallizes at 25 °C to form orthorhombic sulfur (α S_8). Most commercial forms of elemental sulfur, such as 'flowers of sulfur' (formed from sublimation of sulfur vapor to sulfur powder) consist of α S_8 with traces of polymeric sulfur (S_μ) and cyclo S_7. In fact, the well-known bright yellow color of sulfur is caused by these traces of S_7 [16].

Table 1.1. Examples of the different oxidation states of sulfur compounds (after [17]).

oxidation state	compounds
–2	sulfide (H_2S, HS^-, S^{2-})
–1	disulfide (S_2^{2-})
0	sulfur (S_8)
+1	dichlorodisulfane (S_2Cl_2)
+2	sulfur dichloride (SCl_2), sulfoxylate (SO_2^{2-})
+3	dithionite ($S_2O_4^{2-}$)
+4	sulfur dioxide (SO_2), sulfite (SO_3^{2-})
+5	dithionate ($S_2O_6^{2-}$)
+6	sulfate (SO_4^{2-})

Sulfur of oxidation state zero is also present in polysulfide ions, S_x^{2-}. Polysulfide ions can be formed from reaction of sulfide with elemental sulfur. The overall reaction between elemental sulfur in its most common form (S_8 rings) and dissolved sulfide is shown in Eq. 1.5, but polysulfide formation can also occur with other forms of elemental sulfur [18].

$$HS^- + \frac{x-1}{8}S_8 \rightleftarrows S_x^{2-} + H^+ \qquad (1.5)$$

Polysulfide ions are unbranched chains of sulfur atoms, related to the polysulfanes, H_2S_n. The acidity constants of the polysulfanes are so low that polysulfide ions in aqueous solution can be assumed to be unprotonated [17, 19]. Because of difficulties in distinguishing between polysulfide ions of different chain length, the exact distribution of polysulfide ions of different chain length in aqueous solution is not completely clear. At neutral to alkaline pH values S_6^{2-}, S_5^{2-}, and S_4^{2-} are believed to dominate the solution and the shorter chains S_3^{2-} and S_2^{2-} were only observed at very high alkalinity (pH > 14) [20].

Recently, this was confirmed in a study where polysulfide ions were methylated and subsequently separated by chromatography [21]. Chromatograms showed the largest peaks for $(CH_3)_2S_n$ for n = 4, 5, and 6, with trace peaks at n = 2 and 3, and also small peaks at n = 7, 8, and 9. At mildly alkaline conditions and when in equilibrium with excess amounts of sulfur, the reported average chain length, x, varies from x = 4.6 [20], x = 4.8 [22], x = 5.4 [23], x = 5.5 [17]. Under acidic conditions, polysulfide ions are not stable.

Measurement of polysulfide concentrations in aqueous solutions aims at the amount of zero valent sulfur atoms in polysulfide molecules. This concentration, which is termed the *polysulfide excess sulfur concentration*, [S^0 in S_x^{2-}], can be measured with UV spectrophotometry [24, 25] and voltammetry [26]. Both methods cannot distinguish between polysulfide ions of different chain lengths. In this thesis UV spectrophotometry was used for the analysis of polysulfide excess sulfur concentrations.

Polysulfide ions are believed to play an important role in biotechnological H_2S removal processes. First, polysulfide ions are considered to be intermediates in the oxidation of HS^- to elemental sulfur, both in the chemical oxidation catalyzed by metal ions and in the biological oxidation by sulfide-oxidizing bacteria [18, 27] (see also section 2.3.3). Furthermore, formation and oxidation of polysulfide ions may affect the rate of H_2S absorption or the process selectivity for sulfur production. **Chapters 3, 4,** and **5** of this thesis are particularly concerned with polysulfide chemistry.

From pilot plant studies on the removal of H_2S from pressurized natural gas [28] it was observed that more H_2S was absorbed in the gas absorber than could be expected

based on physical absorption. A possible explanation for this is an enhancement of the absorption rate by a heterogeneous reaction between biologically produced sulfur and dissolved hydrogen sulfide, forming polysulfide ions (Eq. 1.5). For a better comprehension of the absorption of H_2S in the gas absorber, knowledge of the kinetics of this reaction is required. **Chapter 3** of this thesis describes the study of the kinetics of polysulfide formation by reaction of sodium sulfide with biologically produced sulfur in aqueous solutions, and **chapter 4** describes the study of the equilibrium of this reaction. Technological implications of the work described in chapters 3 and 4 are investigated in **chapter 6**.

Polysulfide ions formed according to Eq. 1.5 can be oxidized to thiosulfate and elemental sulfur according to Eq. 1.6 [29].

$$S_x^{2-} + \tfrac{3}{2} O_2 \rightarrow S_2O_3^{2-} + (x-2)\, S^0 \qquad (1.6)$$

This reaction decreases process selectivity for elemental sulfur production. Furthermore, hydroxyl ions which are consumed during the absorption of H_2S (Eq. 1.2) are regenerated when sulfur is formed (Eq. 1.3), but not when polysulfide ions are oxidized. Therefore, sodium hydroxide has to be dosed to the bioreactor and a bleed stream is necessary to prevent accumulation. This can be a considerable cost for the process. Knowledge of the kinetics of this reaction may help to prevent thiosulfate formation. This was investigated and results are reported in **chapter 5**.

Furthermore, sometimes excessive foam formation is observed in the process. In the aerated bioreactor stable foam containing solid elemental sulfur can be formed which can result in severe problems such as site pollution and loss of biomass contents of the reactor. To control foam formation more should be known about the mechanism of foam formation and foam stability. Particularly interesting is the role of sulfur particles. The results of the study on foam formation in biotechnological H_2S removal processes is described in **chapter 7**.

References

1. J. J. Middelburg, The geochemical sulfur cycle. In *Environmental technologies to treat sulfur pollution. Principles and engineering* (Eds.: P. N. L. Lens, L. Hulshoff Pol), IWA Publishing, London, **2000**, pp. 33-46.
2. T. Brüser, P. N. L. Lens, H. G. Trüper, The biological sulfur cycle. In *Environmental technologies to treat sulfur pollution. Principles and engineering* (Eds.: P. N. L. Lens, L. Hulshoff Pol), IWA Publishing, London, **2000**, pp. 47-85.
3. B. Johnson, Biological removal of sulfurous compounds from inorganic wastewaters. In *Environmental technologies to treat sulfur pollution. Principles and engineering* (Eds.: P. N. L. Lens, L. Hulshoff Pol), IWA Publishing, London, **2000**, pp. 175-205.
4. J. N. Cape, D. Fowler, A. Davison, Ecological effects of sulfur dioxide, fluorides, and minor air pollutants: Recent trends and research needs, *Environ. Int.* **2003**, *29*, 201-211.

5. A. B. Jensen, C. Webb, Treatment of H_2S-containing gases: A review of microbiological alternatives, *Enzyme Microb. Technol.* **1995**, *17*, 2-10.
6. E. Smet, P. Lens, H. Van Langenhove, Treatment of waste gases contaminated with odorous sulfur compounds, *Crit. Rev. Environ. Sci. Technol.* **1998**, *28*, 89-117.
7. J. E. Burgess, S. A. Parsons, R. M. Stuetz, Developments in odour control and waste gas treatment biotechnology: A review, *Biotechnol. Adv.* **2001**, *19*, 35-63.
8. A. J. H. Janssen, H. Dijkman, G. Janssen, Novel biological processes for the removal of H_2S and SO_2 from gas streams. In *Environmental technologies to treat sulfur pollution. Principles and engineering* (Eds.: P. N. L. Lens, L. Hulshoff Pol), IWA Publishing, London, **2000**, pp. 265-280.
9. C. J. N. Buisman, Biotechnological sulphide removal with oxygen, PhD thesis, Wageningen Agricultural University (Wageningen, The Netherlands), **1989**.
10. A. J. H. Janssen, Formation and colloidal behaviour of elemental sulphur produced from the biological oxidation of hydrogen sulphide, PhD thesis, Wageningen Agricultural University (Wageningen, The Netherlands), **1996**.
11. S. W. S. Kijlstra, A. J. H. Janssen, B. Arena, Biological process for H_2S removal from (high pressure) gas: The Shell-Thiopaq gas desulfurization process. In *Proceedings of the Laurance Reid gas conditioning conference* [CD-ROM], University of Oklahoma, Norman, OK, **2001**, pp. 169-182.
12. C. Cline, A. Hoksberg, R. Abry, A. Janssen, Biological process for H_2S removal from gas streams. The Shell-Paques/Thiopaq gas desulfurization process. In *Proceedings of the Laurance Reid gas conditioning conference* [CD-ROM], University of Oklahoma, Norman, OK, **2003**.
13. J. G. Kuenen, Colourless sulfur bacteria and their role in the sulfur cycle, *Plant Soil* **1975**, *43*, 49-76.
14. J. M. Visser, G. C. Stefess, L. A. Robertson, J. G. Kuenen, *Thiobacillus* sp. W5, the dominant autotroph oxidizing sulfide to sulfur in a reactor for aerobic treatment of sulfidic wastes, *Antonie van Leeuwenhoek* **1997**, *72*, 127-134.
15. R. Guerrero, J. Mas, C. Pedrós-Alió, Buoyant density changes due to intracellular content of sulfur in *Chromatium warmingii* and *Chromatium vinosum*, *Arch. Mircrobiol.* **1984**, *137*, 350-356.
16. R. Steudel, B. Eckert, Solid sulfur allotropes, *Top. Curr. Chem.* **2003**, *230*, 1-79.
17. R. Steudel, The chemical sulfur cycle. In *Environmental technologies to treat sulfur pollution. Principles and engineering* (Eds.: P. N. L. Lens, L. Hulshoff Pol), IWA Publishing, London, **2000**, pp. 1-31.
18. R. Steudel, Mechanism for the formation of elemental sulfur from aqueous sulfide in chemical and microbiological desulfurization processes, *Ind. Eng. Chem. Res.* **1996**, *35*, 1417-1423.
19. G. Schwarzenbach, A. Fischer, Die Acidität der Sulfane und die Zusammensetzung wässeriger Polysulfidlösungen, *Helv. Chim. Acta* **1960**, *169*, 1365-1392.
20. W. Giggenbach, Optical spectra and equilibrium distribution of polysulfide ions in aqueous solution at 20 ºC, *Inorg. Chem.* **1972**, *11*, 1201-1207.
21. A. Kamyshny, A. Goifman, J. Gun, D. Rizkov, O. Lev, Equilibrium distribution of polysulfide ions in aqueous solutions at 25 °C: A new approach for the study of polysulfides' equilibria, *Environ. Sci. Technol.* **2004**, *38*, 6633-6644.

22. R. H. Arntson, F. W. Dickson, G. Tunell, Saturation curves of orthorhombic sulfur in the system S-Na_2S-H_2O at 25 °C and 50 °C, *Science* **1958**, *128*, 716-718.
23. A. Teder, The equilibrium between elementary sulfur and aqueous polysulfide ions, *Acta Chem. Scan.* **1971**, *25*, 1722-1728.
24. A. Teder, Spectrophotometric determination of polysulphide excess sulfur in aqueous solutions, *Svensk Papperst.* **1967**, *6*, 197-200.
25. L. G. Danielsson, X. S. Chai, M. Behm, L. Renberg, UV characterization of sulphide-polysulphide solutions and its application for process monitoring in the electrochemical production of polysulphides, *J. Pulp Paper Sci.* **1996**, *22*, J187-J191.
26. T. F. Rozan, S. M. Theberge, G. W. Luther III, Quantifying elemental sulfur (S^0), bisulfide (HS^-) and polysulfides (S_x^{2-}) using a voltammetric method, *Anal. Chim. Acta* **2000**, *415*, 175-184.
27. D. C. Brune, Isolation and characterization of sulfur globule proteins from *Chromatium vinosum* and *Thiocapsa roseopersicina*, *Arch. Microbiol.* **1995**, *163*, 391-399.
28. A. J. H. Janssen, Demonstration of the Shell-Paques process for high pressure natural gas desulfurization at BEB Erdgas und Erdöl GmbH. In *Reprints of the sulphur 98 conference* [CD-ROM], Tucson, AZ, **1998**, pp. 55-62.
29. R. Steudel, G. Holdt, R. Nagorka, On the autoxidation of aqueous sodium polysulfide, *Z. Naturforsch. B* **1986**, *41*, 1519-1522.

Chapter 2

Biologically produced sulfur*

Abstract

Sulfur compound oxidizing bacteria produce elemental sulfur as an intermediate in the oxidation of hydrogen sulfide to sulfate. Sulfur produced by these microorganisms can be stored in sulfur globules, located either inside or outside the cell. Excreted sulfur globules are colloidal particles which are stabilized against aggregation by electrostatic repulsion or steric stabilization. The formed elemental sulfur has some distinctly different properties as compared to "normal" inorganic sulfur. The density of the particles is for instance lower than the density of orthorhombic sulfur, and the biologically produced sulfur particles have hydrophilic properties whereas orthorhombic sulfur is known to be hydrophobic. The nature of the sulfur and the surface properties of the globules are different for sulfur produced by different bacteria. For example, the globules produced by phototrophic bacteria appear to consist of long sulfur chains terminated with organic groups, whereas chemotrophic bacteria produce globules consisting of sulfur rings (S_8). Adsorbed organic polymers, such as proteins, provide hydrophilic properties to sulfur produced by a mixed culture of *Thiobacilli*. The hydrophilicity of extracellularly stored sulfur globules produced by *Acidithiobacillus ferrooxidans* can probably be explained by the vesicle structure consisting mainly of polythionates ($^{-}O_3S–S_n–SO_3^{-}$). Sulfur compound oxidizing bacteria, especially *Thiobacilli*, can be applied in biotechnological sulfide oxidation installations for the removal of hydrogen sulfide from gas streams and the subsequent oxidation of sulfide to sulfur. Due to the small particle size and the hydrophilic surface, biologically produced sulfur has advantages over sulfur flower in bioleaching and fertilizer applications.

Key words

Sulfur bacteria, colloidal stability, sulfur globules, hydrogen sulfide, biotechnology

* Published in slightly modified form as: W.E. Kleinjan, A. de Keizer, A.J.H. Janssen, Biologically produced sulfur, *Top. Curr. Chem.* **2003**, *230*, 167–188.

2.1. Introduction

2.1.1. Biological sulfur cycle

Biologically produced sulfur (often termed biosulfur, elemental sulfur, or S^0) is a form of sulfur of oxidation state zero that is produced by microorganisms. At the end of the 19th century, first reports on the formation and the identification of sulfur globules were published with *Beggiatoa* bacteria fed with a solution containing hydrogen sulfide (ref. in [1]). Since then, a large variety of bacteria that are capable of sulfur formation have been reported [2-4]. The sulfur formed by these bacteria is an intermediate in the oxidation of sulfide or thiosulfate to sulfate and the bacteria are called sulfur compound oxidizing bacteria (SOB), sulfide-oxidizing bacteria, or just sulfur bacteria. In Figure 2.1 the role of these sulfur compound oxidizing bacteria in the biological sulfur cycle is pointed out.

The biological sulfur cycle consists of a continuous oxidation and reduction of sulfur compounds by microorganisms or plants. On the left-hand side of the cycle in Figure 2.1 the most reduced sulfur compound is shown (sulfide) and on the right hand side the most oxidized form of sulfur (sulfate).

Sulfur compound oxidizing bacteria cover the oxidation of sulfide to sulfate, with reduced sulfur compounds such as sulfur, thiosulfate, and tetrathionate as intermediates. It should be noted that there is a large variety in sulfur compound oxidizing bacteria of which some species are only capable of covering a specific step in the oxidation of sulfide to sulfate (e.g., oxidation of thiosulfate to sulfate). Also the pathways in which the oxidation takes place may vary so that not always the same intermediates are formed. The reduction of sulfate back to sulfide takes place in two

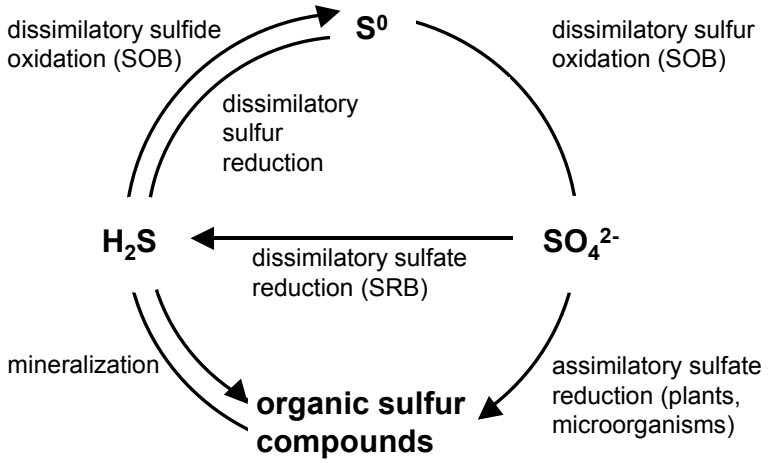

Figure 2.1. The biological sulfur cycle. SOB: sulfur compound oxidizing bacteria; SRB: sulfate-reducing bacteria.

ways. In the first way, sulfate-reducing bacteria (SRB) reduce sulfate via dissimilatory reduction (inorganic compounds reduced to other inorganic compounds). Secondly, inorganic sulfur compounds can be incorporated into organic substrates, such as proteins, by plants or microorganisms (assimilatory reduction). Sulfide is then formed by mineralization of the organic matter.
In natural ecosystems the sulfur cycle should be in balance, meaning that the amount of sulfide that is oxidized should correspond to the amount of sulfate that is reduced. Such a balance can be found in a 'sulfuretum'. This is a syntrophical community of bacteria in which H_2S produced by sulfate reducing bacteria is reoxidized by the sulfur compound oxidizing bacteria.

2.1.2. Sulfur compound oxidizing bacteria

Sulfur compound oxidizing bacteria were often called 'sulfur bacteria', which was used to indicate autolithotrophic (using inorganic compounds to obtain carbon and hydrogen) sulfur compound oxidizing bacteria. These sulfur bacteria consisted of phototrophic (purple and green) and chemotrophic (colorless) bacteria. A number of sulfur bacteria were, however, found to be able to grow organoheterotrophically (using organic compounds as their carbon and hydrogen source) and other bacteria than the sulfur bacteria were found to be able to grow autotrophically. The term 'sulfur bacteria' is therefore not used, but 'sulfur compound oxidizing bacteria' or 'sulfide-oxidizing bacteria' is used instead.

Table 2.1. Properties of some sulfur compound oxidizing bacteria.

Organism	Energy	Carbon source	Sulfur globules	pH of growth	Ref.
Chlorobiaceae	phototrophic	autotrophic	extracellular		[3]
β-Proteobacteria					
Thiobacillus thioparus	chemotrophic	autotrophic	extracellular	6–8	[5]
Thiobacillus denitrificans	chemotrophic	autotrophic	extracellular	6–8	[5]
Thiobacillus sp. W5	chemotrophic	autotrophic	extracellular	7–9	[6]
γ-Proteobacteria					
Allochromatium vinosum[1]	phototrophic	mixotrophic	intracellular	7.5	[3, 7]
Halorhodospira abdelmalekii[2]	phototrophic	mixotrophic	extracellular	8.4	[3, 8]
Beggiatoa alba	chemotrophic	mixotrophic	intracellular		[4, 9]
Acidithiobacillus thiooxidans[3]	chemotrophic	autotrophic	extracellular	2–5	[5]
Acidithiobacillus ferrooxidans[3]	chemotrophic	mixotrophic	extracellular	2–6	[5]
Thioalkalivibrio denitrificans	chemotrophic	autotrophic	extracellular	7.5–10.5	[10]
Thioalkalimicrobium cyclicum	chemotrophic	autotrophic	extracellular	7.5–10.5	[11]
Xanthomonas	chemotrophic	heterotrophic		7	[12]
Cyanobacteria					
Oscillatoria limnetica	phototrophic	autotrophic	extracellular	6.8	[13]

[1] *Allochromatium vinosum* was formerly known as *Chromatium vinosum* [14].

[2] *Halorhodospira abdelmalekii* was formerly known as *Ectothiorhodospira abdelmalekii* [15].

[3] *Acidithiobacillus thiooxidans* and *Acidithiobacillus ferrooxidans* were formerly known as *Thiobacillus thiooxidans* and *Thiobacillus ferrooxidans* [16].

There is a wide variety of sulfur compound oxidizing bacteria, consisting of different groups and genera. Each of the bacteria has its own specific properties, such as the source of energy, carbon, or hydrogen, the sulfide-oxidizing pathway, the size and shape of the bacteria, and the location of storing intermediate sulfur. In Table 2.1 a number of sulfur compound oxidizing bacteria are listed with some of their distinctive properties. Classification of sulfur compound oxidizing bacteria is however not straightforward. Different bacteria of the same bacterial family can have different properties. Each family consists of a wide variety of genera and strains, which can differ substantially in sulfur- oxidizing capacities or other properties. Therefore, the data in Table 2.1 should be seen only as a list of properties of some sulfur compound oxidizing bacteria.

Most important in the classification of sulfur bacteria is the distinction between phototrophic and chemotrophic sulfur bacteria. Phototrophic (purple or green) bacteria use light as energy source to reduce CO_2 to carbohydrates. Reduced sulfur compounds are used as an electron donor for this reduction, which takes place under anaerobic conditions. The oxidation reactions of sulfide to sulfur and sulfate by phototrophic bacteria are called the Van Niel reactions

$$2\ H_2S + CO_2 \xrightarrow{\text{light}} \{CH_2O\} + H_2O + 2\ S^0 \tag{2.1}$$

$$H_2S + 2\ CO_2 + 2\ H_2O \xrightarrow{\text{light}} 2\ \{CH_2O\} + H_2SO_4 \tag{2.2}$$

The first Van Niel reaction (Eq. 2.1) has a strong parallel with the photosynthesis in plants [3]

$$2\ H_2O + CO_2 \xrightarrow{\text{light}} \{CH_2O\} + H_2O + O_2 \tag{2.3}$$

In fact, cyanobacteria are capable of both ways of photosynthesis, which is why it was found difficult to place them in the group of plants (prokaryotes) or bacteria (eukaryotes) [13].

The chemotrophic (colorless) sulfur bacteria obtain energy from the chemical aerobic oxidation of reduced sulfur compounds. Concerning the oxidation of sulfide, the overall reactions occurring are the formation of sulfur (at low oxygen concentrations) and the formation of sulfate (when there is an excess of oxygen)

$$2\ H_2S + O_2 \rightarrow 2\ S^0 + 2\ H_2O \tag{2.4}$$

$$H_2S + 2\ O_2 \rightarrow H_2SO_4 \tag{2.5}$$

Apart from the above mentioned sulfide oxidation reactions, other sulfur compounds, such as sulfur and thiosulfate, can be oxidized by sulfur compound oxidizers. Furthermore, nitrate can be used as oxidant instead of oxygen. In Table 2.2 a list is shown of some other sulfur compound oxidation reactions occurring in chemotrophic

sulfur compound oxidizing bacteria. It should be noted that not all sulfur compound oxidizing bacteria are capable of all the reactions listed in this table.

With respect to the carbon source, the sulfur compound oxidizing bacteria can be classified as heterotrophs, autotrophs, or mixotrophs. Autotrophic bacteria use CO_2 as the major carbon source for production of organic molecules. Heterotrophic bacteria use organic material as carbon source. Obligate autotrophs strictly need CO_2 as carbon source and facultative autotrophs (or mixotrophs) can also grow heterotrophically. Heterotrophic sulfur compound oxidizing microorganisms need a nutrient feed containing organic substrates (e.g., meat or yeast extracts [12]).

Sulfur compound oxidizing bacteria can also be classified according to the nature of the hydrogen source. Lithotrophic bacteria use inorganic substrates (e.g., NH_3, H_2S) as a source for hydrogen atoms. Organotrophic bacteria obtain hydrogen from organic molecules. In most organisms lithotrophy is linked to autotrophy, which means that for instance obligate autotrophic *Thiobacillus* bacteria are also called chemolithotrophic.

Elemental sulfur is often observed as an intermediate product in the oxidation of sulfide to sulfate in sulfur compound oxidizing bacteria. It can be present in considerable concentrations but will eventually be further oxidized to sulfate. The elemental sulfur is stored in sulfur globules, which some bacteria deposit inside the cell membrane and others outside the cell membrane. In section 2.3 the properties of these sulfur globules are discussed.

The optimum pH of growth of the bacteria differs per species. Neutral and acidiphilic sulfur compound oxidizing bacteria have been long known, mostly isolated from marine or freshwater sediments (e.g., [2, 5]). From highly alkaline salt lakes a number of alkaliphilic sulfur compound oxidizing bacteria have been isolated, both phototrophic [8] and chemotrophic [10, 17]. In section 2.4 the technological relevance of alkaliphilic sulfur compound oxidizers is discussed.

Table 2.2. Overall reactions occurring in sulfur compound oxidizing bacteria (after [5]).

Overall reactions	
$S^0 + \frac{3}{2} O_2 + H_2O \rightarrow H_2SO_4$	(2.6)
$S_2O_3^{2-} + 2\ O_2 + H_2O \rightarrow H_2SO_4 + SO_4^{2-}$	(2.7)
$S_2O_3^{2-} + \frac{1}{4} O_2 + \frac{1}{2} H_2O \rightarrow \frac{1}{2} S_4O_6^{2-} + OH^-$	(2.8)
$2\ S_4O_6^{2-} + 7\ O_2 + 6\ H_2O \rightarrow 6\ H_2SO_4 + 2\ SO_4^{2-}$	(2.9)
$5\ H_2S + 2\ HNO_3 \rightarrow 5\ S^0 + N_2 + 6\ H_2O$	(2.10)
$5\ H_2S + 8\ HNO_3 \rightarrow 5\ H_2SO_4 + 4\ N_2 + 4\ H_2O$	(2.11)

2.2. Colloidal stability of sulfur particles

Sulfur particles formed by sulfur compound oxidizing bacteria have particle sizes that fall in the range of the colloidal domain (approximately up to 1.0 μm). The internally stored sulfur particles produced by four different chemotrophic *Beggiatoas* as well as by a phototrophic *Allochromatium* bacterium have a particle diameter around 250 nm (both observed with electron microscopy) [18, 19] but the diameter of internally stored sulfur globules can reach up to 1 μm. Extracellularly stored sulfur globules produced by *Thiobacillus* bacteria in a sulfide-oxidizing reactor initially have approximately the same diameter (observed with electron microscopy and size distribution measured with Single Particle Optical Sizing) [20].

The balance between attractive and repulsive forces governs stability of colloidal sulfur particles. The most important forces are the Van der Waals attraction and electrostatic repulsion, on which the DLVO-theory of colloidal stability is based. The attractive Van der Waals force depends on the size of and the distance between two bodies.

The repulsive electrostatic force originates from the surface charge of the colloidal particles. Apart from this, structural forces (e.g., hydrogen bonding) can stabilize or destabilize colloidal particles depending on the nature of the particles, and adsorption of polymer material at the sulfur-solvent interface can cause steric stabilization.

The origin of charge can be the presence of surface functional groups, such as carboxylic acid or amino groups. Surfaces on which proteins are adsorbed show a dependency of the surface charge on the pH value due to the presence of carboxylic acid and amino groups. At high pH a protein-covered surface will be negatively charged ($-COO^-$ and $-NH_2$ groups) and at low pH the surface will show an overall

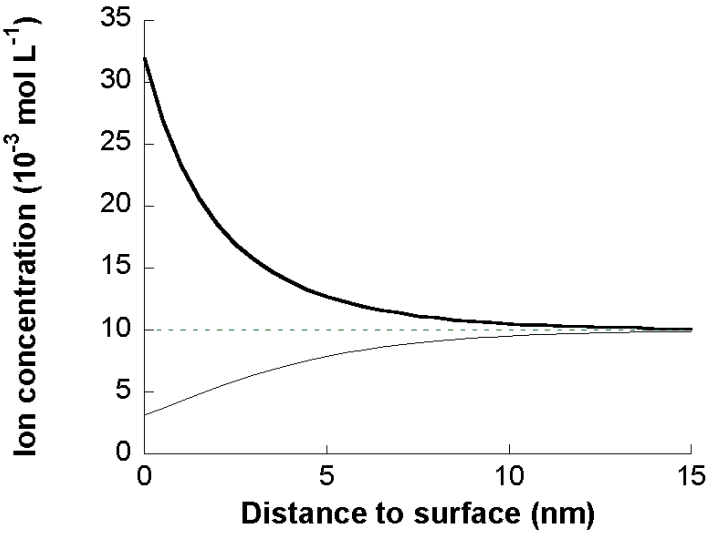

Figure 2.2. Concentration profile of positive (▬) and negative (—) ions in a diffuse electrical double layer near a negatively charged surface. [NaCl] = 0.01 mol L^{-1}.

positive charge (–COOH and $–NH_3^+$ groups). The pH at which the overall surface charge is zero is called the point of zero charge. In the absence of specific adsorption it coincides with the isoelectric point.

This surface charge attracts oppositely charged ions to the surface and equally charged ions are repelled from the surface. This results in an ion concentration profile as is represented in Figure 2.2, which is called the diffuse electrical double layer. Presence of salt causes a screening of the electrical double layer.

The repulsive and attractive energies of two interfaces can be calculated as a function of their distance (Figure 2.3). When salt is added to a colloidal solution the electrostatic repulsion can be screened, resulting in a destabilization of the colloids.

Long chain polymers, such as proteins, can often adsorb to the surface of colloidal particles (because they gain adsorption energy), which can have a significant influence on colloidal stability. Adsorption of polymeric material at an interface takes place in such a way that the chains can extend from the surface into the solution and can rearrange their position and orientation. The effect of polymer adsorption can be both attractive and repulsive but in most cases the effect is repulsive.

Stabilization of colloidal particles by adsorption of an uncharged polymer is called steric stabilization. The two main contributions to this influence are a volume restriction effect and an osmotic effect. The volume restriction effect is caused by the loss of configurational entropy if the adsorbed polymer chain is compressed (less possible configurations of the flexible part of the polymer). The osmotic effect is caused by the increase in osmotic pressure between two particles if the polymer layers of two particles overlap. This effect depends on the quality of the solvent. In a good solvent polymer segments favor contact with the solvent over contact with other

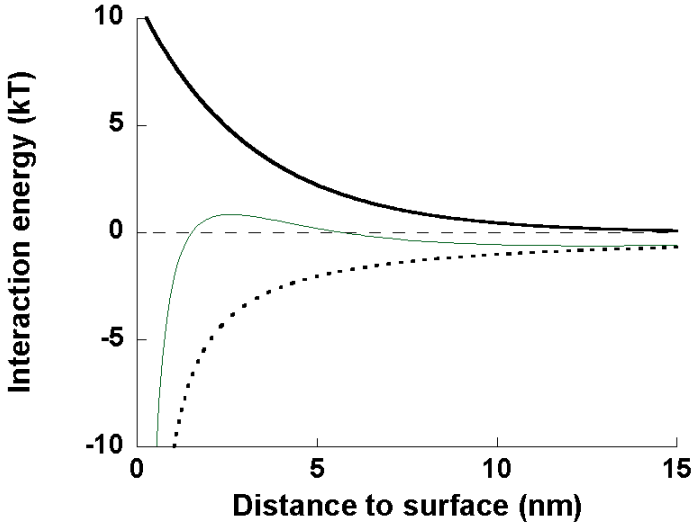

Figure 2.3. Electrostatic repulsive (▬), van der Waals attractive (• • •) and total (—) interaction energies of two approaching spherical particles. Particle radius, r = 100 nm; Stern potential, Ψ_d = 10 mV; Hamaker constant, $A = 0.5 \times 10^{-20}$ J.

polymer segments resulting in repulsion. In a poor solvent, polymer segments favor contact with other polymer segments over contact with the solvent.
Apart from polymer adsorption for uncharged macromolecules, charged macromolecules (polyelectrolytes), such as proteins, can also adsorb at surfaces [21, 22]. Adsorption of a charged macromolecule is different from adsorption of an uncharged polymer in that there is a high dependency on the salt concentration. At a low salt concentration, repulsive electrostatic forces between charged polymer chains will inhibit formation of loops and tails (Figure 2.4). This has been predicted and confirmed, for instance for adsorption of humic acids on iron-oxide particles [23].

2.3. Properties of biologically produced sulfur

In the last 30 years a significant amount of research has been done on sulfur globules that are stored intracellularly (especially sulfur globules of *Al. vinosum* and *Beggiatoa alba*) and that are excreted outside the cell membrane (especially *Thiobacillus* sp.). This section is about the physicochemical properties of those biologically produced sulfur globules stored intracellularly and extracellularly.
Research by Vetter [24] on externally excreted sulfur globules suggested that sulfur is stored as an energy reservoir rather than as a way of detoxification of excess hydrogen sulfide. As long as dissolved sulfide is available, sulfur is stored in globules. When sulfide is depleted, the stored sulfur is oxidized.
The identification of the nature of elemental sulfur in globules produced by sulfur compound oxidizing bacteria is not straightforward. Several studies have been performed with several different techniques but unfortunately the interpretation of the results sometimes seems to be contradictory. Although several studies propose models for the nature of sulfur globules produced by all sulfur compound oxidizing bacteria [25-27] it is safer to distinguish between sulfur globules produced by different bacteria because there are indications that not all sulfur globules are comparable [28, 29]. To give a clear overview of what is known about the nature of sulfur in globules, studies on sulfur globules from each organism are discussed separately.

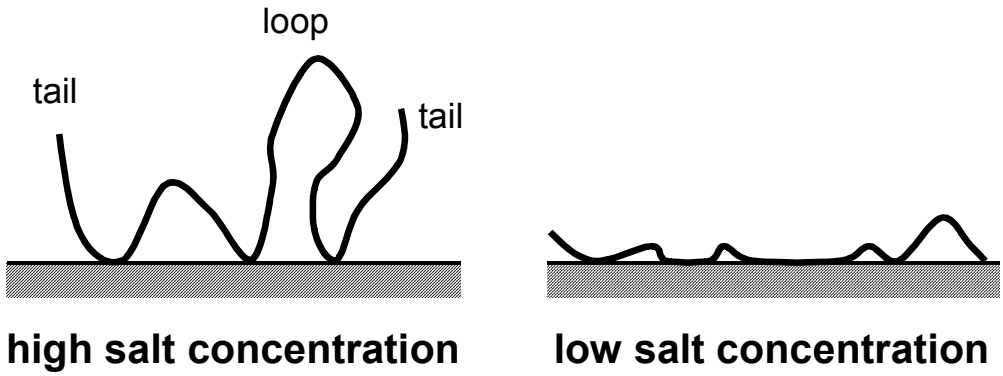

Figure 2.4. The effect of salt concentration on the adsorption of charged polymers at a surface.

2.3.1. Intracellularly stored sulfur

Several sulfide-oxidizing bacteria contain globules inside the cell membrane. The globules are membrane-limited and extracytoplasmic [18, 30]. In this way these globules could also be called extracellular, however, we will call them intracellular because the globules are stored within the cell membrane.

In 1887 Winogradsky already stated that living cells would contain globules of amorphous sulfur while in dead cells the sulfur would crystallize (ref. in [1]). X-ray diffraction (XRD) on intracellularly produced sulfur globules (among which *Allochromatium* sp.) has shown a difference between the isolated sulfur structure of fresh globules in the wet-state and the dried sulfur globules. The XRD pattern for fresh globules resembled the pattern of liquid sulfur whereas the pattern for dried globules and globules that were kept in a wet-state for several days, resembled the pattern of crystalline orthorhombic sulfur [1, 31]. This indicated that the structure of fresh sulfur globules is not crystalline orthorhombic sulfur, but rather a liquid or amorphous form of sulfur, which converts into crystalline orthorhombic sulfur on drying or aging. After this, it was shown that the density of the sulfur globules produced by two *Allochromatium* species is 1.31 g cm^{-3} [32, 33]. This is considerably lower than the density of liquid sulfur (1.89 g cm^{-3}) or that of any form of crystalline sulfur (1.9–2.2 g cm^{-3}) [34], indicating that the globules did not consist of pure liquid sulfur either. The suggestion was made that sulfur globules consist of sulfur and an unidentified moiety, which is probably water. In a model proposed by Steudel *et al*. [35] the globules consist of a nucleus of sulfur rings (S_8) with water around it and long-chain sulfur compounds such as polysulfides or polythionates as amphiphilic compounds at the interface. Polythionate chains were, however, not detected in cultures of *Al. vinosum* storing sulfur globules inside the bacterial cell, thereby limiting the possible amphiphilic compound in the model to long-chain polysulfides or sulfanemonosulfonates [33]. Polythionates in sulfur globules of *Al. vinosum* were also not detected by Prange *et al*. who used X-ray absorption near-edge spectroscopy (XANES) [28]. Moreover, they ruled out the presence of sulfur rings and found the globules to consist of long sulfur chains terminated by organic groups (R–S_n–R), indicating the inapplicability of Steudel's model of a core of sulfur rings surrounded with water and polythionates or polysulfides for *Al. vinosum* sulfur globules. Some controversy has however arisen around these XANES measurements since Pickering *et al*. [26] claimed that the experimental results were misinterpreted due to artifacts and that sulfur globules of *Al. vinosum* consisted of 'simple, solid sulfur'. The discussion around this topic focuses on the measurement mode, with each mode having its own problem (electron yield mode with a sample charging effect; fluorescence mode with a self-absorption effect; transmittance mode with a 'pinhole' effect) [36, 37]. However, the model for sulfur globules of *Al. vinosum* that corresponds best with the available experimental data consists of long sulfur chains

terminated by organic groups as was suggested by Prange *et al*. This can account for the observed low density and does not need to assume that the observed density is erroneously low.

XANES seems to be a useful technique because it can give information on the structure of sulfur globules *in situ*. Prange *et al*. showed that isolation of sulfur globules from the bacteria affects the structure of the sulfur [29], thereby limiting the value of studies with experimental techniques which do require isolation of the sulfur globules (e.g., XRD). There are however also certain limitations of the technique concerning interpretation of the data and availability of reference compounds, such as long chain organic sulfur compounds.

The sulfur globules of the chemotrophic bacteria *B. alba* have also been studied quite extensively. The density of the globules has not been determined but energy-dispersive X-ray microanalysis showed that the globules consisted almost entirely of sulfur [9]. XANES [29] and Raman spectroscopy [27] confirmed that the sulfur globules of *B. alba* consist of S_8 sulfur rings.

Apart from the nature of the sulfur in the globules, the surface of these globules has been studied as well. Studies on sulfur globules produced by *Al. vinosum* showed that the sulfur particle is bounded by a protein membrane, which appears to be sulfur-free [7, 19]. The proteins of the membrane were isolated by extraction and separated by reversed-phase HPLC, revealing three major proteins [38]. Proteins associated with sulfur globules of *Thiocapsa roseopersicina* appeared to correspond to the proteins on the sulfur globules of *Al. vinosum*. Later research was able to locate the genes responsible for the production of these proteins and it was concluded that sulfur globules in *Al. vinosum* are extracytoplasmic due to the presence of this protein cell membrane [28]. Such a cell membrane was also found for sulfur globules in *B. alba*, where it was called sulfur inclusion envelope [18]. The exact function of the protein is still not clear. Because of the similarity to proteins such as keratin or plant cell wall proteins, it has been suggested that the proteins have a structural rather than an enzymatic function [30]. The proteins might also prevent the crystallization of the sulfur in the globule [39].

2.3.2. Extracellularly stored sulfur

Sulfur globules produced by bacteria excreting the globules outside the cell membrane have also been studied. Especially for biotechnological applications these sulfur compound oxidizing bacteria are interesting because they allow an easy separation of the sulfur from the bacteria. In Figure 2.5 sulfur globules can be seen which have been excreted by a *Thiobacillus* bacterium.

Steudel *et al*. proposed a number of models for the composition of bacterial sulfur globules in which they did not always distinguish between intracellularly and extracellularly stored sulfur. In a model proposed for sulfur globules excreted by

Acidithiobacillus ferrooxidans [40] the globules consist of a sulfur nucleus (mainly S_8 rings and small amounts of other sulfur rings) and long-chain polythionates present on the surface. Indeed, HPLC [40] and XANES [29] analysis showed the presence of polythionates in the cultures of *Ac. ferrooxidans* excreting sulfur globules. XANES analysis did, however, also show that S_8 rings were not present. Another model proposed by Steudel [25] consists of vesicles composed of a polythionate membrane. The inside of the vesicle may contain water, and sulfur rings are only present in low concentrations in the membrane part of the vesicle (see Figure 2.6). This model is in accordance with the observed experimental data obtained by XANES analysis and therefore seems suitable for globules produced by *Ac. ferrooxidans*.

It should be noted that polythionates are only stable at low pH [34] and it is therefore unlikely that the polythionate vesicle model is applicable to sulfur globules produced by bacteria growing at another pH than the acidic conditions at which *Ac. ferrooxidans* grows [5].

Janssen *et al*. have studied the properties of sulfur produced by bacteria of the genus *Thiobacillus* grown at neutral to alkaline pH [20, 41]. The sulfur was produced in a bioreactor in which a mixed culture of *Thiobacilli* was present.

X-ray diffraction of sulfur particles excreted by *Thiobacillus* sp. showed the presence of orthorhombic sulfur crystals. The solubility of crystalline orthorhombic sulfur in

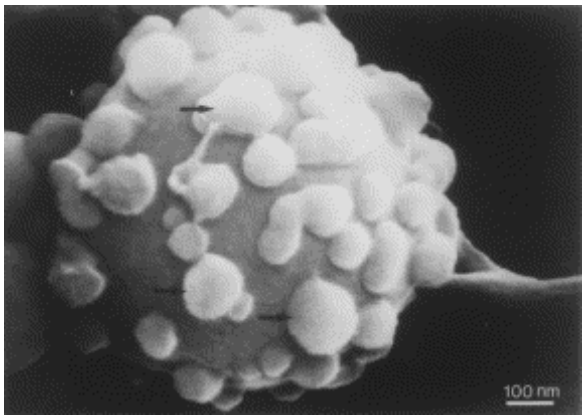

Figure 2.5. Scanning electron micrograph of sulfur excreting *Thiobacillus* [42].

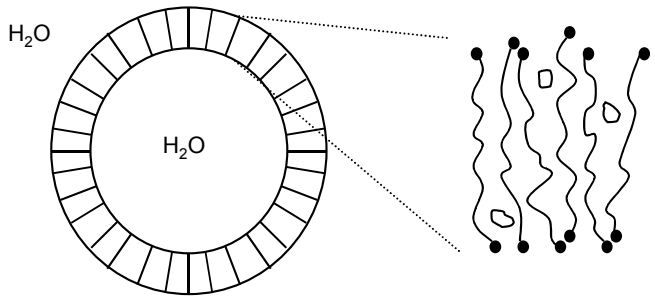

Figure 2.6. Vesicle model proposed by Steudel for sulfur globules excreted by *Ac. ferrooxidans*. Vesicles are composed of long chain polythionates ($^{-}O_3S{-}S_n{-}SO_3^{-}$) in which small amounts of sulfur rings can be present (after [25]).

water is known to be only 5 μg L^{-1} [43]. In the solubility test shown in Figure 2.7 it was seen that the biologically produced sulfur particles can be dispersed in water but not in hexadecane, whereas crystalline orthorhombic sulfur is soluble in hexadecane but not in water. The reason for the observed hydrophilicity of the biologically produced sulfur particles has to be attributed to the hydrophilic properties of the surface of the sulfur particles. Because of the relatively high stability of the biologically produced sulfur particles at high salt concentrations, it is concluded that the colloidal stability is not merely based on electrostatic repulsion. It is known that hydrophobic sulfur can be wetted by *Thiobacillus thiooxidans* bacteria due to formation of organic surface-active substances [44, 45].

It was concluded that the particles are stabilized by long chain polymers, most probably proteins. Indeed, measurements with dynamic light scattering showed a relatively high variation of the determined hydrodynamic radius with changing salt concentration, indicating the presence of relatively thick adsorbed layers on the sulfur particles (see Figure 2.4). This, as well as surface charge density measurements showing values comparable to surface charge densities of bacterial cell walls and humic acids, supports the suggestion of proteins adsorbed on the particles. In addition, electrophoretic mobility experiments showed an isoelectric point comparable to the pK_a value of carboxylic acid groups in proteins (pK_a = 2.3) [46].

As stated above, the presence of proteins on the surface of sulfur globules stored intracellularly has been demonstrated [7, 38]. These well-defined proteins act as a membrane between the cytoplasm and the intracellular sulfur particle. It is not known whether the proteins associated with the sulfur particles excreted by *Thiobacillus* bacteria are well-defined proteins synthesized by the bacterium or if they are originating from organic compounds already present in the liquid reactor system.

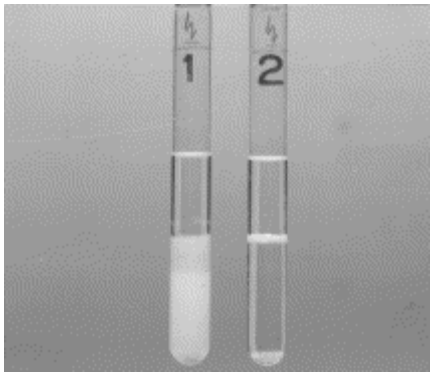

Figure 2.7. Hexadecane-water partition test. Biologically produced sulfur remains in the lower water phase (1) whereas crystalline sulfur remains in the upper hexadecane-phase (2) [42].

2.3.3. Formation of biologically produced sulfur

Biologically produced sulfur is often written as 'S^0', which only indicates that a large part of the sulfur in the sulfur globules is present in oxidation state zero. It should not be mistaken for atomic sulfur, which has a very high enthalpy of formation and therefore cannot exist at ambient temperature [34]. In the previous sections it has been shown that the sulfur in globules can be present as sulfur rings, long-chain polythionates, and long sulfur chains terminated by organic groups. The mechanisms in which these forms of sulfur are formed are not known but the formation of sulfur rings is assumed to proceed through the formation of polysulfides [38].
Steudel [39] proposed a reaction mechanism for the chemical oxidation of sulfide to sulfur rings (S_8), which should take place in a similar way in sulfur compound oxidizing bacteria. In this mechanism HS^- anions are oxidized forming sulfide radicals ($HS^\bullet$ or $S^{\bullet-}$)

$$HS^- \rightarrow HS^\bullet + e^- \quad (2.12)$$

$$HS^\bullet \rightarrow S^{\bullet-} + H^+ \quad (2.13)$$

These radicals are the basis for a complex sequence of reactions involving radicalization of ions and dimerization of radical ions, resulting in polysulfide anions (S_x^{2-}), e.g.,

$$2\ S^{\bullet-} \rightarrow S_2^{2-} \quad (2.14)$$

$$S_2^{2-} + S^{\bullet-} \rightarrow S_3^{\bullet-} \quad (2.15)$$

$$S_3^{\bullet-} + S^{\bullet-} \rightarrow S_4^{2-} \quad (2.16)$$

$$2\ S_3^{\bullet-} \rightarrow S_6^{2-} \quad (2.17)$$

Etc.

Upon acidification of long chain polysulfide anions, elemental sulfur rings are formed.

$$S_9^{2-} + H^+ \rightarrow HS^- + S_8 \quad (2.18)$$

In chemical oxidation reactions, the first oxidation step (forming of sulfide radicals) is catalyzed by metal ions like V^{5+}, Fe^{3+}, and Cu^{2+}. In most sulfur compound oxidizing bacteria, the first step in the oxidation of sulfide to sulfur is catalyzed by the enzyme flavocytochrome c [3]. In a number of bacteria with the capacity to oxidize sulfide to sulfur, flavocytochrome c has not been found and other cytochromes or quinones are believed to catalyze the oxidation of sulfide in these organisms.

Brune [3] has suggested that the location of the catalyst for the acidification of polysulfide anions to elemental sulfur determines whether sulfur is stored extracellularly or intracellularly. Van Gemerden, however, suggested that the location of the electron acceptor in the HS^- oxidation step determines whether sulfur is stored extracellularly or intracellularly [47], as is explained in Figure 2.8. This is supported by research of Then and Trüper [8] on sulfide oxidation in *Halorhodospira abdelmalekii*, excreting sulfur globules extracellularly. They showed the cytochrome c-551 to have a catalytic effect on the oxidation of sulfide and to be located on the outside of the cell membrane. In *Al. vinosum* cytochrome c-551 is located in the periplasmic space, the space between the outer cell wall and the cytoplasmic membrane, which is also the location of storage of sulfur globules [48].

2.4. Sulfur compound oxidizing bacteria in industrial applications

2.4.1. Removal of hydrogen sulfide from gas streams

A number of environmental problems are strongly related to the emission of sulfur compounds, such as SO_2, in the atmosphere. SO_2 emission is mainly due to combustion of fossil fuels containing H_2S or organic S-compounds. In the atmosphere, SO_2 is oxidized forming sulfuric acid resulting in acid rain. Fortunately, the emission of SO_2 has decreased considerably since the 1970s due to selection of low sulfur-content fuels, waste gas treatment and specialized combustion processes.
In order to prevent SO_2 emission, H_2S has to be removed from gas streams prior to combustion. Apart from environmental reasons, removal of H_2S from waste gas streams is also required for health reasons (H_2S is a toxic gas, lethal at concentrations exceeding 600 ppm) and to prevent corrosion of equipment. Gases that can contain H_2S and need treatment are, for instance, natural gas, syngas, and biogas (formed in anaerobic wastewater treatment).

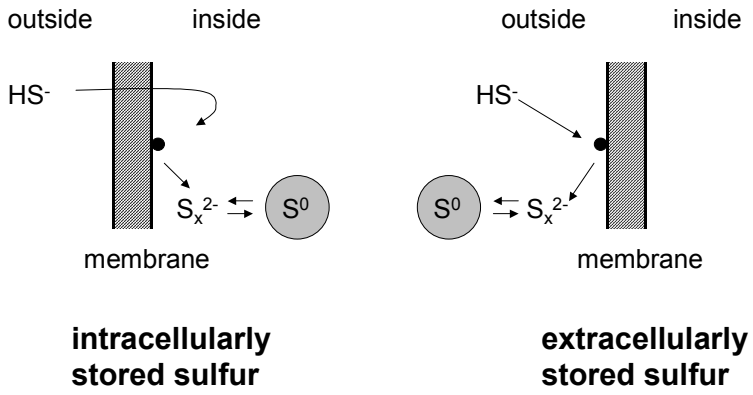

Figure 2.8. Model for the deposition of sulfur inside or outside the cells in which the position of the electron acceptor on the membrane (●) determines the location of sulfur storage (after [47]).

Removal of H_2S from gas streams is generally done in two steps. In the first step, H_2S is separated from the gas stream and in the second step, the removed H_2S (dissolved in liquid or as concentrated gas) is converted into elemental sulfur. Several processes exist that purify gases according to these two steps.
The method most commonly used is based on absorption of H_2S in an amine solution and the subsequent stripping of the dissolved H_2S from this solution forming a concentrated gas ('Claus gas') which is then converted into elemental sulfur in the Claus process. In the Claus process, a third of the H_2S gas is first burned to SO_2 after which the remaining H_2S reacts with the formed SO_2 to elemental sulfur.

$$H_2S + \tfrac{1}{2}O_2 \rightarrow \tfrac{2}{3}H_2S + \tfrac{1}{3}SO_2 + \tfrac{1}{3}H_2O \qquad (2.19)$$

$$\tfrac{2}{3}H_2S + \tfrac{1}{3}SO_2 \rightleftarrows S^0 + \tfrac{2}{3}H_2O \qquad (2.20)$$

$$H_2S + \tfrac{1}{2}O_2 \rightleftarrows S^0 + H_2O \qquad (2.21)$$

In other methods H_2S is absorbed in a solution after which the dissolved H_2S is converted to elemental sulfur without stripping the gas from the solution. Differences between different methods basically consist of a different absorption solution or a different oxidation catalyst. Disadvantages of physicochemical processes are generally the high operational costs due to high pressures and high temperatures and the need of special chemicals (catalysts).

2.4.2. Biotechnological removal of hydrogen sulfide from gas streams

To overcome the disadvantages of physicochemical processes for H_2S removal, the use of microorganisms can be an interesting alternative. Several microorganisms are capable of the oxidation of H_2S at ambient temperatures and pressures, and both phototrophic and chemotrophic organisms have been studied for their industrial application. The phototrophic sulfur oxidizing bacteria *Chlorobium limicola* forma *thiosulfatophilum* has been studied [49, 50] but phototrophic bacteria have the disadvantage of the requirement of light and therefore the need of a transparent reactor surface and reaction solutions. Of the chemotrophic bacteria, heterotrophs as well as autotrophs have been studied. The heterotrophic *Xanthomonas* bacterium has been studied for H_2S removal [12] but showed lower removal rates than other autotrophic bacteria and, in addition, heterotrophic organisms have the disadvantage of the requirement of organic compounds. Chemoautotrophic bacteria (especially *Thiobacilli*) are the types of sulfur oxidizing bacteria that have been studied and used mostly in H_2S removal processes.

The use of *Thiobacillus* species has been studied quite extensively. Sublette and Sylvester especially focused on the use of *Thiobacillus denitrificans* [51-53] for aerobic or anaerobic oxidation of sulfide to sulfate. In the anaerobic oxidation NO_3^- was used as an oxidant instead of oxygen (confer Table 2.2). Buisman *et al*. used a mixed culture of *Thiobacilli* for the aerobic oxidation of sulfide to elemental sulfur and studied technological applications [54-56]. Visser *et al*. showed the dominant organism in this mixed culture to be a new organism named *Thiobacillus* sp. W5 [6].
The production of sulfur from sulfide has some distinct advantages over the production of sulfate. First, elemental sulfur is seen as a less harmful form of sulfur than sulfate. Secondly, the separation of the insoluble sulfur from aqueous streams is easier than the separation of sulfate and thirdly less oxygen is needed for the oxidation, which saves energy costs for aeration. Furthermore, hydroxyl ions that are consumed during the absorption of H_2S (Eq. 2.25) are regenerated when sulfur is formed (Eq. 2.26). This saves in costs of adding OH^- to the system.

$$2\ H_2S + O_2 \rightarrow 2\ S^0 + 2\ H_2O \qquad (2.22)$$

$$H_2S + 2\ O_2 \rightarrow H_2SO_4 \qquad (2.23)$$

According to Kuenen, the formation of sulfate yields more energy than the formation of sulfur [2]. To stimulate formation of sulfur, the oxygen concentration should be limited [57, 58].
There are several reactor systems for the biotechnological removal of H_2S from a gas. Currently, three types of biotechnological process systems are being used; bioscrubber, biotrickling filter, and biofilter. Since in the last two processes, sulfate is produced and not elemental sulfur, it is not within the scope of this chapter to elaborate on these (see [59]). The technology of the bioscrubber is, however, relevant because it is used in practice for the production of biosulfur.
The principle of a bioscrubber system is explained in Figure 2.9. It consists of a bioscrubber or gas absorber (G) and a bioreactor (B). In the gas absorber H_2S is scrubbed from a gas stream by an alkaline solution.

$$H_2S(g) \rightarrow H_2S(aq) \qquad (2.24)$$

$$H_2S(aq) + OH^- \rightarrow HS^- + H_2O \qquad (2.25)$$

After this the dissolved hydrogen sulfide is oxidized to elemental sulfur in a bioreactor.

$$HS^- + \tfrac{1}{2}O_2 \rightarrow S^0 + OH^- \qquad (2.26)$$

The formed elemental sulfur is then separated from the liquid by sedimentation in a settler (S). Here, aggregates of sulfur are formed, which can grow to particles with a diameter of up to 3 mm but which can also be easily ground down [40].
A limitation to the alkalinity of the liquid recycle is the optimum pH of growth of the bacteria in the bioreactor. Use of alkaliphilic sulfur compound oxidizing bacteria is therefore very interesting from a technological point of view.
Apart from this, a number of side reactions take place. In the gas absorber polysulfide ions (S_x^{2-}, with $x \leq 6$) can be formed by reaction of hydrogen sulfide with sulfur.

$$HS^- + (x-1)\,S^0 \rightarrow S_x^{2-} + H^+ \qquad (2.27)$$

The sulfur particles are fed to the gas absorber by the liquid recycle due to an incomplete separation of solid sulfur in the separation step of the process. In the bioreactor, the polysulfide anions either decompose into sulfide and sulfur (Eq. 2.28), or are oxidized to thiosulfate (Eq. 2.29). Sulfate can also be formed by oxidation of HS^- (Eq. 2.30).

$$S_x^{2-} + H^+ \rightarrow HS^- + (x-1)\,S^0 \qquad (2.28)$$

$$S_x^{2-} + \tfrac{3}{2}\,O_2 \rightarrow S_2O_3^{2-} + (x-2)\,S^0 \qquad (2.29)$$

$$HS^- + 2\,O_2 \rightarrow SO_4^{2-} + H^+ \qquad (2.30)$$

In principal, oxygen from air is the only reagent needed for this process. However, due to the occurrence of sulfate and thiosulfate formation, extra sodium hydroxide has to be dosed to the bioreactor and a bleed stream is necessary to prevent accumulation

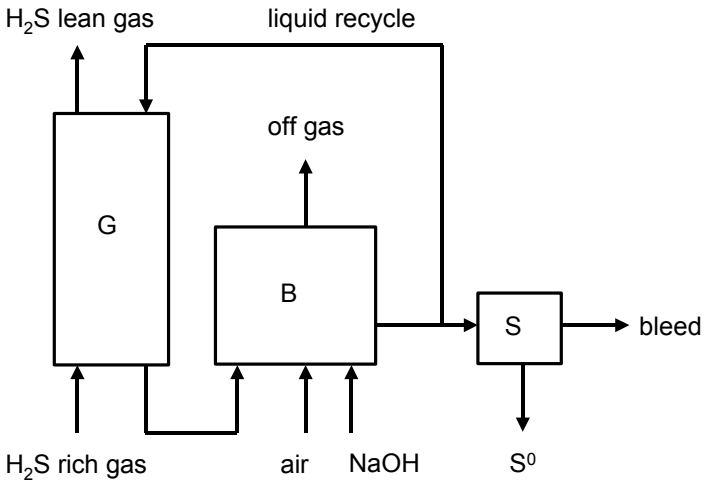

Figure 2.9. Scheme of the process for the biotechnological removal of H_2S from gas streams. G = Gas absorber; B = Bioreactor; S = Settler.

of sodium salts. The amount of NaOH that has to be added to the bioreactor can be minimized if the occurrence of (thio)sulfate formation is minimized. Previous research showed that sulfide oxidation to sulfate can be selectively prevented by applying a low oxygen concentration [57]. The oxidation of anionic polysulfides however, cannot easily be prevented by controlling of the oxygen concentration because the oxidation rate of polysulfides is higher than the oxidation rate of sulfide, as was suggested by Chen and Morris [60]. In order to determine the best way to prevent the thiosulfate formation, more should be known about the role of the polysulfide anions and their specific interaction with the biologically produced sulfur particles.

2.5. Applications of biologically produced sulfur

Sulfur produced by microorganisms in H_2S removal plants, such as described in the previous section, can be handled in a number of ways. Dried sulfur solids can be used in sulfuric acid production (99% sulfur purity needed) or the formed sulfur sludge can be directed to a 'smelter' where it is converted into high purity sulfur (>99.9%). Unfortunately, currently more sulfur is produced worldwide than is needed as pure chemical and therefore sulfur is also stored in landfill (95–98% sulfur purity needed). Although solid sulfur is considered as a non-hazardous refinery waste, landfill is an undesirable option, partly because acidification by oxidation has to be prevented.

To avoid the landfill, possible applications of the biologically produced sulfur have been investigated. In bioleaching and in agriculture, it was found that the specific properties of biologically produced sulfur (small particle size, hydrophilic surface) have clear advantages over the use of inorganic sulfur.

Bioleaching is used in mining to dissolve metals from sulfide ores. The aim of bioleaching is to achieve pH values that are low enough to solubilize a maximum of metals. In some cases additional elemental sulfur is added as substrate for bacteria [61], which oxidize the sulfur forming sulfuric acid, and thereby decrease the pH. Tichý *et al*. compared the use of sulfur flower with biologically produced sulfur, produced by sulfide oxidation of *Thiobacilli* under oxygen limitation [62]. They concluded that the hydrophilic properties of biologically produced sulfur have a

Table 2.3. Grain yield of Breton Canola for different sulfur sources.

Sulfur source	Grain yield (kg ha^{-1})
None	14.6
K_2SO_4	15.9
T90CR	17.4
S95	18.0
Claus sulfur	17.1
Biosulfur paste	22.3
Biosulfur powder	19.8

positive effect in bioleaching because they cause an increase of the rate of sulfuric acid production.

Another field in which biologically produced sulfur can be used is agriculture. Sulfur is an important nutrient for plants, which can take up sulfur by their leaves from the atmosphere as very reduced (COS, CS_2 and H_2S) up to highly oxidized compounds (SO_2). Most of the sulfur, however, is taken up by plant roots as water-soluble sulfate. Partly due to the decrease in SO_2 emissions since the 1970s, there is a widespread sulfur deficiency in soils that are used for cultivation of several highly S-demanding crops, especially oilseed rape and cereals in Denmark, England, Germany, and Scotland. In those circumstances additional S feeding is required.

First results of studies [63] on the yield of canola showed that the grain yield is higher when biologically produced sulfur is used than when other commercially available sulfur sources were used (Table 2.3).

2.6. Conclusions

Elemental sulfur produced by sulfur compound oxidizing bacteria ("biosulfur") has properties distinctly different from those of crystalline elemental sulfur. The hydrophilic properties of "biosulfur" are the most striking of these differences. As a result of this, biologically produced sulfur can be dispersed in aqueous solutions, whereas crystalline inorganic sulfur is hydrophobic and will not be wetted by an aqueous solution.

The origin of the hydrophilicity of biologically produced sulfur is however not the same for sulfur produced by different bacteria. Intracellularly stored sulfur globules produced by *Al. vinosum* consist of long sulfur chains terminated with organic groups. These organic end groups are likely to be responsible for the hydrophilic character of the sulfur globules. The hydrophilicity of extracellularly stored sulfur globules produced by *Ac. ferrooxidans* probably can be explained by the vesicle structure consisting mainly of polythionates ($^{-}O_3S–S_n–SO_3^{-}$). Adsorbed organic polymers, such as proteins, are the cause of the hydrophilic properties of sulfur produced in biotechnological sulfide oxidation installations by a mixed culture of *Thiobacilli*.

Due to the small particle size and hydrophilic surface, biologically produced sulfur has advantages over other available sulfur sources in bioleaching and fertilizer applications.

Abbreviations

SOB	Sulfur compound oxidizing bacteria
SRB	Sulfate reducing bacteria
XANES	X-ray absorption near-edge spectroscopy
XRD	X-ray diffraction
HPLC	High pressure liquid chromatography
Al.	*Allochromatium*

Ac. *Acidithiobacillus*
B. *Beggiatoa*

References

1. H. G. Trüper, J. C. Hathaway, Orthorhombic sulphur formed by photosynthetic sulphur bacteria, *Nature* **1967**, *215*, 435-436.
2. J. G. Kuenen, Colourless sulfur bacteria and their role in the sulfur cycle, *Plant Soil* **1975**, *43*, 49-76.
3. D. C. Brune, Sulfur oxidation by phototrophic bacteria, *Biochim. Biophys. Acta* **1989**, *975*, 189-221.
4. T. Brüser, P. N. L. Lens, H. G. Trüper, The biological sulfur cycle. In *Environmental technologies to treat sulfur pollution. Principles and engineering* (Eds.: P. N. L. Lens, L. Hulshoff Pol), IWA Publishing, London, **2000**, pp. 47-85.
5. H. G. Schlegel, *General microbiology*, 7th ed. Cambridge University Press, Cambridge, **1995**.
6. J. M. Visser, G. C. Stefess, L. A. Robertson, J. G. Kuenen, *Thiobacillus* sp. W5, the dominant autotroph oxidizing sulfide to sulfur in a reactor for aerobic treatment of sulfidic wastes, *Antonie van Leeuwenhoek* **1997**, *72*, 127-134.
7. G. L. Schmidt, G. L. Nicolson, M. D. Kamen, Composition of the sulfur particle of *Chromatium vinosum* strain D, *J. Bacteriol.* **1971**, *105*, 1137-1141.
8. J. Then, H. G. Trüper, Sulfide oxidation in *Ectothiorhodospira abdelmelekii*. Evidence for the catalytic role of cytochrome c-551, *Arch. Microbiol.* **1983**, *135*, 254-258.
9. N. H. Lawry, V. Jani, T. E. Jensen, Identification of the sulfur inclusion body in *Beggiatoa alba* B18LD by energy-dispersive X-ray microanalysis, *Curr. Microbiol.* **1981**, *6*, 71-74.
10. D. Y. Sorokin, J. G. Kuenen, M. S. M. Jetten, Denitrification at extremely high pH values by the alkaliphilic, obligately chemolithoautotrophic, sulfur-oxidizing bacterium *Thioalkalivibrio denitrificans* strain ALJD, *Arch. Microbiol.* **2001**, *175*, 94-101.
11. D. Y. Sorokin, V. M. Gorlenko, T. P. Tourova, A. I. Tsapin, K. H. Nealson, G. J. Kuenen, *Thioalkalimicrobium cyclicum* sp. nov. and *Thioalkalivibrio jannaschii* sp. nov., novel species of haloalkaliphilic, obligately chemolithoautotrophic sulfur-oxidizing bacteria from hypersaline alkaline Mono Lake (California), *Int. J. Syst. Evol. Microbiol.* **2002**, *52*, 913-920.
12. K. S. Cho, M. Hirai, M. Shoda, Degradation of hydrogen sulfide by *Xanthomonas* sp. strain DY44 isolated from peat, *Appl. Environ. Microbiol.* **1992**, *58*, 1183-1189.
13. Y. Cohen, E. Padan, M. Shilo, Facultative anoxygenic photosynthesis in the cyanobacterium *Oscillatoria limnetica*, *J. Bacteriol.* **1975**, *123*, 855-861.
14. J. F. Imhoff, J. Suling, R. Petri, Phylogenetic relationships among the *Chromatiaceae*, their taxonomic reclassification and description of the new genera *Allochromatium*, *Halochromatium*, *Isochromatium*, *Marichromatium*, *Thiococcus*, *Thiohalocapsa* and *Thermochromatium*, *Int. J. Syst. Bacteriol.* **1998**, *48*, 1129-1143.
15. J. F. Imhoff, J. Suling, The phylogenetic relationship among *Ectothiorhodospiraceae*: A reevaluation of their taxonomy on the basis of 16S rDNA analyses, *Arch. Microbiol.* **1996**, *165*, 106-113.

16. D. P. Kelly, A. P. Wood, Reclassification of some species of *Thiobacillus* to the newly designated genera *Acidithiobacillus* gen. nov., *Halothiobacillus* gen. nov. and *Thermithiobacillus* gen. nov., *Int. J. Syst. Evol. Microbiol.* **2000**, *50*, 511-516.
17. D. Y. Sorokin, L. A. Robertson, J. G. Kuenen, Isolation and characterization of alkaliphilic, chemolithoautotrophic, sulphur-oxidizing bacteria, *Antonie van Leeuwenhoek* **2000**, *77*, 251-262.
18. W. R. Strohl, I. Geffers, J. M. Larkins, Structure of the sulfur inclusion envelopes from four *Beggiatoas*, *Curr. Microbiol.* **1981**, *6*, 75-79.
19. G. L. Nicolson, G. L. Schmidt, Structure of the *Chromatium* sulfur particle and its protein membrane, *J. Bacteriol.* **1971**, *105*, 1142-1148.
20. A. Janssen, A. de Keizer, A. van Aelst, R. Fokkink, H. Yangling, G. Lettinga, Surface characteristics and aggregation of microbiologically produced sulphur particles in relation to the process conditions, *Colloids Surf. B-Biointerfaces* **1996**, *6*, 115-129.
21. J. Lyklema, Inference of polymer adsorption from electrical double layer measurements, *Pure Appl. Chem.* **1976**, *46*, 149-156.
22. J. Lyklema, G. J. Fleer, Electrical contributions to the effect of macromolecules on colloid stability, *Colloids Surfaces* **1987**, *25*, 357-368.
23. C. L. Tiller, C. R. O'Melia, Natural organic matter and colloidal stability: Models and measurements, *Colloids Surf. A-Physicochem. Eng. Asp.* **1993**, *73*, 89-102.
24. R. D. Vetter, Elemental sulfur in the gills of three species of clams containing chemoautotrophic symbiotic bacteria: A possible inorganic storage compound, *Mar. Biol.* **1985**, *88*, 33-42.
25. R. Steudel, On the nature of the "elemental sulfur" (S^0) produced by sulfur-oxidizing bacteria - A model for S^0 globules. In *Autotrophic bacteria* (Eds.: H. G. Schlegel, B. Bowien), Science Technology Publishers, Madison, WI, **1989**, pp. 289-303.
26. I. J. Pickering, G. N. George, E. Y. Yu, D. C. Brune, C. Tuschak, J. Overmann, J. T. Beatty, R. C. Prince, Analysis of sulfur biochemistry of sulfur bacteria using X-ray absorption spectroscopy, *Biochemistry* **2001**, *40*, 8138-8145.
27. J. D. Pasteris, J. J. Freeman, S. K. Goffredi, K. R. Buck, Raman spectroscopic and laser scanning confocal microscopic analysis of sulfur in living sulfur-precipitating marine bacteria, *Chem. Geol.* **2001**, *180*, 3-18.
28. A. Prange, I. Arzberger, C. Engemann, H. Modrow, O. Schumann, H. G. Trüper, R. Steudel, C. Dahl, J. Hormes, In situ analysis of sulfur in the sulfur globules of phototrophic sulfur bacteria by X-ray absorption near edge spectroscopy, *Biochim. Biophys. Acta* **1999**, *1428*, 446-454.
29. A. Prange, R. Chauvistre, H. Modrow, J. Hormes, H. G. Trüper, C. Dahl, Quantitative speciation of sulfur in bacterial sulfur globules: X-ray absorption spectroscopy reveals at least three different species of sulfur, *Microbiology (UK)* **2002**, *148*, 267-276.
30. K. Pattaragulwanit, D. C. Brune, H. G. Truper, C. Dahl, Molecular genetic evidence for extracytoplasmic localization of sulfur globules in *Chromatium vinosum*, *Arch. Microbiol.* **1998**, *169*, 434-444.
31. G. J. Hageage, E. D. Eanes, R. L. Gherna, X-ray diffraction studies on the sulfur globules accumulated by *Chromatium* species, *J. Bacteriol.* **1970**, *101*, 464-469.

32. R. Guerrero, J. Mas, C. Pedrós-Alió, Buoyant density changes due to intracellular content of sulfur in *Chromatium warmingii* and *Chromatium vinosum*, *Arch. Mircrobiol.* **1984**, *137*, 350-356.
33. J. Mas, H. van Gemerden, Influence of sulfur accumulation and composition of sulfur globule on cell volume and buoyant density of *Chromatium vinosum*, *Arch. Microbiol.* **1987**, *146*, 362-369.
34. R. Steudel, The chemical sulfur cycle. In *Environmental technologies to treat sulfur pollution. Principles and engineering* (Eds.: P. N. L. Lens, L. Hulshoff Pol), IWA Publishing, London, **2000**, pp. 1-31.
35. R. Steudel, G. Holdt, P. T. Visscher, H. van Gemerden, Search for polythionates in cultures of *Chromatium vinosum* after sulfide incubation, *Arch. Microbiol.* **1990**, *153*, 432-437.
36. G. N. George, I. J. Pickering, E. Y. Yu, R. C. Prince, X-ray absorption spectroscopy of bacterial sulfur globules, *Microbiology (UK)* **2002**, *148*, 2267-2268.
37. A. Prange, C. Dahl, H. G. Trüper, R. Chauvistre, H. Modrow, J. Hormes, X-ray absorption spectroscopy of bacterial sulfur globules: A detailed reply, *Microbiology (UK)* **2002**, *148*, 2268-2270.
38. D. C. Brune, Isolation and characterization of sulfur globule proteins from *Chromatium vinosum* and *Thiocapsa roseopersicina*, *Arch. Microbiol.* **1995**, *163*, 391-399.
39. R. Steudel, Mechanism for the formation of elemental sulfur from aqueous sulfide in chemical and microbiological desulfurization processes, *Ind. Eng. Chem. Res.* **1996**, *35*, 1417-1423.
40. R. Steudel, G. Holdt, T. Goebel, W. Hazeu, Chromatographic separation of higher polythionates $S_nO_6^{2-}$ (n=3..22) and their detection in cultures of *Thiobacillus ferrooxidans*; molecular composition of bacterial sulfur secretions, *Angew. Chem.-Int. Edit. Eng.* **1987**, *26*, 151-152.
41. A. J. H. Janssen, A. de Keizer, G. Lettinga, Colloidal properties of a microbiologically produced sulphur suspension in comparison to a LaMer sulphur sol, *Colloids Surf. B-Biointerfaces* **1994**, *3*, 111-117.
42. A. J. H. Janssen, G. Lettinga, A. de Keizer, Removal of hydrogen sulphide from wastewater and waste gases by biological conversion to elemental sulphur. Colloidal and interfacial aspects of biologically produced sulphur particles, *Colloids Surf. A-Physicochem. Eng. Asp.* **1999**, *151*, 389-397.
43. J. Boulègue, Solubility of elemental sulfur in water at 298 K, *Phosphorus Sulfur Silicon Relat. Elem.* **1978**, *5*, 127-128.
44. G. E. Jones, R. L. Starkey, Surface-active substances produced by *Thiobacillus thiooxidans*, *J. Bacteriol.* **1961**, *82*, 788-789.
45. G. E. Jones, A. A. Benson, Phosphatidyl glycerol in *Thiobacillus thiooxidans*, *J. Bacteriol.* **1965**, *89*, 260-261.
46. W. E. Kleinjan, A. de Keizer, A. J. H. Janssen, Kinetics of the reaction between dissolved sodium sulfide and biologically produced sulfur, *Ind. Eng. Chem. Res.* **2005**, *44*, 309-317. *This thesis, chapter 3*.
47. H. van Gemerden, The sulfide affinity of phototrophic bacteria in relation to the location of elemental sulfur, *Arch. Microbiol.* **1984**, *139*, 289-294.
48. G. O. Gray, D. B. Knaff, The role of a cytochrome c-552-cytochrome c complex in the oxidation of sulfide in *Chromatium vinosum*, *Biochim. Biophys. Acta* **1982**, *680*, 290-296.

49. B. W. Kim, H. N. Chang, Removal of hydrogen sulfide by *Chlorobium thiosulfatophilum* in immobilized-cell and sulfur settling free-cell recycle reactors, *Biotechnol. Prog.* **1991**, *7*, 495-500.
50. D. J. Cork, R. Garunas, A. Sajjad, *Chlorobium limicola* forma *thiosulfatophilum*: Biocatalyst in the production of sulfur and organic carbon from a gas stream containing H_2S and CO_2, *Appl. Environ. Microbiol.* **1983**, *45*, 913-918.
51. K. L. Sublette, N. D. Sylvester, Oxidation of hydrogen sulfide by mixed cultures of *Thiobacillus denitrificans* and heterotrophs, *Biotechnol. Bioeng.* **1987**, *24*, 759-761.
52. K. L. Sublette, N. D. Sylvester, Oxidations of hydrogen sulfide by continuous cultures of *Thiobacillus denitrificans*, *Biotechnol. Bioeng.* **1987**, *24*, 753-758.
53. K. L. Sublette, N. D. Sylvester, Oxidation of hydrogen sulfide by *Thiobacillus denitrificans*: Desulfurization of natural gas, *Biotechnol. Bioeng.* **1987**, *24*, 249-257.
54. C. J. N. Buisman, B. G. Geraats, P. IJspeert, G. Lettinga, Optimization of sulphur production in a biotechnological sulphide-removing reactor, *Biotechnol. Bioeng.* **1990**, *35*, 50-56.
55. C. J. N. Buisman, P. IJspeert, A. Hof, A. J. H. Janssen, R. ten Hagen, G. Lettinga, Kinetic parameters of a mixed culture oxidizing sulfide and sulfur with oxygen, *Biotechnol. Bioeng.* **1991**, *38*, 813-820.
56. C. J. N. Buisman, G. Lettinga, C. W. M. Paasschens, L. H. A. Habets, Biotechnological sulfide removal from effluents, *Water Sci. Technol.* **1991**, *24*, 347-356.
57. A. J. H. Janssen, S. Meijer, J. Bontsema, G. Lettinga, Application of the redox potential for controlling a sulfide oxidizing bioreactor, *Biotechnol. Bioeng.* **1998**, *60*, 147-155.
58. R. V. Gadre, Removal of hydrogen sulfide from biogas by chemoautotrophic fixed-film bioreactor, *Biotechnol. Bioeng.* **1989**, *34*, 410-414.
59. V. Herrygers, H. van Langenhove, E. Smet, Biological treatment of gases polluted by volatile sulfur compounds. In *Environmental technologies to treat sulfur pollution. Principles and engineering* (Eds.: P. N. L. Lens, L. Hulshoff Pol), IWA Publishing, London, **2000**, pp. 281-304.
60. K. Y. Chen, J. C. Morris, Kinetics of oxidation of aqueous sulfide by O_2, *Environ. Sci. Technol.* **1972**, *6*, 529-537.
61. R. Tichý, Treatment of solid materials containing inorganic sulfur compounds. In *Environmental technologies to treat sulfur pollution. Principles and engineering* (Eds.: P. N. L. Lens, L. Hulshoff Pol), IWA Publishing, London, **2000**, pp. 329-354.
62. R. Tichý, A. Janssen, J. T. C. Grotenhuis, G. Lettinga, W. H. Rulkens, Possibilities for using biologically-produced sulfur for cultivation of *Thiobacilli* with respect to bioleaching processes, *Bioresour. Technol.* **1994**, *48*, 221-227.
63. S. W. S. Kijlstra, A. J. H. Janssen, B. Arena, Biological process for H_2S removal from (high pressure) gas: The Shell-Thiopaq gas desulfurization process. In *Proceedings of the Laurance Reid Gas Conditioning Conference* [CD-ROM], University of Oklahoma, Norman, OK, **2001**.

Chapter 3

Kinetics of the reaction between dissolved sodium sulfide and biologically produced sulfur*

Abstract

The kinetics of the heterogeneous reaction between dissolved sodium sulfide and biologically produced sulfur particles has been studied by measuring the formation of polysulfide ions, S_x^{2-}, in time (pH = 8.0, T = 30–50 °C). Detailed knowledge of this reaction is essential to understand its effect on a biotechnological hydrogen sulfide removal process. The data were fitted with a reaction rate model in which heterogeneous reaction kinetics, decreasing particle size, and a nonuniform particle size distribution were incorporated. Polysulfide ions formed in this reaction have an autocatalytic effect. The observed reaction rate of the autocatalyzed reaction is limited by chemical reaction, contrary to earlier reports for the reaction of sulfide with "inorganic" granular sulfur, which was diffusion-rate-limited. The small particle size or the specific hydrophilic surface properties probably make the surface of the biologically produced sulfur particles more easily available for reaction than the surface of granular sulfur.

Keywords

Biologically produced sulfur, polysulfide, hydrogen sulfide, heterogeneous kinetics, autocatalysis

* W.E. Kleinjan, A. de Keizer, A.J.H. Janssen, Kinetics of the reaction between dissolved sodium sulfide and biologically produced sulfur, *Ind. Eng. Chem. Res.* **2005**, *44*, 309-317.

3.1. Introduction

To overcome disadvantages of physicochemical processes for hydrogen sulfide removal (e.g., high pressure, high temperature, need for special chemicals), the use of microorganisms can be an interesting alternative. Several microorganisms are capable of oxidizing H_2S at ambient temperatures and pressures, and both phototrophic and chemotrophic organisms have been studied for application in biotechnological H_2S removal systems (for a review, see [1]). Phototrophic bacteria have the disadvantage of the requirement of light and the need for transparent reactor surface and reaction solutions. Therefore, chemotrophic bacteria (especially the chemoautotrophic *Thiobacilli*) are the types of bacteria that have been studied and used mostly in H_2S removal processes. Sublette and Sylvester [2] especially focused on the use of *Thiobacillus denitrificans* for aerobic or anaerobic oxidation of sulfide to sulfate. Buisman *et al*. [3] used a mixed culture of *Thiobacilli* for the aerobic oxidation of sulfide to elemental sulfur and studied technological applications. Visser *et al*. [4] showed the dominant organism in this mixed culture to be the new organism *Thiobacillus* sp. W5. This process was further developed and is currently used in a number of full-scale installations [5, 6].

In this process, the formation of polysulfide ions can occur. Dissolved hydrogen sulfide can react with biologically produced sulfur, a form of elemental sulfur that is produced by sulfide-oxidizing bacteria, resulting in an aqueous solution of polysulfide ions, S_x^{2-}. The overall reaction between elemental sulfur in its most common form (S_8 rings) and dissolved sulfide is shown in Eq. 3.1, but polysulfide formation can also occur with other forms of elemental sulfur [7].

$$HS^- + \frac{x-1}{8} S_8 \rightleftarrows S_x^{2-} + H^+ \qquad (3.1)$$

For a proper understanding of the hydrogen sulfide removal process, detailed knowledge of the kinetics of the reaction between dissolved hydrogen sulfide and biologically produced sulfur is required.

The hydrogen sulfide removal process consists of a gas absorber, where gaseous H_2S is scrubbed from a gas stream by an alkaline solution (Eqs. 3.2 and 3.3), and a bioreactor in which the dissolved HS^- is microbiologically converted to elemental sulfur (Eq. 3.4). Part of the sulfur is then fed back into the gas absorber with a liquid recycle stream, and the remaining part is separated from the liquid in a settler.

$$H_2S(g) \rightleftarrows H_2S(aq) \qquad (3.2)$$

$$H_2S(aq) + OH^- \rightarrow HS^- + H_2O \qquad (3.3)$$

$$HS^- + \tfrac{1}{2}O_2 \rightarrow S^0 + OH^- \qquad (3.4)$$

The biologically produced sulfur is of oxidation state zero and is therefore often written as S^0, although it should not be mistaken for atomic sulfur. Biologically produced sulfur can occur in different modifications for different sulfide-oxidizing bacteria (for a review, see [8]). Studies by X-ray absorption near-edge spectroscopy (XANES) [9] indicated that sulfur globules produced by phototrophic bacteria consist of long sulfur chains terminated by organic groups (R–S_n–R), whereas sulfur globules produced by chemotrophic bacteria appear to consist of either S_8 rings or polythionates. Because polythionates are not stable at the alkaline conditions of the process, their presence in the sulfur globules of the dominating chemotrophic *Thiobacillus* sp. W5 is not likely, and therefore, sulfur atoms are probably present as S_8 rings.

Janssen *et al*. [10, 11] have studied the characteristics of the sulfur particles formed in this process. The particles can grow up to 1 μm in size but can form aggregates of up to 3 mm. The nature of the sulfur structure was studied by X-ray diffraction, confirming the presence of sulfur rings in the particles. Studies on the surface characteristics showed the particles to be hydrophilic and dispersible in water, contrary to inorganic sulfur, which is very poorly soluble in water (5 μg L^{-1}) [12] and strongly hydrophobic. Because of the relatively high stability of the biologically produced sulfur particles at high salt concentrations, it was concluded that the colloidal stability is based on more than just electrostatic repulsion. The hydrodynamic radius of the particles showed a relatively high dependence on salt concentration, indicating the presence of relatively thick adsorbed layers on the particles. This fact, as well as surface charge density and electrophoretic mobility measurements, supported the suggestion of organic polymers, such as proteins, adsorbed on the particles, providing steric and electrical stabilization to the particles. In this chapter, we use the term biologically produced sulfur to refer to sulfur produced in a biotechnological H_2S removal process in which the chemotrophic *Thiobacillus* sp. W5 is the dominating organism.

Reaction of biologically produced sulfur particles with dissolved hydrogen sulfide results in the formation of polysulfide anions, S_x^{2-}. Polysulfide ions are unbranched chains of sulfur atoms, related to the polysulfanes H_2S_x. The acidity constants of the polysulfanes are not known accurately, but they are so low that polysulfide ions in aqueous solution will practically always be completely deprotonated [13, 14]. At neutral to intermediate alkalinities, S_6^{2-}, S_5^{2-}, and S_4^{2-} ions dominate the solution. The shorter chains S_3^{2-} and S_2^{2-} have been observed only at very high alkalinities (pH > 14) [15]. Reported average chain lengths of polysulfide ions at mildly alkaline conditions and when in equilibrium with excess sulfur vary from $x = 4.6$ [15] and $x = 4.8$ [16] to $x = 5.4$ [17] and $x = 5.5$ [14]. Under acidic conditions, polysulfide ions are

not stable. Somewhat contradictory results have been reported on the effect of temperature on the average polysulfide ion chain length. According to Teder [17], the average chain length increases with increasing temperature (x = 5.0 at 25 °C; x = 6.5 at 80 °C), whereas Giggenbach [18] reported only small variations of x up to 180 °C ($x = 4.5 \pm 0.1$).

Already in 1949, Gerischer [19] reported that the presence of polysulfide ions as a(n) (auto)catalyst increases the rate of dissolution of elemental sulfur into an aqueous sulfide solution. Hartler *et al.* [20] further investigated the kinetics of polysulfide formation, showing that the reaction takes place at the surface of sulfur granules. The specific properties of biologically produced sulfur (especially small particle size) are likely to affect the formation of polysulfide ions. Because of the small particle size, it is expected that the rate of polysulfide formation is faster with biologically produced sulfur than with the inorganic sulfur granules used by Hartler *et al.*

The reaction rate is determined by measuring the polysulfide concentration spectrophotometrically in time. For interpretation, the obtained reaction rate is compared to modeled reaction kinetics.

3.2. Materials and methods

3.2.1. Chemicals used

Biologically produced sulfur was obtained from a bioreactor of the wastewater treatment plant of Industriewater Eerbeek (Eerbeek, The Netherlands). The obtained suspension was dialyzed in deaerated water to remove salts until the conductivity of the sulfur suspension was no higher than 40 μS cm^{-1} (approximately 0.1 mM $NaHCO_3$ + 0.1 mM $Na_2S_2O_3$). Suspensions were then filtered over a 3-μm filter to remove large sulfur aggregates.

Sulfide solutions were prepared by removing the oxidized surface of $Na_2S{\cdot}9H_2O$ crystals by flushing with deaerated water and subsequently dissolving the crystals in deaerated water. The flasks were septum-sealed, and the solutions were kept under argon. For each experiment, sulfide solutions were freshly prepared.

3.2.2. Analysis

Sulfide concentrations were determined spectrophotometrically by the methylene blue method as described by Trüper and Schlegel [21]. The concentration of polysulfide was determined spectrophotometrically at a wavelength of 285 nm. At this wavelength, the polysulfide excess sulfur concentration (the total amount of zero valent sulfur atoms in polysulfide ions, [S^0 in S_x^{2-}]) can be determined, approximately independent of pH and ratio X_S [22, 23].

$$X_S = \frac{[S^0 \text{ in } S_x^{2-}]}{[S^{2-}]_{total}} = \frac{\sum_0^{x_{max}} (x-1)[S_x^{2-}]}{\sum_0^{x_{max}} [S_x^{2-}] + [H_2S] + [HS^-] + [S^{2-}]} \quad (3.5)$$

Calibration was performed with polysulfide solutions made by reaction of a known amount of sulfur with an excess of sulfide. The molar extinction coefficients were determined for pH 8 (1390 L mol^{-1} cm^{-1}) and pH 10 (1350 L mol^{-1} cm^{-1}) and were found to be approximately the same as literature data (1360 L mol^{-1} cm^{-1} [23]; 1325 L mol^{-1} cm^{-1} [13]).
The total sulfur concentration was determined by weight after filtration over a 0.22-μm filter and subsequent drying at 50 °C.

3.2.3. Sulfur particle characterization

The particle size distribution was determined with a Coulter Laser LS 230. The particle size distribution was calculated from the data according to a Fraunhofer model, in which the refractive index of sulfur (α S_8) was incorporated (1.998) [24].
The electrophoretic mobility was measured with a Malvern Instruments Zetasizer 2000. Suspensions were diluted with solutions containing 0.010 M NaCl and additional NaOH or HCl to obtain the desired pH.

3.2.4. Method of measuring the kinetics

In a thermostated 500-mL round-bottom flask, a buffered solution (35 mM K_2HPO_4, pH = 8.0) of $Na_2S{\cdot}9H_2O$ was mixed with a dialyzed suspension of biologically produced sulfur, both at the desired temperature. The contents of the glass flask were pumped through a flow-through quartz cuvette, and the UV absorption was measured in time (λ = 285 nm). The total liquid volume for each experiment was 200 mL. The sulfide concentration varied from 7 to 20 mM and the sulfur concentration from 0.35 to 1.10 mM (sulfur concentration in moles of zerovalent sulfur atoms per liter). In all cases, there was an excess of sulfide, and eventually, all sulfur was “dissolved”, leaving an optically clear yellow solution. Compared to the total reaction time, the mixing can be seen as instantaneous. The total pump tube volume was 5 mL, and the pump speed was 6 mL min^{-1}, so the retention time of the liquid outside the flask was approximately 50 s.
A correction to the absorbance was made for the scattering of colloidal sulfur particles present in the suspension. The correction method is illustrated in Figure 3.1. The dotted line represents the original uncorrected data. From these data, the varying contribution of the scattering can be determined, assuming that, initially, the measured intensity is completely due to scattering and, finally, no scattering is measured because all sulfur particles have dissolved. Initially, the scattering intensity is at a

maximum, and the initial intensity (except for the first seconds, because of mixing) is called ΔI_{max}. Eventually, the scattering intensity reaches zero, and the measured intensity originates completely from UV absorption of the dissolved chemicals (I_0).
The scattering intensity is proportional to the number of particles and to the squared volume of the particle that scatters the light (Rayleigh scattering) [25]. Assuming a monodisperse particle size, one infers that the volume of a sulfur particle at a time t is proportional to the amount of polysulfide excess sulfur originating from this particle when it is completely dissolved. Therefore, the volume of a sulfur particle, V_t is also proportional to the quantity ($I_0 - I_{t,\text{corrected}}$). Here, we have assumed that the final measured intensity (I_0) is completely due to the absorbance of polysulfide excess sulfur. For the scattering intensity at time t we can then write

$$\Delta I_t \propto V_t^2 \propto \left(I_0 - I_{t,\text{corrected}}\right)^2 = C \cdot \left(I_0 - \left(I_{t,\text{measured}} - \Delta I_t\right)\right)^2 \tag{3.6}$$

Because ΔI_t can vary from ΔI_{max} to 0, the boundary conditions are

$t = 0$: $\Delta I_t = \Delta I_{max} = I_{t,\text{measured}}$

$t = \infty$: $\Delta I_t = 0$ and $I_{t,\text{measured}} = I_0$

From the first condition it follows that $C = \Delta I_{max} / I_0^2$ and therefore

$$\Delta I_t = \Delta I_{max} \frac{\left(I_0 - \left(I_{t,\text{measured}} - \Delta I_t\right)\right)^2}{I_0^2} \tag{3.7}$$

The part of the measured intensity that is due to scattering at a given time t, ΔI_t, can then be determined by iteration. Corrected intensities are then obtained by subtracting

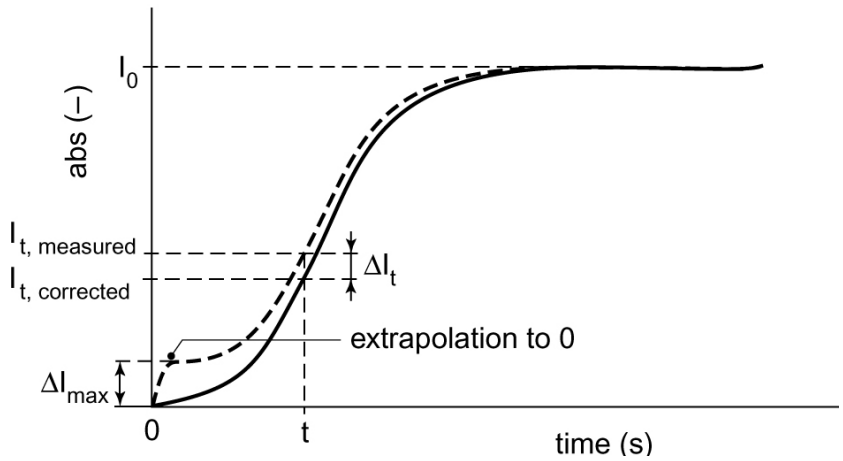

Figure 3.1. Method of correction for the scattering of sulfur particles in the measurement of the kinetics of the reaction between an aqueous sulfide solution and biologically produced sulfur. The dashed line represents the original uncorrected data; the solid line represents the intensity that is due to UV absorption of dissolved chemicals.

ΔI_t from $I_{t,\text{measured}}$. Effects of a heterogeneous particle size distribution were neglected in this correction.

3.3. Modeling the kinetics of polysulfide formation

The reaction in Eq. 3.1 is an overall reaction and does not provide any insight into the mechanism. Formation of a mixture of polysulfides from reaction of hydrogen sulfide with elemental sulfur (S_8 rings) is initiated by the opening of the S_8 ring by the strong nucleophile (species with an unshared electron pair, or Lewis base) HS^- (Eq. 3.8), after which the resulting long-chain polysulfide ion rearranges by reaction with another HS^- ion to shorter polysulfide ions (Eqs. 3.9 and 3.10) [14]

$$HS^- + S_8 \rightleftarrows HS_9^- \rightleftarrows S_9^{2-} + H^+ \tag{3.8}$$

$$S_9^{2-} + HS^- \rightleftarrows 2\ S_5^{2-} + H^+ \tag{3.9}$$

$$2\ S_5^{2-} \rightleftarrows S_4^{2-} + S_6^{2-} \tag{3.10}$$

Polysulfide ions are also strong nucleophiles and therefore capable of opening the S_8 ring as well. The presence of polysulfide ions was even found to accelerate the dissolution of elemental sulfur, and therefore, formation of polysulfide ions has an autocatalytic effect on the rate of sulfur dissolution in aqueous sulfide solutions [20]. In the proposed mechanism, the S_8 ring is first opened by a polysulfide molecule, forming a long-chain polysulfide ion. It has been suggested that especially the short chain ions S_2^{2-} and S_3^{2-} would initiate the ring opening because they would be the strongest nucleophiles [26]. On the other hand, although the speciation of the various polysulfide ions is not well known, these short chains are generally agreed to be practically absent at intermediate pH's and in the presence of sulfur. We have therefore assumed that the S_8 ring is opened by polysulfide ions of the average chain length x. Possible pathways for the breakdown of the long chain are then the uncatalyzed reaction (back reaction Eq. 3.11) and the reaction of this long chain with sulfide (Eq. 3.12) or with a proton (Eq. 3.13). The sequence of reaction steps is then described by Eqs. 3.11–3.14, after which the long-chain polysulfide ion (S_9^{2-}) can rearrange through the reactions in Eqs. 3.9 and 3.10 to polysulfide ions with shorter chain lengths [20, 27].

$$S_x^{2-} + S_8 \rightleftarrows S_{x+8}^{2-} \tag{3.11}$$

$$S_{x+8}^{2-} + HS^- \rightleftarrows S_x^{2-} + HS_9^- \tag{3.12}$$

$$S_{x+8}^{2-} + H^+ \rightleftarrows HS_{x+8}^- \rightleftarrows S_x^{2-} + S_8 + H^+ \tag{3.13}$$

$$HS_9^- \rightleftarrows S_9^{2-} + H^+ \tag{3.14}$$

For the modeling of the kinetics, some assumptions can be made to facilitate the calculations. First, Eqs. 3.8–3.14 are all equilibrium reactions, but for the kinetics we will assume that they are not, except for the ring-opening reactions in Eqs. 3.8 and 3.11. This is justified because the back reactions in Eqs. 3.9, 3.12, and 3.13 will be much slower than the forward reactions because short-chain polysulfide ions are much more stable than long-chain polysulfide ions. Second, the average polysulfide chain is assumed to consist of 5.0 S atoms, which permits the polysulfide shift reaction (Eq. 3.10) to be ignored. Third, the two equilibria concerning the intermediate HS_9^- (Eq. 3.8) are taken as one equilibrium. This results in Eqs. 3.15 and 3.16 for the uncatalyzed formation of polysulfide from sulfide and sulfur.

$$HS^- + S_8 \underset{k_{-1}}{\overset{k_1}{\rightleftarrows}} S_9^{2-} + H^+ \tag{3.15}$$

$$S_9^{2-} + HS^- \xrightarrow{k_2} 2\,S_5^{2-} + H^+ \tag{3.16}$$

When polysulfide ions are present, the reactions in Eqs. 3.15 and 3.16 can take place as well. Using the same assumptions as for the uncatalyzed reactions, the following additional reactions take place

$$S_5^{2-} + S_8 \underset{k_{-3}}{\overset{k_3}{\rightleftarrows}} S_{13}^{2-} \tag{3.17}$$

$$S_{13}^{2-} + HS^- \xrightarrow{k_4} S_5^{2-} + S_9^{2-} + H^+ \tag{3.18}$$

$$S_{13}^{2-} + H^+ \xrightarrow{k_5} S_5^{2-} + S_8 + H^+ \tag{3.19}$$

In these reactions, the long-chain intermediate S_{13}^{2-} is degraded in three different ways: uncatalyzed (back reaction of Eq. 3.17), with HS^- (Eq. 3.18), or catalyzed by a proton (Eq. 3.19).

Because of the poor solubility of S_8 rings, the reaction will essentially not take place in solution but rather at the surface of sulfur particles. In the kinetic equations, the *concentration of the surface*, A_c ($m^2\ m^{-3}$), is used, which is the surface area of the sulfur particles per solvent volume. This term is also called the "extent of the system" [28].

$$A_c = c_{S^0} M_{S^0} A_s \tag{3.20}$$

Here, c_{S0} is the total concentration of solid sulfur in solution (mol m^{-3}), M_S is the molar mass of a sulfur atom (g mol^{-1}), and A_s is the specific surface area of the sulfur particles ($m^2\ g^{-1}$). In a steady-state situation, the rate of S_9^{2-} formation must be equal to the rate of S_9^{2-} consumption. Therefore

$$k_1[HS^-]A_c + k_4[S_{13}^{2-}][HS^-] - k_{-1}[S_9^{2-}][H^+] - k_2[HS^-][S_9^{2-}] = 0 \quad (3.21)$$

From this steady-state situation, an expression can be derived for the concentration of the intermediate product S_9^{2-}.

$$[S_9^{2-}] = \frac{k_1[HS^-]A_c + k_4[S_{13}^{2-}][HS^-]}{k_{-1}[H^+] + k_2[HS^-]} \quad (3.22)$$

Similarly, an expression for the concentration of the intermediate product S_{13}^{2-} can be derived.

$$k_3[S_5^{2-}]A_c - k_{-3}[S_{13}^{2-}] - k_4[S_{13}^{2-}][HS^-] - k_5[S_{13}^{2-}][H^+] = 0 \quad (3.23)$$

$$[S_{13}^{2-}] = \frac{k_3[S_5^{2-}]A_c}{k_{-3} + k_4[HS^-] + k_5[H^+]} \quad (3.24)$$

By substitution of the expressions 3.22 and 3.24 for the concentrations of the intermediate products S_9^{2-} and S_{13}^{2-} into the expression for the rate of polysulfide formation (Eq. 3.25), it can be seen that the last four terms sum to zero, leaving only the first term. This results in Eq. 3.26.

$$\frac{d[S_5^{2-}]}{dt} = 2k_2[S_9^{2-}][HS^-] + k_{-3}[S_{13}^{2-}] + k_4[S_{13}^{2-}][HS^-] + k_5[S_{13}^{2-}][H^+] - k_3[S_5^{2-}]A_c \quad (3.25)$$

$$\frac{d[S_5^{2-}]}{dt} = \frac{2k_2[HS^-]^2 A_c \left(k_1 + \frac{k_3 k_4 [S_5^{2-}]}{k_{-3} + k_4[HS^-] + k_5[H^+]} \right)}{k_{-1}[H^+] + k_2[HS^-]} \quad (3.26)$$

When no polysulfide is present, this relation rearranges to

$$\left(\frac{d[S_5^{2-}]}{dt} \right)_{t=0} = \frac{2k_1 k_2 [HS^-]^2 A_c}{k_{-1}[H^+] + k_2[HS^-]} \quad (3.27)$$

Two extremes can be distinguished. When the relative rate of the back-reaction of Eq. 3.15 is much faster than the reaction rate of Eq. 3.16 ($k_{-1}[H^+] >> k_2[HS^-]$), the rate of polysulfide formation can be written as

$$\left(\frac{d[S_5^{2-}]}{dt} \right)_{t=0} = \frac{2k_1 k_2 [HS^-]^2 A_c}{k_{-1}[H^+]} \quad (3.28)$$

In the other extreme ($k_{-1}[H^+] << k_2[HS^-]$) the rate of polysulfide formation can be rearranged to

$$\left(\frac{\mathrm{d}[S_5^{2-}]}{\mathrm{d}t}\right)_{t=0} = 2k_1[HS^-]A_c \tag{3.29}$$

Hartler *et al.* [20] reported that the reaction between elemental sulfur and sulfide, in the absence of polysulfide, is approximately second order with regard to sulfide ions and directly proportional to the specific surface area of sulfur, which corresponds to the rate expressed in Eq. 3.28. Therefore $k_{-1}[H^+] >> k_2[HS^-]$, in which we should note that the relative rate of the back-reaction of Eq. 3.15 ($k_{-1}[H^+]$) depends not only on the rate of protonation of S_9^{2-} (fast) but also on the stability of the intermediate product HS_9^- (Eq. 3.8), which is ignored in Eq. 3.15.

The rate of polysulfide formation in the presence of polysulfide can now be written as

$$\frac{\mathrm{d}[S_5^{2-}]}{\mathrm{d}t} = \frac{2k_2[HS^-]^2 A_c}{k_{-1}[H^+]}\left(k_1 + \frac{k_3 k_4[S_5^{2-}]}{k_{-3} + k_4[HS^-] + k_5[H^+]}\right) \tag{3.30}$$

Now, three extreme situations can be distinguished, depending on the rates of the back-reaction of Eq. 3.17 (k_{-3}), and the rates of reaction in Eq. 3.18 ($k_4[HS^-]$) and 3.19 ($k_5[H^+]$). From the study of Hartler *et al.* [20] it is known that, in the presence of polysulfide ions, the reaction rate was of mixed first order with respect to sulfide. This suggests that $k_4[HS^-]$ dominates over the terms k_{-3} and $k_5[H^+]$, resulting in the total reaction rate as described by Eq. 3.31

$$\frac{\mathrm{d}[S_5^{2-}]}{\mathrm{d}t} = \frac{A_c[HS^-]}{[H^+]}\left(k_1^*[HS^-] + k_2^*[S_5^{2-}]\right) \tag{3.31}$$

with

$$k_1^* = \frac{2k_1k_2}{k_{-1}} \tag{3.32}$$

$$k_2^* = \frac{2k_2k_3}{k_{-1}} \tag{3.33}$$

Unlike the situation with the S_9^{2-} ion (where the reaction with H^+ dominates the reaction with HS^-), the reaction rate of the longer polysulfide chain S_{13}^{2-} with HS^- is faster than its reaction with H^+. The origin of this difference probably lies in the difference in stability of the polysulfide ions of different chain lengths. The maximum chain length in water is believed to be nine, whereas longer chains have not been detected because of their very short lifetime [14]. Formation of the long-chain intermediate HS_{13}^- (see Eq. 3.13, ignored in Eq. 3.19) is therefore probably less favorable than breaking of the long chain by an HS^- ion (Eq. 3.18).

The expression for the rate of the polysulfide formation (Eq. 3.31) permits the calculation of the polysulfide concentration in time for a given reaction system and

therefore a fitting of the modeled reaction with experimental data. Reaction rate constants k_1^* and k_2^* can be used as fit parameters. The polysulfide concentrations that have been determined experimentally are defined as polysulfide excess sulfur (concentrations of zerovalent sulfur atoms in polysulfide molecules, [S^0 in S_x^{2-}]). For comparison of the experimental data with the modeled reaction rate, each [S_x^{2-}] term in Eq. 3.31 should be divided by (x–1).

To calculate the S_x^{2-} concentration as a function of time, it is necessary to relate [HS^-] and the total surface area of the sulfur particles per volume solution, A_c, to [S^0 in S_x^{2-}]. The relation between [HS^-] and [S^0 in S_x^{2-}] can be determined from the mass balance of the sulfide concentration.

$$[HS^-] = [HS^-]_0 - \frac{[S^0 \text{ in } S_x^{2-}]}{x-1} \tag{3.34}$$

The relation between A_c and [S^0 in S_x^{2-}] depends on the size of the sulfur particles or, in a heterogeneous system, on the particle size distribution. When the particle size distribution is divided into j fractions, the relation between A_c and [S^0 in S_x^{2-}] is

$$A_c = A_{c,1} + ... + A_{c,j} = n_1 A_1 + ... + n_j A_j = n_1 J V_1^{2/3} + ... + n_j J V_j^{2/3}$$

$$= \sum_{i=1}^{i=j} n_i J \left(\frac{M_S c_{S^0 i}}{n_i \rho} \right)^{2/3}$$

$$= \sum_{i=1}^{i=j} \frac{n_i^{1/3} J M_S^{2/3}}{\rho^{2/3}} \left(c_{S^0 i,0} - [S^0 \text{ in } S_x^{2-}]_i \right)^{2/3} \tag{3.35}$$

Here, A_i is the surface area of one particle of fraction i (m^2), V_i is the volume of one particle of fraction i (m^3) and n_i is the number of sulfur particles of fraction i per unit volume (m^{-3}). Furthermore, $J = A_{sphere} / V_{sphere}^{2/3} = 4\pi r^2 / (^4/_3 \pi r^3)^{2/3} = 4.84$, the shape factor for spherical objects, M_S is the molar mass of a sulfur atom, and ρ is the density of biologically produced sulfur.

The number of particles of a given size per solvent volume, n_i can be related to the original total sulfur concentration in the suspension, $c_{S0(0)}$ (mol m^{-3}):

$$n_i = \frac{c_{S^0_i} M_S}{\rho \frac{4}{3} \pi r_i^3} = \frac{f_i c_{S^0_0} M_S}{\rho \frac{4}{3} \pi r_i^3} \tag{3.36}$$

Here, f_i is the volume (or molar) fraction of particles of fraction i. Combining Eqs. 3.35 and 3.36 results in:

$$A_c = \sum_{i=1}^{i=j} \frac{f_i^{1/3} c_{S^0_0}^{1/3}}{r_i} Q\left(f_i c_{S^0_0} - [S^0 \text{ in } S_x^{2-}]_i\right)^{2/3} \tag{3.37}$$

in which the constant Q is

$$Q = \frac{JM_S}{\rho\left(\frac{4}{3}\pi\right)^{1/3}} = \frac{3M_S}{\rho} \tag{3.38}$$

The total rate of polysulfide formation follows from Eqs. 3.31, 3.34, and 3.37 as

$$\frac{d[S_x^{2-}]}{dt} = \sum_{i=1}^{i=j} \left(Q \frac{f_i^{1/3} c_{S^0_0}^{1/3}}{r_i [H^+]} \left([HS^-]_0 - \frac{[S^0 \text{ in } S_x^{2-}]}{x-1} \right) \left(f_i c_{S^0_0} - [S^0 \text{ in } S_x^{2-}]_i\right)^{2/3} \times \ ... \right.$$

$$\left. ... \left(k_1^* \left([HS^-]_0 - \frac{[S^0 \text{ in } S_x^{2-}]}{x-1} \right) + k_2^* \frac{[S^0 \text{ in } S_x^{2-}]}{x-1} \right) \right) \tag{3.39}$$

in which the total polysulfide excess sulfur concentration, $[S^0 \text{ in } S_x^{2-}]$, consists of the sum of the polysulfide concentrations originating from the particles of all fractions

$$[S^0 \text{ in } S_x^{2-}] = \sum_{1}^{i=j} [S^0 \text{ in } S_x^{2-}]_i \tag{3.40}$$

3.4. Results and discussion

3.4.1. Characterization of sulfur particles

The measured particle size distribution of a dialyzed sulfur suspension that was filtered over a 3-μm filter is shown in Figure 3.2. It can be seen that the sulfur suspension consists of a bimodal volume-based particle size distribution. The larger fraction probably consists of aggregated sulfur particles. It should be noted that, because of the difference in refractive indices of sulfur (1.99) and water (1.33), bacteria present in the suspension would make a very minor contribution to the measured distribution.

The electrophoretic mobility is measured as a function of pH, illustrated in Figure 3.3. As can be seen, the surface of the particles is negatively charged at neutral to alkaline pH, and the isoelectric point is 2.3. This value corresponds to pK_a values of carboxylic acid groups in proteins [29]. This is in agreement with previous work by Janssen *et al.* [11] who showed that the isoelectric point of biologically produced sulfur particles was at a pH lower than 3.8. They also showed that the point of zero charge of biologically produced sulfur particles is at a pH of 5.8. The difference between the

isoelectric point and the point of zero charge was explained by an inhomogeneous charge distribution in the polymer layer. Because of the high electron density of the sulfur nucleus, cationic groups are probably located more in the interior of the polymer layer, and anionic carboxylic acid groups are probably located more at the outside of the polymer layer.

The density of biologically produced sulfur is not known exactly. Studies on the density of sulfur globules produced by the phototrophic bacterium *Allochromatium vinosum* revealed a sulfur globule density of 1.31 g cm^{-3} [30], whereas crystalline forms of sulfur have a higher density (1.9–2.2 g cm^{-3}). This difference was explained by the presence of water in the "hydrated sulfur globule" that was later attributed to organic groups on the ends of sulfur chains [9]. The biologically produced sulfur particles produced by the chemotrophic *Thiobacillus* sp. W5 used in our experiments are most likely to consist of S_8 rings and therefore probably less hydrated than sulfur globules produced by *Allochromatium vinosum*. The total particle density is therefore expected to be higher than 1.31 g cm^{-3}. On the other hand, organic polymer chains are

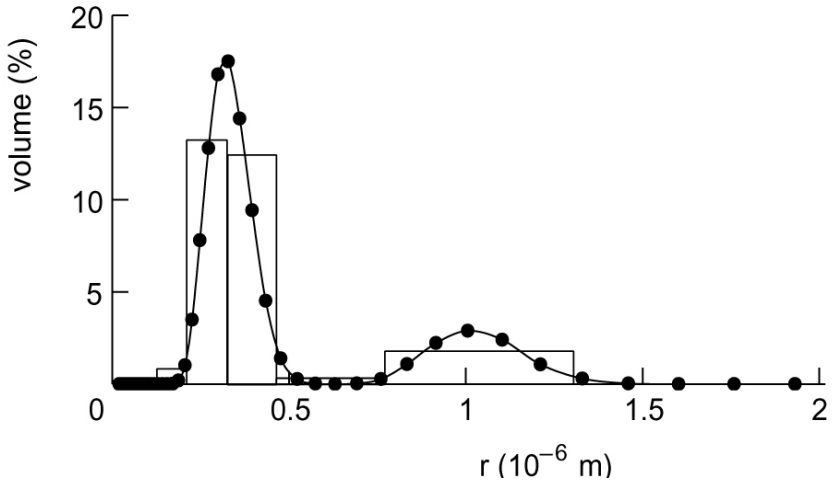

Figure 3.2. Particle size distribution of biologically produced sulfur particles (filtered over a 3-μm filter).

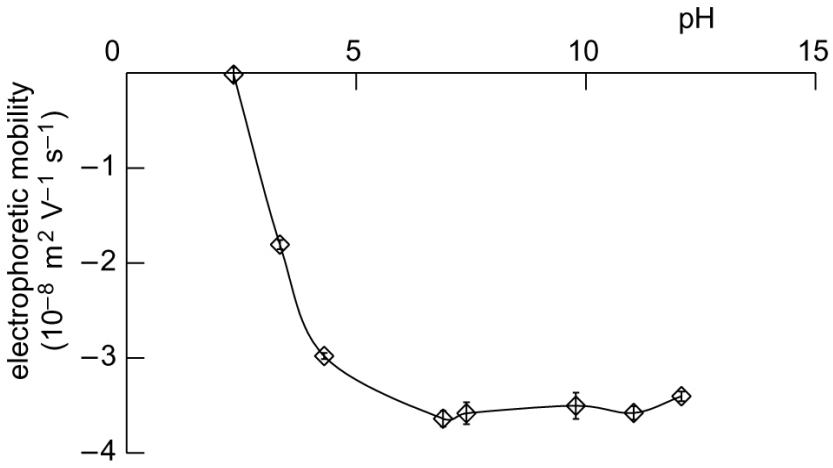

Figure 3.3. Electrophoretic mobility of biologically produced sulfur particles as a function of pH. [NaCl] = 0.010 M.

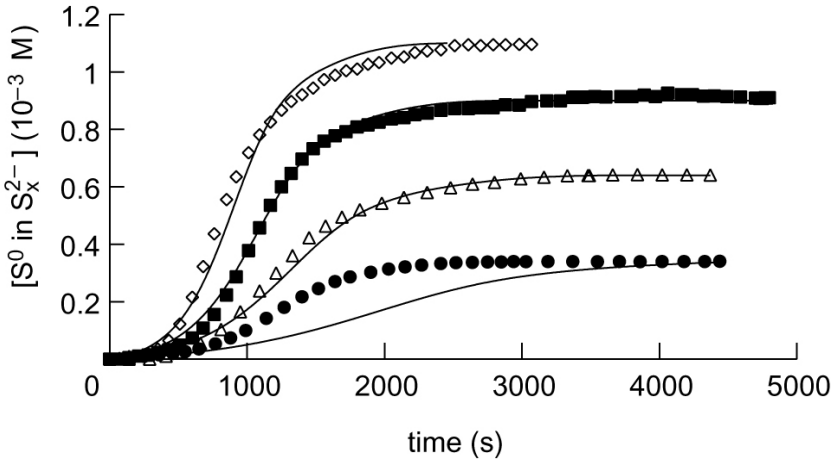

Figure 3.4. Polysulfide excess sulfur concentration in time for different initial sulfur concentrations; 1.10 mM (◊); 0.90 mM (■); 0.64 mM (Δ); 0.35 mM (●). T = 50 ºC; pH = 8.0; [HS^-] = 10 mM. Only a selection of the data points of each curve is shown. The solid lines represent the modeled reaction rate with the best-fit values of the reaction rate constants k_1^* = 5.78 × 10^{-14} m s^{-1} and k_2^* = 1.33 × 10^{-10} m s^{-1}.

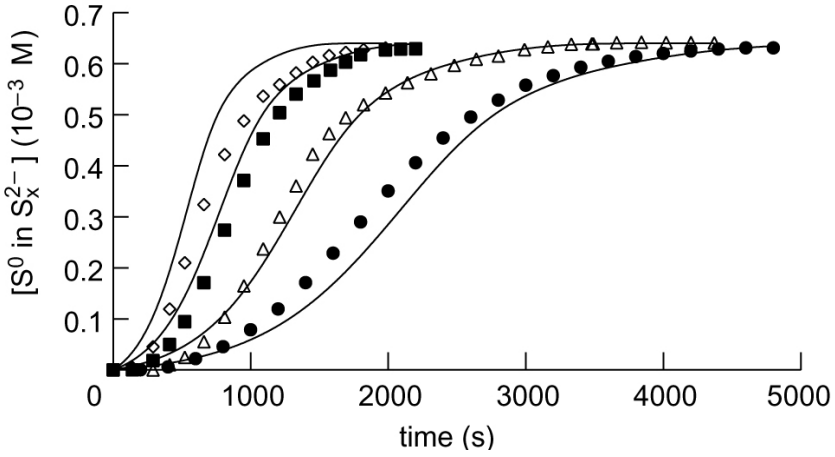

Figure 3.5. Polysulfide excess sulfur concentration in time for different initial sulfide concentrations; 20 mM (◊); 15 mM (■); 10 mM (Δ); 7 mM (●). T = 50 ºC; pH = 8.0; c_{S0}= 0.64 mM. Only a selection of the data points of each curve is shown. The solid lines represent the modeled reaction rate with the best-fit values of the reaction rate constants k_1^* = 5.78 × 10^{-14} m s^{-1} and k_2^* = 1.33 × 10^{-10} m s^{-1}.

Table 3.1. Best-fit values of reaction rate constants k_1^* and k_2^* for each experiment and average values and mean deviations of these constants. T = 50 ºC; for varying sulfur content [HS^-] = 10 mM, for varying sulfide concentrations c_{S0} = 0.64 mM.

c_{S^0} **(mM)**	k_1^* **(× 10^{-14} m s^{-1})**	k_2^* **(× 10^{-10} m s^{-1})**
0.35	6.52	(2.42)
0.64	5.65	1.42
0.90	3.40	1.42
1.10	8.50	1.14
[HS^-] (mM)		
7	8.90	1.28
10	5.65	1.42
15	3.44	1.39
20	4.31	1.06
average	5.78	1.33
mean deviation	2.23	0.20

on the surface of the sulfur particles, and therefore, the total particle density is expected to be lower than the density of crystalline forms of sulfur. In our calculations, we used an estimate for the total particle density of 1.7 g cm^{-3}.

3.4.2. Kinetics

In Figure 3.4, the measured polysulfide concentration is plotted as a function of time for four different sulfur concentrations (data points). In Figure 3.5, the curves are shown with varying sulfide concentrations, and in Figure 3.6, the effect of temperature is shown. All curves are S-shaped, which is typical for autocatalyzed reactions [28]. Initially, sulfur reacts with sulfide according to Eqs. 3.8–3.10. After these reactions have taken place, polysulfide is present as a catalyst, and reactions can also take place according to Eqs. 3.11–3.14. When all sulfur is converted to polysulfide, a constant polysulfide concentration is reached. A linearization of the autocatalytic reaction rate data as was reported for the autocatalytic oxidation of ferrous iron [31] is not possible here because of the heterogeneous particle size distribution. Instead, a fit was made of the reaction rate data with the modeled reaction rate (Eq. 3.39), using the reaction rate constants k_1* and k_2* as fit parameters.

Table 3.2. Best-fit values of reaction rate constants k_1^* and k_2^* for different temperatures. [HS^-] = 10 mM; c_{S0} = 0.64 mM.

T (°C)	k_1^* ($\times 10^{-14}$ m s^{-1})	k_2^* ($\times 10^{-10}$ m s^{-1})
30	3.04	0.30
35	3.12	0.39
40	4.23	0.45
45	5.19	0.67
50	5.78	1.33

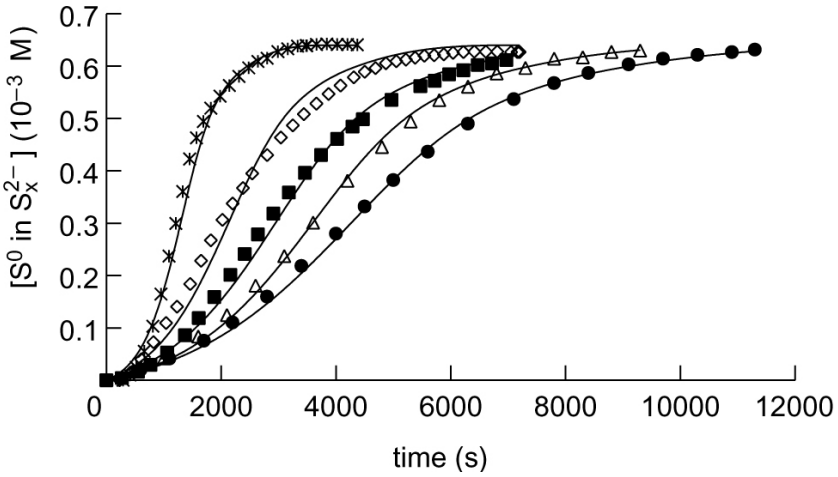

Figure 3.6. Polysulfide excess sulfur concentration in time for different temperatures; 50 °C (*); 45 °C (◊); 40 °C (■); 35 °C (Δ); 30 °C (●). pH = 8.0; c_{S0} = 0.64 mM; [HS^-] = 10 mM . Only a selection of the data points of each curve is shown. The solid lines represent the modeled reaction rate with the best-fit values of reaction rate constants k_1^* and k_2^*.

The polysulfide concentration can be calculated as a function of time by solving Eq. 3.39 for the five fractions into which the measured particle size distribution was divided (Figure 3.2). For each experiment, a best fit was made using a minimization procedure in Matlab with reaction rate constants k_1^* and k_2^* as fit parameters. The data are shown in Table 3.1. The model curves corresponding to the average values of these fits are shown in Figures 3.4 and 3.5 (solid lines). It should be noted that the measured distribution of the particle size is essential for effectively fitting the data. Using an average particle radius resulting from dynamic light scattering, the specific shape of the data cannot be fitted because the plateau value is reached too fast (result not shown). This is because large particles have a lower specific surface, and therefore, the reaction will take place more slowly. The relatively high ionic strength, required for the buffer, is not expected to have a large effect on the reaction rate constants because the rate-determining reaction step in both the uncatalyzed (Eq. 3.8) and catalyzed (Eq. 3.11) processes is a reaction between an ion and an uncharged molecule. This type of reaction is generally unaffected by ionic strength [28].
The effect of temperature on the rate of polysulfide formation is shown in Figure 3.6. The best fit k_1^* and k_2^* values for each temperature are reported in Table 3.2 and shown in an Arrhenius plot (Figure 3.7), obtained using Eq. 3.41, in which A is a preexponential factor and E_a is the activation energy. From the observed linearities in Figure 3.7, it can be concluded that the chemical reaction is reaction-rate-limited. The activation energy for the uncatalyzed reaction (29.6 kJ mol^{-1}) is lower than for the catalyzed reaction (56.2 kJ mol^{-1}).

$$\ln(k) = A - \frac{E_a}{RT} \tag{3.41}$$

In their research on the reaction of sulfide with granulated sulfur, Hartler *et al.* found a similar value for the activation energy for the reaction in the absence of polysulfide

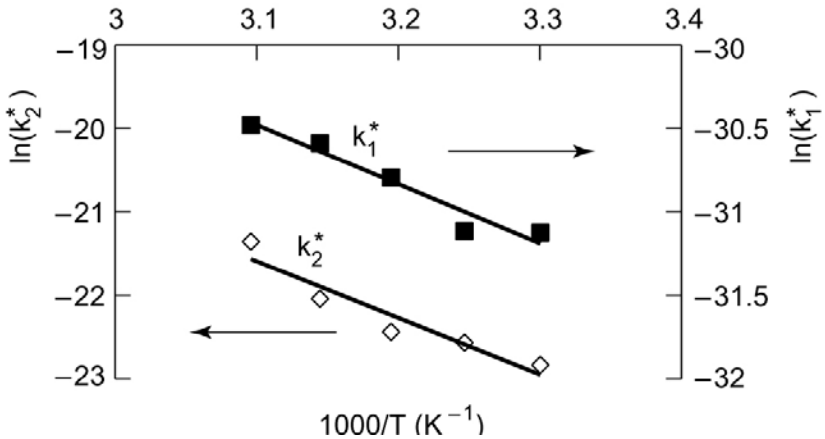

Figure 3.7. Arrhenius plots for determination of activation energy of the reaction between biologically produced sulfur particles with a solution of sodium sulfide in the presence (◊) and in the absence (■) of polysulfide ions.

(31.3 kJ mol^{-1}) [20]. However, they reported a lower activation energy for the reaction in the presence of polysulfide (10.4 kJ mol^{-1}), whereas we find a higher value (56.2 kJ mol^{-1}). Hartler *et al.* concluded that the reaction of sulfide with granulated sulfur was limited by the chemical reaction rate in the absence of polysulfide ions and by the diffusion rate in the presence of polysulfide ions. In the absence of polysulfide ions, the reaction of sulfide with sulfur is relatively slow so that diffusion of sulfide ions to the hydrophobic sulfur surface is not rate limiting. Reaction of polysulfide ions on the sulfur surface is faster, so that the diffusion of polysulfide ions to the hydrophobic sulfur surface becomes rate limiting.

The apparent activation energy for the reaction of sulfide with granulated sulfur in the presence of polysulfide ions is therefore expected to be dependent on the stirring rate and sulfur granule size. These effects on activation energy were not reported, however.

From the values of the activation energies that we find for the reaction of sulfide with biologically produced sulfur, we conclude that the reaction of sulfide with biologically produced sulfur is limited by the chemical reaction rate both in the presence and in the absence of polysulfide ions. This conclusion is also supported by the observed linearities in the Arrhenius plots. For granular sulfur, the catalyzed reaction was diffusion-rate-limited. The difference must be attributed to either a slower reaction on the surface of the biologically produced sulfur particles or a faster diffusion to these particles. The first could be due to differences in sulfur structure. This is not very likely, however, because both sulfur forms are believed to consist of sulfur rings (S_8). Furthermore, no significant difference in the activation energy is observed for the uncatalyzed reaction of sulfide with granular sulfur or biosulfur. A faster diffusion of reactants to biologically produced sulfur compared to granular sulfur could be caused by a higher specific area or by the hydrophilic surface properties of the biosulfur particles.

The k_1^* / k_2^* ratio corresponds to the ratio k_1 / k_3, indicating the ratio between the rates of the ring-opening reactions with a bisulfide or polysulfide ion (Eqs. 3.15 and 3.17). Depending on temperature, the reaction rate constant for S_8 ring opening with S_x^{2-} is between 1000 (30 ºC) and 2300 (50 ºC) times higher than that with HS^-. The stronger nucleophile (Lewis base) S_x^{2-} can cleave the S–S bonds in elemental sulfur faster than the weaker nucleophilic HS^- ions. The stronger nucleophilicity of S_x^{2-} is related to the acidity constants of polysulfides [32]. These are not known accurately, but the pK_{a2} value of the polysulfane H_2S_x must be lower than the pK_{a1} value of H_2S because polysulfides are completely deprotonated in aqueous solution [14].

Comparison of the reaction rates with reported data of granulated sulfur is somewhat difficult. First, the exact specific surface area of the sulfur used in the research by Hartler *et al.* is not reported so that a comparison in reaction rate per unit reactant surface area is not possible. Furthermore, the total amount of sulfur that was present

in the system in our investigation was approximately 1000 times lower (by weight) than in the research done by Hartler, to make it possible to continuously measure the complete reaction.

The reaction rate constants k_1^* and k_2^* have been determined for pH 8.0, and the experimental data can be described by the kinetic expression in Eq. 3.31. This expression might not be suitable for describing the kinetics of polysulfide formation at other pH values. For example, at higher pH, the condition $k_{-1}[H^+] >> k_2[HS^-]$ (see Eq. 3.27) might not be valid, resulting in a different overall kinetic equation. Furthermore, the experiments were performed with biologically produced sulfur obtained from a bioreactor in which the dominating organism is *Thiobacillus* sp. W5, which is believed to be composed of a core of sulfur rings with polymeric organic compounds adsorbed on the particle surface. Other sulfide-oxidizing bacteria are known to produce sulfur globules consisting of polythionates (e.g., *Acidithiobacillus ferrooxidans*) or long sulfur chains terminated by organic groups (e.g., *Allochromatium vinosum*) [9]. The reaction kinetics of dissolved sulfide with these forms of biologically produced sulfur might be substantially different.

3.5. Conclusions

The kinetics of formation of polysulfides from the reaction of dissolved hydrogen sulfide and biologically produced sulfur particles was determined at pH 8.0 and at temperatures between 30 and 50 °C. This was done by measuring the reaction product (polysulfide ions) in time and subsequently fitting the data with a modeled reaction rate in which reaction kinetics, decreasing particle size, and a heterogeneous particle size distribution were incorporated. The reaction takes place at the surface of the biologically produced sulfur particles. Polysulfides formed in this reaction have an autocatalytic effect on the reaction rate, which can be described by the reaction rate in Eq. 3.42

$$\frac{\mathrm{d}[S_5^{2-}]}{\mathrm{d}t} = \frac{A_c\ [HS^-]}{[H^+]} \left(k_1^*[HS^-] + k_2^*[S_5^{2-}]\right) \qquad (3.42)$$

with the reaction rate constants $k_1^* = (5.8 \pm 2.2) \times 10^{-14}$ m s^{-1} and $k_2^* = (1.33 \pm 0.20) \times 10^{-10}$ m s^{-1} (T = 50 ºC). At pH values strongly deviating from pH 8.0, the values for the reaction rate constants might not be applicable, and the overall kinetic expression might have a different form. The observed reaction rate is limited by chemical reaction both in the absence and in the presence of polysulfide ions. The activation energy is 29.6 kJ mol^{-1} in the absence of polysulfide ions and 56.2 kJ mol^{-1} in the presence of polysulfide ions. An earlier study on the reaction of sulfide with granular sulfur in the presence of polysulfide, showed this reaction to be diffusion-rate-limited. The difference suggests that diffusion to the biologically produced sulfur is faster than that to granular sulfur, which might be due to the small particle size or the specific hydrophilic surface properties of the biologically produced sulfur.

Acknowledgement

The authors thank Rachel van Ooteghem for help on estimating fit parameters.

Nomenclature

[A]	concentration of component A	mol m^{-3}
$[A]_0$	initial concentration of component A	mol m^{-3}
$[S^0$ in $S_x^{2-}]$	polysulfide excess sulfur concentration	mol m^{-3}
A	preexponential factor	s^{-1}
A_i	surface area of a particle of fraction i	m^2
$A_{c,i}$	concentration of surface of particles of fraction i	m^2 m^{-3}
c_{S0}	concentration of dispersed solid sulfur	mol m^{-3}
E_a	activation energy	kJ mol^{-1}
f_i	volume fraction of particles of fraction i	-
J	shape factor for spherical objects [= 4.84]	-
V_i	volume of a particle of fraction i	m^3
k_1	reaction rate constant in Eq. 3.15	m s^{-1}
k_{-1}	reaction rate constant in Eq. 3.15	m^3 mol^{-1} s^{-1}
k_2	reaction rate constant in Eq. 3.16	m^3 mol^{-1} s^{-1}
k_3	reaction rate constant in Eq. 3.17	m s^{-1}
k_{-3}	reaction rate constant in Eq. 3.17	s^{-1}
k_4	reaction rate constant in Eq. 3.18	m^3 mol^{-1} s^{-1}
k_5	reaction rate constant in Eq. 3.19	m^3 mol^{-1} s^{-1}
k_1^*	overall reaction rate constant	m s^{-1}
k_2^*	overall reaction rate constant	m s^{-1}
M	molecular weight	g mol^{-1}
n_i	sulfur particles of fraction i per unit volume	m^{-3}
Q	constant in Eq. 3.37	m^3 mol^{-1}
r_i	radius of particles of fraction i	m
T	temperature	°C or K
ρ	density of particles	g m^{-3}
λ	wavelength	nm

References

1. J. E. Burgess, S. A. Parsons, R. M. Stuetz, Developments in odour control and waste gas treatment biotechnology: A review, *Biotechnol. Adv.* **2001**, *19*, 35-63.
2. K. L. Sublette, N. D. Sylvester, Oxidation of hydrogen sulfide by *Thiobacillus denitrificans*: Desulfurization of natural gas, *Biotechnol. Bioeng.* **1987**, *24*, 249-257.
3. C. J. N. Buisman, B. G. Geraats, P. IJspeert, G. Lettinga, Optimization of sulphur production in a biotechnological sulphide-removing reactor, *Biotechnol. Bioeng.* **1990**, *35*, 50-56.
4. J. M. Visser, G. C. Stefess, L. A. Robertson, J. G. Kuenen, *Thiobacillus* sp. W5, the dominant autotroph oxidizing sulfide to sulfur in a reactor for aerobic treatment of sulfidic wastes, *Antonie van Leeuwenhoek* **1997**, *72*, 127-134.

5. A. J. H. Janssen, R. Sleyster, C. van der Kaa, A. Jochemsen, J. Bontsema, G. Lettinga, Biological sulphide oxidation in a fed-batch reactor, *Biotechnol. Bioeng.* **1995**, *47*, 327-333.
6. C. Cline, A. Hoksberg, R. Abry, A. Janssen, Biological process for H_2S removal from gas streams. The Shell-Paques/Thiopaq gas desulfurization process. In *Proceedings of the Laurance Reid gas conditioning conference* [CD-ROM], University of Oklahoma, Norman, OK, **2003**.
7. R. Steudel, Mechanism for the formation of elemental sulfur from aqueous sulfide in chemical and microbiological desulfurization processes, *Ind. Eng. Chem. Res.* **1996**, *35*, 1417-1423.
8. W. E. Kleinjan, A. de Keizer, A. J. H. Janssen, Biologically produced sulfur, *Top. Curr. Chem.* **2003**, *230*, 167-188. *This thesis, chapter 2*.
9. A. Prange, R. Chauvistre, H. Modrow, J. Hormes, H. G. Trüper, C. Dahl, Quantitative speciation of sulfur in bacterial sulfur globules: X-ray absorption spectroscopy reveals at least three different species of sulfur, *Microbiology (UK)* **2002**, *148*, 267-276.
10. A. J. H. Janssen, G. Lettinga, A. de Keizer, Removal of hydrogen sulphide from wastewater and waste gases by biological conversion to elemental sulphur. Colloidal and interfacial aspects of biologically produced sulphur particles, *Colloids Surf. A-Physicochem. Eng. Asp.* **1999**, *151*, 389-397.
11. A. Janssen, A. de Keizer, A. van Aelst, R. Fokkink, H. Yangling, G. Lettinga, Surface characteristics and aggregation of microbiologically produced sulphur particles in relation to the process conditions, *Colloids Surf. B-Biointerfaces* **1996**, *6*, 115-129.
12. J. Boulègue, Solubility of elemental sulfur in water at 298 K, *Phosphorus Sulfur Silicon Relat. Elem.* **1978**, *5*, 127-128.
13. G. Schwarzenbach, A. Fischer, Die Acidität der Sulfane und die Zusammensetzung wässeriger Polysulfidlösungen, *Helv. Chim. Acta* **1960**, *169*, 1365-1392.
14. R. Steudel, The chemical sulfur cycle. In *Environmental technologies to treat sulfur pollution. Principles and engineering* (Eds.: P. Lens, L. Hulshoff Pol), IWA Publishing, London, **2000**, pp. 1-31.
15. W. Giggenbach, Optical spectra and equilibrium distribution of polysulfide ions in aqueous solution at 20 ºC, *Inorg. Chem.* **1972**, *11*, 1201-1207.
16. R. H. Arntson, F. W. Dickson, G. Tunell, Saturation curves of orthorhombic sulfur in the system S-Na_2S-H_2O at 25 °C and 50 °C, *Science* **1958**, *128*, 716-718.
17. A. Teder, The equilibrium between elementary sulfur and aqueous polysulfide ions, *Acta Chem. Scan.* **1971**, *25*, 1722-1728.
18. W. Giggenbach, Equilibria involving polysulfide ions in aqueous sulfide solutions up to 240 ºC, *Inorg. Chem.* **1974**, *13*, 1724-1730.
19. H. Gerischer, Über die Auflösungsgeschwindigkeit von Schwefel in Sulfid- und Polysulfidlösungen, *Z. Anorg. Allg. Chem.* **1949**, *259*, 220.
20. N. Hartler, J. Libert, A. Teder, Rate of sulfur dissolution in aqueous sodium sulfide, *Ind. Eng. Chem. Proc. Des. Develop.* **1967**, *6*, 398-406.
21. H. G. Trüper, H. G. Schlegel, Sulphur metabolism in Thiorhodaceae I. Quantitative measurements on growing cells of *Chromatium okenii*, *Antonie van Leeuwenhoek* **1964**, *30*, 225-238.
22. L. G. Danielsson, X. S. Chai, M. Behm, L. Renberg, UV characterization of sulphide-polysulphide solutions and its application for process monitoring in

the electrochemical production of polysulphides, *J. Pulp Paper Sci.* **1996**, *22*, J187-J191.
23. A. Teder, Spectrophotometric determination of polysulphide excess sulfur in aqueous solutions, *Svensk Papperst.* **1967**, *6*, 197-200.
24. *Handbook of chemistry and physics*, 82nd ed. (Ed.: D. R. Lide), CRC Press, Boca Raton, FL, **2001**, p 4-155.
25. J. Lyklema, *Fundamentals of interface and colloid science. Volume I: Fundamentals*, Academic Press, London, **1991**, p 7.52.
26. R. Steudel, Inorganic polysulfides S_n^{2-} and radical anions $S_n^{\bullet-}$, *Top. Curr. Chem.* **2003**, *231*, 127-152.
27. W. Pasiuk-Bronikowska, J. Ziajka, T. Bronikowski, Mechanism and kinetics of sulphide sulphur autoxidation. In *Autoxidation of sulphur compounds*, Ellis Horwood Limited, Chichester, **1992**, pp. 63-79.
28. P. L. Brezonik, *Chemical kinetics and process dynamics in aquatic systems*, Lewis Publishers, Boca Raton, **1994**, p 157 and 189.
29. A. M. James, Charge properties of microbial cell surfaces. In *Microbial cell surface analyses* (Eds.: N. Mozes, P. S. Handley, H. J. Busscher, P. G. Rouxhet), VCH Publishers Inc., New York, **1991**, pp. 223-262.
30. R. Guerrero, J. Mas, C. Pedrós-Alió, Buoyant density changes due to intracellular content of sulfur in *Chromatium warmingii* and *Chromatium vinosum*, *Arch. Microbiol.* **1984**, *137*, 350-356.
31. W. Sung, J. J. Morgan, Kinetics and product of ferrous iron oxygenation in aqueous systems, *Environ. Sci. Technol.* **1980**, *14*, 561-568.
32. I. Suzuki, Oxidation of inorganic sulfur compounds: chemical and enzymatic reactions, *Can. J. Microbiol.* **1999**, *45*, 97-105.

Chapter 4

Equilibrium of the reaction between dissolved sodium sulfide and biologically produced sulfur*

Abstract

The equilibrium of the heterogeneous reaction between dissolved sodium sulfide and biologically produced sulfur particles has been studied. Biologically produced sulfur was obtained from a bioreactor of a hydrogen sulfide removal process in which the dominating organism is *Thiobacillus* sp. W5. Detailed knowledge of this reaction is essential to understand its effect on the process. The results were compared with the equilibrium of the reaction of sulfide with 'inorganic' elemental sulfur. The equilibrium between dissolved sodium sulfide and biologically produced sulfur particles can be described by an equilibrium constant, K_x, which consists of a weighted sum of constants for polysulfide ions of different chain length, rather than a true single equilibrium constant. For biologically produced sulfur pK_x = 9.10 ± 0.08 (21 °C) and 9.17 ± 0.09 (35 °C) with an average polysulfide chain length x = 4.91 ± 0.32 (21 °C) and 4.59 ± 0.31 (35 °C). The pK_x value for biologically produced sulfur is significantly higher than for reaction of dissolved sodium sulfide with inorganic sulfur (pK_x = 8.78; 21 °C). This difference is probably caused by the negatively charged polymeric organic layer, which is present on biologically produced sulfur but absent with "inorganic" sulfur. Specific binding of polysulfide ions to the organic layer results in a higher polysulfide concentration at the reaction site compared to the bulk concentration. This results in an apparent decrease of the measured equilibrium constant, K_x.

Keywords

Biologically produced sulfur, polysulfide, hydrogen sulfide, heterogeneous equilibrium, *Thiobacillus*

* W.E. Kleinjan, A. de Keizer, A.J.H. Janssen, Equilibrium of the reaction between dissolved sodium sulfide and biologically produced sulfur, *Colloids Surf. B-Biointerfaces* (in press).

4.1. Introduction

As an alternative to physicochemical processes for the removal of hydrogen sulfide from gas streams, which generally require high temperature, high pressure, and special chemicals, the use of a biotechnological process can be an interesting option. Several microorganisms have been studied for application in biotechnological H_2S removal systems (see for a review [1]) but the chemoautotrophic bacteria of the genus *Thiobacillus* have been studied and used mostly. Buisman *et al*. [2] used a mixed culture of *Thiobacilli* for the aerobic oxidation of sulfide to elemental sulfur and studied technological applications. Visser *et al*. [3] showed the dominant organism in this mixed culture to be the new organism *Thiobacillus* sp. W5. This process was further developed and is currently used in a number of full-scale installations [4, 5].
The hydrogen sulfide removal process basically consists of a gas absorber, where gaseous H_2S is absorbed from a gas stream by a mildly alkaline solution (Eqs. 4.1 and 4.2), and a bioreactor in which the dissolved HS^- is microbiologically converted to elemental sulfur and a hydroxyl ion is regenerated (Eq. 4.3). Part of the sulfur is then led back to the gas absorber, suspended in a regenerated liquid recycle stream. The net produced elemental sulfur is separated from the liquid in a settler.

$$H_2S(g) \rightleftarrows H_2S(aq) \tag{4.1}$$

$$H_2S(aq) + OH^- \rightarrow HS^- + H_2O \tag{4.2}$$

$$HS^- + \tfrac{1}{2}O_2 \rightarrow S^0 + OH^- \tag{4.3}$$

The biologically produced sulfur (or 'biosulfur') is of oxidation state zero and is therefore often described as S^0, although it should not be mistaken for atomic sulfur. Biologically produced sulfur can occur in different modifications for different sulfide-oxidizing bacteria (see for a review [6]). In this paper we will use the term biologically produced sulfur to refer to sulfur produced in a biotechnological H_2S removal process in which the chemotrophic *Thiobacillus* sp. W5 is the dominating organism.
The exact nature of the biologically produced sulfur particles produced in the process is not completely clear but it is likely that sulfur in the particles is present as S_8 rings. Studies by X-ray absorption near edge spectroscopy (XANES) [7] indicated that sulfur globules produced by chemotrophic bacteria, such as the dominating organism *Thiobacillus* sp. W5 [3], consist of either S_8 rings or polythionates. Because polythionates are not stable at the alkaline conditions of the process, their presence in the sulfur particles is not likely. X-ray diffraction studies showed that sulfur rings are present in the sulfur particles produced in this process [8], and it is therefore most likely that the sulfur atoms are present as S_8 rings.

Biologically produced sulfur is hydrophilic and dispersible in water, contrary to 'inorganic' elemental sulfur (S_8), which is very poorly soluble in water (5 μg L^{-1}) [9] and strongly hydrophobic. Biologically produced sulfur consists of particles which can grow up to 1 μm in size but which can form aggregates of up to 3 mm [10]. The sulfur particles consist of a core of sulfur, on the surface of which polymeric organic compounds such as proteins are adsorbed. These organic polymers give sterical and electrical stabilization of the colloidal particles.

Reaction of biologically produced sulfur particles with dissolved hydrogen sulfide results in formation of polysulfide anions S_x^{2-}. The overall reaction between elemental sulfur in its most common form (S_8 rings) and dissolved sulfide is shown in Eq. 4.4, but polysulfide formation can also occur with other forms of elemental sulfur [11].

$$HS^- + \frac{x-1}{8} S_8 \rightleftarrows S_x^{2-} + H^+ \qquad (4.4)$$

Polysulfide ions are unbranched chains of sulfur atoms, related to the polysulfanes H_2S_n. The acidity constants of the polysulfanes are not known accurately, but must be so low that polysulfide ions in aqueous solution will practically always be completely deprotonated [12, 13]. At neutral to intermediate alkalinities S_6^{2-}, S_5^{2-} and S_4^{2-} ions dominate the solution. The shorter chains S_3^{2-} and S_2^{2-} have only been observed at very high alkalinities (pH > 14) [14]. Recently, this was confirmed in a study where polysulfide ions were methylated and subsequently separated by chromatography [15]. Chromatograms showed the largest peaks for $(CH_3)_2S_n$ for n = 4, 5, and 6, with trace peaks at n = 2 and 3, and also small peaks at n = 7, 8, and 9. At mildly alkaline conditions and when in equilibrium with excess sulfur, the reported average chain lengths vary from x = 4.6 [14], 4.8 [16], 5.4 [17], to 5.5 [13]. Under acidic conditions polysulfide ions are not stable. Somewhat contradictory results have been reported on the effect of temperature on the average polysulfide ion chain length. According to Teder [17] the average chain length increases with increasing temperature (x = 5.0 at 25 °C; x = 6.5 at 80 °C), whereas Giggenbach [18] reported only small variations of x up to 180 °C (x = 4.5 ± 0.1).

For a good understanding of the hydrogen sulfide removal process, detailed knowledge of the kinetics and equilibrium of the heterogeneous reaction between dissolved hydrogen sulfide and biologically produced sulfur is required. In a previous study [19] we investigated the kinetics of this reaction and compared it to a study on the reaction of sulfide with 'inorganic' elemental sulfur [20]. For both types of elemental sulfur the reaction takes place at the surface of the solid sulfur and presence of polysulfide ions as (auto)catalyst increases the rate of dissolution of elemental sulfur. The observed reaction rate of the reaction of sulfide with 'biosulfur' is limited by chemical reaction rate, contrary to earlier reported for the reaction of sulfide with 'inorganic' granular sulfur, which was diffusion rate limited. The small particle size

or the specific hydrophilic surface properties probably make the surface of the biologically produced sulfur particles more easily available for reaction than the surface of granular sulfur.

Teder [17] studied the equilibrium of the reaction between sulfide and granular sulfur (Eq. 4.4). The reaction was defined as

$$(n-1)\,S^0 + HS^- + OH^- \rightleftarrows S_n^{2-} + H_2O \tag{4.5}$$

and assumed that when elemental sulfur is present in excess, the activity of elemental sulfur can be considered constant so that the equilibrium constant of the reaction between elemental sulfur and polysulfide ions of different size (n = 2–6) can be written as

$$K_n = \frac{[S_n^{2-}]}{[HS^-][OH^-]} \times \frac{\gamma_{S_n^{2-}}}{\gamma_{HS^-}\gamma_{OH^-}} \tag{4.6}$$

The values of K_n for polysulfide ions of different chain length (K_2–K_6) are not well known. However, at a given temperature the relative amounts of the ions of different chain lengths will be constant when sulfur is present in excess.

$$[HS^-]\gamma_{HS^-}[OH^-]\gamma_{OH^-} = \frac{[S_2^{2-}]\gamma_{S_2^{2-}}}{K_2} = \frac{[S_3^{2-}]\gamma_{S_3^{2-}}}{K_3} = \ldots = \frac{[S_x^{2-}]\gamma_{S_x^{2-}}}{K_x} \tag{4.7}$$

Therefore, the corresponding average polysulfide ion chain length x will be constant as well. The average chain length x is defined by the ratio of the so-called *polysulfide excess sulfur concentration* (the total concentration of zero valent sulfur atoms in polysulfide ions, [S^0 in S_x^{2-}]) and the polysulfide ion concentration, [S_x^{2-}].

$$x = \frac{[S^0 \text{ in } S_x^{2-}]}{[S_x^{2-}]} = \frac{\sum_{n=2}^{n_{max}} \left((n-1)[S_n^{2-}]\right)}{\sum_{n=2}^{n_{max}} [S_n^{2-}]} \tag{4.8}$$

It is therefore possible to calculate the equilibrium constant K_x for polysulfide ions of the average chain length x in equilibrium with excess sulfur, without exact knowledge of K_2–K_6. The equilibrium constant K_x is therefore given by

$$K_x = \frac{[S_x^{2-}][H^+]}{[HS^-]} \times \frac{\gamma_{S_x^{2-}}\gamma_{H^+}}{\gamma_{HS^-}} = 10^{-pK_x} \tag{4.9}$$

Teder reported values of the ratio B = [HS^-][OH^-]/[S^0 in S_x^{2-}] of 1.5 × 10^{-6} M (25 °C) and 2.8 × 10^{-6} M (80 °C). When rewritten in the form of K_x and using the corresponding reported average polysulfide chain lengths, x = 5.0 (25 °C) and x = 6.5 (80 °C), the pK_x values are 8.78 (25 °C) and 9.19 (80 °C).

Because of differences in crystalline sulfur structure and surface properties between biologically produced sulfur and granular elemental sulfur, the equilibrium constants determined by Teder for the reaction of sodium sulfide with granular sulfur may not be directly applicable for biologically produced sulfur. It is therefore our objective to determine the equilibrium constant of the reaction between HS^- with biologically produced sulfur particles and compare it to the equilibrium between HS^- and 'inorganic' elemental sulfur. The principle of the experimental method reported by Teder to be the most accurate, the stepwise acidification of a polysulfide solution until elemental sulfur is formed in equilibrium with polysulfide ions, was used to verify the data reported by Teder for inorganic elemental sulfur. However, this method cannot be used to determine the equilibrium constant for the reaction of sodium sulfide with biologically produced sulfur. Elemental sulfur formed after acidification of a polysulfide solution does not have the specific properties of biologically produced sulfur particles, even if the polysulfide solution was originally made from reaction of sodium sulfide and 'biosulfur'. Therefore, the equilibrium constant for biologically produced sulfur was obtained by measuring concentrations of reagents, after equilibrium of the reaction of sodium sulfide with 'biosulfur' was established.

4.2. Materials and methods

4.2.1. Chemicals used

Biologically produced sulfur was obtained from a bioreactor of the wastewater treatment plant of Industriewater Eerbeek B.V. (The Netherlands). The suspension was dialyzed in deaerated water in order to remove salts until the conductivity of the sulfur suspension was below 40 μS cm^{-1} (approximately 0.1 mM $NaHCO_3$ + 0.1 mM $Na_2S_2O_3$). Suspensions were then filtered over a 3-μm filter in order to remove large sulfur aggregates.

Polysulfide solutions were prepared by dissolving crystals of Na_2S_4 (Alfa Aesar, H_2O content 5 % max) in deaerated water. Flasks were septum-sealed and solutions kept under an argon blanket. Furthermore, polysulfide solutions for UV spectroscopy calibration were prepared by reaction of granular sulfur (Aldrich, 99.99+ %) with a sodium sulfide solution until all sulfur was 'dissolved' (see section 4.2.3).

Sulfide solutions were prepared by removing the oxidized surface of $Na_2S{\cdot}9H_2O$ crystals (J.T. Baker) by flushing with deaerated water and subsequent dissolution of the crystals in deaerated water. The flasks were septum-sealed and the solutions were kept under argon. For each experiment sulfide solutions were freshly prepared.

4.2.2. Analysis

Sulfide concentrations were determined spectrophotometrically by the methylene blue method as described by Trüper and Schlegel [21]. The concentration of polysulfide

ions was determined spectrophotometrically at a wavelength of 285 nm. At this wavelength the polysulfide excess sulfur concentration (the total amount of zero valent sulfur atoms in polysulfide ions, [S^0 in S_x^{2-}]) can be determined, approximately independent of pH and ratio X_S [22, 23]. X_S consists of the ratio of polysulfide and total sulfide concentration in solution and should not be confused with the average polysulfide chain length x, which is defined in Eq. 4.8.

$$X_S = \frac{[S^0 \text{ in } S_x^{2-}]}{[S^{2-}]_{total}} = \frac{\sum_{n=2}^{n_{max}} \left((n-1)[S_n^{2-}] \right)}{\sum_{n=2}^{n_{max}} \left([S_n^{2-}] \right) + [H_2S] + [HS^-] + [S^{2-}]} \tag{4.10}$$

When dealing with polysulfide concentrations it is essential to distinguish polysulfide ion concentrations, [S_x^{2-}] from polysulfide excess sulfur concentrations, [S^0 in S_x^{2-}]. It is possible to calculate one from the other when the average chain length x is known.

$$(x-1)[S_x^{2-}] = [S^0 \text{ in } S_x^{2-}] \tag{4.11}$$

The total sulfur concentration was determined by weight, after filtration over a 0.22-μm filter and subsequent washing with demineralized water to remove any salts. The pH was determined with a calibrated pH-combination electrode (Schott).

4.2.3. Calibration

Calibration of the spectrophotometric method for measuring the polysulfide excess sulfur concentration was performed in two ways. First, polysulfide solutions were made from reaction of known amounts of sulfur with sulfide until all sulfur was 'dissolved'. This was done at different X_S ratios and different pH values. Second, polysulfide solutions were made by dissolving crystals of Na_2S_4.

Figure 4.1.a (pH = 10) and Figure 4.1.b (pH = 8) show calibration curves of polysulfide solutions made from reaction of granular sulfur with sodium sulfide until all sulfur is dissolved, for X_S = 0.2 and 2.0. The pH was adjusted to the desired value by addition of NaOH or HCl. The molar extinction coefficient ε is based on the so-called polysulfide excess sulfur concentration and therefore independent of the average chain length x. It can be seen that the ratio X_S has no significant effect on the molar extinction coefficient. The molar extinction coefficient does vary somewhat with pH. At higher pH the extinction coefficient decreases, possibly because of a shorter average chain length of the polysulfide chains at higher pH. The values of the molar extinction coefficients (pH = 8: 1390 L mol^{-1} cm^{-1}; pH = 10: 1350 L mol^{-1} cm^{-1}) are approximately equal to literature data (1360, 1325 L mol^{-1} cm^{-1} [12, 23]). In further experiments, the molar extinction coefficient determined for pH = 10 was used for the measurements at the pH range 9.0–11.2. Below pH = 9.0, we used the value determined for pH = 8.

From Figure 4.1.c it can be seen that the molar extinction coefficient of dissolved Na_2S_4 is considerably lower than of polysulfide solutions made from reaction of granular sulfur with sodium sulfide (1024 L mol^{-1} cm^{-1}). The explanation is probably in some impurities of the Na_2S_4 crystals. Due to rapid oxidation with oxygen commercial polysulfides usually contain some thiosulfate as impurity [24]. For this reason in further measurements the molar extinction coefficients determined from reaction of elemental sulfur and sodium sulfide are used: 1390 (pH = 8) or 1350 L mol^{-1} cm^{-1} (pH = 10). The polysulfide concentration of a polysulfide solution prepared by dissolving Na_2S_4 crystals is therefore also measured by UV spectroscopy using these extinction coefficients.

4.2.4. Method of measuring the equilibrium

For determining the equilibrium constant with biologically produced sulfur, a set of 8 mixtures was made of a dialyzed sulfur suspension and a deaerated $Na_2S{\cdot}9H_2O$ solution (total volume 50 mL). The ratio total sulfur / total sulfide was varied from 1.95 to 19.5. The septum-sealed samples were kept under argon and mixed with magnetic stirrers in a thermostated hood until equilibrium was reached (≈ 16 h). After mixing, the total sulfide and polysulfide excess sulfur concentrations were measured, as well as the pH. This was done at 21 °C and 35 °C.

For 'inorganic' granular sulfur the above method was not found suitable due to the very slow dissolution of the sulfur at low temperatures (> 6 d). Instead, the equilibrium constant was determined by acidification of a polysulfide solution of known composition and concentration. A polysulfide solution was prepared by dissolving Na_2S_4 crystals in deaerated water. The polysulfide excess sulfur concentration was then measured by UV spectroscopy (ε = 1350 L mol^{-1} cm^{-1}; [S^0 in

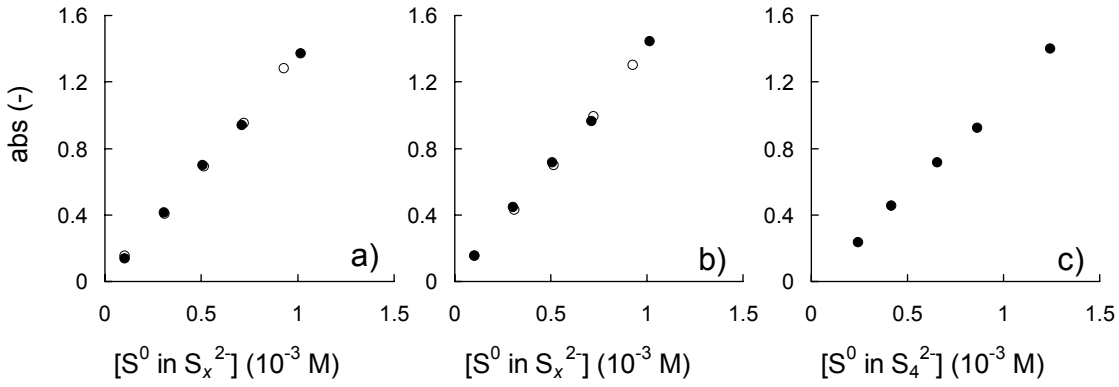

Figure 4.1.a) Calibration curves for polysulfide solutions made from reaction of granular sulfur with sodium sulfide at pH = 10 for X_S = 2.0 (○) and X_S = 0.2 (●), ε = 1350 L mol^{-1} cm^{-1}. **b)** Same for pH = 8, ε = 1390 L mol^{-1} cm^{-1}. **c)** Calibration curve for polysulfide solutions made by dissolving crystals of Na_2S_4, ε = 1024 L mol^{-1} cm^{-1}.

S_x^{2-}] = 0.75 mM). 250 mL of this solution was charged under argon to a 500 mL thermostated (T = 21 °C) septum-sealed round bottom glass flask. Subsequently the pH was decreased stepwise (approximately from pH 11 to 6) by addition of a concentrated HCl solution with a syringe through the septum. During the acidification sulfur precipitated and the polysulfide concentration decreased. After each step, the solution was thoroughly mixed until the pH reached a stable value and the polysulfide excess sulfur concentration was measured. This experiment was performed with polysulfide solutions of three different ratios X_S (3.0, 0.39, and 0.21), by changing the concentration of additional sodium sulfide to the polysulfide solution.

4.3. Modeling the equilibrium between elemental sulfur and a sulfide solution

4.3.1. Henry constant, equilibrium constants, and activity coefficients

The equilibrium between the partial H_2S pressure and the H_2S concentration in the liquid (water) phase can be described with the Henry constant H (Pa m^3 mol^{-1}). At constant pressure and sufficiently low $[H_2S]_L$, the equilibrium can be described with

$$p_{H_2S} = H_{H_2S}[H_2S]_L \tag{4.12}$$

Edwards *et al*. [25] reported the Henry constant of H_2S as function of temperature

$$\ln H_{H_2S}' = \frac{B_1}{T} + B_2 \ln T + B_3 T + B_4 \tag{4.13}$$

with $B_1 = -13236.8$, $B_2 = -55.0551$, $B_3 = 0.0595651$, and $B_4 = 342.595$. H_{H2S}' has the units (atm kg mol^{-1}) and is related to H_{H2S} with

$$H_{H_2S} = 1.01325 \times 10^5 H_{H_2S}' / \rho_w \tag{4.14}$$

in which ρ_w is the density of water (kg m^{-3}). The equilibrium between gas and liquid phase is also often described in terms of the distribution coefficient m, a dimensionless form of the Henry constant. The H_2S concentrations (mol m^{-3}) in gas- and liquid phases at the interface are related to m through

$$[H_2S]_L = m[H_2S]_G \tag{4.15}$$

The distribution coefficient m can be calculated from the Henry constant using

$$m = RT / H_{H_2S} \quad (m_G^3 / m_L^3) \tag{4.16}$$

Hydrogen sulfide dissolved in water is in equilibrium with HS^- and S^{2-}. At 20 °C the equilibrium constants are [13]

$$K_1 = \frac{[HS^-][H^+]}{[H_2S]} \times \frac{\gamma_{HS^-}\gamma_{H^+}}{\gamma_{H_2S}} = 10^{-7} \qquad \text{mol L}^{-1} \tag{4.17}$$

$$K_2 = \frac{[S^{2-}][H^+]}{[HS^-]} \times \frac{\gamma_{S^{2-}}\gamma_{H^+}}{\gamma_{HS^-}} = 0.8 \times 10^{-17} \text{ mol L}^{-1} \quad (4.18)$$

In earlier reports other values of K_2 have been reported, e.g., [26], but in all cases K_2 is so low that the equilibrium with S^{2-} can be neglected at intermediate pH values.
The activity coefficients in Eqs. 4.17 and 4.18 can be calculated with the extended Debye-Hückel law, which applies for values of the ionic strength I up to approximately 0.1 M [27]. For an activity coefficient γ_i for component i

$$\log \gamma_i = -\frac{z_i^2 A\sqrt{I}}{1+\beta a_i \sqrt{I}} \quad (4.19)$$

In this relation A and β are constants characteristic for the solvent. For water at 25 °C, A = 0.509 (mol$^{-½}$ L^{½}), and β = 0.328 × 10^8 (mol$^{-½}$ L^{½} m^{-1}). Furthermore, a_i is the effective ionic diameter or the distance of closest approach to the central ion i (m), and the ionic strength I (mol L^{-1}) is given by Eq. 4.20. Estimates of the effective ionic diameters can be made for different ions and are shown in Table 4.1.

$$I = \tfrac{1}{2}\sum z_i^2[\mathrm{i}] \quad (4.20)$$

4.4. Results and discussion

4.4.1. Biologically produced sulfur

A set of 8 mixtures of a dialyzed biologically produced sulfur suspension and a deaerated sulfide solution was made and stirred in a thermostated hood. The total sulfur concentration before equilibrium was 32.5 mM and the total sulfide concentration before equilibrium varied from 1.67 to 16.7 mM. When equilibrium was reached (≈ 16 h), the total sulfide and polysulfide excess sulfur concentrations were again measured, as well as the pH. Data are reported in Tables 4.2 (21 °C) and 4.3 (35 °C).
A comparison between the total sulfide concentrations before and after equilibrium is shown in Figure 4.2.a. Before equilibrium, only free sulfide (H_2S, HS^-, and S^{2-}) contributes to the measurement. After equilibrium however, part of the sulfide is bound to elemental sulfur in polysulfide ions. The total sulfide concentrations before

Table 4.1. Estimates of the effective ionic diameter for calculation of activity coefficients from extended Debye-Hückel law. Values for HS^- and H^+ are from [28]. The value for S_x^{2-} is an estimate.

component	a_i (× 10^{-10} m)
HS^-	3.0
S_x^{2-}	4.0
H^+	9.0

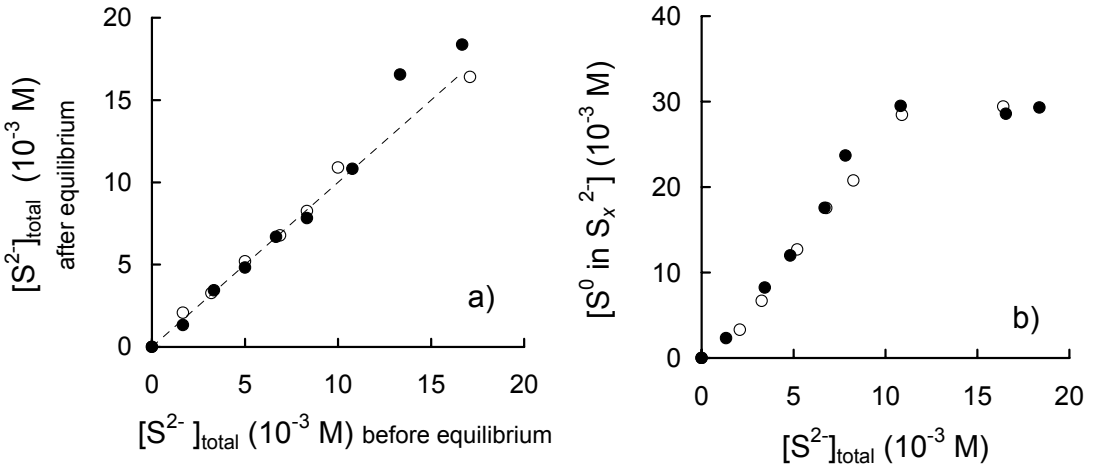

Figure 4.2.a) The total sulfide concentration before and after equilibrium of its reaction with biologically produced sulfur. The straight line represents the case where the total sulfide concentrations before and after equilibrium are equal. **b)** Polysulfide excess sulfur concentration as a function of the total sulfide concentration after equilibrium of the reaction between sodium sulfide and biologically produced sulfur. Initial total sulfur concentration, c_{S0} = 32.5 mM. T = 21 °C (●) and 35 °C (○).

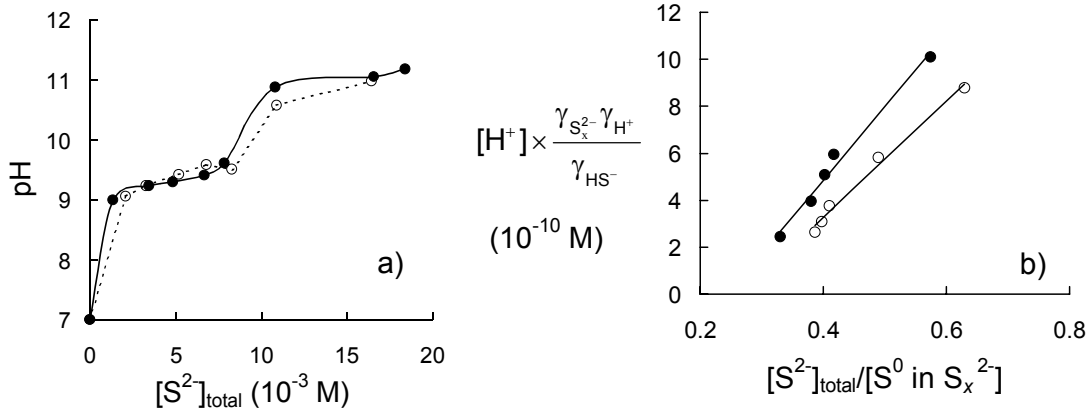

Figure 4.3.a) pH as a function of the total sulfide concentration after equilibrium of the reaction between sodium sulfide and biologically produced sulfur. **b)** Linearization of the equilibrium data of the reaction between sodium sulfide and biologically produced sulfur according to Eq. 4.23. The intercept at the vertical axis equals $-K_x$ and the slope equals $(x-1)K_x$. Initial total sulfur concentration, c_{S0} = 32.5 mM. T = 21 °C (●) and 35 °C (○).

and after equilibrium are approximately equal. Only at higher sulfide concentrations some deviations from complete equality (the dotted line) were measured. We can therefore conclude that polysulfide ions and sulfide ions contribute in the same way to the total sulfide concentration measurement. This was to be expected because the solution is acidified in the analysis, resulting in the formation of HS^- (reverse of Eq. 4.4). At the experimental pH range (pH = 9.0–11.2), the H_2S and S^{2-} concentrations are negligible and the actual HS^- concentration can be obtained by subtracting the polysulfide concentration from the total sulfide concentration.

$$[HS^-] = [S^{2-}]_{total} - [S_x^{2-}] \tag{4.21}$$

In Figure 4.2.b the polysulfide excess sulfur concentration after equilibrium is shown as a function of the total sulfide concentration after equilibrium. The polysulfide excess sulfur concentration increases linearly with increasing total sulfide concentration until all sulfur is dissolved, resulting in a clear solution. The polysulfide excess sulfur concentration then remains constant. In Figure 4.3.a the pH after equilibrium is shown. Below $[S^{2-}]_{total} \approx 10$ mM, the pH is a result of the polysulfide equilibrium, whereas above this concentration there is an excess of sulfide and therefore a jump in pH.

For the solutions that are in equilibrium with an excess of elemental sulfur ($[S^{2-}]_{total} <$

Table 4.2. Experimental data for measuring the equilibrium constant with biologically produced sulfur particles. Initial total sulfur concentration, $c_{S0} = 32.5$ mM; $T = 21$ °C.

	before equilibrium		**after equilibrium**			
	$[S^{2-}]_{total}$ (mM)	**X_s**		**$[S^0$ in $S_x^{2-}]$ (mM)**	**$[S^{2-}]_{total}$ (mM)**	**pH**
1	1.67	19.5	turbid	2.32	1.33	9.00
2	3.33	9.75	turbid	8.24	3.44	9.23
3	5.00	6.50	turbid	11.99	4.82	9.30
4	6.67	4.88	turbid	17.56	6.69	9.40
5	8.33	3.90	clear	23.68	7.83	9.61
6	10.77	2.79	clear	29.49	10.83	10.87
7	13.33	2.44	clear	28.59	16.55	11.04
8	16.67	1.95	clear	29.31	18.37	11.17

Table 4.3. Experimental data for measuring the equilibrium constant with biologically produced sulfur particles. Initial total sulfur concentration, $c_{S0} = 32.5$ mM; $T = 35$ °C.

	before equilibrium		**after equilibrium**			
	$[S^{2-}]_{total}$ (mM)	**X_s**		**$[S^0$ in $S_x^{2-}]$ (mM)**	**$[S^{2-}]_{total}$ (mM)**	**pH**
1	1.67	19.5	turbid	3.30	2.08	9.06
2	3.19	10.3	turbid	6.68	3.27	9.23
3	5.00	6.50	turbid	12.70	5.20	9.42
4	6.89	4.64	turbid	17.55	6.78	9.58
5	8.33	3.90	clear	20.77	8.26	9.51
6	10.00	3.25	clear	28.44	10.90	10.57
7	16.67	1.95	clear	29.42	16.41	10.97

10 mM), the equilibrium constant K_x can be defined by Eq. 4.9. We can rewrite this relation by combining it with Eqs. 4.11 and 4.21 to

$$K_x = \frac{[S_x^{2-}][H^+]}{[HS^-]} \times \frac{\gamma_{S_x^{2-}}\gamma_{H^+}}{\gamma_{HS^-}} = \frac{[S^0 \text{ in } S_x^{2-}][H^+]}{(x-1)\left([S^{2-}]_{total} - \frac{[S^0 \text{ in } S_x^{2-}]}{(x-1)}\right)} \times \frac{\gamma_{S_x^{2-}}\gamma_{H^+}}{\gamma_{HS^-}} \qquad (4.22)$$

The above relation can be transformed to a linear relation consisting of $[H^+] \times \gamma_{Sx(2-)}\gamma_{H(+)} / \gamma_{HS(-)}$ as a function of $[S^{2-}]_{total} / [S^0 \text{ in } S_x^{2-}]$ (Eq. 4.23).

$$[H^+] \times \frac{\gamma_{S_x^{2-}}\gamma_{H^+}}{\gamma_{HS^-}} = (x-1)K_x \frac{[S^{2-}]_{total}}{[S^0 \text{ in } S_x^{2-}]} - K_x \qquad (4.23)$$

In a plot of $[H^+] \times \gamma_{Sx(2-)}\gamma_{H(+)} / \gamma_{HS(-)}$ vs. $[S^{2-}]_{total} / [S^0 \text{ in } S_x^{2-}]$, $-K_x$ can be determined from the intercept at the $[H^+]\gamma_{Sx(2-)}\gamma_{H(+)}/\gamma_{HS(-)}$-axis and $(x-1)$ can then be obtained from the slope. This is shown in Figure 4.3.b. From this plot we obtain $pK_x = 9.10 \pm 0.08$ with an average polysulfide chain length $x = 4.91 \pm 0.32$ (21 °C) and $pK_x = 9.17 \pm 0.09$ and $x = 4.59 \pm 0.31$ (35 °C). Differences in both pK_x and x at 21 or 35 °C are within the experimental error and therefore not significant. Slopes, intercepts and their standard deviations were calculated with linear regression according to [29]. Although the ratio $[S^{2-}]_{total} / [S^0 \text{ in } S_x^{2-}]$ is not constant in the linearization in Figure 4.3.b, the average chain length x can be considered constant because all mixtures are in equilibrium with excess elemental sulfur.

One can speculate whether the observed equilibrium between biologically produced sulfur and polysulfide ions is a "true" chemical equilibrium. Biologically produced sulfur differs from "inorganic" sulfur in sulfur structure and in surface properties. The sulfur in biologically produced sulfur is believed to consist of an amorphous structure, which is thermodynamically unstable and which will eventually be converted into crystalline elemental sulfur. In this sense, the observed equilibrium may rather be seen as an intermediate- or pseudo-equilibrium. Within the time measured (equilibrium was established after ≈ 16 h and no significant changes in concentrations were measured within 24 h after this), an apparent equilibrium was observed. However, ultimately, all biosulfur will be converted into crystalline sulfur resulting in a different equilibrium.

Furthermore, there is a possibility that reaction of biosulfur with sulfide (Eq. 4.4) contributes to the conversion of biosulfur to crystalline elemental sulfur, as in the back reaction of Eq. 4.4 an "inorganic" form of elemental sulfur may be formed. Initially, the 'nascent' elemental sulfur is formed in short sulfur chains or S_8 rings. This may precipitate to form crystalline elemental sulfur, however, it may also be relocated at the biosulfur particle in the form of an amorphous sulfur structure. This is

not unlikely as the original form of biosulfur is believed to be formed through polysulfide ions [11], just as in the equilibrium described.

4.4.2. Inorganic elemental sulfur

For inorganic elemental sulfur, the equilibrium constant was determined by acidification of a polysulfide solution and measurement of the polysulfide excess sulfur concentration for each pH. Upon acidification of a polysulfide solution of volume V_L in a glass flask with a headspace of volume V_G, sulfur precipitates and HS^- is formed. Also, the equilibrium of HS^- with dissolved and gaseous H_2S rearranges upon acidification of a polysulfide solution. The following reactions take place.

$$S_x^{2-} + H^+ \rightleftarrows (x-1)\,S^0 + HS^- \tag{4.24}$$

$$HS^- + H^+ \rightleftarrows H_2S(aq) \tag{4.25}$$

$$H_2S(aq) \rightleftarrows H_2S(g) \tag{4.26}$$

The corresponding equilibria can be represented with Eqs. 4.9, 4.17, and 4.15, respectively. Because of the low value of K_2 (Eq. 4.18) we have neglected the contribution of S^{2-} ions at the experimental pH range (≈ 6–11).
The total molar sulfide and sulfur balances can be written as

$$\text{total sulfide} = V_G[H_2S]_G + V_L[H_2S] + V_L[HS^-] + V_L[S_x^{2-}] \quad \text{(mol)} \tag{4.27}$$

$$\text{total sulfur} = V_L\,(x-1)[S_x^{2-}] + V_L[S^0] \quad \text{(mol)} \tag{4.28}$$

Here, $V_L[S^0]$ represents the total amount of precipitated elemental sulfur. The maximum polysulfide ion concentration is determined by the total amount of elemental sulfur.

$$0 \le [S_x^{2-}] \le [S_x^{2-}]_{max} = \frac{\text{total sulfur}}{V_L\,(x-1)} \tag{4.29}$$

Solving Eqs. 4.9, 4.15, 4.17, 4.27, and 4.29 for $[S_x^{2-}]$ results in Eq. 4.30. With this relation, the equilibrium polysulfide concentration at given total sulfide and total sulfur contents can be calculated as a function of pH. Comparison of calculated results with measured values allows verification of the reported value of K_x.

$$[S_x^{2-}] = \frac{\text{total sulfide}}{V_L + \dfrac{V_G[H^+]^2\gamma_{S_x^{2-}}\gamma_{H^+}{}^2}{mK_1K_x\gamma_{H_2S}} + \dfrac{V_L[H^+]^2\gamma_{S_x^{2-}}\gamma_{H^+}{}^2}{K_1K_x\gamma_{H_2S}} + \dfrac{V_L[H^+]\gamma_{S_x^{2-}}\gamma_{H^+}}{K_x\gamma_{HS^-}}} \tag{4.30}$$

In Figure 4.4 the measured polysulfide excess sulfur concentration is shown as a function of pH (data points). The lines represent theoretical polysulfide excess sulfur

concentrations calculated with Eq. 4.30. The value of K_x used in this calculation was based on the parameter B, reported by Teder [17], $B = [HS^-][OH^-]/[S^0 \text{ in } S_x^{2-}] = 1.5 \times 10^{-6}$ (M). For an average polysulfide ion chain length $x = 4$, this corresponds to $pK_x = 8.65$. For $x = 5$ this corresponds to $pK_x = 8.78$. Activity coefficients for the ions were calculated using the extended Debye-Hückel law (Eq. 4.19). The activity coefficient for the nonionic component H_2S was taken to be one. The open circles represent the data of a polysulfide solution prepared by dissolving Na_2S_4 crystals without extra sulfide ($X_S = 3.0$). In the other series of data points additional sodium sulfide is added to the same polysulfide solution (black squares: $X_S = 0.39$, open diamonds: $X_S = 0.21$). Upon acidification, the polysulfide concentration decreases and sulfur precipitates. It can be seen that the stability of a polysulfide solution at various pH values is highly dependent on the ratio X_s. Without extra sodium sulfide present ($X_S = 3.0$), polysulfide ions start precipitating already at a pH of 10. At the low X_s ratio of 0.21, polysulfides are stable above pH = 8.0. When an acidified solution is brought back to alkaline pH again, the precipitated sulfur can be redissolved and the polysulfide concentration reaches approximately 99 % of its initial value (result not shown).

Figure 4.4 clearly shows that the experimental data for $X_S = 3.0$ correspond to the values calculated with Eq. 4.30 in which K_x was based on data previously reported by Teder [17]. At a lower ratio of X_S the theoretical lines correspond to the data points at low pH, but show deviations at higher pH. A possible explanation for this is that at the higher pH values no equilibrium was reached. In the heterogeneous reaction equilibrium (Eq. 4.9) the contribution of solid elemental sulfur will be constant as long as there is an excess of solid sulfur. The time needed to establish this equilibrium, however, will not be constant. At the higher pH values of the measurements at $X_S = 0.39$ and 0.21, the excess of elemental sulfur will be smaller than at the lower pH values and therefore equilibrium will be reached faster. In

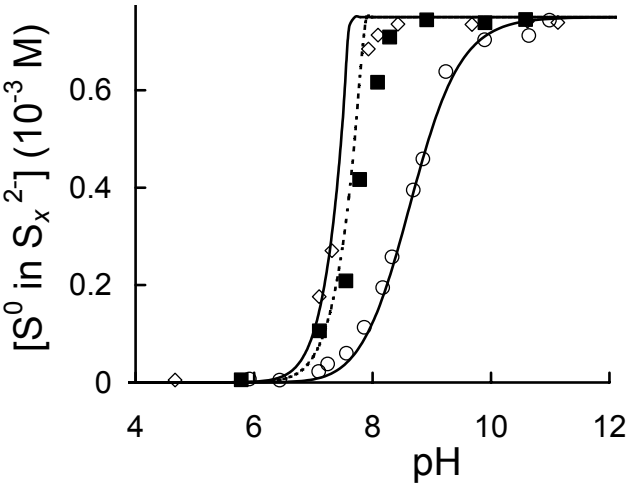

Figure 4.4. Polysulfide excess sulfur concentration as function of pH at different ratios X_S; $X_S = 0.21$ (◊); $X_S = 0.39$ (■); $X_S = 3.0$ (o). The corresponding lines are calculated with Eq. 4.30.

general, heterogeneous reactions are slow to reach equilibrium [27]. Possibly, reaching the equilibrium in the situation with a small amount of excess sulfur takes longer than the time needed to reach an apparently constant pH (for approximately 30 s).

The difference in steepness of the slopes with X_S results from the difference in the amount of sodium sulfide. When there is an excess of sodium sulfide (X_S = 0.39 and 0.21) the polysulfide ion concentration is limited by the total amount of elemental sulfur and at high pH values the equilibrium in Eq. 4.9 is not reached. During acidification the polysulfide concentration remains constant until the $[H^+]$ is high enough to reach the equilibrium of Eq. 4.9. Then the polysulfide ion concentration rapidly decreases. Without extra sulfide present (X_S = 3.0), both the amount of precipitated elemental sulfur and the amount of sulfide gradually increase during acidification. This results in a gradual decrease in polysulfide concentration

The data on the acidification of a polysulfide solution (21 °C) can be described by an average equilibrium constant pK_x = 8.78, which corresponds to an earlier determined constant $B = [HS^-][OH^-]/[S^0 \text{ in } S_x^{2-}] = 1.5 \times 10^{-6}$ (M). This constant involves the reaction of HS^- with 'inorganic' elemental sulfur because this type of sulfur is formed upon acidification of a polysulfide solution. The equilibrium constant of HS^- with biologically produced elemental sulfur particles is higher than for inorganic sulfur, pK_x = 9.10 ± 0.08 (21 °C). This means that with biologically produced sulfur the equilibrium lies more in the direction of elemental sulfur than with inorganic sulfur.

This difference must be either attributed to differences in sulfur structure or in surface properties. Although biologically produced sulfur is likely to be composed mainly of S_8 rings just as inorganic elemental sulfur, biologically produced sulfur is believed to have a more amorphous structure than the crystalline sulfur structure of inorganic sulfur. Isolation, drying, or ageing of sulfur globules have been reported to affect the crystalline structure of sulfur globules from various sulfide-oxidizing bacteria [7, 30, 31]. Thus, biologically produced sulfur can be assumed to be less stable and therefore more reactive. In this sense, one would expect a shift in equilibrium in the direction of polysulfide, contrary to our observations. However, the surface properties of biologically produced sulfur may result in a shift in equilibrium in the direction of biosulfur because of a specific binding of polysulfide ions to the organic polymer layer. This was previously observed in marine sediments where polysulfide ions can react with carbon-carbon unsaturated bonds in organic matter [32]. The equilibrium constant of the heterogeneous reaction K_x, without any specific binding of polysulfide ions, is essentially determined by the concentrations of reagents near the surface. These are related to the concentrations in the bulk by Boltzmann's law, describing the behavior of ions in an electrical double layer. When neglecting activity coefficients this can be described as

$$K_x = \frac{[S_x^{2-}]_s [H^+]_s}{[HS^-]_s} = \frac{[S_x^{2-}]_{bulk} e^{2e\Psi/kT} [H^+]_{bulk} e^{-e\Psi/kT}}{[HS^-]_{bulk} e^{e\Psi/kT}} = \frac{[S_x^{2-}]_{bulk} [H^+]_{bulk}}{[HS^-]_{bulk}} \quad (4.31)$$

Here, e is the elementary charge (C), Ψ the potential (V), and k the Boltzmann constant (J K^{-1}). When part of the polysulfide ions present near the surface are specifically bound to an organic polymer layer, the equilibrium constant can be written as

$$K_x = \frac{\left([S_x^{2-}]_{s,free} + [S_x^{2-}]_{s,bound}\right)[H^+]_s}{[HS^-]_s} = \ldots$$

$$\ldots = \frac{\left([S_x^{2-}]_{bulk,free} e^{2e\Psi/kT} + [S_x^{2-}]_{s,bound}\right)[H^+]_{bulk} e^{-e\Psi/kT}}{[HS^-]_{bulk} e^{-e\Psi/kT}} \quad (4.32)$$

As the bound polysulfide concentration is not measured in the bulk concentration, an apparent equilibrium K_x' is measured instead.

$$K_x' = \frac{[S_x^{2-}]_{bulk} [H^+]_{bulk}}{[HS^-]_{bulk}} < K_x \quad (4.33)$$

When polysulfide ions are bound to the organic layer, the apparent equilibrium constant K_x' will therefore be lower than the equilibrium constant K_x where no polysulfide ions are bound and pK_x' will be higher than pK_x.

Furthermore, shielding of reactants by the polymer layer may play a role. Although this can be expected to mainly affect the kinetics, an effect on equilibrium cannot be excluded completely. The above described effects of the particle surface on the measured equilibrium (especially specific binding of polysulfide ions) will result in a shift in equilibrium in the direction of biosulfur, as was also observed in our experiments. From this we can conclude that the differences in equilibrium between "inorganic" sulfur and polysulfide and the pseudo-equilibrium between biosulfur and polysulfide can mainly be attributed to the surface properties of biologically produced sulfur.

It should be noted that experiments have been performed with biologically produced sulfur obtained from a bioreactor in which the dominating organism is *Thiobacillus* sp. W5, which is believed to be composed of a core of sulfur rings with an organic polymer layer on the particle surface. Other sulfide-oxidizing bacteria are known to produce sulfur globules consisting of polythionates (e.g., *Acidithiobacillus ferrooxidans*) or long sulfur chains terminated with organic groups (e.g., *Allochromatium vinosum*) [7]. Equilibrium constants between dissolved sulfide and these forms of biologically produced sulfur may therefore be somewhat different.

Large sulfur aggregates were removed from the suspension to obtain a more uniform particle size. The same treatment of suspensions was used in a study on the kinetics of

the reaction between biologically produced sulfur and sodium sulfide [19]. Although aggregates of sulfur can be expected to be more crystalline in structure, they keep their hydrophilic properties, indicating that specific binding of polysulfide ions can still occur. A higher apparent pK_x compared to the equilibrium of 'inorganic' sulfur can therefore also be expected for aggregates of biosulfur, although the question to what extent this will occur remains open.

4.5. Conclusions

The equilibrium between dissolved sodium sulfide and biologically produced sulfur particles (from a bioreactor in which the dominating organism is *Thiobacillus* sp. W5) in the presence of an excess of elemental sulfur, can be described with an equilibrium constant for average polysulfide chain length, pK_x. For biologically produced sulfur pK_x = 9.10 ± 0.08 (21 °C) and 9.17 ± 0.09 (35 °C). The average polysulfide chain length x = 4.91 ± 0.32 (21 °C) and 4.59 ± 0.31 (35 °C). The pK_x value for biologically produced sulfur is higher than for reaction of dissolved sulfide with inorganic sulfur (pK_x = 8.78), meaning that with biologically produced sulfur the equilibrium lies more in the direction of elemental sulfur than with inorganic sulfur. The difference between biologically produced sulfur and inorganic sulfur is probably caused by the presence of a negatively charged organic polymer layer on the biosulfur particles. Particularly specific binding of polysulfide ions to the organic matter results in a shift in equilibrium towards biosulfur.

Nomenclature

$[A]_G$	concentration of component A in gas phase	mol L^{-1}
[A]	concentration of component A in liquid phase	mol L^{-1}
$[A]_0$	initial concentration of component A	mol L^{-1}
$[S_x^{2-}]$	concentration of polysulfide ion S_x^{2-}	mol L^{-1}
$[S^0$ in $S_x^{2-}]$	polysulfide excess sulfur concentration	mol L^{-1}
a_i	distance of closest approach to ion i	m
A	constant in Eq. 4.19	$mol^{-1/2}$ $L^{1/2}$
B	= $[HS^-][OH^-]/[S^0$ in $S_x^{2-}]$	mol L^{-1}
B_1–B_4	constants in Eq. 4.13	
c_{S0}	sulfur content	mol m^{-3}
e	elementary charge	C
H	Henry constant	Pa m^3 mol^{-1}
H'	Henry constant	atm kg mol^{-1}
I	ionic strength	mol L^{-1}
k	Boltzmann constant	J K^{-1}
K_1	equilibrium constant	mol L^{-1}
K_2	equilibrium constant	mol L^{-1}
K_x	equilibrium constant	mol L^{-1}
m	distribution coefficient between gas and liquid	m_G^3 m_L^{-3}

M	molar mass	g mol^{-1}
p	partial pressure	Pa
R	gas constant	J mol^{-1} K^{-1}
T	temperature	K or °C
V_G	volume of gas phase	m^3
V_L	volume of liquid phase	m^3
x	average polysulfide ion chain length	-
X_S	ratio S^0/S_x^{2-} in polysulfide ion	-
z	ionic valency	-
β	constant in Eq. 4.19	$mol^{-1/2}$ $L^{1/2}$ m^{-1}
ε	molar extinction coefficient	L mol^{-1} cm^{-1}
γ_i	activity coefficient of component i	-
ρ	density	g m^{-3}
Ψ	surface potential	V

References

1. J. E. Burgess, S. A. Parsons, R. M. Stuetz, Developments in odour control and waste gas treatment biotechnology: A review, *Biotechnol. Adv.* **2001**, *19*, 35-63.
2. C. J. N. Buisman, B. G. Geraats, P. IJspeert, G. Lettinga, Optimization of sulphur production in a biotechnological sulphide-removing reactor, *Biotechnol. Bioeng.* **1990**, *35*, 50-56.
3. J. M. Visser, G. C. Stefess, L. A. Robertson, J. G. Kuenen, *Thiobacillus* sp. W5, the dominant autotroph oxidizing sulfide to sulfur in a reactor for aerobic treatment of sulfidic wastes, *Antonie van Leeuwenhoek* **1997**, *72*, 127-134.
4. A. J. H. Janssen, R. Sleyster, C. van der Kaa, A. Jochemsen, J. Bontsema, G. Lettinga, Biological sulphide oxidation in a fed-batch reactor, *Biotechnol. Bioeng.* **1995**, *47*, 327-333.
5. C. Cline, A. Hoksberg, R. Abry, A. Janssen, Biological process for H_2S removal from gas streams. The Shell-Paques/Thiopaq gas desulfurization process. In *Proc. Laurance Reid gas conditioning conference* [CD-ROM], University of Oklahoma, Norman, OK, **2003**.
6. W. E. Kleinjan, A. de Keizer, A. J. H. Janssen, Biologically produced sulfur, *Top. Curr. Chem.* **2003**, *230*, 167-188. *This thesis, chapter 2*.
7. A. Prange, R. Chauvistre, H. Modrow, J. Hormes, H. G. Trüper, C. Dahl, Quantitative speciation of sulfur in bacterial sulfur globules: X-ray absorption spectroscopy reveals at least three different species of sulfur, *Microbiology (UK)* **2002**, *148*, 267-276.
8. A. J. H. Janssen, A. de Keizer, G. Lettinga, Colloidal properties of a microbiologically produced sulphur suspension in comparison to a LaMer sulphur sol, *Colloids Surf. B-Biointerfaces* **1994**, *3*, 111-117.
9. J. Boulègue, Solubility of elemental sulfur in water at 298 K, *Phosphorus Sulfur Silicon Relat. Elem.* **1978**, *5*, 127-128.
10. A. J. H. Janssen, G. Lettinga, A. de Keizer, Removal of hydrogen sulphide from wastewater and waste gases by biological conversion to elemental sulphur. Colloidal and interfacial aspects of biologically produced sulphur particles, *Colloids Surf. A-Physicochem. Eng. Asp.* **1999**, *151*, 389-397.

11. R. Steudel, Mechanism for the formation of elemental sulfur from aqueous sulfide in chemical and microbiological desulfurization processes, *Ind. Eng. Chem. Res.* **1996**, *35*, 1417-1423.
12. G. Schwarzenbach, A. Fischer, Die Acidität der Sulfane und die Zusammensetzung wässeriger Polysulfidlösungen, *Helv. Chim. Acta* **1960**, *169*, 1365-1392.
13. R. Steudel, The chemical sulfur cycle. In *Environmental technologies to treat sulfur pollution. Principles and engineering* (Eds.: P. Lens, L. Hulshoff Pol), IWA Publishing, London, **2000**, pp. 1-31.
14. W. Giggenbach, Optical spectra and equilibrium distribution of polysulfide ions in aqueous solution at 20 ºC, *Inorg. Chem.* **1972**, *11*, 1201-1207.
15. A. Kamyshny, A. Goifman, J. Gun, D. Rizkov, O. Lev, Equilibrium distribution of polysulfide ions in aqueous solutions at 25 °C: A new approach for the study of polysulfides' equilibria, *Environ. Sci. Technol.* **2004**, *38*, 6633-6644.
16. R. H. Arntson, F. W. Dickson, G. Tunell, Saturation curves of orthorhombic sulfur in the system S-Na_2S-H_2O at 25 °C and 50 °C, *Science* **1958**, *128*, 716-718.
17. A. Teder, The equilibrium between elementary sulfur and aqueous polysulfide ions, *Acta Chem. Scan.* **1971**, *25*, 1722-1728.
18. W. Giggenbach, Equilibria involving polysulfide ions in aqueous sulfide solutions up to 240 ºC, *Inorg. Chem.* **1974**, *13*, 1724-1730.
19. W. E. Kleinjan, A. de Keizer, A. J. H. Janssen, Kinetics of the reaction between dissolved sodium sulfide and biologically produced sulfur, *Ind. Eng. Chem. Res.* **2005**, *44*, 309-317. *This thesis, chapter 3*.
20. N. Hartler, J. Libert, A. Teder, Rate of sulfur dissolution in aqueous sodium sulfide, *Ind. Eng. Chem. Proc. Des. Develop.* **1967**, *6*, 398-406.
21. H. G. Trüper, H. G. Schlegel, Sulphur metabolism in Thiorhodaceae I: Quantitative measurements on growing cells of *Chromatium okenii*, *Antonie van Leeuwenhoek* **1964**, *30*, 225-238.
22. L. G. Danielsson, X. S. Chai, M. Behm, L. Renberg, UV characterization of sulphide-polysulphide solutions and its application for process monitoring in the electrochemical production of polysulphides, *J. Pulp Paper Sci.* **1996**, *22*, J187-J191.
23. A. Teder, Spectrophotometric determination of polysulphide excess sulfur in aqueous solutions, *Svensk Papperst.* **1967**, *6*, 197-200.
24. R. Steudel, Inorganic polysulfides S_n^{2-} and radical anions $S_n^{\bullet-}$, *Top. Curr. Chem.* **2003**, *231*, 127-152.
25. T. J. Edwards, G. Maurer, J. Newman, J. M. Prausnitz, Vapor-liquid equilibria in multicomponent aqueous solution of volatile weak electrolytes, *AIChE J.* **1978**, *24*, 966-975.
26. G. Maronny, Constantes de dissociation de l'hydrogene sulfure, *Electrochim. Acta* **1959**, *1*, 58-69.
27. P. L. Brezonik, *Chemical kinetics and process dynamics in aquatic systems*, Lewis Publishers, Boca Raton, **1994**, p 155.
28. W. Stumm, J. J. Morgan, *Aquatic chemistry*, Wiley-Interscience, New York, **1970**, p 84.
29. E. L. Bauer, *A statistical manual for chemists*, Academic Press, New York, **1971**, p 109.

30. H. G. Trüper, J. C. Hathaway, Orthorhombic sulphur formed by photosynthetic sulphur bacteria, *Nature* **1967**, *215*, 435-436.
31. G. J. Hageage, E. D. Eanes, R. L. Gherna, X-ray diffraction studies on the sulfur globules accumulated by *Chromatium* species, *J. Bacteriol.* **1970**, *101*, 464-469.
32. A. Vairavamurthy, K. Mopper, B. F. Taylor, Occurrence of particle-bound polysulfides and significance of their reaction with organic matters in marine sediments, *Geophys. Res. Lett.* **1992**, *19*, 2043-2046.

Chapter 5

Kinetics of the chemical oxidation of polysulfide anions in aqueous solution*

Abstract

The kinetic properties of the chemical oxidation of aqueous polysulfide solutions have been studied in phosphate buffered systems at pH 7 to 12, at temperatures between 20 and 40 ºC, and an ionic strength between 0.05 and 0.50 M. Polysulfide solutions were mixed with a buffer solution of known dissolved oxygen concentration, after which the decrease in the oxygen concentration of the solution was measured in time. The rate of oxygen consumption can be described by the empirical relation $d[O_2]/dt = -k[S_x^{2-}][O_2]^{0.59}$. The reaction rate constant k is moderately dependent on pH and goes through a maximum at pH 10. The rate of oxygen consumption for polysulfide solutions is approximately four times higher than for sulfide solutions. At pH values below 9 reaction products were formed according to $S_x^{2-} + 3/2\ O_2 \rightarrow S_2O_3^{2-} + (x-2)\ S^0$. At pH values higher than 9, more thiosulfate and additional sulfide were formed, which is attributed to the low chemical stability of the sulfur of oxidation state zero, formed upon polysulfide oxidation. Our results strongly suggest that hydrolysis of this 'nascent' elemental sulfur to HS^- and $S_2O_3^{2-}$ is faster than hydrolysis of crystalline inorganic sulfur or colloidal particles of biologically produced sulfur, and has a significant contribution already at 30 °C and pH 10.

Keywords

Polysulfide, hydrogen sulfide, kinetics, oxidation, hydrolysis

* W.E. Kleinjan, A. de Keizer, A.J.H. Janssen, Kinetics of the chemical oxidation of polysulfide anions in aqueous solution, *Water Res.* (submitted).

5.1. Introduction

As an alternative to physicochemical processes for the removal of hydrogen sulfide from gas streams, which require special chemicals, and sometimes high temperature and high pressure, the use of a biotechnological process can be an interesting option. Several microorganisms have been studied for application in biotechnological H_2S removal systems (for a review, see ref.[1]) but the chemoautotrophic bacteria of the genus *Thiobacillus* have been studied and used mostly. Buisman *et al*. [2] used a mixed culture of *Thiobacilli* for the aerobic oxidation of sulfide to elemental sulfur and studied technological applications. This process was further developed and is currently used in a number of full-scale installations [3, 4]. The process basically consists of the absorption of H_2S in an alkaline liquid in a gas absorber and the subsequent oxidation of dissolved hydrogen sulfide (HS^-) to solid elemental sulfur in a bioreactor. This solid sulfur is called biologically produced sulfur and differs from "inorganic" sulfur in that it has more hydrophilic properties [5, 6].

In this process, polysulfide ions (S_x^{2-}) can be formed from reaction of biologically produced sulfur with dissolved hydrogen sulfide (Eq. 5.1).

$$HS^- + (x-1)\,S^0 \rightleftarrows S_x^{2-} + H^+ \qquad (5.1)$$

The kinetic properties [7] and equilibrium constants [8] of this reaction have been investigated in previous studies, with special emphasis on the differences between biologically produced sulfur and "inorganic" elemental sulfur. Thiosulfate is an undesired product in the H_2S removal process, just as it is in physicochemical processes, such as the Stretford process [9]. As in the biological oxidation of polysulfide ions mainly sulfate is formed, e.g., [10], it has been suggested that thiosulfate originates from the chemical oxidation of polysulfide ions [11]. Although the kinetics of the oxidation of aqueous sulfide solutions has been studied quite extensively for a number of aqueous systems (e.g., seawater [12], buffer solutions [13, 14], waste water [15]), fairly little is known about the kinetics of the oxidation of polysulfide ions. Most knowledge of the chemical oxidation of aqueous solutions of polysulfide ions stems from studies on the chemical auto-oxidation of sulfide solutions. Here, polysulfide ions appear as intermediates, catalyzing the oxidation of sulfide. In these studies, the concentration of polysulfide intermediate is not well defined and it is therefore difficult to draw quantitative conclusions on the kinetics or the mechanism of polysulfide oxidation. Knowledge of the kinetics of this reaction could however be essential in understanding how to control thiosulfate formation and increase process selectivity for elemental sulfur production.

The chemical oxidation of sulfide solutions has proven to be a complex reaction from which a number of reaction products can be formed, especially sulfur, thiosulfate, sulfite, and sulfate. The reactions are generally catalyzed by metal ions [16] and the

identity of the reaction product depends on conditions such as pH and the sulfide / oxygen ratio, as follows from the overall reactions in Eqs. 5.2–5.5.

$$HS^- + ½\ O_2 \rightarrow S^0 + OH^- \quad (5.2)$$

$$HS^- + O_2 \rightarrow ½\ S_2O_3^{2-} + ½\ H_2O \quad (5.3)$$

$$HS^- + ³⁄₂\ O_2 \rightarrow SO_3^{2-} + H^+ \quad (5.4)$$

$$HS^- + 2\ O_2 \rightarrow SO_4^{2-} + H^+ \quad (5.5)$$

Polysulfide ions have been observed as intermediates at conditions where elemental sulfur is formed from chemical sulfide oxidation, that is around pH 7. It was therefore concluded that elemental sulfur required for the formation of polysulfide ions originates from sulfide oxidation (Eq. 5.2) [13]. Oxidation of polysulfide ions was found to occur more rapidly than oxidation of sulfide ions and therefore polysulfide ions were found to act as catalyst for the oxidation of sulfide. Steudel *et al.* [17] studied the stoichiometry of the oxidation of polysulfide ions by continuously bubbling oxygen through a concentrated polysulfide solution, until the characteristic yellow-to-orange color of the polysulfide solution had completely disappeared (pH = 9–13.5; T = 23–40 °C). The reaction products were thiosulfate and sulfur and the overall reaction is shown in Eq. 5.6. No sulfate, sulfite, or polythionate ($S_xO_6^{2-}$) could be detected.

$$S_x^{2-} + ³⁄₂\ O_2 \rightarrow S_2O_3^{2-} + (x-2)\ S^0 \quad (5.6)$$

The actual mechanism of chemical polysulfide oxidation has not been elucidated. Radical polysulfide anions like $S_2^{\bullet-}$ and $S_3^{\bullet-}$ have been suggested to be the reactive species in oxidation of polysulfide ions [18]. Pasiuk-Bronikowska *et al*. [19] proposed a mechanism in which a sulfane monosulfonic anion, $S_xO_3^{2-}$, is formed as intermediate, whereas Fischer *et al*. [20] suggested the formation of an unstable polythiosulfite species, $S_xO_2^{2-}$, as intermediate.

In a number of cases it was suggested that both sulfite and thiosulfate could be the resulting products in the oxidation [13, 19].The reaction between elemental sulfur and sulfite (or its protonated form, HSO_3^-), however, favors thiosulfate at alkaline conditions, resulting in solutions in which sulfite is almost absent.

$$S^0 + HSO_3^- \rightleftarrows S_2O_3^{2-} + H^+ \quad (5.7)$$

We have investigated the kinetics and stoichiometry of the chemical polysulfide oxidation at pH values ranging from 7–12 and temperatures from 20–40 °C in phosphate buffered aqueous solutions. This was done by continuously measuring the oxygen concentration in time after addition of a polysulfide solution to a buffer

solution of known dissolved oxygen concentration. The reaction orders for polysulfide ions and dissolved oxygen were determined by measuring reaction rates for different initial concentrations of one component while keeping the initial concentration of the other component constant. The reaction rate constant was determined from the initial rate and initial polysulfide and oxygen concentrations.

5.2. Materials and methods

5.2.1. Experimental set-up

Experiments were performed in a thermostated reactor, equipped with a magnetic stirrer (Figure 5.1). A buffer solution was saturated with O_2 by bubbling air through the liquid. The reactor was then closed with a piston containing a calibrated oxygen electrode. The electrode carrier contained a small opening to allow air to be removed from the system and to be able to add reactants to the system via a syringe with a needle. The oxygen electrode was calibrated with air-saturated demineralized water.

The reaction was initiated by injecting 10–80 μL of a sulfide or polysulfide solution (details see below) to 5.0 mL of a buffer solution. After this, the decrease in the O_2 concentration is measured in time. The initial slope, $(d[O_2]/dt)_0$, is taken as a measure of the initial rate of polysulfide oxidation. The initial sulfide or polysulfide concentration was varied by changing the volume of the added stock solution. The initial dissolved O_2 concentration was varied by mixing of an air-saturated buffer solution with a deaerated buffer solution that was bubbled through with N_2 for 30 minutes under vigorous stirring.

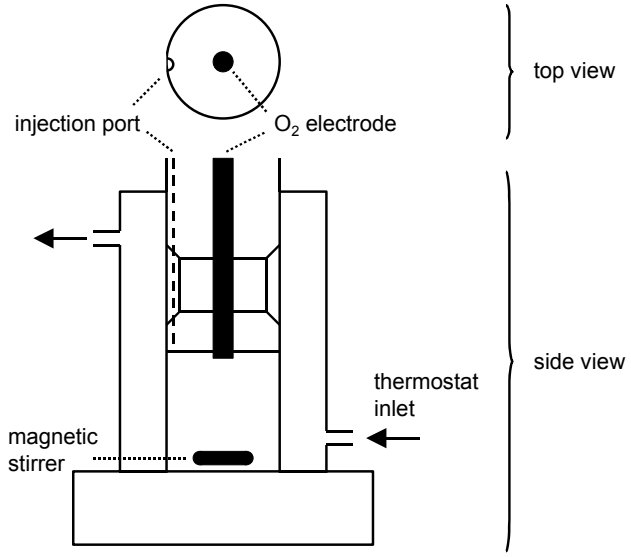

Figure 5.1. Schematic representation of the reactor used for measurements of the polysulfide oxidation rate. Total reaction volume = 5 mL.

5.2.2. Chemicals used

Used buffer solutions were of pH 7.0, 8.0 (both 0.02 M phosphate buffer), 9.0 (0.04 M phosphate buffer), 10.0 (0.08 M phosphate or 0.02 M carbonate buffer), 11.0 (0.04 M phosphate buffer), and 12.0 (0.02 M phosphate or 0.08 M phosphate). The ionic strength of the solutions was adjusted to required values by addition of NaCl. No differences were found for carbonate or phosphate buffers (pH = 10.0), nor was an effect of buffer concentration found (pH = 12.0).

Polysulfide stock solutions were prepared by reaction of 1.5 g of granular sulfur with 50 mL of a 60 mM sulfide solution for 16 h at 50 °C. At this point the polysulfide solution was in equilibrium with excess sulfur. The glass flasks were septum-sealed and a slight N_2 overpressure was maintained to prevent oxidation by air. After reaction, the pH, the total sulfide concentration, and the polysulfide concentration were determined.

Polysulfide solutions prepared this way consist of mixtures of polysulfide ions, S_x^{2-}, and HS^- ions. The mixture is defined by the sulfide-polysulfide equilibrium (Eq. 5.1). In the presence of excess amounts of sulfur, the average polysulfide chain length, x = 4.91 (21 °C) and the equiblibrium can be represented by [8, 21]

$$K_x = \frac{[S_x^{2-}][H^+]}{[HS^-]} = 10^{-8.78} \qquad (5.8)$$

Sulfide solutions were prepared by removing the oxidized surface of $Na_2S{\cdot}9H_2O$ crystals by flushing with deaerated water and subsequent dissolution of the crystals in deaerated water. The flasks were septum-sealed and solutions kept under a N_2 atmosphere. Details of prepared polysulfide solutions are presented in Table 5.1.

5.2.3. Analysis

Sulfide concentrations were determined using the methylene blue method as described by Trüper and Schlegel [22]. Polysulfide concentrations were determined by UV absorption at 285 nm [23]. At this wavelength the amount of zero valent sulfur in

Table 5.1. Preparation of three polysulfide stock solutions used in the polysulfide oxidation batch experiments.

	before equilibrium		**after equilibrium**				
	c_{S0} (mM)	**$[S^{2-}]_{total}$ (mM)[a]**	**$[S^{2-}]_{total}$ (mM)[a]**	**$[S_x^{2-}]$ (mM)[b]**	**$[S_x^{2-}]$ (mM)[c]**	**$[HS^-]$ (mM)[c]**	**pH**
1	936	62.4	63.7	40.9	39.3	24.4	9.06
2	936	20.8	21.2	14.8	14.3	6.90	9.12
3	936	110.2	112.0	79.0	75.9	36.1	9.01

[a] Measured with the methylene blue method.
[b] Measured by UV absorption, assuming that the average polysulfide chain length, x = 4.91.
[c] Calculated according to Eq. 5.8 using the measured $[S^{2-}]_{total}$ and pH after establishing an equilibrium.

polysulfide ions, the *polysulfide excess sulfur concentration*, [S^0 in S_x^{2-}], can be determined independently of pH and ratio X_S [24].

$$X_S = \frac{[S^0 \text{ in } S_x^{2-}]}{[S^{2-}]_{total}} \tag{5.9}$$

Thiosulfate was measured using a Dionex 1999 ion chromatograph. The pH was determined with a calibrated pH-combination electrode (Schott).

5.3. Results and discussion

5.3.1. Reaction order for S_x^{2-} and O_2

The effect of the initial polysulfide concentration on the initial rate of oxygen decrease was measured for different pH values. The initial polysulfide concentration was varied by adding different volumes of a polysulfide stock solution of known concentration to identical buffer solutions of known dissolved oxygen concentration. Assuming the chemical polysulfide oxidation follows the rate law in Eq. 5.10 it is possible to graphically determine the reaction order with respect to S_x^{2-}, α, at constant $[O_2]$, from the slope of a plot of $\ln((d[O_2]/dt)_0)$ vs. $\ln([S_x^{2-}]_0)$.

$$\left(\frac{d[O_2]}{dt}\right)_{t=0} = -k[S_x^{2-}]_0^{\alpha}[O_2]_0^{\beta} \tag{5.10}$$

Figure 5.2 shows that the determined reaction order α is very close to unity at pH values between 7 and 12 ($\alpha = 0.98 \pm 0.08$). We will therefore conclude that the rate of polysulfide oxidation is directly proportional to $[S_x^{2-}]$ and $\alpha = 1$ for pH values between 7 and 12. Similarly, the reaction order with respect to O_2, β, was determined

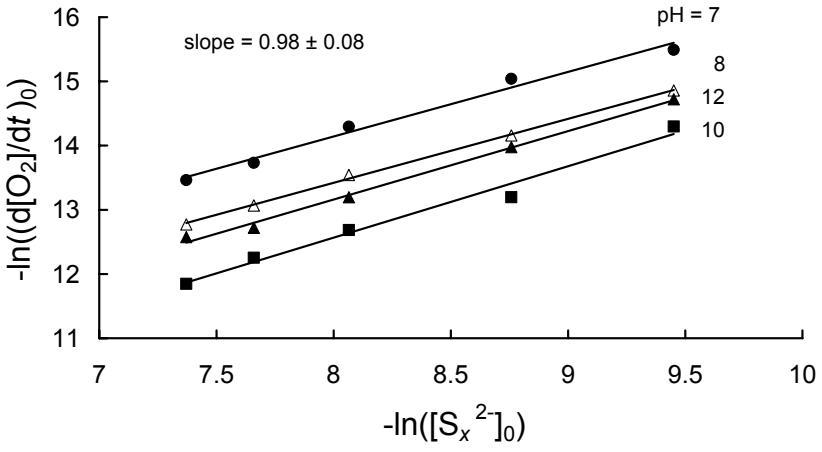

Figure 5.2. Logarithmic plot of the initial polysulfide concentration against the initial rate of oxygen decrease for pH values between 7.0 and 12.0. T = 30 °C; I = 0.10 M; $[O_2]_0$ =2.36 × 10^{-4} M. Reaction order with respect to S_x^{2-}, $\alpha = 0.98 \pm 0.08$.

by varying the dissolved O_2 concentration while maintaining a constant initial S_x^{2-} concentration. From the slopes of the lines in Figure 5.3 it can be seen that $\beta = 0.59 \pm 0.07$.

5.3.2. Effect of pH, ionic strength, and temperature on the reaction rate constant

The specific reaction rate constant k was determined from the initial rate of oxygen consumption and the initial oxygen and polysulfide concentrations, using the empirical relation in Eq. 5.10, with $\alpha = 1$ and $\beta = 0.59$. Results for different pH values are plotted in Figure 5.4. For a pH between 9 and 12, the specific rate constant k is moderately dependent on pH and appears to go through a maximum at pH 10. At pH values below 9 the apparent reaction rate constant is even lower. This is probably because of the fast decrease in polysulfide concentration due to polysulfide acidification. Upon mixing of a polysulfide solution in a buffer of lower pH, the

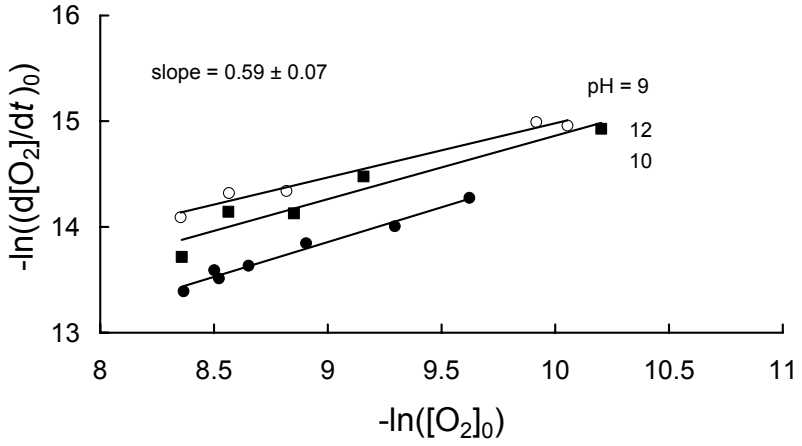

Figure 5.3. Logarithmic plot of the initial oxygen concentration against the initial specific rate of oxygen decrease for pH = 9.0, 10.0, and 12.0. $T = 30$ °C; $I = 0.10$ M; $[S_x^{2-}]_0 = 5.10 \times 10^{-4}$ M. Reaction order with respect to O_2, $\beta = 0.59 \pm 0.07$.

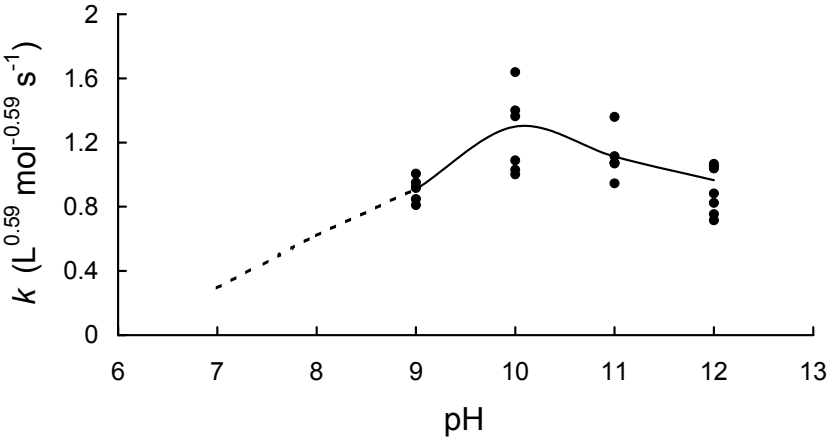

Figure 5.4. Effect of pH on rate constant k, based on $(d[O_2]/dt)_0 = -k\,[S_x^{2-}]_0[O_2]_0^{0.59}$. At pH < 9 acidification of polysulfide ions interferes with oxidation. $T = 30$ °C, $I = 0.10$ M.

equilibrium between HS^- and S_x^{2-} (Eq. 5.1) shifts towards HS^-. This is supported by the fast appearance of whitish sulfur precipitates in solution at pH < 9, whereas at higher pH values only a slow discoloration and increase in turbidity were observed. Furthermore, the effect of polysulfide acidification is in line with the effect of ionic strength on the rate of O_2 decrease. An increase in ionic strength at pH 8, and to a less extent at pH 9, was found to result in an increase in the initial rate of oxygen consumption (Figure 5.5). At higher ionic strength the reaction rate between two oppositely charged ions, such as a polysulfide anion and a proton will decrease due to a shielding of the electrostatic attraction, resulting in a higher initial polysulfide concentration and therefore a higher initial rate of oxygen consumption. This dependence on ionic strength is absent at pH 11 and 12, showing that, here, the reaction rate is not limited by a reaction which is strongly dependent on ionic strength. This suggests that a nonionic reactant, such as an oxygen molecule, is involved in the rate limiting step of polysulfide oxidation.

The effect of polysulfide acidification on the initial rate of oxygen decrease shows that this reaction takes place rapidly, at least in such a way that within the time required for mixing a substantial part of the polysulfide solution has been acidified.

Furthermore, from Figure 5.4 it can be concluded that the reaction rate is only moderately dependent on pH. Upon increasing pH from 9 to 12, the reaction rate constant, calculated based on the initial rate of oxygen decrease, remains fairly constant. At pH 9, $k = 0.95$, then the reaction rate constant goes through a maximum at pH 10 ($k = 1.29$) after which it decreases to $k = 0.96$. The origin of the decrease in reaction rate at pH values above 10 is not clear. Decomposition of the polysulfide ion with OH^- is reported to be far too slow at our experimental conditions [25]. Hydrolysis of elemental sulfur, precipitates of which are formed by oxidation of polysulfide ions, will probably play an increasingly important role with increasing

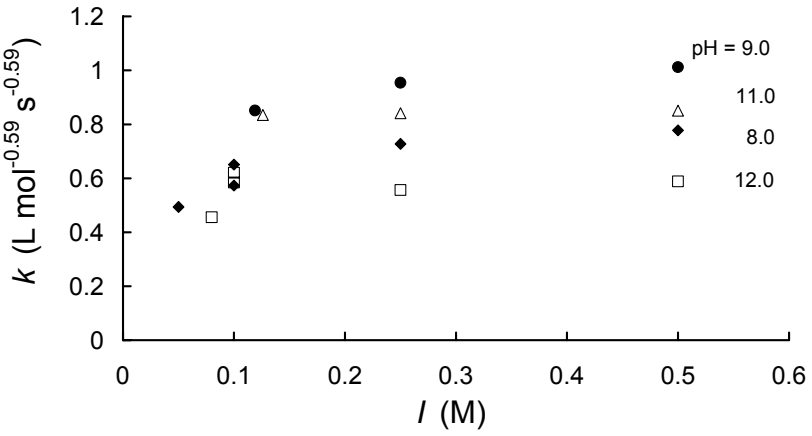

Figure 5.5. Effect of ionic strength on the initial specific rate of oxygen decrease for pH = 8.0 (♦), 9.0 (●), 11.0 (Δ), and 12.0 (□). $T = 30$ °C, $[S_x^{2-}]_0 = 5.10 \times 10^{-4}$ M, $[O_2]_0 = 2.36 \times 10^{-4}$ M.

pH. However, this is not expected to affect the polysulfide concentration or oxygen consumption directly and can therefore not explain the decrease in reaction rate at higher pH values.

The effect of temperature on the reaction rate constant k at pH 12 is shown in Figure 5.6. In this plot it can be seen that the temperature dependence is of Arrhenius behavior (Eq. 5.11). The activation energy is 36.7 kJ mol^{-1}, which is somewhat lower than reported for the oxidation of sulfide solutions at pH 12 (46 kJ mol^{-1}) [12].

$$\ln(k) = A - \frac{E_a}{RT} \tag{5.11}$$

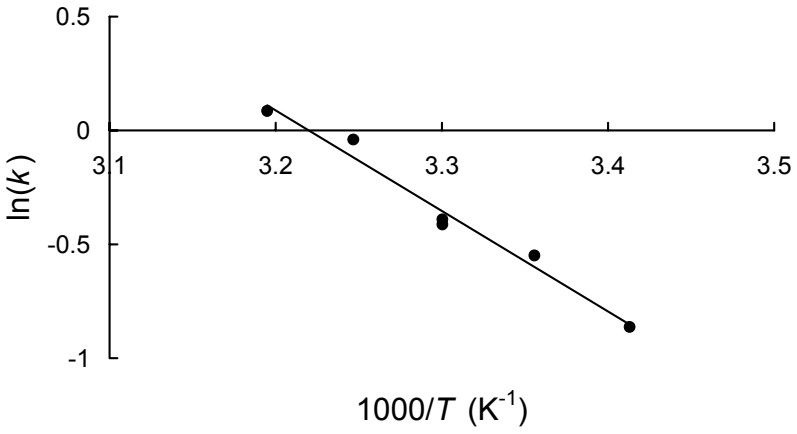

Figure 5.6. Arrhenius plot for temperature dependence of the reaction rate constant. From the slope of the plot the activation energy is obtained, E_a = 36.7 kJ mol^{-1}. $[S_x^{2-}]_0 = 5.10 \times 10^{-4}$ M, $[O_2]_0 = 2.36 \times 10^{-4}$ M, pH = 12, I = 0.10 M.

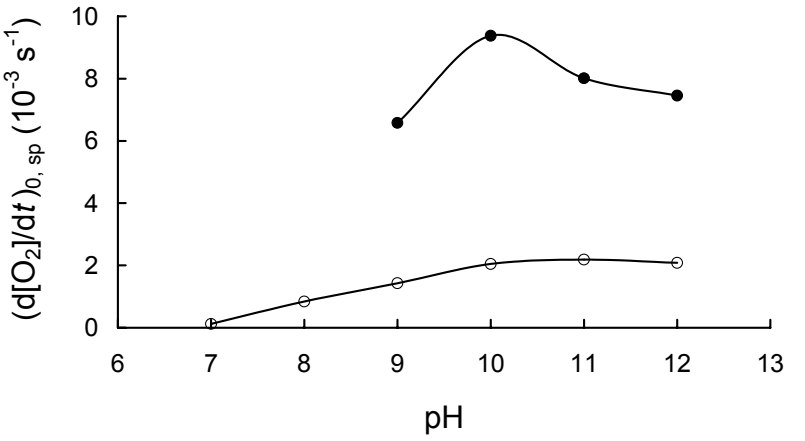

Figure 5.7. Specific rate of oxygen decrease as a function of pH for polysulfide (•) and sulfide solutions (○). $[S_x^{2-}]_0 = 3.04 \times 10^{-4}$ M, $[HS^-]_0 = 4.48 \times 10^{-4}$ M, T = 30 °C, I = 0.10 M.

5.3.3. Comparison of the initial oxidation rates of S_x^{2-} solutions with HS^- solutions

To various air-saturated phosphate buffer solutions of pH 7–12 a solution of dissolved $Na_2S{\cdot}9H_2O$ crystals was added, after which the decrease in dissolved O_2 concentration was measured in time. In Figure 5.7, the specific rate of oxygen consumption for sulfide solutions ($(d[O_2]/dt)_0/[HS^-]_0$) is compared to the specific rate of oxygen consumption for polysulfide solutions ($(d[O_2]/dt)_0/[S_x^{2-}]_0$). At the experimental conditions, the specific rate of oxygen decrease is approximately 3–5 times higher for polysulfide than for sulfide solutions. Earlier observations by e.g., Chen and Morris [13] already strongly suggested a more rapid reaction of polysulfide with O_2 than that of HS^- with O_2 but no quantitative data on the difference in reaction rates have been reported. Our findings give a quantitative comparison between the chemical oxidation rates of polysulfide and sulfide ions. It should however be noted that the rate of sulfide oxidation is known to be dependent on a number of factors, such as the ratio $[S^{2-}]_{total}$ over $[O_2]$, the type of buffer used (HS^- oxidation was found to occur more rapidly in phosphate buffers than in carbonate or acetic acid buffers [13]), and presence of metal ions. In fact, it has been reported that oxidation of HS^- ions can only occur if some form of paramagnetic catalyst, such as metal ions, is present [16].

5.3.4. Mass balance and products formed

To verify the mass balance during the measurements of kinetics of polysulfide oxidation, and to investigate the products formed, we have analyzed the composition of solutions after polysulfide oxidation. The final total sulfide and thiosulfate concentrations were measured for pH values varying between 7 and 12 at constant initial polysulfide
concentration. In all cases thiosulfate was the only reaction product observed. Neither sulfate nor sulfite could be detected with ion chromatography. In Table 5.2 details of experiments on the mass balance of consumption of oxygen and total sulfide, and formation of thiosulfate are shown. From these data the total polysulfide oxidation stoichiometry can be calculated. Comparison of these numbers with reported total stoichiometry in literature (Eq. 5.6) shows some differences. Reasonably good

Table 5.2. Total sulfide mass balance at different pH values. $[S^{2-}]_{total,0} = 4.48 \times 10^{-4}$ M, $[S_x^{2-}]_0 = 3.04 \times 10^{-4}$ M, $T = 30$°C, $I = 0.10$ M.

pH	$\Delta[S^{2-}]_{total}$ (mM) (consumption)	$\Delta[O_2]$ (mM) (consumption)	$\Delta[S_2O_3^{2-}]$ (mM) (formation)	$\Delta[O_2] / \Delta[S^{2-}]_{total}$	$\Delta[S_2O_3^{2-}] / \Delta[S^{2-}]_{total}$
7	0.0772	0.0898	0.0632	1.16	0.818
8	0.145	0.176	0.140	1.21	0.969
9	0.171	0.240	0.176	1.40	1.03
10	0.0719	0.235	0.312	3.26	4.34
11	–0.0223	0.232	0.357	–1.04	–16.0
12	–0.123	0.235	0.446	–1.91	–3.62

agreement with reaction stoichiometry as reported in literature is found for pH values between 7 and 9. Here, approximately one mole thiosulfate formed corresponds to one mole of sulfide consumed. The ratio of consumed oxygen over consumed sulfide is between 1.2 and 1.4, somewhat lower than 1.5. The best agreement with the reported stoichiometry is at pH 9. This is probably because of acidification of polysulfide solutions. At pH 7 and 8 the equilibrium between HS^- and S_x^{2-} shifts towards HS^-. Therefore, sulfide oxidation interferes with polysulfide oxidation at low pH.

At pH 10 and higher, however, there is no correspondence with the reported stoichiometry of polysulfide oxidation. The total sulfide consumption at pH 10.0 is very low, and at pH 11 and 12 there is even an increase in total sulfide concentration. Furthermore, additional thiosulfate is formed. This formation of additional sulfide and thiosulfate can probably be attributed to the hydrolysis of elemental sulfur, S^0, which is formed in the oxidation of polysulfide ions (Eq. 5.6). The overall hydrolysis of elemental sulfur can be described with Eq. 5.12.

$$4\ S^0 + 4\ OH^- \rightarrow S_2O_3^{2-} + 2\ HS^- + H_2O \qquad (5.12)$$

The hydrolysis of elemental sulfur is reported to occur at temperatures close to 100 °C [26]. However, the possibility that hydrolysis of sulfur may ocur at physiological temperatures, particularly with colloidal preparations and freshly precipitated, or ‘nascent’ sulfur, was already suggested in 1970 [27]. Indeed, colloidal particles of biologically produced sulfur were found to undergo considerable hydrolysis already at 55 °C and pH 10 [28]. The hydrolysis was shown to take place at the surface of the particles and the reaction rate increased with increasing pH, although measured reaction rates were still fairly low. However, in the situation where precipitates are formed from solution, the hydrolysis rate can be expected to be higher. The 'nascent' sulfur probably consists of very small clusters of sulfur rings, with a high specific surface area, causing a fast hydrolysis. Furthermore, zero valent sulfur formed upon polysulfide oxidation may consist of short chains of sulfur atoms of a low chemical stability resulting in hydrolysis even before more stable sulfur rings, such as S_8 are formed. Particularly at high pH values, these unstable forms of zero valent sulfur are expected to react with OH^- forming thiosulfate and sulfide. The additional formation of thiosulfate and sulfide strongly suggest that hydrolysis of freshly precipitated elemental sulfur, or 'nascent' sulfur, has a considerable effect already at 30 °C and pH 10 and is therefore considerably faster than hydrolysis of biologically produced sulfur or crystalline inorganic sulfur. Hydrolysis of 'nascent' sulfur may also occur in other systems where sulfur precipitates from solution, e.g., in the preparation of so-called Weimarn sulfur sols. Here, a solution of S_8 in ethanol or acetone is poured into an excess of water. Because of the low solubility of S_8 in the aqueous solution, sulfur precipitates forming a colloidal suspension. The particles are negatively charged due

to the adsorption of anions. Indeed, a drop in pH is observed upon formation of Weimarn sols, which Steudel [29] attributed to hydrolysis of S_8.

The presented data indicate that presence of thiosulfate in biotechnological or physicochemical hydrogen sulfide removal processes is related to the chemical oxidation of polysulfide ions. Polysulfide ions are formed through reaction of elemental sulfur with sulfide and can subsequently be oxidized to thiosulfate and elemental sulfur. Because of a higher rate of polysulfide oxidation than of sulfide oxidation, oxidation of polysulfide ions cannot easily be prevented by applying oxygen-limiting conditions, as is done to prevent oxidation of sulfide to sulfate [30]. The rate of polysulfide oxidation is only moderately dependent on pH. However, at high pH values additional thiosulfate and sulfide are formed, which can probably be explained by the hydrolysis of 'nascent' elemental sulfur, formed upon oxidation of polysulfide ions. This is of particular interest in establishing an optimal pH of operation for aerobic hydrogen sulfide removal processes. On the one hand, the rate of H_2S gas absorption into a liquid will be faster at elevated pH values. On the other hand, however, more thiosulfate will be formed with increasing pH, particularly at a process operating at pH > 9, leading to an overall decrease in process selectivity meaning that less elemental sulfur is produced.

Acknowledgements

We thank Wobby Bosma for performing part of the rate of oxidation measurements. Pim van den Bosch is gratefully acknowledged for assistance with ionic chromatography measurements.

References

1. J. E. Burgess, S. A. Parsons, R. M. Stuetz, Developments in odour control and waste gas treatment biotechnology: A review, *Biotechnol. Adv.* **2001**, *19*, 35-63.
2. C. J. Buisman, B. G. Geraats, P. IJspeert, G. Lettinga, Optimization of sulphur production in a biotechnological sulphide-removing reactor, *Biotechnol. Bioeng.* **1990**, *35*, 50-56.
3. A. J. H. Janssen, R. Sleyster, C. van der Kaa, A. Jochemsen, J. Bontsema, G. Lettinga, Biological sulphide oxidation in a fed-batch reactor, *Biotechnol. Bioeng.* **1995**, *47*, 327-333.
4. C. Cline, A. Hoksberg, R. Abry, A. Janssen, Biological process for H_2S removal from gas streams. The Shell-Paques/Thiopaq gas desulfurization process. In *Proceedings of the Laurance Reid gas conditioning conference* [CD-ROM], University of Oklahoma, Norman, OK, **2003**.
5. A. J. H. Janssen, G. Lettinga, A. de Keizer, Removal of hydrogen sulphide from wastewater and waste gases by biological conversion to elemental sulphur. Colloidal and interfacial aspects of biologically produced sulphur particles, *Colloids Surf. A-Physicochem. Eng. Asp.* **1999**, *151*, 389-397.
6. W. E. Kleinjan, A. de Keizer, A. J. H. Janssen, Biologically produced sulfur, *Top. Curr. Chem.* **2003**, *230*, 167-188. *This thesis, chapter 2*.

7. W. E. Kleinjan, A. de Keizer, A. J. H. Janssen, Kinetics of the reaction between dissolved sodium sulfide and biologically produced sulfur, *Ind. Eng. Chem. Res.* **2005**, *44*, 309-317. *This thesis, chapter 3*.
8. W. E. Kleinjan, A. de Keizer, A. J. H. Janssen, Equilibrium of the reaction between dissolved sodium sulfide and biologically produced sulfur, *Colloids Surf. B-Biointerfaces*, in press. *This thesis, chapter 4*.
9. C. A. Hammond, The Dow Stretford chemical recovery process, *Environ. Progr.* **1986**, *5*, 1-4.
10. H. Banciu, D. Y. Sorokin, R. Kleerebezem, G. Muyzer, E. A. Galinski, J. G. Kuenen, Growth kinetics of haloalkaliphilic, sulfur-oxidizing bacterium *Thioalkalivibrio versutus* strain ALJ 15 in continuous culture, *Extremophiles* **2004**, *8*, 185-192.
11. R. Steudel, Mechanism for the formation of elemental sulfur from aqueous sulfide in chemical and microbiological desulfurization processes, *Ind. Eng. Chem. Res.* **1996**, *35*, 1417-1423.
12. F. J. Millero, S. Hubinger, M. Fernandeze, S. Garnett, Oxidation of H_2S in seawater as a function of temperature, pH, and ionic strength, *Environ. Sci. Technol.* **1987**, *21*, 439-443.
13. K. Y. Chen, J. C. Morris, Kinetics of oxidation of aqueous sulfide by O_2, *Environ. Sci. Technol.* **1972**, *6*, 529-537.
14. C. Buisman, P. IJspeert, A. Janssen, G. Lettinga, Kinetics of chemical and biological sulfide oxidation in aqueous solutions, *Water Res.* **1990**, *24*, 667-671.
15. A. H. Nielsen, J. Vollertsen, T. Hvitved-Jacobsen, Determination of kinetics and stoichiometry of chemical sulfide oxidation in wastewater of sewer networks, *Environ. Sci. Technol.* **2003**, *37*, 3853-3858.
16. R. Steudel, The chemical sulfur cycle. In *Environmental technologies to treat sulfur pollution. Principles and engineering* (Eds.: P. Lens, L. Hulshoff Pol), IWA Publishing, London, **2000**, pp. 1-31.
17. R. Steudel, G. Holdt, R. Nagorka, On the autoxidation of aqueous sodium polysulfide, *Z. Naturforsch. B* **1986**, *41*, 1519-1522.
18. R. Steudel, Inorganic polysulfides S_n^{2-} and radical anions $S_n^{\bullet-}$, *Top. Curr. Chem.* **2003**, *231*, 127-152.
19. W. Pasiuk-Bronikowska, J. Ziajka, T. Bronikowski, Mechanism and kinetics of sulphide sulphur autoxidation. In *Autoxidation of sulphur compounds*, Ellis Horwood Limited, Chichester, **1992**, pp. 63-79.
20. H. Fischer, G. Schulz-Ekloff, D. Wöhrle, Oxidation of aqueous sulfide solutions by dioxygen Part I: Autoxidation reaction, *Chem. Eng. Technol.* **1997**, *20*, 462-468.
21. A. Teder, The equilibrium between elementary sulfur and aqueous polysulfide ions, *Acta Chem. Scand.* **1971**, *25*, 1722-1728.
22. H. G. Trüper, H. G. Schlegel, Sulphur metabolism in Thiorhodaceae I: Quantitative measurements on growing cells of *Chromatium okenii*, *Antonie van Leeuwenhoek* **1964**, *30*, 225-238.
23. A. Teder, Spectrophotometric determination of polysulphide excess sulfur in aqeuous solutions, *Svensk Papperst.* **1967**, *70*, 197-200.
24. L. G. Danielsson, X. S. Chai, M. Behm, L. Renberg, UV characterization of sulphide-polysulphide solutions and its application for process monitoring in the electrochemical production of polysulphides, *J. Pulp Paper Sci.* **1996**, *22*, J187-J191.

25. S. Licht, J. Davis, Disproportionation of aqueous sulfur and sulfide: Kinetics of polysulfide decomposition, *J. Phys. Chem. B* **1997**, *101*, 2540-2545.
26. W. A. Pryor, *Mechanisms of sulfur reactions*, McGraw-Hill Book Company Inc., New York, **1962**, p 12.
27. A. B. Roy, P. A. Trudinger, *The biochemistry of inorganic compounds of sulphur*, Cambridge University Press, London, **1970**, p 13.
28. C. J. N. Buisman, A. J. H. Janssen, R. J. van Bodegraven, Method for desulphurization of gases, Patent PCT/NL00/00155, 2000.
29. R. Steudel, Aqueous sulfur sols, *Top. Curr. Chem.* **2003**, *230*, 153-166.
30. A. J. H. Janssen, S. Meijer, J. Bontsema, G. Lettinga, Application of the redox potential for controlling a sulfide oxidizing bioreactor, *Biotechnol. Bioeng.* **1998**, *60*, 147-155.

Chapter 6

Effect of biologically produced sulfur on gas absorption in a biotechnological hydrogen sulfide removal process*

Abstract

Absorption of hydrogen sulfide in aqueous suspensions of biologically produced sulfur particles was studied in a batch stirred cell reactor, and in a continuous set-up, consisting of a lab-scale gas absorber column and a bioreactor. Presence of biologically produced sulfur particles was found to enhance the absorption rate of H_2S gas in the mildly alkaline liquid. The mechanism for this enhancement was however found to depend on the type of particles used. In the gently stirred cell reactor, enhancement of the H_2S absorption rate can be explained from the heterogeneous reaction between dissolved hydrogen sulfide and solid elemental sulfur to polysulfide ions, S_x^{2-}. Here, large hydrophobic particles could not be kept in suspension and therefore only smaller hydrophilic particles were present (d_p < 3 μm). Conditions favoring enhanced H_2S absorption for these hydrophilic particles are: low liquid side mass transfer (k_L), high sulfur content and presence of polysulfide ions. In the set-up of gas absorber column and bioreactor, both small hydrophilic particles and more hydrophobic particles were continuously produced (d_p up to 20 μm). Here, observed enhancement could not be explained by the heterogeneous reaction between sulfide and sulfur, due to the relatively low specific particle surface area, high k_L, and low [S_x^{2-}]. A more likely explanation for enhancement in this series of experiments is the more hydrophobic behavior of the larger particles. A local increase of the hydrophobic sulfur particle concentration near the gas/liquid interface and specific adsorption of H_2S at the particle surface can result in an increase in the H_2S absorption rate.

Keywords

Biologically produced sulfur, polysulfide, hydrogen sulfide, gas absorption, enhancement factor

* W.E. Kleinjan, J.N.J.J. Lammers, A. de Keizer, A.J.H. Janssen, Effect of biologically produced sulfur on gas absorption in a biotechnological hydrogen sulfide removal process, *Biotechnol. Bioeng.* (submitted).

6.1. Introduction

For the removal of hydrogen sulfide from gas streams, a biotechnological process was developed [1, 2] in which H_2S is converted into elemental sulfur by a mixed culture of sulfide-oxidizing bacteria, mainly of the genus *Thiobacillus* [3]. The process consists of the absorption of H_2S from a gas stream in a gas absorber by an alkaline carbonate solution (Eqs. 6.1–6.3) and the subsequent oxidation of dissolved H_2S to elemental sulfur and hydroxyl ions in a bioreactor (Eq. 6.4).

$$H_2S(g) \rightarrow H_2S(aq) \tag{6.1}$$

$$H_2S + OH^- \rightleftarrows HS^- + H_2O \tag{6.2}$$

$$CO_3^{2-} + H_2O \rightleftarrows HCO_3^- + OH^- \tag{6.3}$$

$$HS^- + \tfrac{1}{2}O_2 \rightarrow S^0 + OH^- \tag{6.4}$$

This process is currently used in a number of full-scale installations for the removal of H_2S from both biogas and natural gas [4]. Biologically produced sulfur (or 'biosulfur') is formed in particles with dimensions of approximately 0.1–1 μm, which are stabilized by organic matter, most likely proteins. The particles can form aggregates of elemental sulfur, with diameters up to 3 mm [5, 6]. Part of the particles formed in the bioreactor is led to the gas absorber. Absorption of H_2S therefore takes place in an aqueous (bi-)carbonate solution containing biologically produced sulfur particles. Absorption of H_2S in (bi-)carbonate solutions is well known and the enhancement factor due to the homogeneous reaction of sulfide with carbonate, $E_{\text{homogeneous}}$ is dependent on pH [7]. At pH > 9, $E_{\text{homogeneous}}$ is so high (up to 3000 at pH 12) that gas-side resistance becomes limiting for H_2S absorption, whereas at lower pH values, $E_{\text{homogeneous}}$ decreases so that liquid-side resistance becomes predominant. The effect of biosulfur particles on the uptake of H_2S is not well known. For a proper understanding of the new H_2S removal process, knowledge of the effect of biosulfur particles on the rate of H_2S absorption is required.

Enhancement of the gas absorption rate due to particles, with an enhancement factor E_{particle}, has been reported for many systems (for a review, see e.g., [8]), including the absorption of H_2S in crystalline sulfur particle suspensions [9, 10]. The enhancement factor for particles is usually defined as the ratio of fluxes into a solution with particles, and an identical solution without particles (Eq. 6.5)

$$E_{\text{particle}} = \frac{J_{\text{with particles}}}{J_{\text{without particles}}} \tag{6.5}$$

The total enhancement factor for the absorption of H_2S in an aqueous (bi-)carbonate solution containing biosulfur particles is determined by both the homogeneous reaction and the enhancement due to particles

$$E_{H_2S} = E_{\text{homogeneous}} \times E_{\text{particle}} \tag{6.6}$$

Several mechanisms of enhanced gas absorption due to particles have been discussed and they can all play a role in different systems. First, some researchers reported a "grazing or shuttle effect" [11, 12]. Adsorption of dissolved gas on the particle surface takes place in the diffusion layer and after diffusion of the particle to the bulk, desorption takes place. The particles therefore act as shuttles. On the one hand, this mechanism has been reported to occur especially at conditions of low mass transfer rates, e.g., low stirring rates, because of the larger diffusion layer [11]. On the other hand, however, Ruthiya *et al.* [13] suggested that the shuttle effect would occur especially in systems of high mixing intensity, due to an increase in visiting frequency of the particles in the diffusion layer.

Second, Vinke *et al*. [14] and Demmink *et al*. [10] considered so called particle-at-interface models in which enhancement of gas absorption depends on two effects, (a) accumulation of particles at the G/L interface, and (b) a high absorption capacity of the particle for the dissolved gas. Accumulation of particles at the G/L interface will occur especially with hydrophobic particles. The importance of this accumulation was supported by experiments in which enhancement in gas absorption rate only occurs with hydrophobic particles. For instance, the enhancement in gas absorption rate of H_2S in crystalline hydrophobic sulfur slurries disappeared upon addition of a surfactant [10], and the enhancement of H_2 absorption in a solution containing hydrophobic carbon-supported particles disappeared when more hydrophilic alumina-supported particles were used instead [14]. The 'absorption capacity' of particles for the gas is quantified as the distribution coefficient m_s.

$$m_s = \frac{\left(\text{amount of solute per particle volume}\right)}{\left(\text{amount of solute per solvent volume}\right)} \tag{6.7}$$

The particle-at-interface models assume absorption of the gas in the particle, based on a high solubility of the gas in the particle. The value of m_s can however also be based on adsorption of the gas onto the particle surface. Enhancement of gas absorption in a continuous system can only take place when desorption can occur as well. Apart from desorption after diffusion of particles from the G/L interface to the bulk (shuttle effect), desorption could take place after rotation of the particles at the G/L interface.

The relevance of the particle-at-interface effect for the absorption of H_2S in a suspension of biosulfur particles depends on the hydrophobicity of the particles and the distribution of H_2S between particle and solvent, the distribution coefficient m_s.

Contrary to hydrophobic crystalline sulfur, biologically produced sulfur particles are generally considered to be hydrophilic due to an organic polymer layer on the particle surface, which provides sterical and electrical stabilization against aggregation. The particles can be dispersed in water and are insoluble in hexadecane [15]. Contact angle and capillary rise measurements also show that biologically produced sulfur particles in their wet native state have a hydrophilic nature with a contact angle θ well below 90º . This is clearly different from the hydrophobic behavior of crystalline elemental sulfur (θ = 119°). However, flotation experiments showed that especially large sulfur aggregates are dragged along air bubbles to the air-liquid interface, indicating that at least part of the biologically produced sulfur is sufficiently hydrophobic to be located at the gas-liquid interface. Furthermore, contact angle measurements on dried biologically produced sulfur show intermediate hydrophobic behavior (θ ≈ 90°). This indicates that the hydrophilic behavior of biologically produced sulfur particles is not constant or uniformly distributed over all particles.

The value of the distribution coefficient m_s for H_2S with biologically produced sulfur particles is not accurately known. Wubs *et al*. [16] determined the maximum value of m_s for the absorption of H_2S in sulfur suspensions as a function of particle size, assuming monolayer or multilayer adsorption of H_2S on the sulfur particle surface. In their model, Demmink *et al*., however, needed values of m_s that were higher than the maximum values determined by Wubs *et al*. (or use values of m_s that corresponded to a particle size that was too small).

A third mechanism for the enhanced gas absorption due to particles is an increase in interfacial area by stabilization of gas bubbles, first reported by Lindner *et al*. [17]. Particle-stabilized bubbles will have a lower coalescence rate than unstabilized bubbles and therefore the bubbles will stay smaller and the interfacial area will be higher. This mechanism may contribute to enhanced gas absorption in bubble columns, it will however not be relevant in absorption experiments in a stirred cell reactor with a flat interface, where no bubbles are present. The contribution of this mechanism to the absorption of H_2S in biosulfur suspensions is difficult to predict due to the lack of knowledge of the effect of biosulfur particles on bubble size. Flotation experiments with biosulfur particles however show that especially larger sulfur particles are located at the G/L interface, where they can possibly stabilize the bubbles [16].

Furthermore, enhancement of gas absorption can take place due to a fourth mechanism, a heterogeneous reaction of the dissolved gas with the particle, as was described by Sada *et al*. [18]. They explained the enhancement of SO_2 uptake from off-gases in suspensions of calcium hydroxide particles, with a fast heterogeneous reaction of SO_2 with these particles. In general, enhanced gas absorption due to a heterogeneous reaction can occur in cases where the surface reaction is fast and the particle size is smaller than the film thickness δ_L [19].

This fourth mechanism seems relevant for the absorption of H_2S in biosulfur suspensions because of the heterogeneous reaction of dissolved hydrogen sulfide with elemental sulfur. In this reaction polysulfide ions, S_x^{2-}, are formed, chains of sulfur atoms with an average chain length x. The reaction between HS^- and elemental sulfur in its most common form (S_8) is represented by Eq. 6.8. At temperatures of 20–35 °C and when a polysulfide solution is in equilibrium with excess elemental sulfur, the value of x is approximately 5 sulfur atoms [20, 21]. The pK_a values of the protonated polysulfides (polysulfanes, H_2S_x) are low [22] indicating that in neutral to alkaline solutions polysulfides are completely deprotonated.

$$HS^- + \frac{x-1}{8} S_8 \rightleftarrows S_x^{2-} + H^+ \tag{6.8}$$

The kinetics of polysulfide formation from reaction of biologically produced sulfur particles with dissolved hydrogen sulfide at pH = 8.0 and T = 30–50 °C, have been determined in batch experiments in a previous study [23]. The kinetic properties were determined with small particles (d_p < 3 μm) and the total sulfur content was relatively low ($c_{S0} \leq 1.10$ mM). It was shown that the reaction takes place at the surface of the sulfur particles and can be described with

$$\frac{d[S_5^{2-}]}{dt} = \frac{A_c\,[HS^-]}{[H^+]} \left(k_1^*[HS^-] + k_2^*[S_5^{2-}] \right) \tag{6.9}$$

The reaction rate constants at 30 °C are: $k_1^* = 3.0 \times 10^{-14}$ m s^{-1} and $k_2^* = 3.0 \times 10^{-11}$ m s^{-1} and the *concentration of the surface* (particle surface area per solvent volume), A_c, depends on the particle size distribution.

This chapter aims to address the question whether presence of biologically produced sulfur particles enhances the uptake of H_2S gas in a biotechnological H_2S removal process and if this can be explained by the heterogeneous reaction between dissolved hydrogen sulfide and biologically produced sulfur particles. This was investigated by measuring the rate of H_2S absorption into aqueous solutions with and without sulfur particles, in a stirred cell reactor with a flat interface. Furthermore, H_2S absorption was measured in a continuous packed bed gas absorber column, which was integrated with a bioreactor where the dissolved sulfide was biologically converted into elemental sulfur. Obtained results were compared with a model for the enhancement of H_2S, based on a pseudo first order approximation of the reaction kinetics of the heterogeneous reaction between biologically produced sulfur and dissolved sulfide.

6.2. Materials and methods

6.2.1. Gas absorption in a stirred cell reactor with a flat interface

The absorption of H_2S was studied in a thermostated stirred cell reactor (Figure 6.1). The reactor is a stainless steel vessel, equipped with connections to allow the dosing of liquid and gas and to take samples. The liquid phase was mixed with a magnetic stirrer with a stirrer speed at which the G/L interface remained flat (55 min^{-1}). The introduction of gas (H_2S) is quantitatively performed from a calibrated dosing cylinder. Pressure measurements in the cell can be performed with an accuracy of ± 1 mbar. The working pressure was up to 1.88 bar. The amount of gas dissolved in the liquid can be calculated from the mass balance. From the initial kinetic data (slope of the line in a plot of ln(p) versus t between 10 and 300 s after each H_2S addition) the ratio of mass transfer coefficients and the enhancement factor E can be calculated, according to Eq. 6.10 [24].

$$\frac{\left(\frac{\mathrm{d}\ln p}{\mathrm{d}t}\right)_{\text{with particles}}}{\left(\frac{\mathrm{d}\ln p}{\mathrm{d}t}\right)_{\text{without particles}}} = \frac{k_\mathrm{L}}{k_\mathrm{L}^0} = E_{\text{particle}} \tag{6.10}$$

The experimental procedure for an absorption test was as follows: to the empty reactor 100 mL of a deaerated test solution was added after which the reactor was closed and a slight vacuum was applied to remove oxygen from the gas and liquid phase. A known amount of H_2S gas (V = 0.198 L) was then injected into the reactor and subsequently the reactor pressure was measured in time and followed for one hour. After this, seven more injections of H_2S were applied. Details on the reactor properties are reported in Table 6.1.

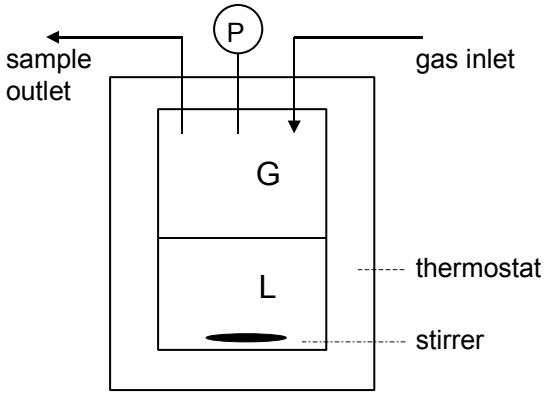

Figure 6.1. Schematic representation of the stirred cell reactor. Total reactor volume 303.7 mL.

Suspensions of biologically produced sulfur particles were obtained from a full-scale biogas treatment facility. Apart from sulfur particles, these suspensions mainly contained a (bi-)carbonate buffer and some sulfate and thiosulfate. Absorption of H_2S in original suspensions resulted, however, in release of CO_2, complicating the pressure decrease measurement. In order to avoid this, the suspension was dialyzed until the conductivity was lower than 40 μS cm^{-1}. Dialyzed suspensions were filtered over a 3.0-μm filter to remove large sulfur aggregates, which could not be kept in suspension at the applied low stirring rate. To the resulting suspension (c_{S0} = 2.0 g L^{-1}) the required amount of phosphate salt was added. Part of this suspension was diluted 10 times with a buffer solution to obtain a suspension of lower sulfur concentration. The particle size distribution of the two sulfur suspensions was therefore identical and is shown in Figure 6.2 (black circles). This resulted in two phosphate buffered solutions ($[PO_4^{3-}]$ = 0.34 M; pH = 8.0) containing biologically produced sulfur particles (c_{S0} = 0.2 and 2.0 g L^{-1}) and one phosphate buffered solution without sulfur, as a reference.

Table 6.1. Experimental conditions and properties of the stirred cell reactor.

Reactor properties		
Total reactor volume	3.037×10^{-4}	m^3
Reactor diameter	0.10	m
Total liquid volume	1.00×10^{-4}	m^3
Gas/liquid interfacial area	7.85×10^{-3}	m^2
Stirrer rate	55	min^{-1}
Temperature	303	K
Total pressure	0.017–1.88	bar

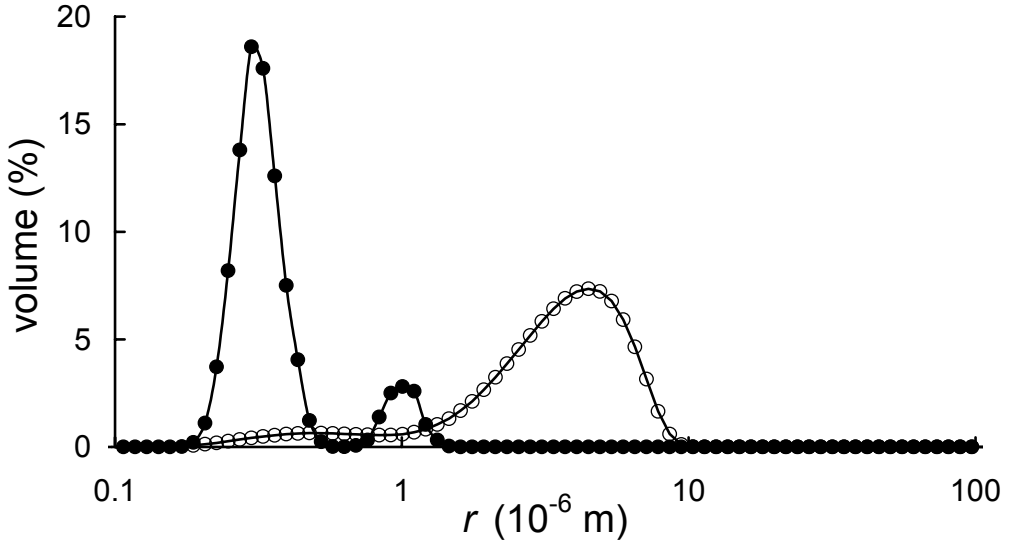

Figure 6.2. Particle size distribution of sulfur suspensions used in stirred cell reactor experiment (•) and continuous gas absorber column experiment (○).

6.2.2. Continuous gas absorption in a lab-scale gas absorber column

In an experimental set-up consisting of an integrated gas absorber and bioreactor, polysulfide formation and H_2S absorption was studied. The process is schematically shown in Figure 6.3. A gas stream consisting of N_2 (99.9 vol%) and H_2S (0.1 vol%) is directed into a packed bed gas absorber column (G), (ring diameter 5 mm, height 10 mm). The gas mixture is contacted with an alkaline liquid stream, into which H_2S dissolves and which flows into a mixing tank (M). The retention time of the liquid in this degassing zone can be controlled by changing the liquid volume in the mixing tank (level control). From the mixing tank the liquid is pumped into a continuous aerated gaslift bioreactor (B) where the dissolved sulfide is oxidized to elemental sulfur. The overflow of the bioreactor ends up in a funnel (F) in which a part of the sulfur particles are allowed to sediment. A liquid recycle stream is pumped from the funnel to the gas absorber. Accumulated sulfur can be removed from the bottom of this funnel and its overflow is the liquid bleed stream of the process. The position of gas and liquid phase sample points is shown in Figure 6.3. Properties and dimensions of the components of the process and process conditions during the experiment are reported in Table 6.2.

The O_2 gas flow into the bioreactor is proportional to the H_2S gas flow. In case of 100% selectivity for sulfur formation, the ratio O_2 / H_2S should be 0.5 based on reaction stoichiometry (see Eq. 6.4). However, as part of the available electrons are required for CO_2 fixation into biomass, this ratio is 0.45 [25]. During part of the period in which the experiment took place the O_2 gas flow was fixed at a ratio of 0.7,

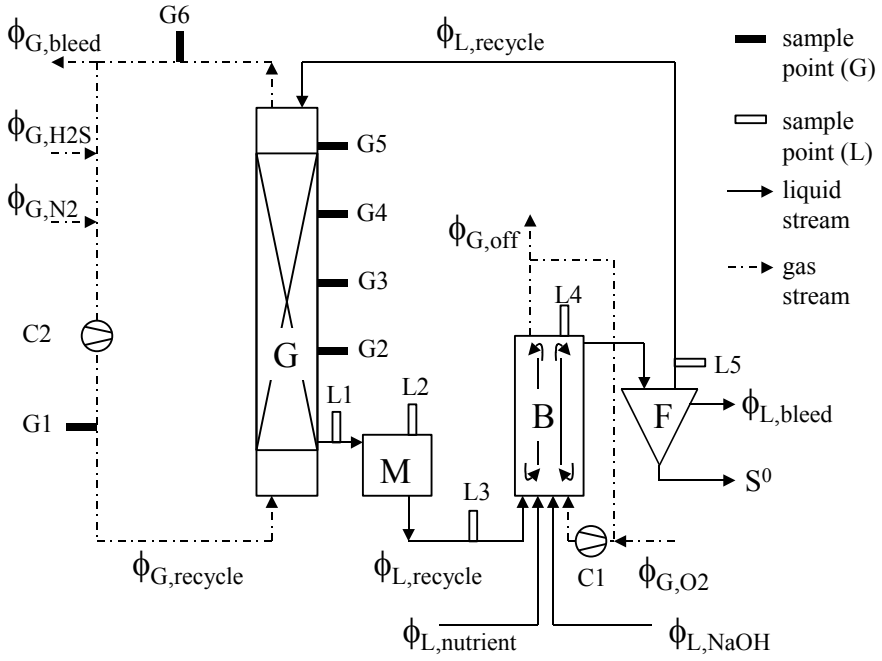

Figure 6.3. Scheme of the experimental set-up for the continuous gas absorber column experiment. G = Gas absorber, M = Mixing tank, B = Bioreactor, F = Funnel; C1 and C2: compressors; G1–G6: gas sample points; L1–L5: liquid sample points.

so that there was a slight excess of oxygen. Alternatively, the O_2 gas flow was controlled by a set point for the redox value (–350 mV; Ag/AgCl-electrode) [25].

During operation, the H_2S concentration in the gas phase was measured in the gas streams flowing into the absorber column (loaded gas), and out of the column (treated gas), as well as on four sample points at the column. The liquid streams flowing into (lean solvent) and out of the absorber column (loaded solvent) were analyzed on pH, polysulfide concentration, and total sulfide concentration.

The absorption of H_2S and the formation of polysulfide ions were studied for varying sulfur concentrations in the lean solvent. This was done in two different ways. First, the sulfur content was varied by adapting the position in the funnel from which the liquid stream was pumped into the gas absorber. This way it was possible to vary the sulfur concentration from 0.73 to 7.6 g L^{-1}, lower sulfur contents could, however, not be reached. As an alternative the bioreactor and gas absorber were uncoupled. Instead of having a continuous liquid recycle from the bioreactor, a synthetically prepared deaerated salt solution containing carbonate, sulfate, and thiosulfate was fed to the gas absorber. Changes in the sulfur content of the salt solution were made by adding varying amounts of a concentrated sulfur suspension. In this way the sulfur content was varied from 0 to 1.1 g L^{-1}. The composition of the salt solution (similar to the composition of experiments with the bioreactor) is shown in Table 6.3. The particle size distribution of the sulfur suspension used is shown in Figure 6.2 (open circles).

Furthermore, the absorption of H_2S and the formation of polysulfide ions were studied for varying H_2S gas concentrations in the ingoing gas stream. The H_2S gas concentration was varied by changing $\Phi_{G,H2S}$, while $\Phi_{G,N2}$ and the compressor C2 (and therefore $\Phi_{G,recycle}$) were kept constant. This way the rate of gas flow in the

Table 6.2. Properties and process conditions of the experimental setup for the continuous gas absorption in a lab-scale gas absorber column.

Properties and process conditions				
column diameter	0.05	m		
column height	1.4	m		
reactor diameter	0.10	m		
reactor height	0.5	m		
mixing tank diameter	0.2	m		
mixing tank height	0.5	m		
funnel diameter top	0.1	m		
funnel height	0.4	m		
$\Phi_{G,\ recycle}$	1.27	$\times 10^{-4}$ $Nm^3\ s^{-1}$	457	$L\ h^{-1}$
$\Phi_{G,\ H2S}$	0.42–1.67	$\times 10^{-7}$ $Nm^3\ s^{-1}$	2.5–10	$mL\ min^{-1}$
$\Phi_{G,\ N2}$	6.67	$\times 10^{-7}$ $Nm^3\ s^{-1}$	40	$mL\ min^{-1}$
$\Phi_{L,\ recycle}$	6.94	$\times 10^{-6}$ $m^3\ s^{-1}$	25	$L\ h^{-1}$
H_2S loading	1.17–4.67	$\times 10^{-2}$ $g\ m^{-3}\ s^{-1}$	1.01–4.04	$kg\ m^{-3}\ d^{-1}$
temperature G	296	K	23	°C
temperature L	303	K	30	°C
gas rate in gas absorber	0.0647	$m\ s^{-1}$	6.47	$cm\ s^{-1}$
gas retention time in gas absorber	21.6	s		

absorber column remains unaffected. When the reactor and gas absorber were running in steady state, with a relatively high H_2S loading rate (4.0 kg m^{-3} d^{-1}; $\Phi_{G,H2S}$ = 10 mL min^{-1}), both gas and liquid phases were analyzed. After this, the H_2S loading rate was decreased stepwise ($\Phi_{G,H2S}$ = 10, 7.5, 5.0, and 2.5 mL min^{-1}). After each step the system was kept for approximately two hours at the same conditions, to allow the column to reach a steady state and subsequently, gas and liquid phases were analyzed. The absorption of H_2S in the gas absorber column and the formation of polysulfide ions were also studied for different retention times in the mixing tank. In a steady state situation ($\Phi_{G,H2S}$ = 7.5 mL min^{-1}, $V_{mixing\ tank}$ = 2.25 L), the gas profile and the sulfide and polysulfide concentrations in the liquid are measured. After this, the mixing tank volume is lowered to 1.70 L, and after that to 1.00 L. After each decrease the system was left for approximately two hours to allow the column to reach steady state. Subsequently, the gas and liquid phases were analyzed.

6.2.3. Analysis

Total sulfide concentrations were determined spectrophotometrically by the methylene blue method as described by Trüper and Schlegel [26]. The concentration of polysulfide was determined spectrophotometrically at a wavelength of 285 nm. At this wavelength the polysulfide excess sulfur concentration (the total amount of zero valent sulfur atoms in polysulfide ions, [S^0 in S_x^{2-}]) can be determined, approximately independent of pH and ratio X_S [27, 28].

$$X_S = \frac{[S^0 \text{ in } S_x^{2-}]}{[S^{2-}]_{total}} \tag{6.11}$$

Thiosulfate and sulfate concentrations were determined by ion chromatography. The H_2S concentration in the gas phase was measured using Dräger tubes. Particle size distributions were determined with a Coulter Laser LS 230. The distribution was calculated from the data according to a Fraunhofer model, with a refractive index of sulfur (α S_8) of 1.998 [29].

Table 6.3. Composition of the salt solution used. The pH was adjusted to 8.5.

component	concentration (M)
$NaHCO_3$	0.117
Na_2CO_3	0.017
Na_2SO_4	0.020
$Na_2S_2O_3 \cdot 5H_2O$	0.129

6.3. Modeling of mass transfer

6.3.1. Henry constant, equilibrium constants, diffusion coefficients, and activity coefficients

The equilibrium between H_2S in the gas phase and in the liquid (water) phase can be described with the Henry constant H (Pa m^3 mol^{-1}). Under constant pressure and at sufficiently low dissolved H_2S concentrations, the equilibrium can be described with

$$p_{H_2S} = H_{H_2S}[H_2S]_L \tag{6.12}$$

Edwards *et al*. [30] reported the Henry constant of H_2S as function of temperature

$$\ln H_{H_2S}' = \frac{B_1}{T} + B_2 \ln T + B_3 T + B_4 \tag{6.13}$$

with $B_1 = -13236.8$, $B_2 = -55.0551$, $B_3 = 0.0595651$, and $B_4 = 342.595$. H_{H2S}' (atm kg mol^{-1}) is related to H_{H2S} (Pa m^3 mol^{-1}) by

$$H_{H_2S} = \frac{1.01325 \times 10^5 H_{H_2S}'}{\rho_w} \tag{6.14}$$

in which ρ_w is the density of water (kg m^{-3}). The equilibrium of a volatile compound between gas and liquid phase is often described in terms of the distribution coefficient m, a dimensionless form of the Henry constant. The H_2S concentrations (mol m^{-3}) in gas and liquid phases are related to m through

$$[H_2S]_L = m[H_2S]_G \tag{6.15}$$

The distribution coefficient m can be calculated from the Henry constant using

$$m = \frac{RT}{H_{H_2S}} \qquad \left(\frac{m^3{}_G}{m^3{}_L}\right) \tag{6.16}$$

Hydrogen sulfide dissolved in water is in equilibrium with HS^- and S^{2-}. At 20 °C the equilibrium constants are [31]

$$K_1 = \frac{[HS^-][H^+]}{[H_2S]} \times \frac{\gamma_{HS^-}\gamma_{H^+}}{\gamma_{H_2S}} = 10^{-7} \qquad (\text{mol L}^{-1}) \tag{6.17}$$

$$K_2 = \frac{[S^{2-}][H^+]}{[HS^-]} \times \frac{\gamma_{S^{2-}}\gamma_{H^+}}{\gamma_{HS^-}} = 0.8 \times 10^{-17} \ (\text{mol L}^{-1}) \tag{6.18}$$

Due to the low value of K_2, the equilibrium with S^{2-} can be neglected at intermediate pH values. The temperature dependence of K_1 can be described with the following expression [30]

$$\ln K_1' = \frac{A_1}{T} + A_2 \ln T + A_3 T + A_4 \tag{6.19}$$

with A_1 = –12995.4, A_2 = –33.5471, A_3 = 0, and A_4 = 218.599. The equilibrium constant K_1' is expressed in (mol kg^{-1}) and is related to K_1 (mol L^{-1}) by

$$K_1 = K_1' \rho_w \tag{6.20}$$

The equilibrium constant between polysulfide and sulfide can be represented by Eq. 6.21. At 30 °C the value for the equilibrium constant pK_x is approximately 9.1 [21].

$$K_x = \frac{[S_x^{2-}][H^+]}{[HS^-]} \times \frac{\gamma_{S_x^{2-}} \gamma_{H^+}}{\gamma_{HS^-}} = 10^{-pK_x} \tag{6.21}$$

The temperature dependence of the equilibrium between carbonate and bicarbonate

$$K_3 = \frac{[CO_3^{2-}][H^+]}{[HCO_3^-]} \times \frac{\gamma_{CO_3^{2-}} \gamma_{H^+}}{\gamma_{HCO_3^-}} \tag{6.22}$$

can also be described by Eq. 6.19, with A_1 = –12431.7, A_2 = –35.4819, A_3 = 0, and A_4 = 220.067 [30].

Estimates for the activity coefficients can be calculated with the extended Debye-Hückel law. This relation generally applies for values of the ionic strength I up to approximately 0.1 M, but can be used (with lower accuracy) above this limit [32]. For an activity coefficient γ_i for component i

$$\log \gamma_i = -\frac{z_i^2 A \sqrt{I}}{1 + \beta a_i \sqrt{I}} \tag{6.23}$$

In this relation A and β are constants characteristic for the solvent. For water at 30 °C, A = 0.514 (mol$^{-½}$ L^{½}), and β = 0.330 × 10^8 (mol$^{-½}$ L^{½} m^{-1}) [33]. Furthermore, a_i is the effective ionic diameter or the distance of closest approach to the central ion i (m), and the ionic strength I (mol L^{-1}) is given by

$$I = \tfrac{1}{2} \sum z_i^2 [i] \tag{6.24}$$

Estimates of the effective ionic diameters can be made for different ions and are shown in Table 6.4.

Diffusion coefficients of H_2S, HS^-, HCO_3^-, and CO_3^{2-} in water at infinite solution and at 25 °C were obtained from [29]. The temperature dependence of the diffusion coefficient of solute A in solvent B, D_{AB} is given by the Stokes-Einstein equation

$$D_{AB} = \frac{k_b T}{6 \pi r_A \eta_B} \tag{6.25}$$

in which k_b is the Boltzmann constant, r_A is the molecular radius of solute A, and η_B the viscosity of solvent B. Within a temperature interval of about 10–15 K, D_{AB}/T is approximately constant [34], and therefore diffusion coefficients at 30 °C can be calculated using the values at 25 °C, by $D_{30\,°C} = D_{25\,°C} \times 303/298$.

6.3.2. Enhanced H_2S absorption due to a homogeneous reaction

The absorption of H_2S from a gas phase to an alkaline carbonate solution can be represented by the homogeneous reactions Eqs. 6.1–6.3. Carbonate concentrations (≈ 20×10^{-3} M) predominate over hydroxyl concentrations (10^{-6}–10^{-5} M for pH 8–9). When we combine Eqs. 6.2 and 6.3, assuming reversible and instantaneous reactions, this gives

$$H_2S\,(aq) + CO_3^{2-} \rightleftarrows HS^- + HCO_3^- \tag{6.26}$$

For this system it can be derived ([19], see Appendix A) that the enhancement factor for H_2S absorption and therefore $E_{homogeneous}$ can be described by Eq. 6.27.

$$E_{homogeneous} = 1 + \frac{D_{HS^-}}{D_{H_2S}}\left(\frac{[HS^-]^* - [HS^-]}{[H_2S]^* - [H_2S]}\right) \tag{6.27}$$

Furthermore, the interfacial carbonate and bicarbonate concentrations can be represented with

$$[CO_3^{2-}]^* = [CO_3^{2-}] - \frac{D_{HS^-}}{D_{CO_3^{2-}}}\left([HS^-]^* - [HS^-]\right) \tag{6.28}$$

$$[HCO_3^-]^* = [HCO_3^-] + \frac{D_{HS^-}}{D_{HCO_3^-}}\left([HS^-]^* - [HS^-]\right) \tag{6.29}$$

With an instantaneous reaction, the equilibrium at the G/L interface is defined by the equilibrium constant

$$K = \frac{[HS^-]^*[HCO_3^-]^*}{[H_2S]^*[CO_3^{2-}]^*} \tag{6.30}$$

Table 6.4. Effective ionic diameters for the calculation of activity coefficients from the extended Debye-Hückel law. All effective ionic diameters are from [35], except for S_x^{2-} (estimate).

component	a_i (× 10^{-10} m)
HS^-	3.0
S_x^{2-}	4.0
H^+	9.0
HCO_3^-	4.0
CO_3^{2-}	5.0

Substitution of relations for the equilibrium distribution of H_2S in gas and liquid phase (Eq. 6.15), and for the interfacial carbonate and bicarbonate concentrations (Eqs. 6.28 and 6.29), in Eq. 6.30 result in a quadratic expression which can be solved for $[HS^-]^*$ (see Appendix A). After this, $E_{homogeneous}$ can also be calculated (Eq. 6.27).

6.3.3. Enhanced H_2S absorption due to particles

There are a number of mechanisms which could potentially cause an enhancement of the H_2S absorption rate due to the presence of biosulfur particles: heterogeneous reaction of dissolved sulfide with biosulfur (polysulfide formation), adsorption of H_2S on hydrophobic biosulfur particles at the G/L interface, and stabilization of gas bubbles by hydrophobic biosulfur particles (for tray columns). In principle, these effects could take place simultaneously. We will term the enhancement due to heterogeneous reaction as $E_{heterogeneous}$ and the combined effect of the latter two mechanisms as $E_{hydrophobic}$.

The mass transfer of H_2S in a three-phase system with a heterogeneous reaction is schematically shown in Figure 6.4. In Figure 6.4.a, the mass transfer of H_2S from gas to liquid and from liquid to solid with subsequent reaction of HS^- on the L/S interface is shown. Resistances to mass transfer on the gas side and on the liquid side of the G/L interface, on the liquid side of the L/S interface, and due to reaction at the solid surface are, in this situation, in series. Figure 6.4.b shows a situation where mass transfer and reaction occur simultaneously, with the resistance to mass transfer lying in the liquid film near the G/L interface. This particularly takes place with fast reactions and small particles.

The total sulfide fluxes can be described by the following relations

gas film: $$J_{H_2S}a = k_G a\left([H_2S]_G - [H_2S]_G^*\right) \tag{6.31}$$

liquid film: $$J_{H_2S}a = E_{H_2S}k_L a\left([H_2S]^* - [H_2S]\right) \tag{6.32}$$

liquid/solid film: $$J_{H_2S}a = k_{LS}A_c\left([H_2S] - [H_2S]_{LS}^*\right) + k_{LS}A_c\left([HS^-] - [HS^-]_{LS}^*\right) \tag{6.33}$$

surface reaction: $$J_{H_2S}a = -R_{H_2S} = k_1'' A_c\left([H_2S]_{LS}^* + [HS^-]_{LS}^*\right) \tag{6.34}$$

Reaction kinetics were reported in an earlier study [23], from which it was concluded that at the given conditions the chemical reaction was rate limiting, instead of the transport of HS^- to the L/S interface. Therefore, we can ignore the transport to the L/S interface (Eq. 6.33) and we will assume that the reaction at the solid surface is proportional to the total sulfide concentration in the bulk. Eq. 6.34 can therefore be replaced by

$$J_{H_2S}a = k_1'' A_c \left([H_2S] + [HS^-] \right) \tag{6.35}$$

Analogously to [19], a relation for the stationary flux can now be derived using Eqs. 6.31, 6.32, and 6.35, combined with relations for the equilibrium distribution of H_2S between gas and liquid phase (Eq. 6.15) and the equilibrium between H_2S and HS^- (Eq. 6.17) (see Appendix B). This results in Eq. 6.36. The three ratios in the denominator of the fraction can be seen as three resistances in series (gas phase resistance, liquid phase resistance, and resistance due to chemical reaction).

$$J_{H_2S}a = \frac{[H_2S]_G}{\frac{1}{k_G a} + \frac{1}{mE_{H_2S}k_L a} + \frac{1}{mk_1'' A_c \left(1 + \frac{K_1}{[H^+]} \times \frac{\gamma_{H_2S}}{\gamma_{HS^-}\gamma_{H^+}} \right)}} \tag{6.36}$$

Enhancement of gas absorption due to chemical reaction can occur when chemical reaction and mass transfer are parallel steps. This is the case when the resistance to mass transfer lies in the liquid film near the G/L interface (Figure 6.4.b), that is for

$$\frac{1}{mk_1'' A_c \left(1 + \frac{K_1}{[H^+]} \times \frac{\gamma_{H_2S}}{\gamma_{HS^-}\gamma_{H^+}} \right)} << \frac{1}{mE_{H_2S}k_L a} + \frac{1}{k_G a} \tag{6.37}$$

where k_L is the mass transfer coefficient from gas to liquid (m s^{-1}), A_c the specific particle surface per reactor volume (m^2 m^{-3}), k_1" the specific first order reaction rate constant (m s^{-1}), and a the specific gas-liquid interfacial area per reactor volume (m^2 m^{-3}).

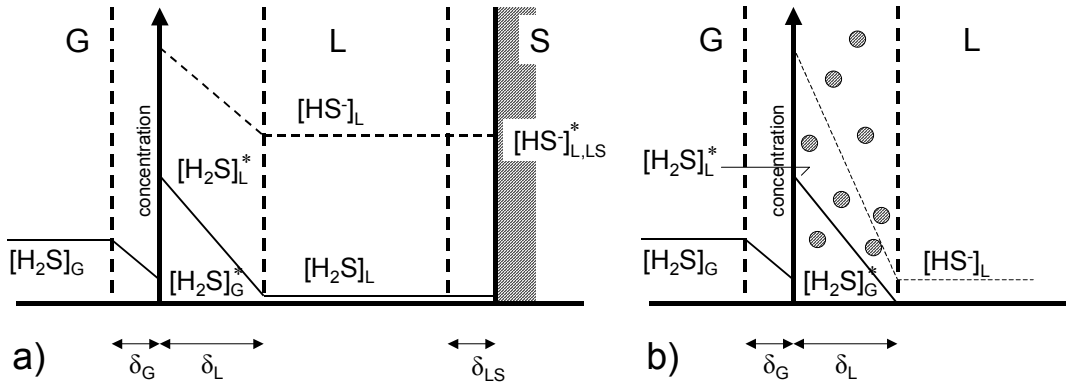

Figure 6.4. Concentration profiles of H_2S and HS^- in mass transfer from gas to liquid to solid with subsequent reaction on the solid surface. **a)** Large sulfur particles, mass transfer and reaction in series; **b)** Small sulfur particles, mass transfer and reaction parallel.

When Eq. 6.37 is valid, mass transfer can be considered parallel to reaction and enhancement can be treated similarly as with homogeneous reaction. According to film theory, enhancement can then be calculated using

$$E = \frac{Ha}{\tanh Ha} \tag{6.38}$$

with

$$Ha = \sqrt{\frac{kD_{H_2S}}{{k_L}^2}} \tag{6.39}$$

where Ha is the Hatta number (-), and k is a pseudo first order reaction constant (s^{-1}). Estimates for k_L (0.8×10^{-4} m s^{-1}) and a (70 m^2 m^{-3}) can be made for packed columns and for stirred cell reactors [19]. The kinetics of the heterogeneous reaction can be described by Eq. 6.9. This reaction is of mixed kinetics, however a pseudo first order approximation can be made

$$\frac{\mathrm{d}[S_5^{2-}]}{\mathrm{d}t} = \frac{k_2^* A_c [HS^-][S_5^{2-}]}{[H^+]} \approx k[HS^-] \tag{6.40}$$

with $k_2^* = 3.0 \times 10^{-11}$ m s^{-1}. For a known particle size distribution, the *concentration of the surface*, A_c, can be calculated from the total sulfur content.

$$A_c = c_{S^0} A_s = \frac{3c_{S^0}}{\rho r} \tag{6.41}$$

The pseudo first order reaction constant k can therefore be calculated for known particle size distribution, pH and polysulfide concentration. This value has to be divided by A_c to obtain the specific pseudo first order reaction rate constant as defined in Eq. 6.37.

$$k_1'' = \frac{k}{A_c} = \frac{k_2^*[S_5^{2-}]}{[H^+]} \tag{6.42}$$

6.3.4. Absorber column model

Consider a packed column divided in n ideally mixed parts (Figure 6.5). The amount of H_2S transferred in each part of the column can be calculated by

$$\Phi = J_{H_2S} a A \mathrm{d}H \qquad (\text{mol } s^{-1}) \tag{6.43}$$

A relation for J_{H2S} can be derived from Eqs. 6.31 and 6.32

$$J_{H_2S} = \frac{[H_2S]_G - \frac{[H_2S]}{m}}{\frac{1}{k_G} + \frac{1}{mE_{H_2S}k_L}} \tag{6.44}$$

In these relations k_G and k_L are mass transfer coefficients of the gas and of the liquid phase, a the interfacial area per packed area, A the column cross section, dH the height of one part of the column, m the H_2S partition coefficient between gas and water, and E_{H2S}
the enhancement factor. Under the assumption that the sulfide concentrations are low so that changes in the volumetric gas and liquid stream are negligible, the following mass balances for a part of the column can be made.

$$\Phi_G[H_2S]_{G,in} = \Phi_G[H_2S]_{G,1} + \frac{aA\mathrm{d}H\left([H_2S]_{G,1} - \frac{[H_2S]_{L,1}}{m}\right)}{\frac{1}{k_G} + \frac{1}{mE_{H_2S}k_L}} \tag{6.45}$$

$$\Phi_L[S^{2-}]_{total,L,1} = \Phi_L[S^{2-}]_{total,L,2} + \frac{aA\mathrm{d}H\left([H_2S]_{G,1} - \frac{[H_2S]_{L,1}}{m}\right)}{\frac{1}{k_G} + \frac{1}{mE_{H_2S}k_L}} \tag{6.46}$$

The driving force in gas absorption is the between $[H_2S]_G$ (at the interface) and $[H_2S]_L$. For known sulfide concentrations at the bottom ($[H_2S]_{G,in}$ and $[H_2S]_{L,out}$) and known gas and liquid flows (Φ_G and Φ_L), H_2S mass transfer in the complete column can be calculated. For the lowest element of the column ("1") the outcoming $[H_2S]_{G,1}$

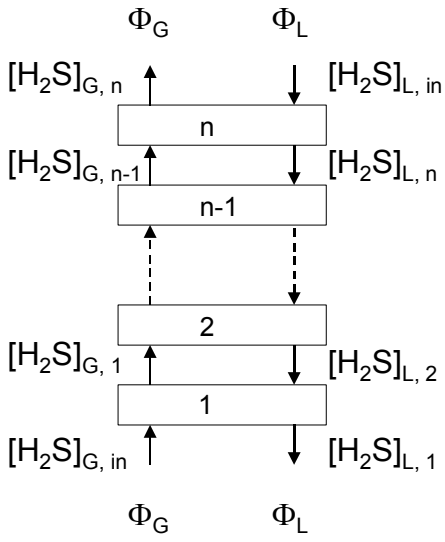

Figure 6.5. Packed column divided in *n* parts.

can be calculated by solving Eq. 6.45, using the known $[H_2S]_{G,in}$ and $[H_2S]_{L,1}$ (= $[H_2S]_{L,out}$). After this, $[S^{2-}]_{total,L,2}$ can be calculated using Eq. 6.46. Corresponding $[H_2S]$, $[HS^-]$, and $[S_x^{2-}]$ follow from the equilibrium between H_2S and HS^- (Eq. 6.17), the equilibrium between polysulfide and sulfide (Eq. 6.21), and the total sulfide mass balance in the liquid phase (Eq. 6.47).

$$[S^{2-}]_{total} = [H_2S] + [HS^-] + [S_x^{2-}] \quad (6.47)$$

Going from bottom to top, the complete sulfide profiles in gas and liquid phases can be calculated this way. The enhancement factor due to homogeneous reaction can be calculated using Eq. 6.27. The pH profile in the column can be based on the measured pH values of the loaded and clean solvent. When the difference of pH in top and bottom is small (buffered system), the pH profile between top and bottom can be assumed to be linear with column height.

6.4. Results and discussion

6.4.1. Gas absorption in a stirred cell reactor

The enhancement factor was calculated as the ratio of the mass transfer coefficients with (k_L) and without (k_L^0) particles according to Eq. 6.10 [24]. Results are shown in Figure 6.6 for c_{S0} = 0.2 and 2.0 g L^{-1} as a function of the total sulfide fraction of the liquid. Apart from the first H_2S injections (f_{H2S} = 0) and the fifth injection for c_{S0} = 2.0 g L^{-1}, the enhancement is more or less independent of the sulfide concentration in the liquid. The enhancement increases with increasing sulfur content; $E_{particle}$ = 1.05 (c_{S0} = 0.2 g L^{-1}), and $E_{particle}$ = 1.45 (c_{S0} = 2.0 g L^{-1}). The lower value of $E_{particle}$ in the first

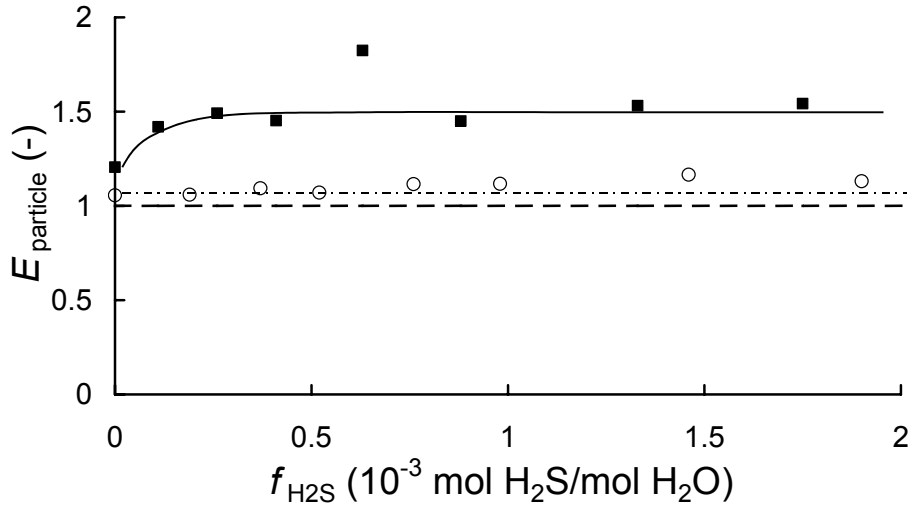

Figure 6.6. Enhancement factor as function of total sulfide fraction based on kinetic data of gas absorption experiments in batch stirred cell reactor for c_{S0} = 0.2 g L^{-1} (○) and 2.0 g L^{-1} (■).

H_2S addition is possibly related to the initial absence of polysulfide ions in the solution. As can be seen from the reaction kinetics (Eq. 6.9), presence of polysulfide ions has an autocatalyzing effect on polysulfide formation. Initially no polysulfide ions are present in the stirred cell reactor and the heterogeneous polysulfide formation reaction will be relatively slow.

6.4.2. Continuous gas absorption in a gas absorber column

The effect of sulfur concentration in the liquid stream on sulfide and polysulfide concentrations in the liquid is shown in Figure 6.7. The sulfur concentration in the liquid was varied in two ways. First, in a system where gas absorber and bioreactor are both operating, the sulfur content was varied by adapting the position in the funnel from which the liquid stream into the gas absorber (lean solvent) is pumped. This way, the sulfur concentration was varied from 0.73 to 7.7 g L^{-1} (diamonds). Secondly, the bioreactor was uncoupled from the gas absorber. A stock suspension was sprayed into the gas absorber as lean solvent. The stock suspension consisted of a salt solution (Table 6.3) and a biosulfur suspension of known sulfur content. In this way, it is easier to apply lower sulfur concentrations in the liquid stream. The sulfur concentration varied from 0–1.12 g L^{-1} (triangles).

Figure 6.7 shows that the total amount of sulfide transferred (open symbols) is approximately independent of the sulfur concentration of the liquid stream. Concentration differences in the liquid stream are based on measurements in loaded

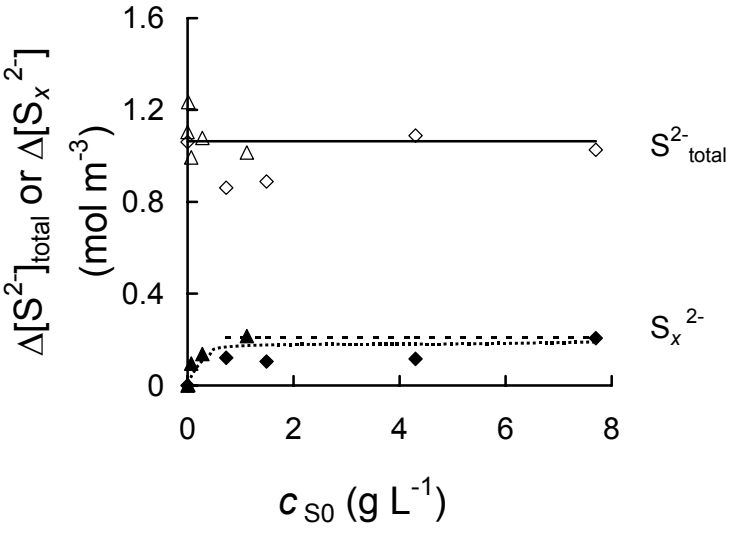

Figure 6.7. Effect of varying the sulfur concentration by adapting the position of the lean solvent inlet in the funnel on the change in total sulfide (◊) and polysulfide (♦) concentrations in the loaded solvent, and by dosing stock suspensions as lean solvent on the change in total sulfide (Δ) and polysulfide (▲) concentrations. Theoretical changes in total sulfide concentration (—) based on mass balance and in polysulfide concentrations (- - -) based on polysulfide equilibrium. The curved dotted line is a guide for the eye.

(L1, see Figure 6.3) and lean solvent (L5). The straight line shows the theoretical total sulfide concentration for the given $[H_2S]_G$, based on the mass balance (Eq. 6.48). Initially, an increase in the sulfur concentration has a strong effect on the polysulfide formation (black symbols), after which the amount of polysulfide formed seems to reach a plateau. This indicates that the equilibrium of polysulfide formation is reached. At the applied conditions ($[S^{2-}]_{total} \approx 1$ mM) elemental sulfur is already in excess at $c_{S0} > 0.03$ g L^{-1}. Once an excess amount of elemental sulfur is present, the polysulfide concentration in equilibrium remains constant. The theoretical concentration of polysulfide ions at equilibrium can be calculated from measured pH and $[S^{2-}]_{total,L}$, and the equilibrium between polysulfide and sulfide (Eq. 6.21). The calculated polysulfide concentration in equilibrium (dashed line) overlaps with the measured data at higher sulfur concentrations, showing that the heterogeneous polysulfide formation reaction in the loaded solvent is close to equilibrium.

The effect of the sulfur concentration on H_2S gas profiles in the gas absorber column is shown in Figure 6.8 (data points). At higher sulfur concentrations the H_2S concentrations in the gas phase in the absorber column are lower, indicating that presence of sulfur induces enhancement of H_2S absorption rate. The lines in Figure 6.8 represent corresponding calculated profiles according to the model described in section 6.3.4. An estimate of $E_{particle}$ was determined by using $E_{particle}$ as fit parameter, set at 1 for $c_{S0} = 0$ g L^{-1}. Fit parameters were obtained by means of least square errors between measured data points and corresponding points of the calculated profiles. The values of these fits are shown as a function of c_{S0} in the inset in Figure 6.8.

Initially, a steep increase in $E_{particle}$ can be seen, after which this increase levels off, possibly reaching a plateau. This behavior seems in line with enhancement of H_2S

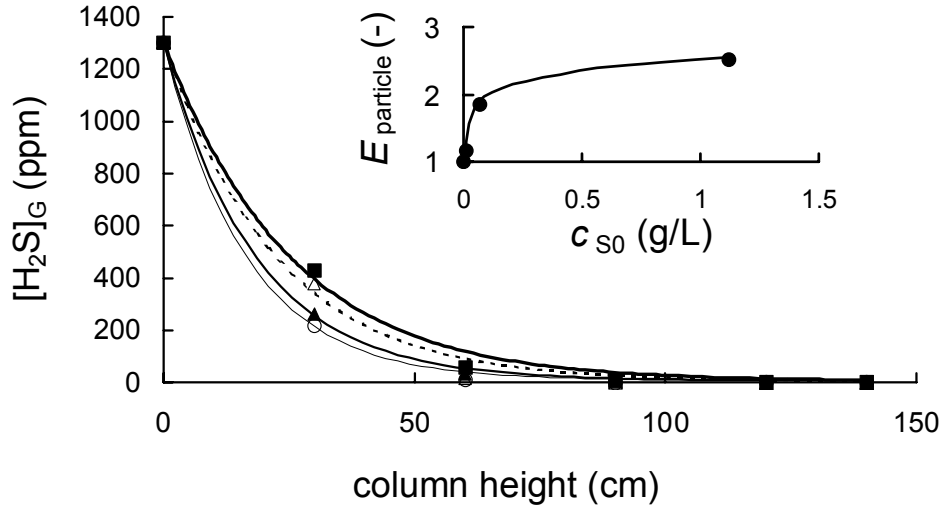

Figure 6.8. Effect of sulfur content on H_2S profiles in the gas absorber. 0 g L^{-1} (■), 0.014 g L^{-1} (Δ), 0.07 g L^{-1} (▲), 1.12 g L^{-1} (○). The lines represent calculated profiles in which $E_{particle}$ is used as fit parameter. Values of $E_{particle}$ are shown in the inset.

absorption by particles due to the heterogeneous polysulfide formation reaction. A linear increase in sulfur concentration, and therefore in A_c and k (see Eq. 6.40) will result in a curved increase in E (Eq. 6.38), approximately similar to the measured increase shown in the inset of Figure 6.8. However, the curved increase of $E_{particle}$ with sulfur concentration may also be related to accumulation of hydrophobic particles at the G/L interface. Once the complete G/L interface is covered with sulfur, a further increase in sulfur concentration will not result in an increase in sulfur concentration near the interface and, therefore, not in an increase in enhancement factor either.

Figure 6.9 shows the effect of the amount of H_2S transferred based on the gas phase ($\Phi_G\Delta[H_2S]_G$), compared to the amount of H_2S transferred based on the liquid phase ($\Phi_L\Delta[S^{2-}]_{total,L}$). Concentration differences in the liquid stream are based on measurements in loaded (L1, see Figure 6.3) and lean solvent (L5). Concentration differences in the gas stream are based on measurements in loaded (G1) and treated gas (G6). It can be seen that the data points (open circles) are in reasonable agreement with the mass balance of H_2S absorption (full line, Eq. 6.48).

$$\Phi_{L,recycle}\Delta[S^{2-}]_{total,L} = \Phi_{G,recycle}\Delta[H_2S]_G \qquad (6.48)$$

The amount of polysulfide formed ($\Phi_L\Delta[S_x^{2-}]_L$, black circles) corresponds to the theoretical equilibrium polysulfide concentration (dotted line) showing that the polysulfide formation reaction is close to equilibrium in the loaded solvent. This was also found in the experiment where the effect of sulfur concentration was investigated (Figure 6.7).

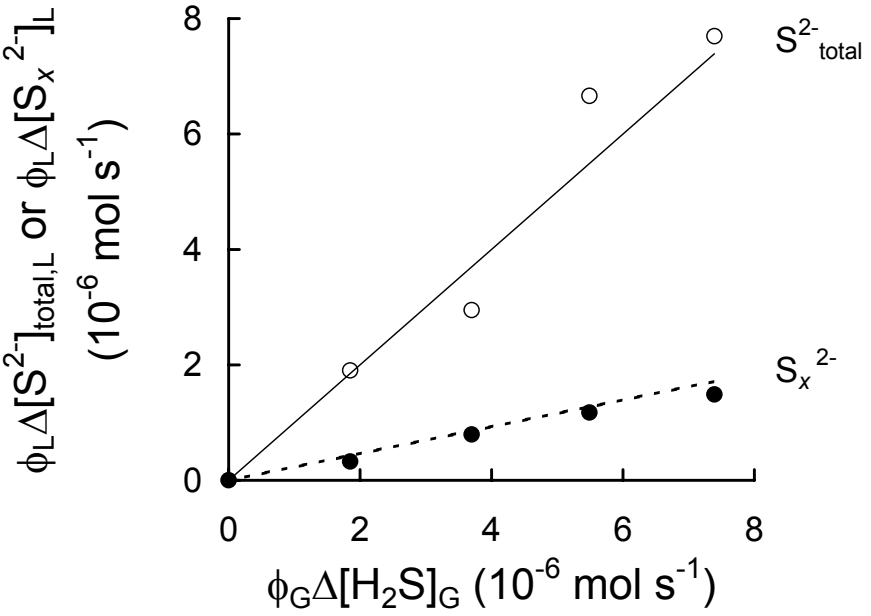

Figure 6.9. Amount of H_2S transferred from the gas phase compared to the amount of total sulfide (○) and polysulfide (•) transferred to the liquid phase. The straight line represents the ideal mass balance. The dotted line shows the polysulfide concentration in equilibrium.

The effect of changing $[H_2S]_G$ on the H_2S gas profile in the gas absorber column is shown in Figure 6.10 (data points). At low H_2S loading (2.5 mL min^{-1} or 0.104 mmol min^{-1}), approximately all H_2S is removed from the gas stream in the first 30 cm whereas at a H_2S flow rate of 7.5 mL min^{-1}, almost the complete column is required. At a H_2S flow rate of 10 mL min^{-1} not all H_2S is removed from the gas stream. The lines in Figure 6.10 represent corresponding calculated profiles, according to the model described in section 6.3.4. Values for $E_{homogeneous}$ vary from bottom to top between 41 and 51, and $E_{particle}$ was taken to be 2.52 (see Figure 6.8). On average, the pH in the liquid at the bottom of the column was about 0.1 pH unit lower than at the top. Values of properties used in the calculation are shown in Table 6.5.

Figure 6.11 shows the effect of the retention time of the liquid in the mixing tank on polysulfide (black symbols) and total sulfide (open symbols) concentrations. The total sulfide concentration is approximately independent of the retention time in the mixing tank. The total sulfide concentration in the mixing tank (L2, open squares) is approximately the same as in the liquid coming from the gas absorber (L1, open diamonds). The straight line shows the theoretical total sulfide concentration for the given $[H_2S]_G$, based on the mass balance (Eq. 6.48). The polysulfide concentrations in the mixing tank (L2, black squares) and in the liquid coming from the gas absorber (L1, black diamonds) are approximately independent of retention time. Within the error margins of the measurement, the concentrations are the same. The dotted line, which shows the expected polysulfide concentration when in equilibrium, corresponds to the measured polysulfide concentrations. The reaction between elemental sulfur and sulfide can therefore be assumed to be in equilibrium in the liquid coming from the gas absorber column.

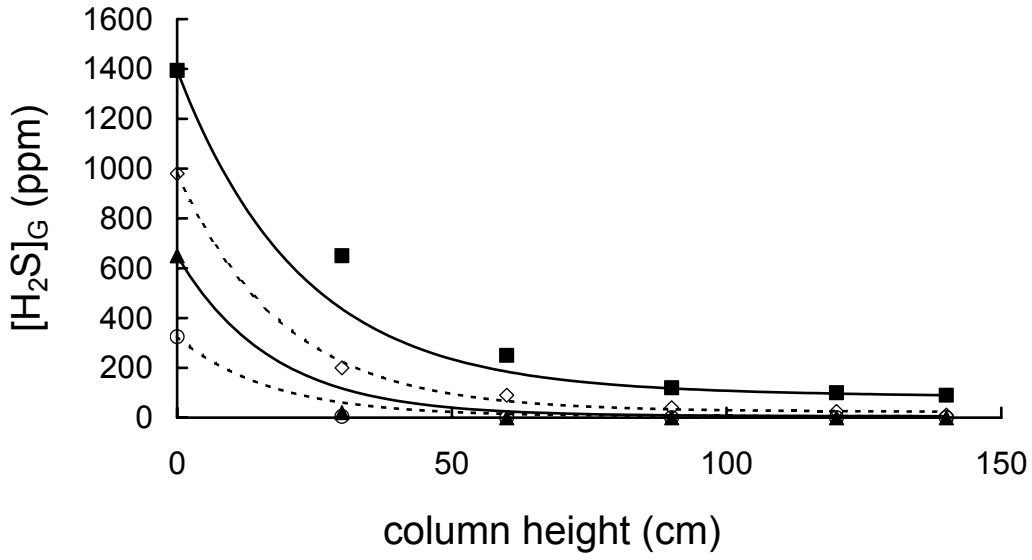

Figure 6.10. H_2S gas profile in the column for different H_2S gas flow rates. $\phi_{G,\,H2S}$ =10 mL min^{-1} (■); 7.5 mL min^{-1} (◊); 5.0 mL min^{-1} (▲); 2.5 mL min^{-1} (○). c_{S0} = 1.5 g L^{-1}. The lines represent the corresponding calculated profiles with $E_{particle}$ = 2.52.

To determine the mechanism of enhancement of H_2S absorption due to particles, it is possible to compare experimental findings with the theoretical contribution of the heterogeneous reaction. For this purpose, the condition expressed in Eq. 6.37 was verified for a stirred cell reactor and a gas absorber, after which E was calculated with Eq. 6.38. The values of properties used in this calculation are shown in Table 6.6. The condition in Eq. 6.37 is valid for a stirred cell reactor. However, for the packed absorber column the condition is not met.

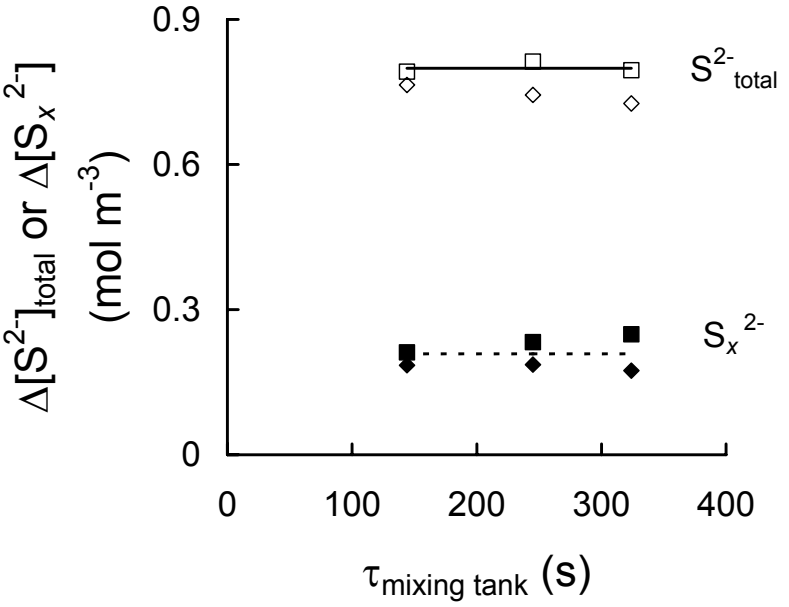

Figure 6.11. Effect of mixing tank retention time on the sulfide (open symbols) and polysulfide concentration (black symbols) in different liquid streams in the process. Gas absorber out, L1 (diamonds), mixing tank L2 (squares). $[H_2S]_G$ = 980 ppm. pH = 8.55.

Table 6.5. Conditions and values of constants used in calculations of $[H_2S]_G$ profiles in the gas absorber column. (Figures 6.8 and 6.10).

Symbol		Value	Unit	Reference
Φ_G	gas flow	1.27×10^{-4}	$m^3\ s^{-1}$	
Φ_L	liquid flow	6.94×10^{-6}	$m^3\ s^{-1}$	
k_L	mass transfer coefficient liquid	0.8×10^{-4}	$m\ s^{-1}$	
a	specific gas-liquid interfacial area	70	$m^2\ m^{-3}$	
A	column area	1.96×10^{-3}	m^2	
n	number of column elements	60	-	
dH	height of column element	0.0235	m	
$[CO_3^{2-}]$	carbonate concentration	20	mol m^{-3}	
$[HCO_3^-]$	bicarbonate concentration	110	mol m^{-3}	
$E_{homogeneous}$	enhancement factor due to homogeneous reaction	41–51	-	
$E_{particle}$	enhancement factor due to particle	1–2.4	-	
D_{H2S}	diffusion coefficient H_2S at 25 °C	1.36×10^{-9}	$m^2\ s^{-1}$	[29]
$D_{HS(-)}$	diffusion coefficient HS^- at 25 °C	1.731×10^{-9}	$m^2\ s^{-1}$	[29]
$D_{HCO3(-)}$	diffusion coefficient HCO_3^- at 25 °C	1.185×10^{-9}	$m^2\ s^{-1}$	[29]
$D_{CO3(2-)}$	diffusion coefficient CO_3^{2-} at 25 °C	0.923×10^{-9}	$m^2\ s^{-1}$	[29]
m	H_2S partition coefficient between gas and water	2.294	$m^3_G\ m^{-3}_L$	[30]
pH		8.40–8.50		

The theoretical enhancement factors due to the heterogeneous reaction (c_{S0} = 0.2 g L^{-1}: E = 1.04, and c_{S0} = 2.0 g L^{-1}: E = 1.37) are reasonably well in agreement with the experimental results (E = 1.05 and 1.45, respectively). This suggests that the heterogeneous reaction is the main contributor to the enhancement due to particles in the stirred cell reactor experiment. Factors that stimulate a high enhancement rate of H_2S for small hydrophilic particles are a low k_L, high [S_x^{2-}], high pH, small particle size, and high c_{S0}. In the stirred cell reactor, only small particles (< 3 μm) were used. The larger sulfur aggregates were removed to prevent them from settling at the reactor bottom. These small particles generally have a more hydrophilic character and therefore accumulation of biosulfur at the G/L interface with adsorption of H_2S at the particles does not take place.

In the continuously operated gas absorber and integrated bioreactor, sulfur particles were continuously produced and are not of uniform size. Larger particles were present and therefore the specific total particle surface area was smaller than in the stirred cell reactor experiment. Furthermore, the high k_L and low [S_x^{2-}] do not favor the reaction rate of the heterogeneous reaction, as can be seen from the kinetic relation in Eq. 6.9.

The observed effect of sulfur content on the H_2S gas profiles in the gas absorber column (Figure 6.8) is therefore probably not caused by heterogeneous reaction. It is more likely that the observed enhancement of H_2S absorption rate in this experiment is caused by the more hydrophobic behavior of the larger particles. This could take place either by adsorption of H_2S at the particle surface, whereby particles act as shuttles, or by an increase in interfacial gas-liquid area by stabilization of gas bubbles.

6.5. Conclusions

In a stirred cell reactor, enhancement of H_2S absorption rate due to particles takes place with small (d_p < 3 μm) biologically produced sulfur particles. These particles are hydrophilic in nature and enhancement of H_2S gas absorption can be explained by

Table 6.6. Values for some properties in the stirred cell reactor and the packed absorber column.

	stirred cell reactor	**absorber column**	
k_{LS}	2.77	2.77	× 10^{-3} m s^{-1}
k_L	0.2	0.8	× 10^{-4} m s^{-1}
k_1"	0.228	0.0754	× 10^{-4} m s^{-1}
A_c	1.10 (c_{S0} = 2.0 g L^{-1})	0.133	× 10^{4} m^2 m^{-3}
	0.11(c_{S0} = 0.2 g L^{-1})		× 10^{4} m^2 m^{-3}
a	78	70	m^2 m^{-3}
pH	8.0	8.5	-
[S_5^{2-}]	7.6	1	mol m^{-3}
$E_{heterogeneous}$	1.37 (c_{S0} = 2.0 g L^{-1})	1.00	-
	1.04 (c_{S0} = 0.2 g L^{-1})		-

the heterogeneous reaction between elemental sulfur and dissolved hydrogen sulfide, forming polysulfide ions. Conditions favoring this enhancement are low liquid side mass transfer, high polysulfide concentration, high pH, high sulfur content, and small particle size.

Enhancement of H_2S gas absorption rate in an aqueous carbonate/bicarbonate solution containing biologically produced sulfur particles, can take place in a continuously operated lab-scale gas absorber. The absorber column was integrated with a bioreactor in which sulfur particles with a broad particle size distribution are formed. At the conditions tested (pH = 8.5) the enhancement factor for homogeneous reaction varies from 41–51. The enhancement factor due to particles reaches values up to 2.5. The heterogeneous reaction between sulfide and elemental sulfur is close to equilibrium in the liquid coming from the gas absorber. Enhancement of H_2S absorption rate can however not be explained by the heterogeneous reaction alone. For larger biosulfur particles the enhancement is probably caused by the more hydrophobic behavior of the particles resulting in a local increase of the hydrophobic sulfur particle concentration near the G/L interface. Specific adsorption of H_2S at the particle surface near the G/L interface with subsequent desorption near the bulk (shuttle mechanism) can then result in an enhancement of the H_2S absorption rate.

Nomenclature

$[A]_G$	concentration of component A in gas phase	mol m^{-3} or ppm
$[A]_L$ or $[A]$	concentration of component A in liquid phase	mol m^{-3}
$[A]^*$	concentration of component A at interface	mol m^{-3}
a	specific gas-liquid interfacial area	m^2 m^{-3}
A_c	concentration of surface	m^2 m^{-3}
A_s	specific surface	m^2 g^{-1}
A_1–A_4	constants in Eq. 6.19	
B_1–B_4	constants in Eq. 6.13	
c_{S0}	solid sulfur content	g m^{-3} or g L^{-1}
d_p	particle diameter	m
dH	height of column element	m
D	diffusion coefficient	m^2 s^{-1}
E	enhancement factor	-
$E_{homogeneous}$	enhancement factor due to homogeneous reaction	-
$E_{heterogeneous}$	enhancement factor due to heterogeneous reaction	-
J	flux	mol m^{-2} s^{-1}
H	Henry constant	Pa m^3 mol^{-1}
H'	Henry constant	atm kg mol^{-1}
Ha	Hatta number	-
k	pseudo first order reaction rate constant	s^{-1}
$k'' = k/A_c$	specific pseudo first order reaction rate constant	m s^{-1}
k_1^*	reaction rate constant	m s^{-1}
k_2^*	reaction rate constant	m s^{-1}

k_b	Boltzmann constant	J K^{-1}
k_G	mass transfer coefficient gas film	m s^{-1}
k_L	mass transfer coefficient liquid film	m s^{-1}
k_{LS}	mass transfer coefficient from liquid to solid	m s^{-1}
K_x	polysulfide/sulfide equilibrium constant	mol m^{-3}
m	distribution coefficient between gas and liquid	m^3_G m^{-3}_L
m_s	distribution coefficient between liquid and solid	-
n	number of column elements	-
p	pressure	Pa
r	particle radius	m
R	gas constant	J mol^{-1} K^{-1}
t	time	s
T	temperature	K
V_G	volume of the gas phase	m^3
V_L	volume of the liquid phase	m^3
x	number of sulfur atoms in a polysulfide molecule	-
X_S	ratio S^0/S^{2-} in polysulfide molecule	-

Greek symbols

Φ_L	liquid flow	mol s^{-1}
Φ_G	gas flow	mol s^{-1}
η	dynamic viscosity	N s m^{-2}
θ	contact angle	°
ρ	density	kg m^{-3}
τ	retention time	s
ζ	fraction of G/L interface covered with particles	-

Subscripts/superscripts

G	concerning the gas phase
L	concerning the liquid phase
LS	concerning the liquid/solid film or interface

References

1. C. J. Buisman, B. G. Geraats, P. IJspeert, G. Lettinga, Optimization of sulphur production in a biotechnological sulphide-removing reactor, *Biotechnol. Bioeng.* **1990**, *35*, 50-56.
2. A. J. H. Janssen, R. Sleyster, C. van der Kaa, A. Jochemsen, J. Bontsema, G. Lettinga, Biological sulphide oxidation in a fed-batch reactor, *Biotechnol. Bioeng.* **1995**, *47*, 327-333.
3. J. M. Visser, G. C. Stefess, L. A. Robertson, J. G. Kuenen, *Thiobacillus* sp. W5, the dominant autotroph oxidizing sulfide to sulfur in a reactor for aerobic treatment of sulfidic wastes, *Antonie van Leeuwenhoek* **1997**, *72*, 127-134.
4. C. Cline, A. Hoksberg, R. Abry, A. Janssen, Biological process for H_2S removal from gas streams. The Shell-Paques/Thiopaq gas desulfurization process. In *Proceedings of the Laurance Reid gas conditioning conference* [CD-ROM], University of Oklahoma, Norman, OK, **2003**.
5. A. J. H. Janssen, G. Lettinga, A. de Keizer, Removal of hydrogen sulphide from wastewater and waste gases by biological conversion to elemental

sulphur. Colloidal and interfacial aspects of biologically produced sulphur particles, *Colloids Surf. A-Physicochem. Eng. Aspects* **1999**, *151*, 389-397.
6. W. E. Kleinjan, A. de Keizer, A. J. H. Janssen, Biologically produced sulfur, *Top. Curr. Chem.* **2003**, *230*, 167-187. *This thesis, chapter 2*.
7. M. Wallin, S. Olausson, Simultaneous absorption of H_2S and CO_2 into a solution of sodium carbonate, *Chem. Eng. Comm.* **1993**, *123*, 43-59.
8. A. A. C. M. Beenackers, W. P. M. van Swaaij, Mass-transfer in gas-liquid slurry reactors, *Chem. Eng. Sci.* **1993**, *48*, 3109-3139.
9. A. Mehra, M. Sharma, Absorption of hydrogen sulfide in aqueous solutions of iodides containing dissolved iodine: Enhancements in rates due to precipitated sulfur, *Chem. Eng. Sci.* **1988**, *43*, 1071-1081.
10. J. F. Demmink, A. Mehra, A. A. C. M. Beenackers, Gas absorption in the presence of particles showing interfacial affinity: Case of fine sulfur precipitates, *Chem. Eng. Sci.* **1998**, *53*, 2885-2902.
11. E. Alper, B. Wichtendahl, W.-D. Deckwer, Gas absorption mechanism in catalytic slurry reactors, *Chem. Eng. Sci.* **1980**, *35*, 217-222.
12. G. Quicker, E. Alper, W.-D. Deckwer, Effect of fine activated carbon particles on the rate of CO_2 absorption, *AIChE J.* **1987**, *33*, 871-875.
13. K. C. Ruthiya, J. van der Schaaf, B. F. M. Kuster, J. C. Schouten, Mechanisms of physical and reaction enhancement of mass transfer in a gas inducing stirred slurry reactor, *Chem. Eng. J.* **2003**, *96*, 55-69.
14. H. Vinke, P. J. Hamersma, J. M. H. Fortuin, Enhancement of the gas-absorption rate in agitated slurry reactors by gas-adsorbing particles adhering to gas bubbles, *Chem. Eng. Sci.* **1993**, *48*, 2197-2210.
15. A. J. H. Janssen, A. de Keizer, G. Lettinga, Colloidal properties of a microbiologically produced sulphur suspension in comparison to a LaMer sulphur sol, *Colloids Surf. B-Biointerfaces* **1994**, *3*, 111-117.
16. H. J. Wubs, A. A. C. M. Beenackers, R. Krishna, Absorption of hydrogen sulfide in aqueous solutions of iodine - a critical review, *Chem. Eng. Sci.* **1991**, *46*, 703-706.
17. D. Lindner, M. Werner, A. Schumpe, Hydrogen transfer in slurries of carbon supported catalyst (HPO process), *AIChE J.* **1988**, *34*, 1691-1697.
18. E. Sada, H. Kumazawa, M. A. Butt, Single gas absorption with reaction in a slurry containing fine particles, *Chem. Eng. Sci.* **1977**, *32*, 1165-1170.
19. K. R. Westerterp, W. P. M. van Swaaij, A. A. C. M. Beenackers, *Chemical reactor design and operation*, John Wiley & Sons, Chichester, **1990**, p 413, 426, and 487.
20. A. Teder, The equilibrium between elementary sulfur and aqueous polysulfide ions, *Acta Chem. Scan.* **1971**, *25*, 1722-1728.
21. W. E. Kleinjan, A. de Keizer, A. J. H. Janssen, Equilibrium of the reaction between dissolved sodium sulfide and biologically produced sulfur, *Colloids Surf. B-Biointerfaces*, in press. *This thesis, chapter 4*.
22. R. Steudel, Mechanism for the formation of elemental sulfur from aqueous sulfide in chemical and microbiological desulfurization processes, *Ind. Eng. Chem. Res.* **1996**, *35*, 1417-1423.
23. W. E. Kleinjan, A. de Keizer, A. J. H. Janssen, Kinetics of the reaction between dissolved hydrogen sulfide and biologically produced sulfur, *Ind. Eng. Chem. Res.* **2005**, *44*, 309-317. *This thesis, chapter 3*.

24. G. F. Versteeg, P. M. M. Blauwhoff, W. P. M. van Swaaij, The effect of diffusivity on gas-liquid mass-transfer in stirred vessels. Experiments at atmospheric and elevated pressures, *Chem. Eng. Sci.* **1987**, *42*, 1103-1119.
25. A. J. H. Janssen, S. Meijer, J. Bontsema, G. Lettinga, Application of the redox potential for controlling a sulfide oxidizing bioreactor, *Biotechnol. Bioeng.* **1998**, *60*, 147-155.
26. H. G. Trüper, H. G. Schlegel, Sulphur metabolism in Thiorhodaceae I: Quantitative measurements on growing cells of *Chromatium okenii*, *Antonie van Leeuwenhoek* **1964**, *30*, 225-238.
27. L. G. Danielsson, X. S. Chai, M. Behm, L. Renberg, UV characterization of sulphide-polysulphide solutions and its application for process monitoring in the electrochemical production of polysulphides, *J. Pulp Paper Sci.* **1996**, *22*, J187-J191.
28. A. Teder, Spectrophotometric determination of polysulphide excess sulfur in aqueous solutions, *Svensk Papperst.* **1967**, *6*, 197-200.
29. D. R. Lide, *Handbook of chemistry and physics*, 82nd ed. (Ed.: D. R. Lide), CRC Press, Boca Raton, FL, **2001**, p 4-155.
30. T. J. Edwards, G. Maurer, J. Newman, J. M. Prausnitz, Vapor-liquid equilibria in multicomponent aqueous solution of volatile weak electrolytes, *AIChE J.* **1978**, *24*, 966-975.
31. R. Steudel, The chemical sulfur cycle. In *Environmental Technologies to treat sulfur pollution. Principles and engineering* (Eds.: P. Lens, L. Hulshoff Pol), IWA Publishing, London, **2000**, pp. 1-31.
32. P. L. Brezonik, *Chemical kinetics and process dynamics in aquatic systems*, Lewis Publishers, Boca Raton, FL, **1994**, p 155.
33. M. W. Kemp, *Physical Chemistry*, Marcel Dekker, New York, **1979**, p 295.
34. R. H. Perry, D. W. Green, J. O. Maloney, *Perry's chemical engineers' handbook*, 7th ed. (Eds.: R. H. Perry, D. W. Green, J. O. Maloney), McGraw-Hill, New York, **1997**, p 5-50.
35. W. Stumm, J. J. Morgan, *Aquatic chemistry*, Wiley-Interscience, New York, **1970**, p 84.

Appendix 6.A

Absorption of H_2S into a carbonate solution can be represented with an instantaneous reversible reaction.

$$H_2S\,(g) \rightarrow H_2S\,(aq) \qquad (6.A.1)$$

$$H_2S\,(aq) + CO_3^{2-} \rightleftarrows HS^- + HCO_3^- \qquad (6.A.2)$$

The fluxes of the components at the G/L interface and at distance Δy from the interface, are shown in Figure 6.A.1.

From reaction stoichiometry we can conclude that the total amount of sulfide transferred through the liquid film is the sum of the amount of H_2S and the amount of HS^- transferred.

$$\left(J_{H_2S}\right)_0 = \left(J_{HS^-}\right)_{\Delta y} + \left(J_{H_2S}\right)_{\Delta y} \tag{6.A.3}$$

In terms of the film theory this can be described as

$$J_{H_2S} = \frac{D_{H_2S}}{\delta}\left([H_2S]^* - [H_2S]\right) + \frac{D_{HS^-}}{\delta}\left([HS^-]^* - [HS^-]\right) \tag{6.A.4}$$

in which δ is the film thickness and $[HS^-]_L^*$ the concentration at y = 0. The total sulfide flux can also be described in terms of an enhancement factor

$$J_{H_2S} = E_{H_2S}\frac{D_{H_2S}}{\delta}\left([H_2S]^* - [H_2S]\right) \tag{6.A.5}$$

From the above two relations the enhancement factor follows

$$E_{H_2S} = 1 + \frac{D_{HS^-}}{D_{H_2S}}\left(\frac{[HS^-]^* - [HS^-]}{[H_2S]^* - [H_2S]}\right) \tag{6.A.6}$$

The relations for the interfacial carbonate and bicarbonate concentrations (Eqs. 6.28 and 6.29) follow from

$$-\left(J_{CO_3^{2-}}\right)_{\Delta y} = \left(J_{HS^-}\right)_{\Delta y} \tag{6.A.7}$$

$$\frac{D_{CO_3^{2-}}}{\delta}\left([CO_3^{2-}] - [CO_3^{2-}]^*\right) = \frac{D_{HS^-}}{\delta}\left([HS^-]^* - [HS^-]\right) \tag{6.A.8}$$

$$[CO_3^{2-}]^* = [CO_3^{2-}] - \frac{D_{HS^-}}{D_{CO_3^{2-}}}\left([HS^-]^* - [HS^-]\right) \tag{6.A.9}$$

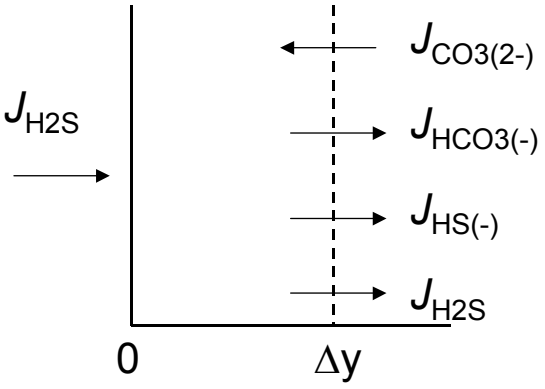

Figure 6.A.1. Fluxes at interfaces

and

$$\left(J_{HCO_3^-}\right)_{\Delta y} = \left(J_{HS^-}\right)_{\Delta y} \tag{6.A.10}$$

$$\frac{D_{HCO_3^-}}{\delta}\left([HCO_3^-]^* - [HCO_3^-]\right) = \frac{D_{HS^-}}{\delta}\left([HS^-]^* - [HS^-]\right) \tag{6.A.11}$$

$$[HCO_3^-]^* = [HCO_3^-] + \frac{D_{HS^-}}{D_{HCO_3^-}}\left([HS^-]^* - [HS^-]\right) \tag{6.A.12}$$

Substitution of relations for the equilibrium distribution of H_2S in gas and liquid phase (Eq. 6.15), and for the interfacial carbonate and bicarbonate concentrations (Eqs. 6.A.9 and 6.A.12), in Eq. 6.30, result in a quadratic equation which can be solved for $[HS^-]^*$. The analytical solution for $[HS^-]^*$ is

$$[HS^-]^* = \frac{-[HCO_3^-] + C[HS^-] - K'GD \pm \sqrt{Q}}{2C} \tag{6.A.13}$$

in which

$$C = \frac{D_{HS^-}}{D_{HCO_3^-}}, \quad D = \frac{D_{HS^-}}{D_{CO_3^{2-}}}, \quad G = m[H_2S], \quad K' = K \times \frac{\gamma_{H_2S}\gamma_{CO_3^{2-}}}{\gamma_{HS^-}\gamma_{HCO_3^-}}, \text{ and}$$

$$Q = [HCO_3^-]^2 + 2[HCO_3^-]\left(K'DG - C[HS^-]\right) + C^2[HS^-]^2 + \ldots$$

$$\ldots + C^2[HS^-]^2 + 2K'CDG[HS^-] + 4K'CG[CO_3^{2-}] + K'^2 D^2 G^2 \tag{6.A.14}$$

Appendix 6.B

The total sulfide fluxes for gas film, liquid film, and surface reaction (Eqs. 6.31, 6.32, and 6.35) can be rewritten using the equilibria in Eqs. 6.15 and 6.17.

$$J_{H_2S}a = k_G a\left([H_2S]_G - \frac{[H_2S]^*}{m}\right) \tag{6.A.15}$$

$$J_{H_2S}a = E_{H_2S}k_L a\left([H_2S]^* - [H_2S]\right) + k_L a\left(\frac{K_1[H_2S]^*}{[H^+]} - \frac{K_1[H_2S]}{[H^+]}\right) \times \frac{\gamma_{H_2S}}{\gamma_{HS^-}\gamma_{H^+}} \tag{6.A.16}$$

$$J_{H_2S}a = k_1'' A_c\left([H_2S] + \frac{K_1[H_2S]}{[H^+]} \times \frac{\gamma_{H_2S}}{\gamma_{HS^-}\gamma_{H^+}}\right) \tag{6.A.17}$$

This set of equations can be solved for $[H_2S]$. Substitution of the resulting expression for $[H_2S]$ in Eq. 6.A.17 results in Eq. 6.36.

Chapter 7

Foam formation in a biotechnological process for the removal of hydrogen sulfide from gas streams*

Abstract

Foam formation in aqueous suspensions of biologically produced sulfur is studied in a foam generator at 30 °C, with the objective of describing trends and phenomena that govern foam formation in a biotechnological hydrogen sulfide removal process. Air is bubbled through a suspension and the development of the foam height in time is measured, showing essentially two types of foam, unstable foam of constant foam height and stable foam with a rapidly increasing foam height. The transition between these types of foam can occur when the local sulfur concentration near the surface of the liquid is higher than a critical concentration, so that a stable network structure can be formed. Sulfur particles are transported to the top of the liquid by flotation. Upon foam formation large aggregates of sulfur fall apart into smaller fractions. Especially the larger fraction of the sulfur particles is present in the foam, indicating that these particles have the right hydrophobicity to form a network structure. Furthermore, polysulfide anions were found to have antifoaming properties in biologically produced sulfur suspensions, either because of the changing of the surface properties of the biologically produced sulfur or because of the antifoaming properties of the hydrophobic elemental sulfur formed upon the chemical oxidation of polysulfide ions.

Keywords

Foam, froth, biologically produced sulfur, particles, antifoaming

* W.E. Kleinjan, C.L.M. Marcelis, A. de Keizer, A.J.H. Janssen, M.A. Cohen Stuart, Foam formation in a biotechnological process for the removal of hydrogen sulfide from gas streams, *Colloids Surf. A-Physicochem. Eng. Asp.* (submitted).

7.1. Introduction

Before gas streams such as natural gas, synthesis gas, or biogas can be combusted, hydrogen sulfide has to be removed to prevent environmental problems caused by emission of S-compounds, corrosion of equipment, and for reasons of toxicity. Biotechnological processes can be an interesting option for this task because they generally lack some of the disadvantages of physicochemical processes (e.g., need of special catalysts, high temperature or pressure) and can therefore be cheaper and safer.

Several microorganisms have been studied for application in biotechnological H_2S removal processes (for a review, see ref. [1]) but the chemoautotrophic bacteria of the genus *Thiobacillus* have been studied and used mostly. Sublette and Sylvester [2] focused on the use of *Thiobacillus denitrificans* for the oxidation of sulfide to sulfate. Buisman *et al*. [3] used a mixed culture of *Thiobacilli* for the aerobic oxidation of sulfide to elemental sulfur. Visser *et al*. [4] showed the dominant organism in this process to be the new organism *Thiobacillus* sp. W5. This process was further developed and is currently used in a number of full-scale installations [5, 6].

The elemental sulfur formed (biologically produced sulfur, or biosulfur) is in the shape of particles with dimensions of approximately 0.1–1 μm. The particles can form aggregates of elemental sulfur, which can grow up to 3 mm. Contrary to hydrophobic 'inorganic' sulfur, biologically produced sulfur has a more hydrophilic character and can be dispersed in water [7]. The particles are believed to be composed of a core of sulfur rings in an amorphous structure, with organic polymers adsorbed on the surface providing sterical and electrical stabilization against aggregation [8].

The process in which these particles are formed basically consists of the washing of H_2S from a gas stream in a gas absorber by an alkaline solution, and the subsequent oxidation of dissolved H_2S to elemental sulfur in a bioreactor. In the aerated bioreactor, air is led into an aqueous solution containing a mixture of surface-active components (e.g., polymeric organic components, particles) and some foam is usually produced. This foam can be of short lifetime, forming only small amounts of foam, but also a very stable foam can be formed, resulting in excessive foam formation. To prevent site pollution, loss of biomass contents, and reactor operation below full capacity, it is crucial to control foam formation in the bioreactor.

In general, foaming can be a problem in a number of biotechnological processes where gas is mixed with aqueous solutions of surface-active organic components, such as proteins. Often some type of antifoaming is used to reduce foam formation, e.g., in fermentation [9] and food processing [10]. This is usually the addition of some component to the process but also mechanical foam breaking, e.g., spraying with water, is used. Usually, the term antifoaming refers to the prevention of foam

formation, whereas defoaming refers to foam breaking. However, the terms are often used interchangeably.

To establish an effective type of antifoaming for the biotechnological H_2S removal process, knowledge of the aspects governing the stability of the foam formed in this process, is required. Because the foam formed in the H_2S removal process seems to contain fairly large amounts of solid elemental sulfur, the role of the sulfur particles on foam stability is particularly interesting.

Foams are dispersions of gas in a liquid, which are thermodynamically unstable but can be kinetically stabilized. Foams consisting of gas in aqueous solutions of mildly surface-active components (short-chain fatty acids, alcohols) have a short lifetime (up to seconds) and are often called unstable or transient foams. Metastable or permanent foams from aqueous solutions of soap, protein, or other surface active components can have lifetimes of hours or days, or can persist almost infinitely when no disturbances occur. Foam stability is generally described in terms of film drainage, the thinning of films by a flow of liquid towards the interconnection points in the film network (Plateau borders), and film rupture, the breaking of a film by random disturbances, depending on surface elasticity (or the Gibbs-Marangoni effect). Furthermore, particles can have an important effect on foam stability.

The effect of presence of solid particles in surfactant-stabilized aqueous foams on foam stability depends on a number of parameters, such as particle hydrophobicity, particle size, and concentration. Particles can have a stabilizing or a destabilizing effect on foams. Large hydrophobic particles, roughly the size of the thickness of foam films, such as Teflon particles [11, 12] have been found to destabilize foams and are often used in antifoaming agents [13, 14]. The basic mechanism for this destabilizing effect of large smooth hydrophobic particles is schematically shown in Figure 7.1.a. For a high G/L contact angle, the curvature will induce a high Laplace pressure in the film next to the particle, leading to an increase in film drainage and therefore rupture at the L/S interface.

More hydrophilic particles that are partially wetted can reduce the rate of film drainage, thereby providing stabilization for the foam film (see Figure 7.1.b).

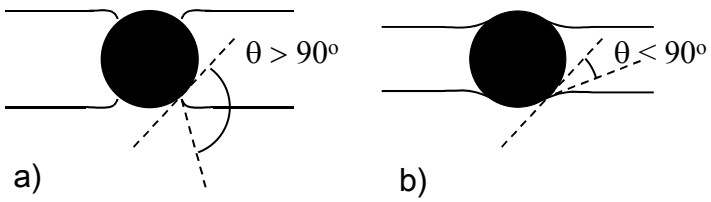

Figure 7.1. Effect of large smooth spherical particle on foam film. **a)** particle dewetting and film destabilization caused by a hydrophobic particle with $\theta_{A/W} > 90°$, **b)** partial particle wetting and film stabilization caused by a hydrophilic particle with $\theta_{A/W} < 90°$ (after [13]).

Research by Johansson and Pugh [15] on the effect of finely ground quartz particles of varying hydrophobicity and size fractions, showed that there was an optimum in foam stability for particles of intermediate hydrophobicity. More hydrophilic particles did not appear to affect foam stability and more hydrophobic particles decreased the foam stability.

In general, small fully wetted hydrophilic particles tend to stabilize foam films by an increase in bulk viscosity (and therefore a decrease in film drainage). Partially wetted small particles can provide mechanical stability to the film. Hudales *et al*. [16] reported, however, that small (< 1 μm) hydrophilic glass particles decrease foam stability whereas the larger particles (up to 10 μm) provided foam stabilization. Small hydrophobic particles are reported to be ineffective as antifoamers [14] or even to increase foam stability [17].

Furthermore, the shape of particles is of importance in foam stability. Frye and Berg [12] reported that nonspherical hydrophobic particles with sharp edges are more effective in foam destabilization than smooth hydrophobic particles.

Antifoamers typically consist of hydrophobic particles, oil, or a combination of both (hydrophobic particles dispersed in an oil phase). The effect of hydrophobic particles is explained above and illustrated in Figure 7.1. The mechanism of oil as antifoamer is basically the formation of an oil lens or film on the G/L interface, causing a reduction in viscosity, surface tension, or elasticity, and thereby decreasing the stability of the foam film. To increase the penetration of the oil into the foam, the oil can be dispersed as emulsion droplets or solubilized in micelles. Mixtures of oil and hydrophobic particles are generally most efficient as antifoamers because of the combination of good foam penetration of emulsion droplets with good foam breaking properties of the hydrophobic particles. Some antifoaming agents are soluble in water at low temperatures, whereas they are insoluble at higher temperatures. For some processes, these cloud-point antifoamers can be used as insoluble antifoamers at high process temperatures. Upon cooling, the antifoamer dissolves which can be useful for an easy separation of reaction product from the antifoamer.

Foam formation has been studied in a wide variety of systems by different methods. The foaming behavior of a solution is usually studied in some type of column where gas is introduced into a liquid through an orifice (sparging) and where foam height or foam volume is then measured. As an alternative, dispersion techniques consisting of mechanical shaking or whipping have been used, but these have the disadvantage of a poor control of the amount of gas incorporated in the liquid [13]. For unstable foams, from aqueous solutions containing mildly surface active components, Tuinier *et al*. [18] defined the foamability as the foam height in the steady state situation. For metastable foams, from aqueous solutions of stronger surface-active components, e.g., surfactants or proteins, the foam height often does not reach a steady state and therefore the increase of foam height in time is represented. This was for instance

done by Hudales and Stein [16], who studied foaming behavior of hydrophilic glass particles in cationic surfactant solutions (CTAB), and by Christiano and Fey [10], who studied foaming behavior of aqueous solutions of nonionic surfactants.
To control foam formation in a biotechnological H_2S removal process we tried to establish the mechanism of foam formation and foam stability. Experiments were performed in a foam generator and particular emphasis was given to the effect of biologically produced sulfur particles.

7.2. Materials and methods

7.2.1. Experimental set-up

Foam formation upon aeration of sulfur suspensions present in a bioreactor, is investigated with a foam generator (see Figure 7.2). The foam generator consists of a glass column (d = 60 or 100 mm) with a sintered glass plate at the bottom. The generator can contain 0.5–2.0 L of liquid, through which gas can be bubbled. The gas is pumped through the liquid with a compressor and the flow rate can be measured and adjusted (0–2.5 L min^{-1}), as well as the gas pressure before the sintered glass plate (0–350 mbar overpressure). There was a small opening at the top of the foam generator to prevent pressure fluctuations above the foam. After charging of a liquid to the foam generator air was pumped through the liquid at maximum flow rate for approximately 10 s in order to open all pores of the sintered glass plate. Subsequently, the gas flow was adjusted to the desired flow rate and the evolution of the foam height was measured.
After an experiment, any stable foam sticking on the glass wall could be mixed with the liquid by means of a recycle pump, which pumps the liquid from the bulk below to the top. For this, an opening on the side of the column (approximately 3 cm above the sintered glass plate) was used. The recycled liquid is then sprayed against the glass wall of the column to mix any stable foam attached to the glass wall with the contents of the foam generator.

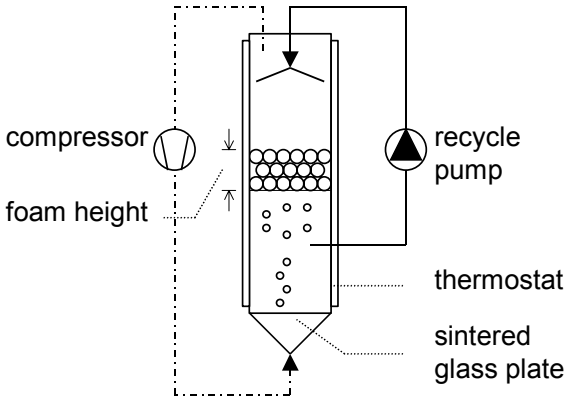

Figure 7.2. Experimental set-up used in foam tests (foam generator).

7.2.2. Chemicals used

Biologically produced sulfur was obtained from a full-scale biogas treatment facility (Thiopaq™). Four batches of stock suspensions were used, termed A, B, C, and D. Sulfur suspensions of different concentrations were prepared by centrifugation of 4 L of an original suspension at 10000 rpm (Beckman Coulter Avanti J-25I centrifuge), after which part of the solid material was redispersed with approximately 1 L of the resulting supernatant (suspension A). Furthermore, a suspension was prepared by centrifugation of approximately 20 L of an original suspension with a continuous centrifuge (Heraeus Sepatech) at 7500 rpm, resulting in a concentrated suspension and a supernatant (suspensions B and C). Suspension D was used as received. Specific conductivities of the suspensions varied from 40–46 mS cm^{-1}, corresponding to approximately 0.32–0.36 M NaCl. The properties of these suspensions are shown in Table 7.1. Prepared sulfur suspensions were stored at 4 °C. Standard yellow sulfur powder was used as inorganic sulfur (Sigma Aldrich). Polysulfide solutions were prepared by dissolving crystals of Na_2S_4 (Alfa Aesar, H_2O content 5% max) in deaerated water.

7.2.3. Sulfur characterization

The particle size distribution was measured using a Coulter Laser LS 230. The particle size distribution was calculated from the data according to a Fraunhofer model, in which the refractive index of sulfur (α S_8) was incorporated (1.998) [19].
Contact angles of dried and original biosulfur, and inorganic sulfur have been determined with a Krüss contact angle microscope G1. Measurements were performed with surfaces of sulfur pellets, prepared with an IR spectroscopy press at a pressure of 34.5 bar. Because no equilibrium contact angle could be found, results for the advancing contact angle (increase in drop volume) are reported. These contact angles will be higher than the equilibrium contact angles. Results are shown in Table 7.2. Samples of biosulfur dried at 80 or 85 °C show moderate hydrophobic behavior

Table 7.1. Properties of the four sulfur suspensions used.

	original	**concentrated**	**supernatant**
suspension A	[protein] = 15 mg L^{-1}	-	-
	C = 46.2 mS cm^{-1}	-	-
	c_{S0} = 8.4 g L^{-1}	c_{S0} = 32.4 g L^{-1}	c_{S0} < 0.1 g L^{-1}
suspension B	[protein] = 18 mg L^{-1}	[protein] = 29 mg L^{-1}	[protein] = 22 mg L^{-1}
	C = 41.7 mS cm^{-1}	-	-
	c_{S0} = 7.1 g L^{-1}	c_{S0} = 35.8 g L^{-1}	c_{S0} < 0.1 g L^{-1}
suspension C	[protein] = 23 mg L^{-1}	[protein] = 31 mg L^{-1}	[protein] = 24 mg L^{-1}
	C = 40.2 mS cm^{-1}	-	-
	c_{S0} = 7.3 g L^{-1}	c_{S0} = 36.0 g L^{-1}	c_{S0} < 0.1 g L^{-1}
suspension D	C = 45.8 mS cm^{-1}	-	-
	c_{S0} = 3.1 g L^{-1}		

with contact angles of approximately 90 °. The biosulfur sample dried at 40 °C shows considerable water penetration in the pellet and therefore a reliable contact angle could not be determined. It must be concluded that the sulfur is hydrophilic and the contact angle is much lower than 90 °. Inorganic sulfur is very hydrophobic (θ = 119 °).

7.2.4. Analysis

Sulfur suspensions from a bioreactor consist of a mixture of sulfur particles of different particle sizes and a complex mixture of dissolved components. This 'background solution' contains salts, proteins, and other dissolved organic matter. Suspensions are characterized according to sulfur concentration, particle size distribution, conductivity and free protein concentration. The solid sulfur concentration is determined by filtration of a suspension, flushing the solid residue with water to remove salts, drying of the solid material on the filter, and measuring the weight increase of the filter. The protein concentration is determined according to the Bradford method (Biorad, Inc. USA).

7.3. Results

7.3.1. Effect of sulfur concentration

The effect of sulfur concentration on foam formation was investigated by measuring the height of the foam layer in time for suspensions of varying sulfur content. Suspensions of varying sulfur concentration were prepared by centrifugation of the original sulfur suspension A (see Table 7.1, c_{S0} = 8.4 g L^{-1}) to remove all solid sulfur. The supernatant was a slightly turbid liquid (c_{S0} < 0.1 g L^{-1}) and was used for dilution of concentrated sulfur suspensions. This way 7 suspensions of each 0.50 L were made of equal particle size distribution and 'background solution' but varying sulfur concentrations (c_{S0} from 0 to 12.8 g L^{-1}). The development of the foam height was investigated for each suspension in a foam generator (d = 60 mm) for 6 flow rates of air, varying from 0.25 to 1.20 L min^{-1}, starting with the lowest gas flow rate. Results are shown for three flow rates (0.25, 0.80, and 1.20 L min^{-1}) in Figure 7.3.

Table 7.2. Air/water contact angles of different types of sulfur. Sulfur pellets were formed at 34.5 bar.

type of sulfur	contact angle
biosulfur, dried at 80 °C (paddle dryer)	91.0 °
biosulfur, dried at 85 °C (fluid bed dryer)	89.5 °
biosulfur, dried at 40 °C (vacuum oven)	< 90 °
inorganic sulfur	119 °

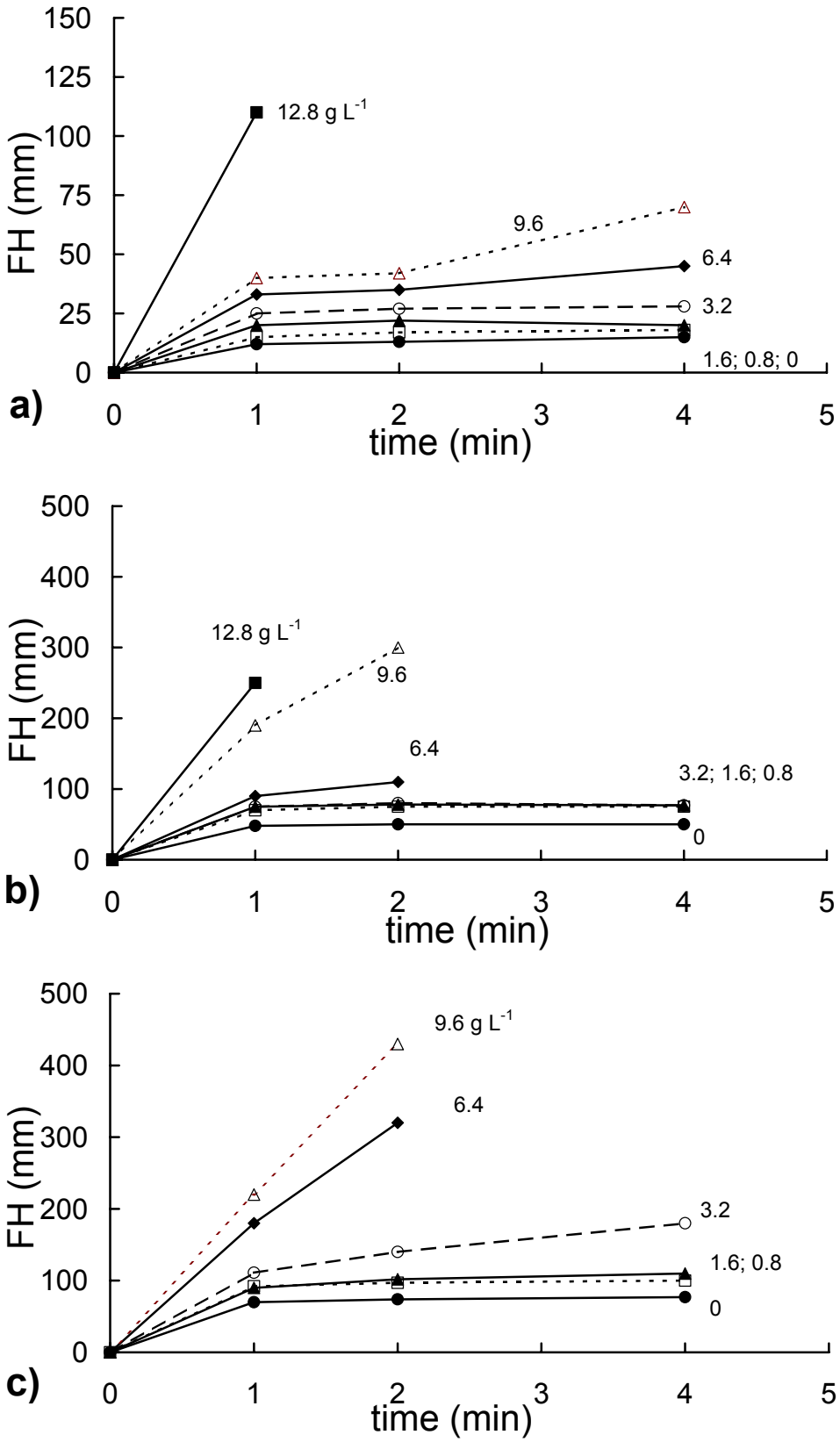

Figure 7.3. Development of foam height for different sulfur concentrations and different gas flow rates. **a)** 0.25 L min^{-1}, **b)** 0.80 L min^{-1}, **c)** 1.20 L min^{-1}. Sulfur concentration was varied by diluting a concentrated sulfur suspension with the supernatant of a centrifuged suspension. c_{S0} = 0 g L^{-1}(●), 0.8 g L^{-1} (□), 1.6 g L^{-1} (▲), 3.2 g L^{-1} (○), 6.4 g L^{-1} (♦), 9.6 g L^{-1} (Δ), 12.8 g L^{-1} (■). Column diameter = 60 mm; V = 0.50 L; T = 30 °C; Specific conductivity = 46 mS cm^{-1}.

In Figure 7.3.a, the effect of sulfur content on measured foam height is shown for an airflow rate of 0.25 L min^{-1}. It can be seen that at low sulfur concentration ($c_{S0} \leq 6.4$ g L^{-1}) a steady state foam height is reached, which increases with increasing sulfur concentration. At a sulfur concentration of 9.6 g L^{-1}, however, the foam height first seems to reach a steady state value, but then drastically increases after approximately 3 min. This is accompanied by a change of the appearance of the foam layer from small spherical bubbles to a polyhedral structure of larger dimensions. Films are formed which cover the complete area of the column and which rise up to 400 mm, where they break. A fairly large amount of solid sulfur seems to be present in the lamellae between the gas bubbles. Upon breaking of the films, solid material is released and part of it remains sticking on the glass wall of the column. At a sulfur concentration of 12.8 g L^{-1} no apparent steady state situation is reached and the foam height increases almost immediately, forming a polyhedral structure of large dimensions (up to 50 mm) and films covering the complete column area.
Figures 7.3.b and c show the effect of sulfur concentration on measured foam height for airflow rates of 0.80 and 1.20 g L^{-1}, respectively. At low sulfur concentrations ($c_{S0} \leq 3.2$ g L^{-1}) the foam height remains constant during the time measured, whereas at higher sulfur concentrations a transition in foaming behavior occurs resulting in large lamellae and films, containing solid material. The transition occurs faster with higher sulfur concentration and higher flow rate. In Figure 7.4 photographs of the development of the foaming behavior at a high sulfur concentration are shown.

7.3.2. Effect of liquid volume

The effect of sulfur particles on foam formation is further investigated by measuring the foamability of identical sulfur suspensions of different volumes. The concentrated suspension B (see Table 7.1) was diluted with supernatant from centrifugation, resulting in a suspension with $c_{S0} = 3.2$ g L^{-1}. With this suspension the effect of liquid

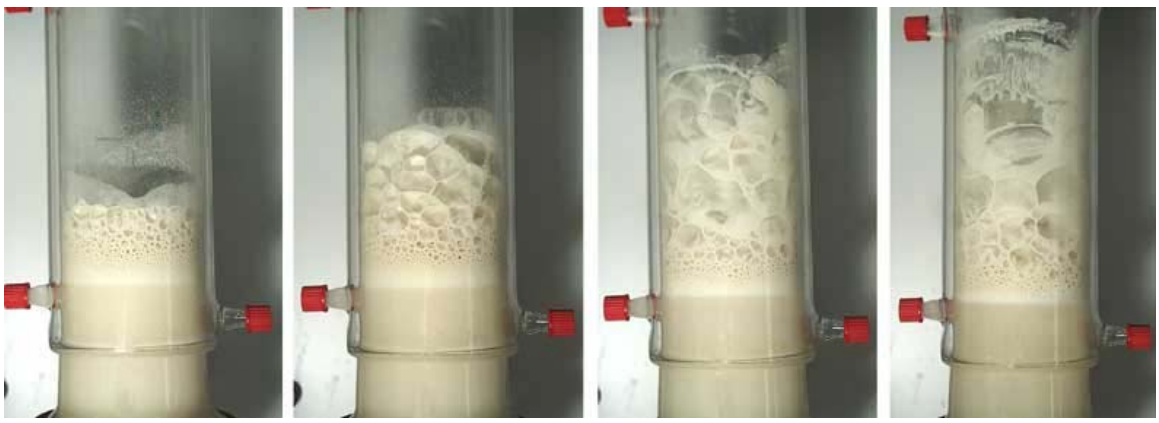

Figure 7.4. Transition from foam consisting of small spherical bubbles to foam of larger dimension of a polyhedral structure. Solid material (sulfur) is eventually sticking on the glass wall.

volume (V = 1.0, 1.5, and 2.0 L) is measured for three different air flow rates (ϕ_G = 0.25, 0.80, and 1.20 L min^{-1}). Results are shown in Figure 7.5. During the time measured (≈ 10 min) all reported foam heights remained constant. For all three air flow rates an increase of liquid volume causes an increase in the steady state foam height, showing the effect of total sulfur content, rather than sulfur concentration. This is probably caused by a higher concentration of sulfur particles near the G/L interface for a higher total sulfur content. Sulfur particles are dragged from the bulk to the top of the liquid by flotation. A high sulfur concentration near the G/L interface stimulates foam formation. This effect is most pronounced at the relatively high air flow rates of 1.20 and 0.80 L min^{-1}. At the lower air flow rate of 0.25 L min^{-1} the air velocity is probably too low for the sulfur particles to reach the liquid surface.

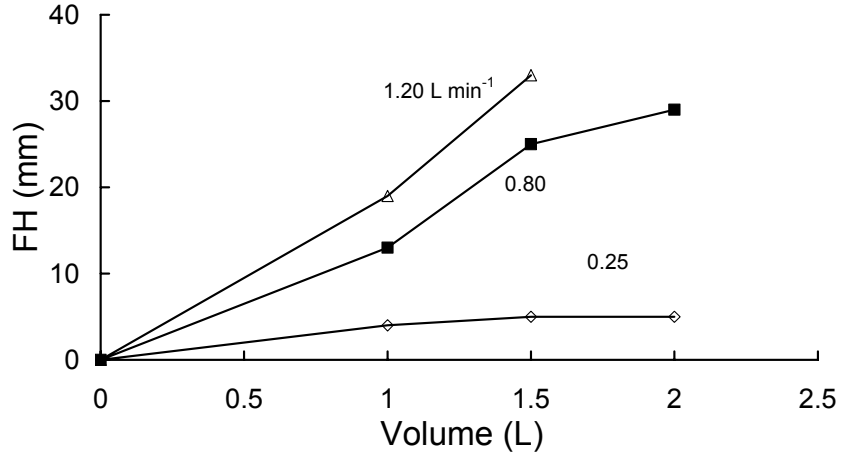

Figure 7.5. Effect of liquid volume on steady state foam height for different gas flow rates. Φ = 0.25 L min^{-1} (◊), 0.80 L min^{-1} (■), 1.20 L min^{-1} (Δ). c_{S0} = 3.2 g L^{-1}; Column diameter = 100 mm; T = 30 °C.

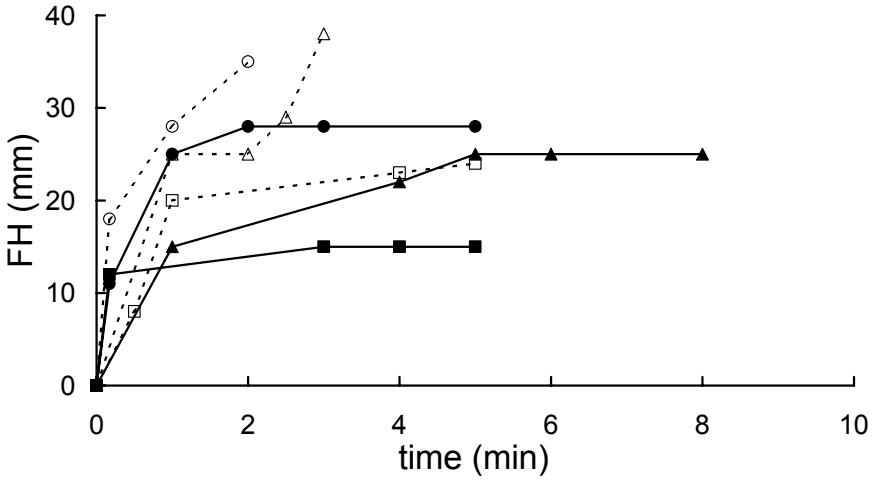

Figure 7.6. Development of foam height for different sulfur concentrations and liquid volumes. c_{S0} = 3.2 g L^{-1}: V = 1.0 (■), 1.5 (▲), and 2.0 L (●). c_{S0} = 4.2 g L^{-1}: V = 1.0 (□), 1.5 (Δ), and 2.0 L (○). Φ_G = 0.80 L min^{-1}; Column diameter = 100 mm; T = 30 °C.

To further distinguish between the effect of sulfur content and sulfur concentration, we performed additional experiments with sulfur suspensions of a higher concentration (c_{S0} = 4.2 g L^{-1}, prepared from concentrated suspension B). Results for ϕ_G = 0.80 L min^{-1} are shown in Figure 7.6. Foam heights with 3.2 g L^{-1} suspensions (black symbols) reach a steady state foam height for all liquid volumes used (see also Figure 7.5). For suspensions of 4.2 g L^{-1} (open symbols) this is, however, not the case. The foam height of 1.0 L of a 4.2 g L^{-1} suspension appears to reach a steady state situation. At the higher liquid volumes of 1.5 and 2.0 L, the foam height does not remain constant, but large lamellae and films are formed. Of particular interest is the comparison between 1.5 L of a 4.2 g L^{-1} suspension and 2.0 L of a 3.2 g L^{-1} suspension, as the total sulfur contents are comparable (6.3 g and 6.4 g, respectively.). With the suspension of the higher sulfur concentration and lower liquid volume, there is a transition between foam consisting of small spherical bubbles and foam of large lamella and films. This transition is absent with the suspension of the lower sulfur concentration and higher volume, at least within the time measured. In the concentrated suspension of low liquid volume the accumulation of sulfur at the G/L interface will occur faster than in the more diluted suspension of higher volume. The distance to the G/L interface is shorter and therefore less coalescence of gas bubbles will occur and the bubble size will be smaller, resulting in a higher specific bubble/liquid interfacial area.

7.3.3. Dynamic sulfur concentration in the bulk during foam formation

To investigate the behavior of sulfur particles in solution upon foam formation, the dynamic sulfur concentration in the bulk of the liquid have been measured. Upon foam formation, samples were taken from the bulk of the liquid, through the opening on the side of the column, and sulfur concentrations were measured. Results are

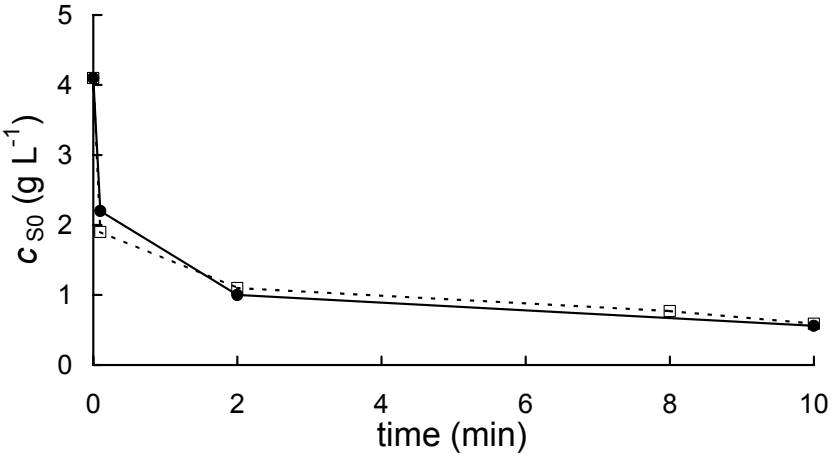

Figure 7.7. Dynamic sulfur concentration of the liquid bulk during plug formation at Φ = 0.80 (●) and 1.20 L min^{-1} (□). Column diameter = 100 mm; V = 2.0 L; c_{S0} = 4.2 g L^{-1}; T = 30 °C.

shown in Figure 7.7 for c_{S0} = 4.2 g L^{-1} and V = 2.0 L (from suspension B). At the gas flow rates applied, no steady state foam height was reached and large lamella and films were formed almost instantaneously. It can be seen that the sulfur concentration in the bulk decreases when air is bubbled through the liquid, indicating that the majority of the solid sulfur content of the original suspension ends up in the foam layer.

7.3.4. Effect of background solution

To investigate the role of the dissolved organic material in the background solution, a comparison was made between a sulfur suspension with an original background solution (mainly consisting of $NaHCO_3$ and Na_sSO_4) and a suspension with a NaCl solution as background. The concentrated sulfur suspension C (see Table 7.1) was diluted with a supernatant from centrifugation (specific conductivity = 40.2 mS cm^{-1}; [protein] = 24 μg mL^{-1}), or with a NaCl solution of equal conductivity, resulting in suspensions of c_{S0} = 2.0 g L^{-1} and 3.0 g L^{-1}.

The development of the foam height for these suspensions is shown in Figure 7.8. In the cases of suspensions without solid elemental sulfur, the foam consists of small spherical bubbles and the foam height is low (< 5 mm). No transition to foam of a larger polyhedral structure occurs. The foam height of a sulfur suspension of 2.0 g L^{-1} sulfur with a NaCl solution as background remains constant within the time interval measured and the foam consists of small spherical bubbles. When the supernatant is used as a background solution, the initially formed foam consists of small bubbles, however, after approximately 2 min a transition occurs to foam consisting of a polyhedral structure with larger lamellae. For the suspensions with a sulfur content of 3.0 g L^{-1}, no apparent steady state situation is reached and large lamellae are formed

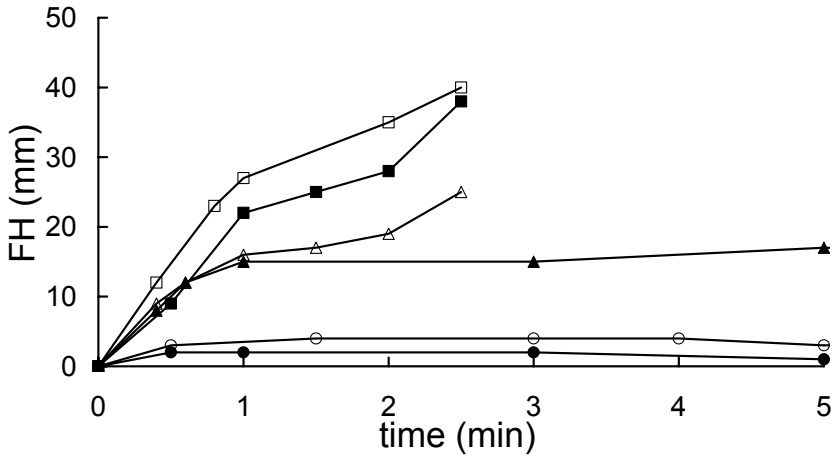

Figure 7.8. Development of foam height for suspensions with a centrifuged supernatant from an original suspension, or a NaCl solution as background. c_{S0} = 0 g L^{-1}: supernatant (○), salt (●); c_{S0} = 2.0 g L^{-1}: supernatant (Δ), salt (▲); c_{S0} = 3.0 g L^{-1}: supernatant (□), salt (■); Column diameter = 100 mm; V = 1.0 L; Φ_G = 0.80 L min^{-1}; conductivity = 40.2 mS cm^{-1}; T = 30 °C.

after approximately 1 min, both for a suspension with a NaCl solution and supernatant as background.

The transition from small spherical foam bubbles to large foam is stimulated by the concentration of solid sulfur particles, as was also concluded from the experiments described in section 7.3.1. The transition is further stimulated by the background solution in the supernatant of a sulfur suspension. This supernatant consists of salt and dissolved organic material, which is likely to be surface active.

7.3.5. Effect of foam formation on particle size distribution

Upon investigation of the dynamic sulfur concentration in the bulk of the liquid, during foam formation, we observed that part of the sulfur content ended up in the foam layer, whereas another part remained in the bulk. To distinguish between these

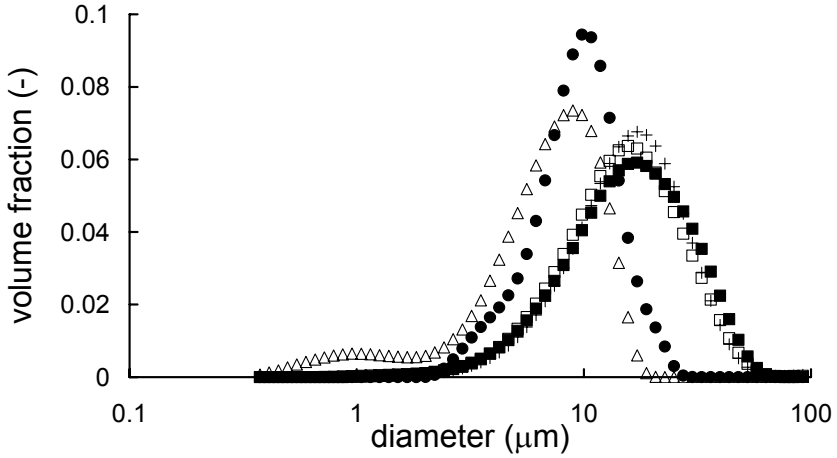

Figure 7.9. Particle size distributions of suspension C. Sulfur particles in foam (•), in suspension of foam remixed with bulk after foam formation (Δ), of a suspension concentrated by centrifugation (+), and of original suspensions stored at 4 °C (□) and 21 °C (■).

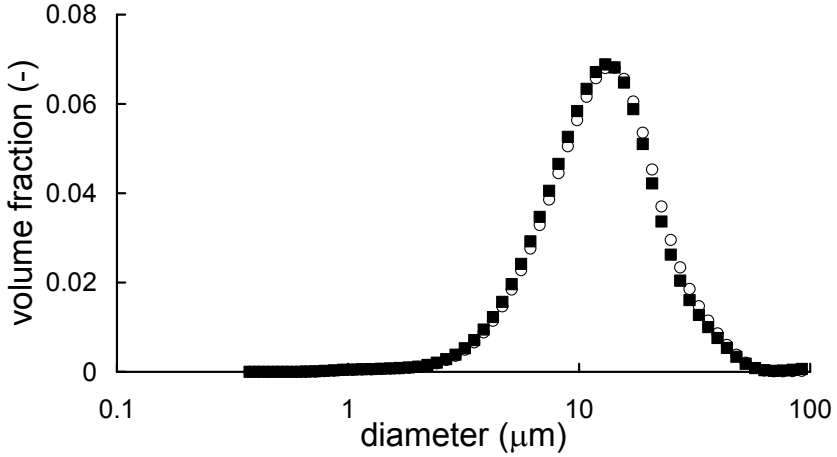

Figure 7.10. Particle size distribution of sulfur suspension pumped with peristaltic pump (■) compared to original suspension (○).

fractions we measured the particle size distribution of the original sulfur suspension D (see Table 7.1) before and after foaming, and of the fraction of sulfur particles that end up in the foam. The fraction of particles in the foam was collected by removing the bulk of the liquid through an opening of the foam generator (see Figure 7.2) after foam formation. The stable foam remained present on the glass wall of the column and was collected by flushing with a salt solution. The measured particle size distribution is shown in Figure 7.9 (black circles). The average particle size of the fraction in the foam ($d_p \approx 10$ μm) is considerably smaller than of the original suspension ($d_p \approx 17$ μm, open squares). The open triangles show the particle size distribution of a sulfur suspension after formation of stable foam, however, remixed with the bulk of the solution. Here, two smaller fractions can clearly be seen. One peak at a particle diameter of approximately 9 μm and a fraction with a diameter of approximately 1 μm. Apparently, large sulfur aggregates have fallen apart in smaller particles. This is possibly due to high shear forces that can occur upon the burst of a gas bubble, or a change in particle properties may have occurred upon the forming or breaking of a network structure in the stable foam. Possible breaking of aggregates due to shearing in the peristaltic pump was ruled out in a control experiment (Figure 7.10). The particle size of the larger fraction of the remixed suspension is comparable to the diameter of the particles in the stable foam, whereas the smaller fraction of the mixed suspension is not present in the stable foam. This indicates that the larger particles end-up in the stable foam. It is likely that the larger particles are more hydrophobic and therefore more likely to be present at the liquid-gas interface. Gas bubbles drag them into the foam more rapidly than the more hydrophilic smaller particles (flotation).

Figure 7.9 furthermore shows the effect of the storing conditions on the particle size distribution of sulfur suspensions. Concentration of an original suspension by centrifugation (plusses) and storing of the suspension at 21 °C (black squares) result only in small differences with the original suspension.

7.3.6. Effect of polysulfide anions on foam formation

In Figure 7.9 the particle size distribution of a sulfur suspension stored in a closed flask at 4 °C is compared to one stored at 21 °C. The plot shows a small increase in average particle diameter at higher temperature, although the difference is small. However, the appearance of the two stored suspensions were not identical. The suspension stored at 21 °C showed the formation of a yellow color within approximately three weeks, whereas the sulfur suspension stored at 4 °C kept its milk white appearance. This yellow color was attributed to the formation of polysulfide anions, S_x^{2-}, in the solution. Contact with air resulted in the disappearance of the yellow color, probably because of the chemical oxidation of polysulfide anions, which occurs rapidly at ambient conditions [20]. Furthermore, the foaming behavior of the

suspension stored in a closed flask at 21 °C was considerably different from the foaming behavior of a suspension stored in a closed flask at 4 °C. Less foam was formed in the suspension stored at 21 °C. To verify if this was caused by polysulfide ions, experiments were performed where 900 mL of the original sulfur suspension D was mixed with 100 mL of a 39 mM polysulfide solution (Na_2S_4) and the foaming behavior was investigated. The foaming behavior of suspensions with polysulfide is shown in Figure 7.11 (open symbols) and was compared with a mixed suspension of the original suspension with demineralized water (black symbols).

Whereas with the original sulfur suspensions a foaming behavior comparable to the previous experiments was observed, in the presence of polysulfide ions the amount of foam formed was much lower. In fact, barely any foam was produced, except for some unstable bubbles at the surface. Hardly any solid material appeared to be located in the bubbles. This effect could be caused by an interaction of polysulfide ions with the sulfur particles, changing the surface properties of the particles. Adsorption of polysulfide ions to sediments was previously observed [21]. It could also be related to the oxidation of polysulfide ions. Upon oxidation of polysulfide ions thiosulfate and elemental sulfur is formed. This elemental sulfur formed probably has a hydrophobic nature, and could therefore act as an antifoaming agent.

7.4. Discussion

Foam formation in suspensions of biologically produced sulfur is a complex process which depends on several properties, such as gas flow rate, sulfur concentration, total sulfur content, sulfur particle size distribution, and presence of organic surface active components. In experiments where we bubbled gas through a liquid in a foam generator we observed basically two types of foam. At low sulfur content or gas flow

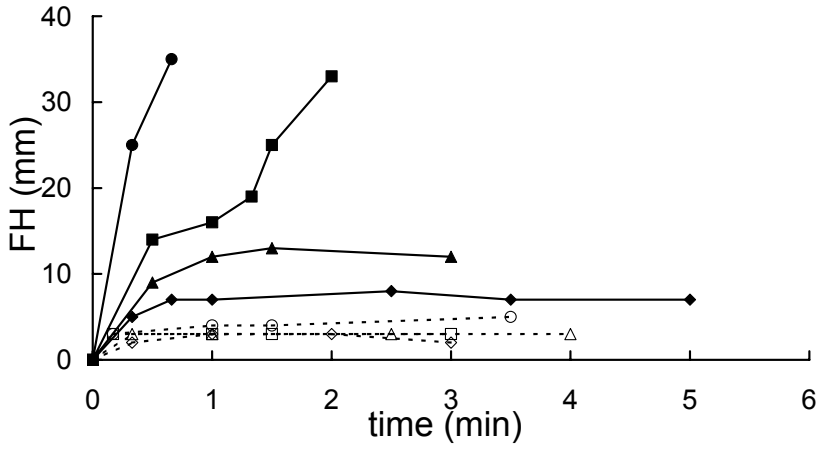

Figure 7.11. Development of foam height of an original sulfur suspension and a suspension with additional Na_2S_4 at different gas flow rates. Original: Φ_G = 0.5 (♦), 1.0 (▲), 1.5 (■), and 2.0 L min^{-1} (●). With additional 3.9 mM Na_2S_4: Φ_G = 0.5 (◊), 1.0 (Δ), 1.5 (□), and 2.0 L min^{-1} (○). c_{S0} = 2.8 g L^{-1}; V = 1.0 L; T = 30 °C.

rate, foam consisting of small spherical bubbles (< 5 mm) with a constant foam height was observed. At high sulfur content or gas flow rate, the foam was of a polyhedral structure of larger dimensions (up to 50 mm). Also films are formed which cover the complete area of the column (d = 100 mm) and rise up to 400 mm. A large part of the solid sulfur content of the aerated suspension ends up in this more stable foam, which results in the release of solid sulfur upon breaking of the films. In a foam generator no steady state in foam height is reached for this last type of foam. At intermediate sulfur content and gas flow rate, initially an apparent steady state foam height can be observed, with foam consisting of small spherical bubbles. After some time, e.g., 2 min, a transition to more stable foam can take place, resulting in a sudden increase in foam height.

Presence of sulfur particles stimulates foam formation. The observed steady state foam height is higher for a higher sulfur concentration, and a transition to the more stable foam occurs faster at higher sulfur concentration. During a foaming experiment, the sulfur concentration in the bulk of the liquid rapidly decreases, showing that sulfur particles are transported from the bulk of the liquid to the top by flotation. An increase in total liquid volume stimulates foam formation, showing that total sulfur content, apart from sulfur concentration, plays an important role as well. This indicates that foam formation is for a large part determined by the local sulfur concentration at the top of the liquid.

At intermediate sulfur content and gas flow, the foam height in the foam generator can initially be constant, with foam consisting of small spherical bubbles. After some time, however, a fast transition to the more stable foam consisting of large lamellae can take place. This suggests that the initial local sulfur particle concentration near the liquid/foam interface is too low for the formation of the stable type of foam. During the foaming experiment, the local sulfur particle concentration near this interface will increase due to flotation of particles. When the local sulfur particle concentration is sufficiently high, build-up of the more stable foam can occur.

Another possible explanation for the time needed for the transition to the more stable foam is that during the foaming experiment the properties of the particles change. This was observed from particle size distribution measurements indicating that an original sulfur suspension of approximately uniform particle size ($d \approx 17$ μm), consisted of two fractions ($d \approx 1$ μm and 9 μm) after intensive foaming. Large sulfur aggregates have fallen apart into smaller particles. The shearing forces required for the breaking of the aggregates probably originate from the burst of gas bubbles when these reach the surface of the liquid. Especially the particles of this larger fraction are present in the stable foam formed. The difference in foaming behavior of the two fractions might be due to particle size but could also be caused by a difference in hydrophobicity of the two fractions. The larger sulfur particles are likely to be more

hydrophobic than the smaller ones, and will therefore be more likely to be transported to the top of the column by flotation.

Presence of organic material in the 'background' of a biosulfur suspension stimulates foam formation and the transition from the small spherical foam bubbles to the more stable foam (see Figure 7.8). These dissolved organic components are likely to be surface active and therefore stimulate foam formation. The finding that the presence of this background solution also stimulates the formation of the more stable foam suggests that these components are also present in the foam.

The observed trends show that biologically produced sulfur is an important contributor to foam formation. Sulfur particles stabilize foam films either by partial wetting of the particles or by formation of a network. Sulfur particles can be transported to the top of the liquid by flotation. Especially the more hydrophobic particles will adhere to the G/L interface of rising gas bubbles. At the same time, sulfur particles will sediment in the liquid due to gravity. This will result in the formation of a concentration gradient of sulfur particles in the column. The net rise or fall of sulfur particles in the liquid will depend on the balance between flotation and sedimentation. An increase in particle concentration at the top of the liquid in the column will take place when this balance favors flotation, that is at a high gas flow rate, a high G/L interfacial area (small gas bubbles), and with hydrophobic particles. After reaching a critical interfacial particle concentration, particles of the right hydrophobicity will be able to form a network-structure forming a relatively stable film at the top of the liquid in the column. Because of this stable film, bubbles reaching the surface of the liquid cannot burst. Therefore an increase in coalescence rate of gas bubbles will occur, resulting in larger bubbles and a fast increase in foam height.

The performed experiments in a foam generator indicate the trends that will be important in foam formation in hydrogen sulfide removal processes. In installations sometimes unstable foam with a short lifetime is produced, and sometimes excessive foaming can take place, forming a more stable type of foam. This type of excessive foaming, as is sometimes observed in full-scale installations, can probably be compared to the stable type of foam that is produced in foam generator experiments at high sulfur content and high gas flow rate. Similar to experiments in a foam generator, excessive foaming in a bioreactor will take place when a critical local concentration at the top of the liquid has been reached. At this point, a network structure of sulfur will be formed, resulting in stable films and a high coalescence rate of gas bubbles below the films. When the local sulfur concentration is below this critical value no excessive foaming occurs.

Furthermore, from laboratory reactors it is known that foaming problems can occur in cases of biomass lyses, e.g., by an osmotic shock due to a sudden change in salt concentration [unpublished results]. This will result in an increase in the concentration

of dissolved organic surface-active material and therefore also in an increase in foaming tendency. This observation from practice is in line with the foam stimulating properties of the organic components in the background solution, as was observed in our foam generator experiments.
The local concentration of sulfur near the surface of the liquid results from the balance between flotation of sulfur from the bulk to the top and sedimentation from the top to the bulk of the liquid. Flotation depends on conditions such as the gas flow rate, the G/L interfacial area, the hydrophobicity of the particles, and the hydrodynamics of the liquid. Although the superficial gas rates applied in our study are comparable to applied rates in full-scale installations, the hydrodynamics and the G/L interfacial areas are not identical. In bioreactors in H_2S removal processes, a circulation of liquid is generated (air-lift loop reactors). Furthermore, as the bioreactor is much larger, the rising bubbles will have more time to coalesce with other bubbles, resulting in a lower G/L interfacial area. In operating H_2S removal processes, the sulfur concentration in the liquid may therefore be much higher than in the experiments in the foam generator. It is therefore difficult to draw quantitative conclusions from our experiments on the operation of a biotechnological H_2S removal process. However, the trends described in this study provide tools that can help control foam formation.

7.5. Conclusions

The bubbling of air through aqueous suspensions of biologically produced sulfur, obtained from a biotechnological H_2S removal process, can result in the formation of basically two types of foam. At low sulfur content and air flow rate, an unstable foam is formed consisting of small spherical bubbles and of constant foam height. At higher sulfur content and air flow rate, a very stable foam with a polyhedral structure is formed. The transition between unstable and stable foam occurs when the local sulfur concentration near the the surface of the liquid is higher than a critical concentration. Then a film, effectively stabilized by a network structure of sulfur particles, can be formed which prevents air bubbles to burst at the surface. This results in an increase in bubble coalescence rate, the formation of large bubbles, lamellae, and films, and a fast increase in foam height.
Sulfur particles are transported from the bulk of the liquid to the top by flotation. Especially hydrophobic particles will adhere to the interface of rising air bubbles. When the bubble reaches the surface of the liquid, it will burst after which the adhering sulfur particles will sediment back to the bulk of the liquid, or be incorporated into the foam films. After foam formation, large aggregates of sulfur particles ($d \approx 17$ μm) have fallen apart into two smaller fractions ($d \approx 1$ μm and ≈ 9 μm). The foam especially contains particles of the larger of these two fractions, and practically no particles of the smaller fraction. The smaller particles are possibly too

hydrophilic to be located at the G/L interface of rising gas bubbles or in the film. The larger fraction is probably somewhat more hydrophobic and it therefore has an intermediate hydrophobicity that on the one hand causes the particles to be hydrophobic enough to be located at the G/L interface, and on the other hand not hydrophobic enough to act as antifoamer. The formation of a network structure results from the layer of organic polymeric material on the sulfur particles.
Furthermore, polysulfide anions were found to have antifoaming properties in biologically produced sulfur suspensions, either because of the changing of the surface properties of the biologically produced sulfur or because of the antifoaming properties of the hydrophobic elemental sulfur formed upon the chemical oxidation of polysulfide ions.

Acknowledgement

We thank Tanya Goloub for providing data on contact angle measurements. Albert Prins is gratefully acknowledged for discussions.

References

1. J. E. Burgess, S. A. Parsons, R. M. Stuetz, Developments in odour control and waste gas treatment biotechnology: A review, *Biotechnol. Adv.* **2001**, *19*, 35-63.
2. K. L. Sublette, N. D. Sylvester, Oxidation of hydrogen sulfide by *Thiobacillus denitrificans*: Desulfurization of natural gas, *Biotechnol. Bioeng.* **1987**, *24*, 249-257.
3. C. J. Buisman, B. G. Geraats, P. IJspeert, G. Lettinga, Optimization of sulphur production in a biotechnological sulphide-removing reactor, *Biotechnol. Bioeng.* **1990**, *35*, 50-56.
4. J. M. Visser, G. C. Stefess, L. A. Robertson, J. G. Kuenen, *Thiobacillus* sp. W5, the dominant autotroph oxidizing sulfide to sulfur in a reactor for aerobic treatment of sulfidic wastes, *Antonie van Leeuwenhoek* **1997**, *72*, 127-134.
5. A. J. H. Janssen, R. Sleyster, C. van der Kaa, A. Jochemsen, J. Bontsema, G. Lettinga, Biological sulphide oxidation in a fed-batch reactor, *Biotechnol. Bioeng.* **1995**, *47*, 327-333.
6. C. Cline, A. Hoksberg, R. Abry, A. Janssen, Biological process for H_2S removal from gas streams. The Shell-Paques/Thiopaq gas desulfurization process. In *Proceedings of the Laurance Reid gas conditioning conference* [CD-ROM], University of Oklahoma, Norman, OK, **2003**.
7. A. J. H. Janssen, G. Lettinga, A. de Keizer, Removal of hydrogen sulphide from wastewater and waste gases by biological conversion to elemental sulphur. Colloidal and interfacial aspects of biologically produced sulphur particles, *Colloids Surf. A-Physicochem. Eng. Asp.* **1999**, *151*, 389-397.
8. W. E. Kleinjan, A. de Keizer, A. J. H. Janssen, Biologically produced sulfur, *Top. Curr. Chem.* **2003**, *230*, 167-187. *This thesis, chapter 2*.
9. J. Varley, A. K. Brown, J. W. R. Boyd, P. W. Dodd, S. Gallagher, Dynamic multi-point measurement of foam behaviour for a continuous fermentation over a range of key process variables, *Biochem. Eng. J.* **2004**, *20*, 61-72.

10. S. P. Christiano, K. C. Fey, Silicone antifoam performance enhancement by nonionic surfactants in potato medium, *J. Ind. Microbiol. Biotechnol.* **2003**, *30*, 13-21.
11. G. C. Frye, J. C. Berg, Mechanisms for the synergistic antifoam action by hydrophobic solid particles in insoluble liquids, *J. Colloid Interface Sci.* **1989**, *130*, 54-59.
12. G. C. Frye, J. C. Berg, Antifoam action by solid particles, *J. Colloid Interface Sci.* **1989**, *127*, 222-238.
13. R. J. Pugh, Foaming, foam films, antifoaming and defoaming, *Adv. Colloid Interface Sci.* **1996**, *64*, 67-142.
14. R. Pelton, A review of antifoam mechanisms in fermentation, *J. Ind. Microbiol. Biotechnol.* **2002**, *29*, 149-154.
15. G. Johansson, R. J. Pugh, The influence of particle-size and hydrophobicity on the stability of mineralized froths, *Int. J. Min. Process.* **1992**, *34*, 1-21.
16. J. B. M. Hudales, H. N. Stein, The influence of solid particles on foam and film drainage, *J. Colloid Interface Sci.* **1990**, *140*, 307-313.
17. F. Q. Tang, Z. Xiao, J. A. Tang, J. A. Long, The effect of SiO_2 particles upon stabilization of foam, *J. Colloid Interface Sci.* **1989**, *131*, 498-502.
18. R. Tuinier, C. G. J. Bisperink, C. van den Berg, A. Prins, Transient foaming behavior of aqueous alcohol solutions as related to their dilational surface properties, *J. Colloid Interface Sci.* **1996**, *179*, 327-334.
19. *Handbook of chemistry and physics*, 82nd ed. (Ed.: D. R. Lide), CRC Press, Boca Raton, FL, **2001**,
20. W. E. Kleinjan, A. de Keizer, A. J. H. Janssen, Kinetics of the chemical oxidation of polysulfide anions in aqueous solution, *Water Res.*, submitted. *This thesis, chapter 5*.
21. A. Vairavamurthy, K. Mopper, B. F. Taylor, Occurrence of particle-bound polysulfides and significance of their reaction with organic matters in marine sediments, *Geophys. Res. Lett.* **1992**, *19*, 2043-2046.

Chapter 8

Summary and concluding remarks

Summary

This thesis deals with the effects of particles of biologically produced sulfur (or 'biosulfur') on a biotechnological process for the removal of hydrogen sulfide from gas streams. Particular emphasis is given to the role of polysulfide ions in such a process. These polysulfide ions are formed from reaction of sulfide with biologically produced sulfur. The basic concepts of this H_2S removal process were developed at the department of Environmental Technology of Wageningen University and the process is currently commercialized by Paques B.V. and Shell Global Solutions Int. B.V. as the Shell-Paques or Thiopaq™ process. It was originally designed for the removal of H_2S from 'biogas', which is a product from anaerobic wastewater treatment plants. Currently it is also used for the treatment of natural gas.

The process basically consists of a gas absorber and a bioreactor. In the gas absorber, H_2S is absorbed from an untreated gas stream by an alkaline liquid. The dissolved hydrogen sulfide (HS^-) is then led into the bioreactor where it is biologically oxidized to elemental sulfur by sulfide-oxidizing bacteria, mainly of the genus *Thiobacillus*. The solid sulfur formed is separated from the liquid by sedimentation and a liquid recycle flows from the bioreactor back to the gas absorber. To prevent oxidation of sulfide to sulfate, oxygen-limiting conditions are applied in the bioreactor. Production of elemental sulfur is preferred over the production of sulfate as elemental sulfur is less harmful than sulfate. Furthermore hydroxyl ions, consumed in the absorption of H_2S in the alkaline liquid, are regenerated upon oxidation of sulfide to elemental sulfur. This saves costs of dosing caustic (NaOH) to the process. Solid elemental sulfur is also easily separated from the solution by sedimentation and the resulting sulfur product can be reused.

Elemental sulfur has a very low solubility in water and the solid material is formed in the shape of particles, or 'globules'. In **chapter 2** an overview is given of reported studies on the properties of biologically produced sulfur. This concerns sulfur as it is produced in the biotechnological process by *Thiobacilli*, but also sulfur produced by other sulfide-oxidizing bacteria. Sulfide-oxidizing bacteria produce elemental sulfur as an intermediate in the oxidation of hydrogen sulfide to sulfate. Sulfur produced by these microorganisms can be stored in sulfur globules, located either inside or outside the cell. Excreted sulfur globules are colloidal particles that are stabilized against aggregation by electrostatic repulsion or steric stabilization. The formed elemental sulfur has some distinctly different properties as compared to "normal" inorganic sulfur. The density of the particles is for instance lower than the density of orthorhombic sulfur and the biologically produced sulfur particles have hydrophilic properties whereas orthorhombic sulfur is known to be hydrophobic. The nature of the sulfur and the surface properties of the globules are different for sulfur produced by different bacteria. For example, the globules produced by phototrophic bacteria

appear to consist of long sulfur chains terminated with organic groups, whereas chemotrophic bacteria produce globules consisting of sulfur rings (S_8). Extracellularly stored sulfur globules produced by *Acidithiobacillus ferrooxidans* have hydrophilic properties that can probably be explained by a vesicle structure consisting mainly of polythionates ($^{-}O_3S–S_n–SO_3^{-}$). Adsorbed organic polymers, such as proteins, provide hydrophilic properties to sulfur produced by a mixed culture of *Thiobacilli* in a biotechnological H_2S removal process. The small particle size and the hydrophilic properties of these particles provide advantages over other commercially available forms of sulfur in bioleaching and fertilizer applications.

A central question in this thesis is how biologically produced sulfur particles can affect the absorption of H_2S in the gas absorber. A possibly occurring effect is an enhancement of the absorption rate of gaseous H_2S by a heterogeneous reaction of the dissolved sulfide with biologically produced sulfur particles. To assess the role of this reaction in the enhancement of the H_2S absorption rate, the kinetics of this reaction has been studied, as has been described in **chapter 3**. The kinetics of the heterogeneous reaction between dissolved sodium sulfide and biologically produced sulfur particles has been studied by measuring the formation of polysulfide ions, S_x^{2-}, in time. Experiments were performed at pH 8.0 and at temperatures ranging from 30 to 50 °C. The obtained data were fitted with a reaction rate model. To describe the heterogeneous reaction kinetics, a detailed reaction mechanism for the polysulfide formation reaction has been proposed. Furthermore, a decreasing particle size and a nonuniform particle size distribution were incorporated in this reaction rate model. Results for the reaction of sulfide with biosulfur were compared with an earlier published study on the reaction of sulfide with “inorganic” granular sulfur. Whereas the reaction rate of sulfide with granular sulfur was limited by diffusion, the reaction rate of sulfide with biologically produced sulfur is limited by chemical reaction. This is probably caused by the smaller particle size or the specific hydrophilic properties of the biologically produced sulfur. This makes the surface of the biosulfur particles more easily available for reaction than the surface of granular sulfur.

The effect of the specific properties of biologically produced sulfur on the equilibrium constant of the reaction between biologically produced sulfur and sodium sulfide is described in **chapter 4**. Results were compared with the equilibrium of the reaction of sulfide with “inorganic” elemental sulfur. The equilibrium can be described by an equilibrium constant pK_x. For biologically produced sulfur, pK_x = 9.10 ± 0.08 (21 °C) and 9.17 ± 0.09 (35 °C) with an average polysulfide chain length x = 4.91 ± 0.32 (21 °C) and 4.59 ± 0.31 (35 °C). The pK_x value for biologically produced sulfur is significantly higher than for reaction of dissolved sodium sulfide with “inorganic” sulfur (pK_x = 8.78; 21 °C). This difference is probably caused by specific binding of polysulfide ions in the organic polymer layer, adsorbed on the surface of the sulfur particles.

As was described in chapters 3 and 4, polysulfide ions can be produced from reaction of dissolved hydrogen sulfide with biologically produced sulfur. In a hydrogen sulfide removal process, these polysulfide ions can be oxidized to form thiosulfate. The basic concept of the H_2S removal process is the absorption of H_2S from a gas stream, in which OH^- is consumed, and the subsequent biological oxidation of HS^- to elemental sulfur (OH^- is produced). By oxidation of polysulfide ions to thiosulfate, the biological oxidation of sulfide to elemental sulfur is prevented, resulting in a net loss of OH^-. This means that an OH^- solution has to be dosed to the process, which can involve considerable costs. To control thiosulfate formation in the H_2S removal process, more knowledge of the chemical oxidation of polysulfide ions in aqueous solutions is required. Therefore, the kinetics of this reaction and the reaction products formed, have been studied, which is described in **chapter 5**. Experiments were performed in phosphate buffered solutions at pH 7 to 12, at temperatures between 20 and 40 °C, and an ionic strength between 0.05 and 0.50 M. Polysulfide solutions were mixed with a buffer solution of known dissolved oxygen concentration, after which the decrease in the oxygen concentration of the solution was measured in time. The rate of oxygen consumption can be described by the empirical relation $d[O_2]/dt = -k[S_x^{2-}][O_2]^{0.59}$. The reaction rate constant k is moderately dependent on pH and goes through a maximum at pH 10. The rate of oxygen consumption for polysulfide solutions is approximately four times higher than for sulfide solutions. At pH values below 9, reaction products were formed according to $S_x^{2-} + 3/2\ O_2 \rightarrow\ S_2O_3^{2-} + (x-2)\ S^0$. At pH values higher than 9, more thiosulfate and additional sulfide were formed, which is attributed to the low chemical stability of the sulfur of oxidation state zero, formed upon polysulfide oxidation. The results strongly suggest that hydrolysis of this 'nascent' elemental sulfur to HS^- and $S_2O_3^{2-}$ is faster than hydrolysis of crystalline inorganic sulfur or colloidal particles of biologically produced sulfur, and has a significant contribution already at 30 °C and pH 10.

With knowledge of the measured reaction kinetics from chapter 3 it is possible to calculate the theoretical contribution of the heterogeneous reaction between sulfide and biosulfur to the enhancement of the H_2S absorption rate. This is described in **chapter 6**. Based on a pseudo-first order approximation of the kinetics, theoretical enhancement factors have been calculated. These have been compared with experimentally determined enhancement factors. Experiments on H_2S absorption in a suspension containing small (< 3 μm) biosulfur particles have been performed in a stirred cell reactor with a constant gas-liquid interfacial area. The observed enhancement of H_2S absorption in these experiments can be explained by the heterogeneous reaction. Here, large hydrophobic particles could not be kept in suspension and therefore only smaller hydrophilic particles were present ($d_p < 3\mu m$). However, the observed enhancement of H_2S absorption in a gas absorber column,

coupled with a bioreactor, cannot be explained by the heterogeneous reaction alone. In these experiments both small hydrophilic particles and larger, more hydrophobic particles were present (d_p up to 20μm). In the gas absorber column, there was therefore a relatively low available specific surface area. Furthermore, a high k_L and low [S_x^{2-}] prevented enhancement due to the heterogeneous reaction. A more likely explanation for enhancement of the H_2S absorption rate in this series of experiments is the more hydrophobic behavior of the larger particles. A local increase of the hydrophobic sulfur particle concentration near the gas/liquid interface and specific adsorption of H_2S at the particle surface can result in an increase in the H_2S absorption rate.

In the aerated bioreactor of the biotechnological H_2S removal process, sometimes stable foam is formed, which contains fairly large amounts of solid elemental sulfur. For a good operation of the process it is required to control foam formation and therefore knowledge of the nature of the foam and the mechanism of foam formation is needed. The effect of biologically produced sulfur particles on foam formation is particularly interesting. In **chapter 7** a study on foam formation in aqueous suspensions of biologically produced sulfur particles is described, with the objective of describing trends and phenomena that govern foam formation in a biotechnological H_2S removal process. Air is bubbled through a suspension and the development of the foam height in time is measured, showing essentially two types of foam: unstable foam of constant foam height and stable foam with a rapidly increasing foam height. The transition between these types of foam can occur when the local sulfur concentration near the surface of the liquid is higher than a critical concentration, so that a stable network structure can be formed. Sulfur particles are transported to the top of the liquid by flotation. Upon foam formation large aggregates of sulfur fall apart into smaller fractions. Especially the larger fraction of the sulfur particles is present in the foam, indicating that these particles have the right hydrophobicity to form a network structure. Furthermore, polysulfide anions were found to have antifoaming properties in biologically produced sulfur suspensions, either because of the changing of the surface properties of the biologically produced sulfur or because of the antifoaming properties of the hydrophobic elemental sulfur formed upon the chemical oxidation of polysulfide ions.

Concluding remarks

The results of the research described in this thesis can provide tools that can be used in the control and design in a new biotechnological H_2S removal processes. Several aspects of the process have been studied and it can be concluded that processes that are beneficial for one aspect of the process may be a considerable draw back for another aspect. For a good process control strategy an integral view of the process is therefore required.

The chemistry of polysulfide ions plays an important role in a number of aspects of the biotechnological H_2S removal process. The idea may occur that formation of polysulfide ions is on the one hand desirable, as it stimulates the rate of H_2S absorption in the gas absorber and suppresses foam formation, and on the other hand undesirable, as it decreases process selectivity due to formation of thiosulfate. Unfortunately, the draw back may be bigger than the advantages. Although the heterogeneous reaction forming polysulfide ions can result in an enhancement of H_2S absorption when only small hydrophilic sulfur particles are present, this is probably not the case in a gas absorber in a continuous process where more larger hydrophobic particles are present (chapter 6). The results from the research presented in this thesis suggest that formation of polysulfide has little effect on the enhancement of H_2S absorption rate in a gas absorber. Formation of polysulfide ions will, however, result in a decrease in process selectivity as oxidation and hydrolysis to thiosulfate occurs (chapter 5). This will be especially the case at high pH because hydrolysis of sulfur will play an increasingly important role.

Presence of particles of biologically produced sulfur has several effects on a biotechnological H_2S removal process. On the one hand, the presence of the more hydrophobic particles can induce an enhancement of the H_2S absorption rate by a so-called shuttle effect. On the other hand, an increase in sulfur particles can stimulate excessive foam formation, which can result in site pollution and loss of biomass contents.

Furthermore, it may be beneficial to operate the process at a high pH as this stimulates the rate of H_2S absorption in the gas absorber. However, more thiosulfate will be formed with increasing pH, particularly at a process operating at pH > 9, leading to an overall decrease in process selectivity, meaning that less elemental sulfur is produced and additional NaOH has to be dosed.

For the control of foam formation in the H_2S removal process a number of recommendations can be made. High sulfur concentrations should be prevented as they can stimulate foam formation. Accumulation of surface-active organic components should be prevented, particularly the lyses of bacteria by sudden changes in salt concentrations or pH. Dosing of additional sulfide will result in formation of polysulfide ions. This may help in preventing foam formation or destabilizing any foam formed, however, it will also lead to a decrease in process selectivity.

Experiments described in this thesis were performed with biologically produced sulfur obtained from a full-scale bioreactor in which the dominating organism is *Thiobacillus* sp. W5. This biologically produced sulfur is believed to consist of a core of sulfur rings with polymeric organic compounds adsorbed on the particle surface. Other sulfide-oxidizing bacteria are known to produce sulfur globules consisting of polythionates (e.g., *Acidithiobacillus ferrooxidans*) or long sulfur chains terminated with organic groups (e.g., *Allochromatium vinosum*). Specific properties found for

biosulfur particles in this thesis (e.g., kinetics and equilibrium of its reaction with sulfide) may not be valid for other forms of biologically produced sulfur.

In chapter 3 of this thesis the study of the kinetics of polysulfide formation was described. A detailed reaction mechanism was proposed which can be described by a fairly simple kinetic equation. With this it was possible to explain the observed kinetics at pH 8. It should however be noted that the obtained kinetic expression might not be suitable for describing the kinetics of polysulfide formation at other pH values. For example, at higher pH the condition $k_{-1}[H^+] >> k_2[HS^-]$ (see Eq. 3.27) might not be valid, resulting in a different overall kinetic equation. Further research would be needed to resolve the kinetic behavior at other pH values. However, in general, it can be expected that a higher pH would result in a higher rate of polysulfide formation.

In chapter 7 of this thesis foam formation with dispersions of biologically produced sulfur is studied with the objective of indicating the trends that will be important in full-scale installations of biotechnological H_2S removal processes. Although the superficial gas rates applied in our study are comparable to applied rates in full-scale installations, the hydrodynamics and the G/L interfacial area are not identical. In bioreactors in H_2S removal processes, a circulation of liquid is generated (air-lift loop reactors). Furthermore, as the bioreactor is much larger, the rising bubbles will have more time to coalesce with other bubbles, resulting in a lower G/L interfacial area. In operating H_2S removal processes, the sulfur concentration in the liquid may therefore be much higher than in the experiments in the foam generator. It is therefore difficult to draw quantitative conclusions from these experiments on the operation of a biotechnological H_2S removal process but the observed trends and phenomena may be useful for the control of foam formation.

Future research will focus on the operation of the process at higher pH, as this is beneficial for the rate of absorption of H_2S in the gas absorber. Microbiological studies on microorganisms that can resist high pH and high salt concentration have been performed but more research is required, both microbiological as technological. It should be noted, however, that increasing hydrolysis of sulfur at high pH (not of biologically produced sulfur, but rather of 'nascent' elemental sulfur formed upon oxidation of polysulfide ions) will result in a decrease of process selectivity.

The technique used to study the kinetics of the reaction between sulfur and sulfide may also be used for the study of the reaction between sulfur and methylmercaptans.

Furthermore, promising results have been obtained in the study of applications of biosulfur as fungicide, fertilizer, or in bioleaching. It has been found that the specific properties of biologically produced sulfur (small particle size, hydrophilic surface) have clear advantages over other forms of commercial, inorganic sulfur. This is particularly interesting as currently more sulfur is produced worldwide than is needed as pure chemical and therefore sulfur is also stored in landfill. Although solid sulfur is

considered a non-hazardous waste, landfill is an undesirable option, partly because acidification by oxidation has to be prevented. Further research in the application of biologically produced sulfur in agriculture is therefore needed.

Samenvatting en slotopmerkingen

Samenvatting

Dit proefschrift gaat over de effecten die biologisch gevormde zwaveldeeltjes ('biozwavel') kunnen hebben op een biotechnologisch proces voor de verwijdering van waterstofsulfide (H_2S) uit gasstromen. Met name is gekeken naar de rol van polysulfide ionen in zo'n proces. Deze polysulfide ionen worden gevormd in de reactie van sulfide met biologisch gevormd zwavel. De basisprincipes van het proces zijn ontwikkeld op de afdeling milieutechnologie van Wageningen Universiteit en het wordt momenteel op de markt gebracht door Paques B.V. en Shell Global Solutions International B.V. als het *Shell-Paques* of het *Thiopaq*™ proces. Oorspronkelijk is het ontworpen voor de verwijdering van H_2S uit biogas, een product van anaërobe waterzuivering. Tegenwoordig wordt het ook gebruikt voor de behandeling van aardgas.

Het proces bestaat uit een *gasabsorber* en een bioreactor. In de gasabsorber wordt H_2S vanuit het onbehandelde gas geabsorbeerd in een alkalische vloeistof. Het opgeloste sulfide (HS^-) wordt dan naar een bioreactor geleid waar het biologisch tot elementair zwavel wordt geoxideerd door sulfide oxiderende bacteriën, voornamelijk *Thiobacilli*. Het gevormde vaste zwavel wordt van de vloeistof gescheiden door sedimentatie en een *recycle* leidt de resterende vloeistof terug naar de gasabsorber. Om te voorkomen dat sulfide wordt geoxideerd tot sulfaat worden zuurstof limiterende condities toegepast in de bioreactor. Vorming van zwavel heeft de voorkeur boven vorming van sulfaat omdat elementair zwavel minder schadelijk is dan sulfaat. Verder worden OH^- ionen die geconsumeerd worden bij de absorptie van H_2S geregenereerd bij de vorming van zwavel maar niet bij de vorming van sulfaat. Bij vorming van zwavel is het hierdoor dus niet nodig extra loog (NaOH) te doseren. Elementair zwavel is ook makkelijk van een vloeistof te scheiden door sedimentatie en het zwavel kan worden hergebruikt.

Elementair zwavel heeft een zeer lage oplosbaarheid in water en het vaste materiaal precipiteert in de vorm van deeltjes. In **hoofdstuk 2** wordt een overzicht gegeven van beschikbare studies naar de eigenschappen van biologisch gevormde zwaveldeeltjes. Hierbij is gekeken naar biozwavel zoals dat is gevormd in een biotechnologisch proces door *Thiobacilli* maar ook naar biozwavel dat is geproduceerd door andere sulfide oxiderende bacteriën. Sulfide oxiderende bacteriën produceren elementair zwavel als een tussenproduct in de oxidatie van sulfide naar sulfaat. Dit zwavel kan door de micro-organismen worden opgeslagen in *globules*, die zich zowel binnen als buiten de celwand kunnen bevinden. Uitgescheiden zwavelglobules kunnen worden opgevat als kolloïdale deeltjes die gestabiliseerd worden door elektrostatische repulsie of sterische stabilisatie. Het gevormde biozwavel heeft een aantal duidelijk andere eigenschappen dan "gewoon" kristallijn zwavel. De dichtheid van de biozwaveldeeltjes is bijvoorbeeld lager dan de dichtheid van kristallijn

orthorhombisch zwavel en verder heeft biologisch gevormd zwavel hydrofiele eigenschappen terwijl van orthorhombisch zwavel bekend is dat het sterk hydrofoob is. De aard van het zwavel en de oppervlakte-eigenschappen van de globules kunnen verschillen voor verschillende bacteriën. Zwaveldeeltjes geproduceerd door fototrofe bacteriën lijken bijvoorbeeld te bestaan uit lange zwavelketens met organische groepen aan het uiteinde, terwijl chemotrofe bacteriën vaak globules produceren die voornamelijk uit zwavelringen (S_8) bestaan. Zwavelglobules die buiten de cel worden opgeslagen van *Acidithiobacillus ferrooxidans* hebben hydrofiele eigenschappen die waarschijnlijk veroorzaakt worden door een *vesicle* structuur van polythionaten ($^{-}O_3S{-}S_n{-}SO_3^{-}$). Het hydrofiele karakter van het biozwavel dat geproduceerd is in het biotechnologische proces wordt veroorzaakt door adsorptie van organische polymeren zoals eiwitten. Verder blijkt dat de kleine deeltjesgrootte en het hydrofiele karakter van biozwaveldeeltjes voordelen kunnen bieden boven andere commercieel beschikbare zwavelmiddelen die bijvoorbeeld gebruikt worden als kunstmest of in mijnbouw (*bioleaching*).

Een belangrijke vraag in dit proefschrift is hoe biologisch gevormde zwaveldeeltjes de absorptie van H_2S in een gasabsorber kunnen beïnvloeden. Een verschijnsel dat mogelijk zou kunnen optreden is een versnelling van de H_2S absorptie doordat er een reactie optreedt van opgelost sulfide met de biozwaveldeeltjes. Om te voorspellen hoe deze reactie het proces beïnvloedt is de kinetiek van deze reactie bestudeerd. Dit is beschreven in **hoofdstuk 3**. De kinetiek van de reactie tussen biologisch gevormde zwaveldeeltjes en opgelost sulfide is bestudeerd door de vorming van polysulfide ionen, S_x^{2-}, in de tijd te meten bij pH 8 en temperaturen variërend van 30 tot 50 °C. De verkregen data zijn gemodelleerd aan de hand van een reactiesnelheidsmodel, waarin heterogene reactiekinetiek, afnemende deeltjesgrootte en een niet-uniforme deeltjesgrootteverdeling zijn meegenomen. Een gedetailleerd reactiemechanisme voor de optredende polysulfidevormingsreactie is hierbij voorgesteld. Resultaten voor de kinetiek van de reactie van opgelost sulfide met biologisch gevormde zwaveldeeltjes zijn vergeleken met een eerder onderzoek naar polysulfidevorming uit reactie van sulfide met “anorganisch” granulair zwavel. Waar in dit eerdere onderzoek de reactie gelimiteerd is door diffusie, is deze in het geval van reactie van sulfide met biologisch zwavel gelimiteerd door chemische reactie. Dit wordt waarschijnlijk veroorzaakt door de kleinere deeltjesgrootte of de specifiek hydrofiele eigenschappen van het biologisch gevormd zwavel. Hierdoor is het oppervlak van biologisch gevormd zwavel beter beschikbaar voor reactie met sulfide dan het oppervlak van anorganisch granulair zwavel.

Naast de reactiesnelheid van de reactie tussen waterstofsulfide en biologisch gevormd zwavel in waterige oplossing is de ligging van het evenwicht van deze reactie van belang. De studie naar de evenwichtsligging is beschreven in **hoofdstuk 4**. De evenwichtsconstante van deze heterogene reactie is bepaald, alsmede de bijbehorende

gemiddelde polysulfide ketenlengte, x (x = 4.91 ± 0.32; T = 21 °C). Uit vergelijking van de evenwichtsconstante voor biologisch gevormd zwavel met de experimenteel bepaalde evenwichtsconstante voor anorganisch zwavel volgt dat het evenwicht met biologisch gevormd zwavel meer in de richting van zwavel ligt dan het evenwicht met anorganisch zwavel. Dit wordt waarschijnlijk veroorzaakt door specifieke adsorptie van polysulfide ionen in de organische polymeerlaag van de biozwaveldeeltjes.

Zoals is beschreven in de hoofdstukken 3 en 4 kunnen polysulfide ionen worden gevormd uit de reactie van sulfide met biologisch gevormd zwavel. In een H_2S verwijderingsproces kunnen deze polysulfide ionen verder worden geoxideerd tot thiosulfaat. In deze ongewenste nevenreactie worden polysulfide ionen chemisch geoxideerd tot elementair zwavel en thiosulfaat. De vorming van dit thiosulfaat betekent een verlaging van de selectiviteit van het proces. Het basisprincipe van het proces bestaat uit de absorptie van H_2S uit een gasstroom (kost OH^-) en vervolgens de biologische oxidatie van HS^- tot S^0 (levert OH^- op). Door oxidatie van polysulfide ionen tot thiosulfaat wordt de biologische oxidatie van (poly)sulfide verhinderd, wat netto OH^- ionen kost. Bij het optreden van chemische polysulfide oxidatie moet dus een loogoplossing worden gedoseerd, wat in de praktijk een belangrijke kostenpost kan zijn. Het onderzoek naar deze reactie is beschreven in **hoofdstuk 5**. Chemische oxidatie van waterige polysulfide oplossingen is bestudeerd bij een pH van 7 tot 12, een temperatuur van 20 tot 40 °C en een ionsterkte van 0.05 tot 0.5 M. Oxidatiesnelheden zijn bepaald door de afname van de zuurstofconcentratie van een gebufferde oplossing te meten vanaf het tijdstip van toevoeging van een polysulfide oplossing. Een empirische relatie voor de snelheid van afname van de zuurstofconcentratie is bepaald: $d[O_2]/dt = k\ [S_x^{2-}][O_2]^{0.59}$. De reactiesnelheidsconstante k is enigszins afhankelijk van pH en gaat door een maximum bij pH 10. Bij pH ≤ 9.0 worden reactieproducten gevormd volgens een ook eerder gepubliceerde verhouding van $S_x^{2-} + 3/2\ O_2 \rightarrow S_2O_3^{2-} + (x-2)\ S^0$. Bij pH > 9.0 wordt echter extra $S_2O_3^{2-}$ en ook HS^- gevormd. Dit wordt waarschijnlijk veroorzaakt door de lage chemische stabiliteit van het bij polysulfide oxidatie gevormde elementair zwavel ("S^0"). Hydrolyse van dit "pas gevormde" zwavel tot HS^- en $S_2O_3^{2-}$ is sneller dan de hydrolyse van kristallijn anorganisch zwavel of van kolloïdale deeltjes van biologisch gevormd zwavel.

Met kennis van de gemeten reactiekinetiek (hoofdstuk 3) is het mogelijk een inschatting te maken van de bijdrage van de heterogene reactie tussen sulfide en biologisch gevormd zwavel aan versnelde H_2S gasabsorptie. Dit is beschreven in **hoofdstuk 6**. Op basis van een pseudo-eerste orde benadering van de reactiekinetiek zijn theoretische versnellingsfactoren uitgerekend. Deze zijn vergeleken met experimenteel bepaalde versnellingsfactoren. Experimenten naar de versnelling van H_2S absorptie in een suspensie bestaande uit kleine (< 3 μm) biozwaveldeeltjes,

uitgevoerd in een geroerde cel reactor met een constant gas-vloeistof grensvlak, kunnen worden verklaard door de reactiekinetiek van de heterogene reactie tussen H_2S en biologisch gevormd zwavel. Geobserveerde versnelling van H_2S absorptie in een gekoppelde gasabsorberkolom met bioreactor (laboratorium schaal) kan echter niet door de gemeten reactiekinetiek verklaard worden, met name vanwege een relatief lage hoeveelheid beschikbaar zwaveloppervlak (veel grote deeltjes; diameter < 20μm). Dat er in deze situatie toch een versnelling van H_2S absorptie wordt gemeten wijst erop dat afgezien van versnelling door heterogene reactie ook een ander mechanisme een rol speelt. Een mogelijke verklaring ligt in het meer hydrofobe karakter van de grotere deeltjes. Hierdoor zal er een verhoogde concentratie van zwaveldeeltjes aan het gas-vloeistof grensvlak zijn. Bij absorptie van H_2S aan deze deeltjes in het grensvlak zouden de deeltjes als shuttle tussen bulk en grensvlak kunnen optreden en daardoor zorgen voor versnelde H_2S absorptie.

In de beluchte bioreactor van het proces kan soms een stabiel schuim worden gevormd dat relatief veel vast elementair zwavel bevat. Voor een goede procesvoering is het noodzakelijk de schuimvorming te beheersen en daarvoor is kennis van de aard van het schuim en het mechanisme van schuimvorming nodig. Met name de invloed van de biologisch gevormde zwaveldeeltjes op schuimvorming is van belang. In **hoofdstuk 7** is het onderzoek beschreven naar schuimvorming in waterige suspensies van biozwaveldeeltjes. Experimenten zijn uitgevoerd waarin suspensies met biologisch gevormd zwavel in een schuimkolom belucht zijn, waarna de ontwikkeling van de schuimlaag is gemeten. Suspensies waren afkomstig van een in de praktijk werkende bioreactor van een afvalwaterzuiveringsinstallatie. Gebleken is dat er een overgang kan plaatsvinden van een kort levend schuim dat bestaat uit kleine belletjes (< 5 mm), naar een stabiel schuim dat bestaat uit grotere, niet-bolvormige structuren (< 50 mm). Dit stabiele schuim bevat relatief grote hoeveelheden vast zwavel dat vrijkomt op het moment dat een film in het schuim knapt. Deze overgang in schuimvorming wordt gestimuleerd door biologische zwaveldeeltjes, opgelost oppervlakteactief organisch materiaal in de suspensie en door hoge beluchtingsnelheden. Zwaveldeeltjes worden door flotatie in de richting van het schuim getransporteerd en dalen door sedimentatie weer af naar de bulk. Als de balans tussen flotatie en sedimentatie in het voordeel is van flotatie (door hoge gassnelheid of hoge deeltjesconcentratie) vindt ophoping van deeltjes aan het gas-vloeistof grensvlak plaats. Als een kritische deeltjesconcentratie aan dit grensvlak is bereikt kan een relatief stabiele film aan het gas-vloeistof grensvlak worden gemaakt. Hierdoor vindt onder deze film een versnelde coalescentie plaats, wat resulteert in grotere bellen en een snel stijgende schuimhoogte. Een opmerkelijke rol van aanwezigheid van polysulfide ionen is ontdekt. Aanwezigheid van polysulfide ionen gaat schuimvorming tegen. Mogelijke verklaringen hiervan zijn de chemische oxidatie van polysulfide ionen, waarbij hydrofoob (anorganisch) vast zwavel wordt

gevormd dat kan optreden als een effectieve schuimbreker, of de adsorptie van polysulfide ionen aan het biozwaveloppervlak waardoor de oppervlakte-eigenschappen van de biozwaveldeeltjes veranderen.

Slotopmerkingen

De resultaten van het onderzoek dat is beschreven in dit proefschrift bieden aanwijzingen die gebruikt kunnen worden bij de procesvoering en het ontwerp van biotechnologische processen voor de verwijdering van H_2S uit gas. Verschillende aspecten van het proces zijn bestudeerd, en geconcludeerd kan worden dat effecten die gunstig kunnen zijn voor een deel van het proces juist nadelig kunnen zijn voor een ander deel van het proces. Een integrale blik op het proces is dus nodig om een goed overzicht te krijgen van de optimale procesvoering.
De chemie van polysulfide ionen speelt een belangrijke rol bij een aantal aspecten van het proces. Het beeld zou kunnen ontstaan dat vorming van polysulfide ionen aan de ene kant wenselijk is, aangezien het kan bijdragen aan de versnelling van de absorptie van H_2S in de gasabsorber en schuimvorming tegengaat en, aan de andere kant, onwenselijk aangezien de selectiviteit wordt verlaagd door vorming van thiosulfaat. Het nadeel lijkt echter zwaarder te wegen dan de voordelen. Hoewel de polysulfidevormingsreactie inderdaad kan resulteren in een versnelling van H_2S absorptie als alleen kleine deeltjes aanwezig zijn, is dit waarschijnlijk niet of veel beperkter het geval in een gasabsorber in een continu proces waar ook grotere deeltjes aanwezig zijn (hoofdstuk 6). Vorming van polysulfide ionen zal echter wel resulteren in een daling van de selectiviteit door oxidatie en hydrolyse tot thiosulfaat (hoofdstuk 5). Dit zal met name bij hogere pH een rol spelen aangezien hydrolyse van zwavel dan een belangrijkere rol speelt.
Aanwezigheid van zwaveldeeltjes kan het proces eveneens op verschillende manieren beïnvloeden. Aanwezigheid van meer hydrofobe deeltjes kan leiden tot een versnelling van H_2S absorptie door een zogenaamd shuttle-effect. Een verhoogde concentratie van deze deeltjes kan echter ook leiden tot excessieve schuimvorming.
Verder zou het gunstig kunnen zijn het proces bij hogere pH te bedrijven, aangezien dit de absorptie van H_2S stimuleert. Bij hogere pH zal echter waarschijnlijk ook meer thiosulfaat gevormd worden wat resulteert in een daling van de selectiviteit van het proces.
Om schuimvorming in het proces tegen te gaan kunnen een aantal aanbevelingen gedaan worden. Hoge zwavelconcentraties zouden voorkomen moeten worden, aangezien hoge zwavelconcentraties schuimvorming stimuleren. Verder dient de accumulatie van oppervlakteactieve stoffen, met name door het afsterven van bacteriën door plotselinge veranderingen in zoutconcentraties of pH, vermeden te worden. Toevoeging van extra sulfide aan een systeem waar zwavel in overmaat aanwezig is zal resulteren in de vorming van polysulfide ionen. Dit zou kunnen

helpen bij het voorkomen van schuimvorming of het afbreken van reeds gevormd schuim. Het zal echter ook resulteren in een daling van de proces selectiviteit.
De experimenten zoals die zijn beschreven in dit proefschrift zijn uitgevoerd met biologisch gevormd zwavel dat is verkregen uit een bioreactor van een werkend proces, waarin het dominerende organisme *Thiobacillus* sp. W5 is. Dit biologisch gevormde zwavel bestaat uit een kern van voornamelijk ringvormige zwavelverbindingen (S_8) met organische polymeren geadsorbeerd aan het oppervlak. Andere sulfide oxiderende bacteriën produceren zwaveldeeltjes die bestaan uit polythionaten (bijvoobeeld *Acidithiobacillus ferrooxidans*) of uit lange zwavelketens met organische eindgroepen (bijvoorbeeld *Allochromatium vinosum*). De specifieke eigenschappen voor de vorm van biozwavel zoals die is gebruikt in dit onderzoek zouden voor andere vormen van biozwavel dus anders kunnen zijn.
In hoofdstuk 3 van dit proefschrift is de kinetiek van polysulfidevorming beschreven waarbij een gedetailleerd reactiemechanisme en een daaruit volgende kinetiekvergelijking is gebruikt. Hiermee was het mogelijk de uitgevoerde experimenten (pH 8) te beschrijven. Het moet worden opgemerkt dat de verkregen kinetiekvergelijking mogelijk niet geschikt is voor de beschrijving van kinetiekresultaten bij pH waarden die behoorlijk afwijken. Zo zou bij hogere pH de voorwaarde $k_{-1}[H^+] >> k_2[HS^-]$ (zie vergelijking 3.27) mogelijk niet meer gelden, wat zou resulteren in een andere kinetiekvergelijking. Meer onderzoek zou dus nodig zijn om het kinetiekgedrag bij andere pH waarden te bepalen, hoewel in het algemeen verwacht kan worden dat bij hogere pH de vormingssnelheid van polysulfide ionen toeneemt.
In hoofdstuk 7 van dit proefschrift is het onderzoek naar schuimvorming in suspensies van biozwavel beschreven waarbij de doelstelling was de trends te bepalen die van belang zijn bij de procesvoering van een *full-scale* installatie van het H_2S verwijderingsproces. Hoewel de superficiële gassnelheden die in de experimenten zijn toegepast vergelijkbaar zijn met condities in full-scale installaties, zijn de hydrodynamica en het gas-vloeistof oppervlakvlak dat echter niet. In bioreactoren wordt een circulatie van vloeistof gegenereerd (*air-lift loop* reactoren) en aangezien een bioreactor groter is zullen stijgende bellen meer tijd hebben voor coalescentie, wat resulteert in een kleiner gas-vloeistof oppervlak. In werkende H_2S verwijderingsprocessen zou de gebruikte zwavelconcentratie dus een stuk hoger kunnen zijn dan in de experimenten in de schuimbuis (*foam generator*). Het is daarom moeilijk kwantitatieve conclusies te trekken uit deze experimenten over de procesvoering van een full-scale proces, maar de geobserveerde trends en effecten kunnen wel nuttig zijn het voorkomen van excessieve schuimvorming.
Verder onderzoek naar de procesvoering bij hogere pH is wenselijk aangezien dit gunstig is voor de absorptie van H_2S in de gasabsorber. Microbiologische studies naar bacteriën die hoge pH en zoutconcentratie kunnen weerstaan zijn beschikbaar, maar

meer onderzoek is wenselijk, zowel naar de microbiologie als de technologie van het proces. Tevens moet worden onderzocht in welke mate vorming van thiosulfaat bij hogere pH de selectiviteit verlaagt.
De techniek die gebruikt is om de kinetiek van de reactie tussen biozwavel en sulfide te bestuderen zou ook gebruikt kunnen worden voor de kinetiek van de reactie tussen biozwavel en mercaptanen.
Verder zijn veelbelovende resultaten gevonden in onderzoeken naar de toepassing van biologisch gevormd zwavel in kunstmest, mijnbouw (*bioleaching*) en als fungicide. De specifieke eigenschappen van biozwavel (kleine deeltjesgrootte, hydrofiel oppervlak) verschaffen het biozwavel een voordeel boven andere commercieel beschikbare vormen van zwavel. Dit is met name interessant omdat er momenteel meer zwavel geproduceerd wordt dan nodig is voor toepassing in de chemische industrie. Dit overschot aan zwavel wordt daarom soms opgeslagen in de grond (*landfill*). Alhoewel vast elementair zwavel beschouwd kan worden als een ongevaarlijk afvalproduct is dit toch onwenselijk, onder meer omdat verzuring door oxidatie dient te worden voorkomen. Meer onderzoek naar toepassingen van het zwavel zijn daarom wenselijk.

Dankwoord

Hoewel zwavel door de eeuwen heen voornamelijk is geassocieerd met hel, verdoemenis, ontploffingen en stank is mijn persoonlijke associatie met zwavel een stuk positiever. Ik denk dan aan het onderzoek dat ik de afgelopen jaren met veel plezier heb gedaan en aan de mensen die me daarbij hebben geholpen. Je zou dus kunnen zeggen dat waar andere mensen denken aan hel en verdoemenis, ik denk aan Albert en Arie.

Albert, je bent de grote inspirator van dit onderzoek geweest. Ondanks de fysieke afstand heb ik nooit het gevoel gehad dat je "op afstand" bij dit project betrokken was. Dit dankzij de vele e-mails, telefoontjes en regelmatige besprekingen die we hier in Wageningen hebben gehad. Arie, veel dank voor de vele besprekingen en je gedetailleerde commentaren op mijn teksten. Ik vond onze samenwerking niet alleen heel plezierig, het heeft me ook steeds weten te motiveren. Aan jullie beide, veel dank voor jullie inzet voor dit project en mijn begeleiding in het bijzonder.

Een deel van het experimentele werk is uitgevoerd bij Paques (Balk, Friesland). Grote hulp heb ik hier gehad van Wobby Bosma en Wim Bourgonje, waarvoor mijn dank. Pim en Rene bedank ik voor het gastvrije verblijf dat ze mij boden in hun huis in Sneek. Andere experimenten heb ik uitgevoerd bij Shell (Amsterdam). Hiervoor bedank ik Rini Seelen voor de hulp. Dank aan Jos Lammers voor nuttige discussies over verschillende onderdelen van dit proefschrift.

De vakgroep Fysko wil ik eigenlijk als geheel bedanken voor de leuke tijd. Om het toch wat te specificeren zou ik ten eerste op het 'zakelijke' gebied graag Martien willen bedanken voor zijn commentaar en suggesties en Chris voor de samenwerking aan het schuimproject. Verdere assistentie bij verschillende metingen heb ik onder meer gekregen van Tanya, Ab, Remco en Wim Threels: dank daarvoor!

Ten tweede, op het gebied van de sfeer wil ik de vele activiteiten van de vakgroep toch wel even roemen. Voetballen, fietsen, roeien en hardlopen, ik zou bijna van mezelf gaan denken dat ik heel sportief ben. Dit natuurlijk afgezien van de aio-uitjes, labuitjes en het bierbrouwen. Voor dat laatste hartelijke dank aan mijn kamergenoot Stefan. En wat mijn andere kamergenoten betreft: Guido, dank voor al het fruit, Ivaylo, thanks for all the cookies. En Wim, bedankt voor de leuke tijd en de anekdotes die ik over je kan vertellen.

Speciale dank aan Merel! En Mirjam natuurlijk, bedankt voor alles de afgelopen tijd en ook alvast voor alles de komende tijd.

Wilfred

Levensloop

Wilfred Kleinjan werd geboren op 4 oktober 1974 te Zwolle. In 1993 behaalde hij zijn VWO-diploma aan de C.S.G. Jan van Arkel te Hardenberg. Hierna begon hij aan een studie Chemische Technologie aan de Universiteit Twente. Tijdens zijn studie deed hij een stageproject bij het Exxon Chemical Research Centre in Machelen (België) en in 1999 studeerde hij af met een afstudeeropdracht bij de vakgroep Membraantechnologie. Eind 1999 begon hij aan een promotieonderzoek op het Laboratorium voor Fysische Chemie en Kolloïdkunde, in samenwerking met het subdepartement Milieutechnologie. De resultaten van dit onderzoek staan beschreven in dit proefschrift.